Course 620B

Experimental Methods in High-Energy Physics

CALORIMETRY

Francois Corriveau

IPP / McGill University

1994-2004

CALORIMETRY

INCOMING PARTICLE

$\leq 1\,\mu s$

COLLISIONS
IONISATION
LIGHT EMISSION
...

$\sim 1\,s$

HEAT

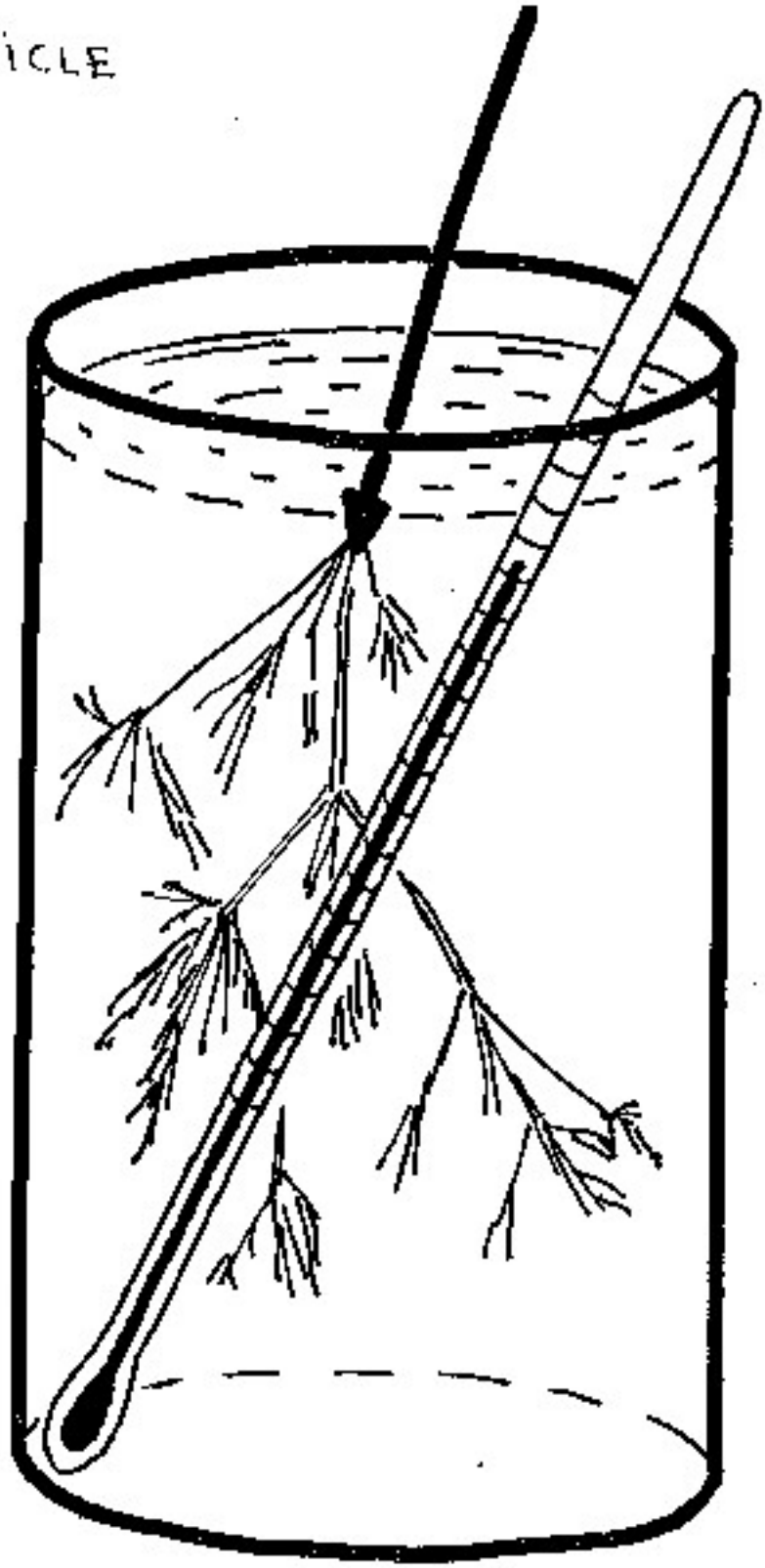

Example: 1 TeV in 10 tons produces $\Delta T \sim 10^{-19}\,^{\circ}K$

PARTICLE PHYSICS DETECTORS

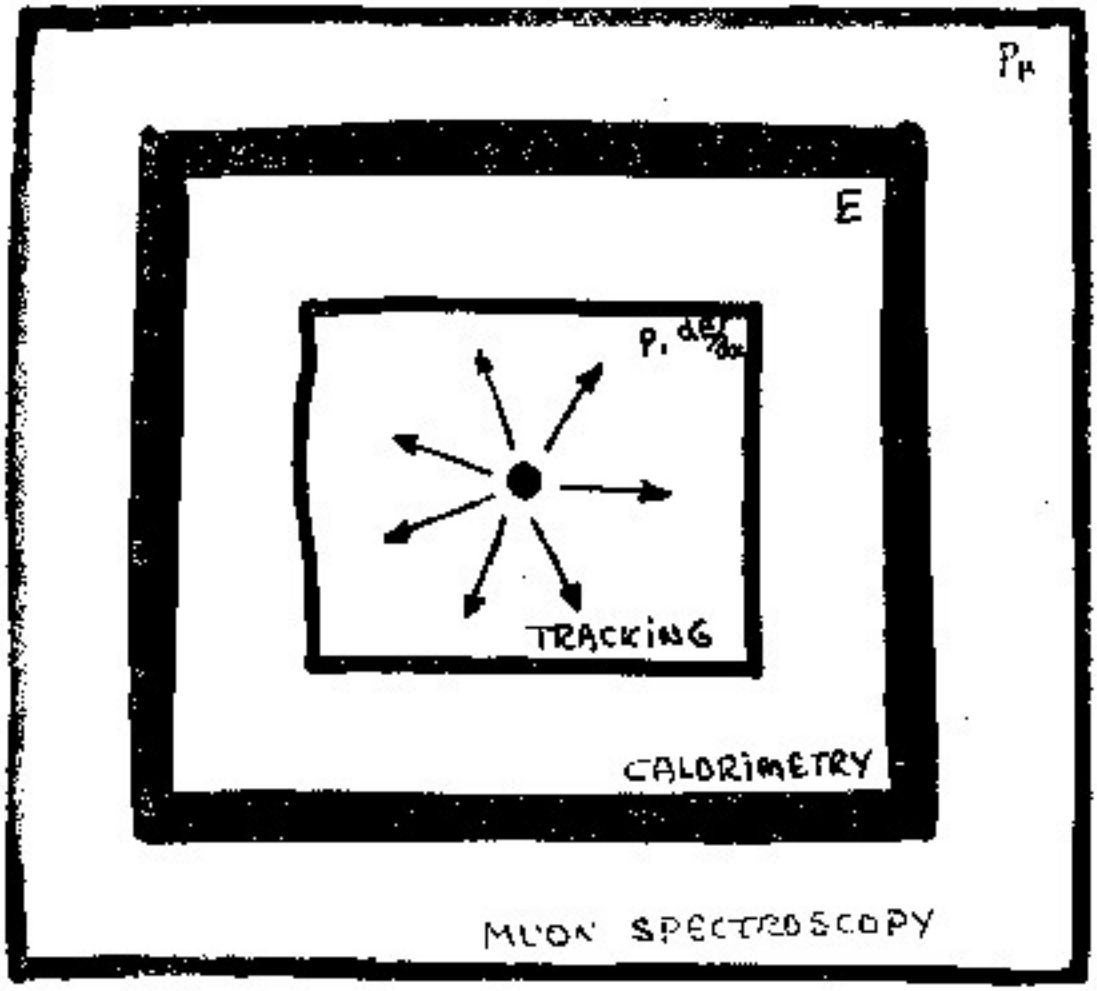

FOR CHARGED AND NEUTRAL PARTICLES

OVER A WIDE RANGE OF ENERGIES

WITH A $\sim 4\pi$ ACCEPTANCE

PARTICLE DETECTION

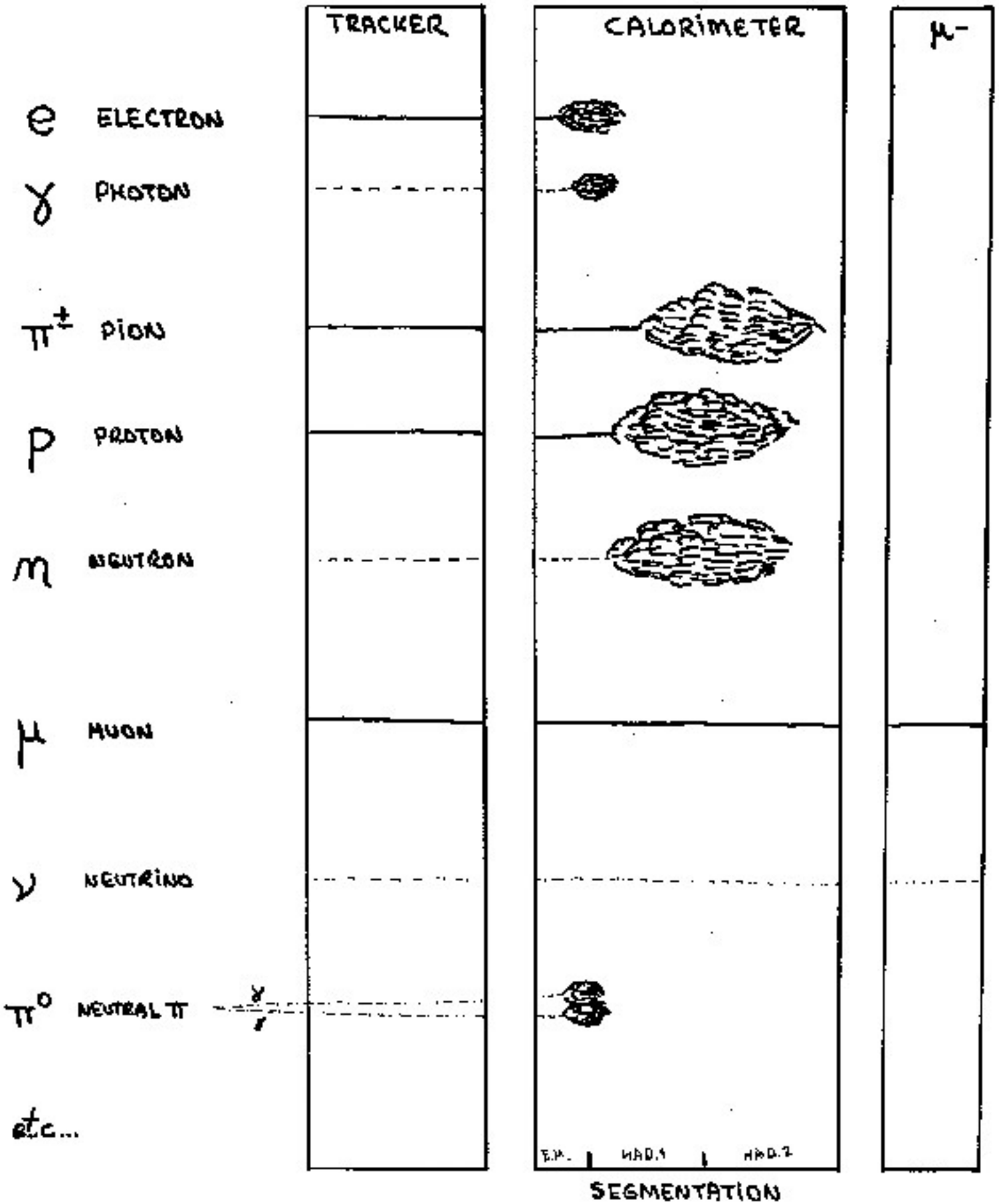

CALORIMETERS

A CALORIMETER IS ESSENTIALLY A PIECE OF MATERIAL WHICH INTERCEPTS A PARTICLE, IN WHICH THE SUBSEQUENT SHOWER DEVELOPS AND WHICH CAN CONVERT A FRACTION OF THE ENERGY DEPOSITION INTO A MEASURABLE SIGNAL.

A SHOWER IS THE GLOBAL PROCESS BY WHICH THE INCOMING ENERGY IS DISSIPATED BY A CASCADE OF LOWER ENERGY PARTICLES.

ONE DISTINGUISHES 2 TYPES OF SHOWERS:
ELECTROMAGNETIC ($e^{\pm}, \gamma$) OR HADRONIC ($\pi^{\pm}, p, n \ldots$)

TOTAL ABSORPTION MEANS THE SHOWER IS CONTAINED

PROPERTIES

- SIGNAL ~ DEPOSITED ENERGY
- DETECTS BOTH CHARGED AND NEUTRAL: PARTICLES
- 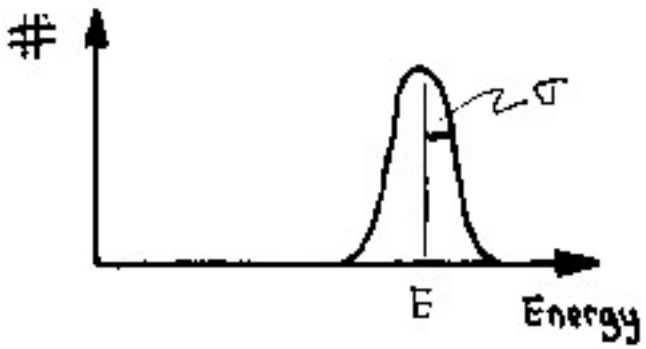

  RESOLUTION:

  $$\frac{\sigma}{E} \sim \frac{1}{\sqrt{\langle N \rangle}} \sim \frac{1}{\sqrt{E}}$$

  SINCE THE ENERGY DEGRADATION THROUGH A SHOWER IS A STATISTICAL PROCESS, VIA $\langle N \rangle$ SECONDARY PARTICLES

- THE SHOWER LENGTHS, HENCE THE CALORIMETER DEPTH, SCALE AS

  $$L \sim \log(E)$$

  MAGNETIC SPECTROMETERS : $\sim \sqrt{p}$

ADVANTAGES

- DIMENSIONS CAN BE FURTHER REDUCED BY USING HIGH-Z MATERIALS
- RESPONSE DEPENDS ON THE TYPE OF PARTICLE AND ALLOWS PARTICLE IDENTIFICATION BETWEEN
  e, μ AND HADRONS
- GRANULARITY (LATERALLY) AND SEGMENTATION (LONGITUDINALLY) ENABLE POSITION AND ANGLE DETERMINATIONS.
- THE TIME RESPONSE IS USUALLY VERY FAST. THE DETECTOR CAN WORK IN HIGH RATE ENVIRONMENT AND THE SIGNALS CAN BE USED IN EVENT TRIGGERS.
- THE COST RANGE CAN ALSO BE VERY WIDE.

ELECTROMAGNETIC SHOWERS

ARE CASCADES OF ELECTROMAGNETIC PROCESSES INVOLVING ELECTRONS $e^{\pm}$ AND PHOTONS γ.

→ UNDERSTAND ENERGY LOSSES IN MATTER

ELECTRON ENERGY LOSS IN MATTER

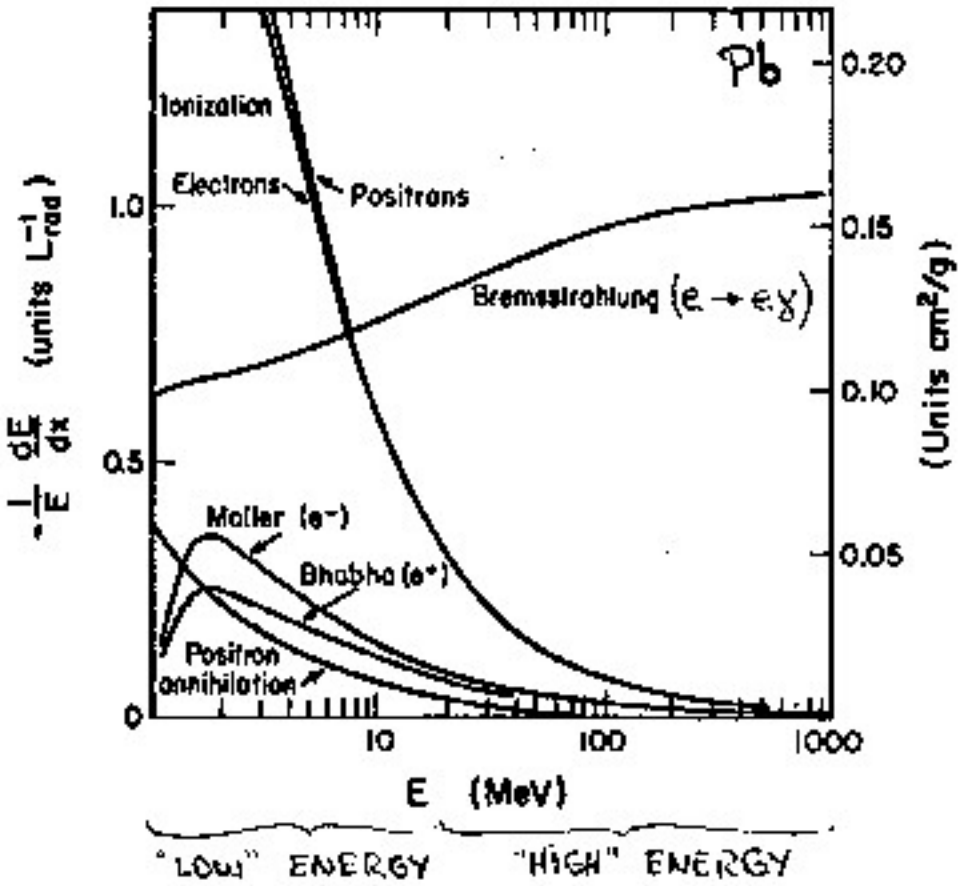

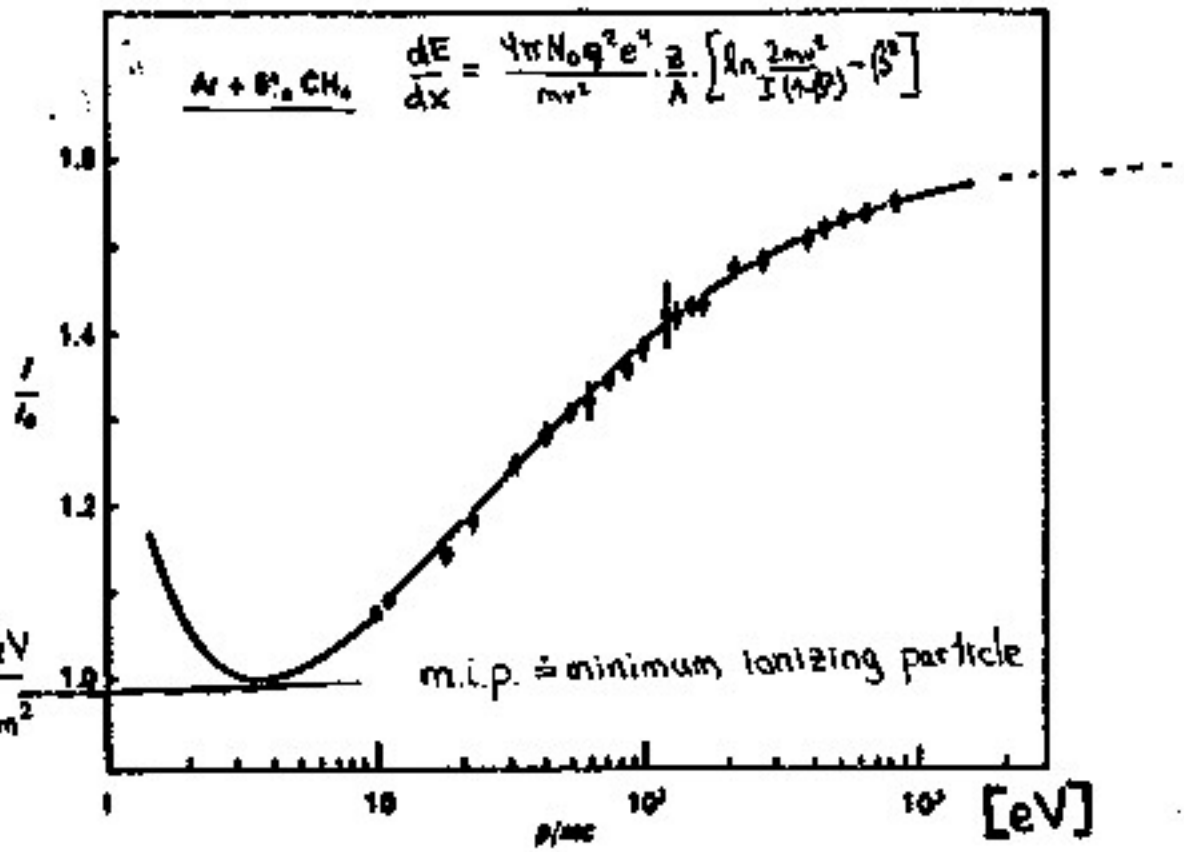

$\left(\frac{dE}{dx}\right)_{min} \approx 1.5 \frac{MeV}{g/cm^2}$

ELECTRON ENERGY LOSSES ARE PROPORTIONAL TO:

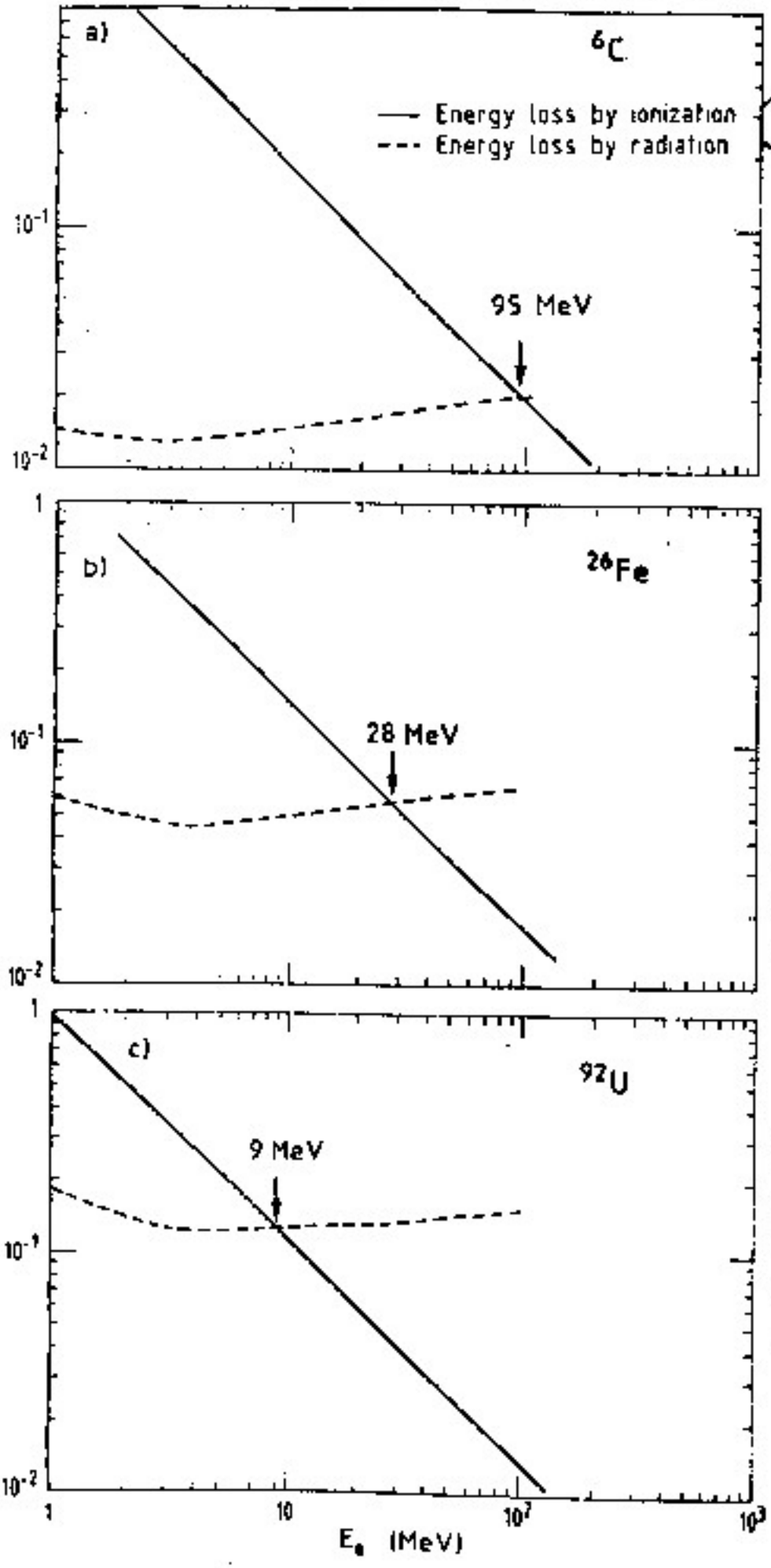

$\sim Z, \ln E$

$\sim Z^2, E$

ONE DEFINES THE CRITICAL ENERGY

$$E_c \sim \frac{1}{Z}$$

AS A SORT OF SCALE BETWEEN DIFFERENT MATERIALS

PHOTON ENERGY LOSS

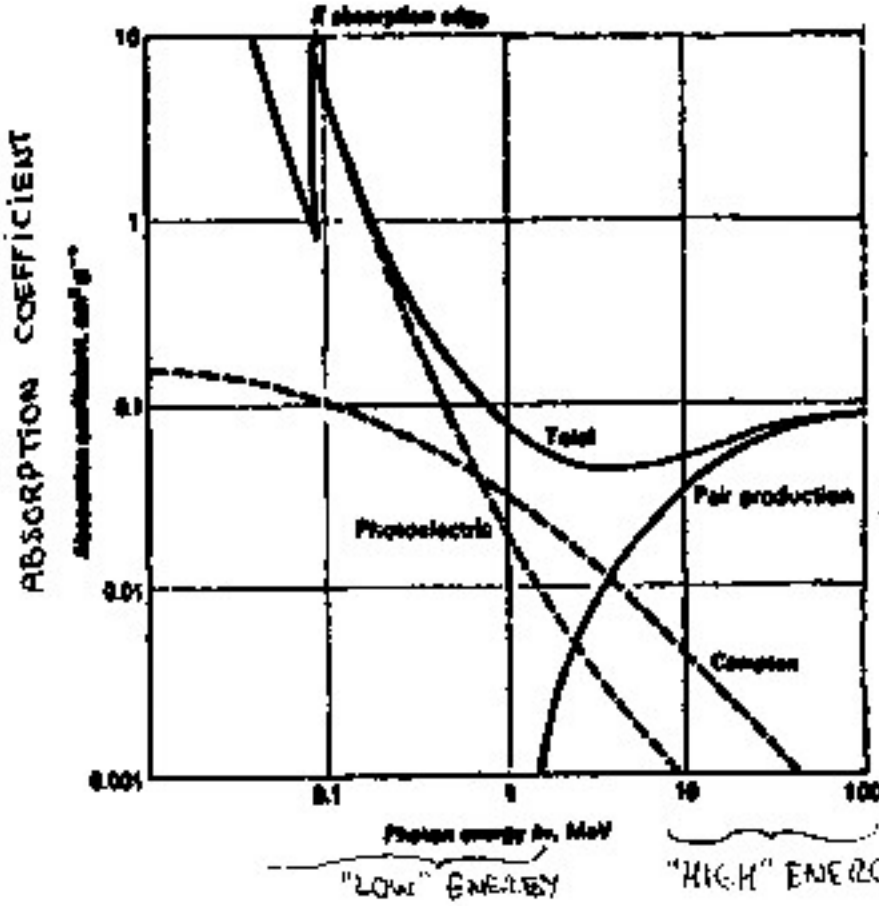

CROSS-SECTION:

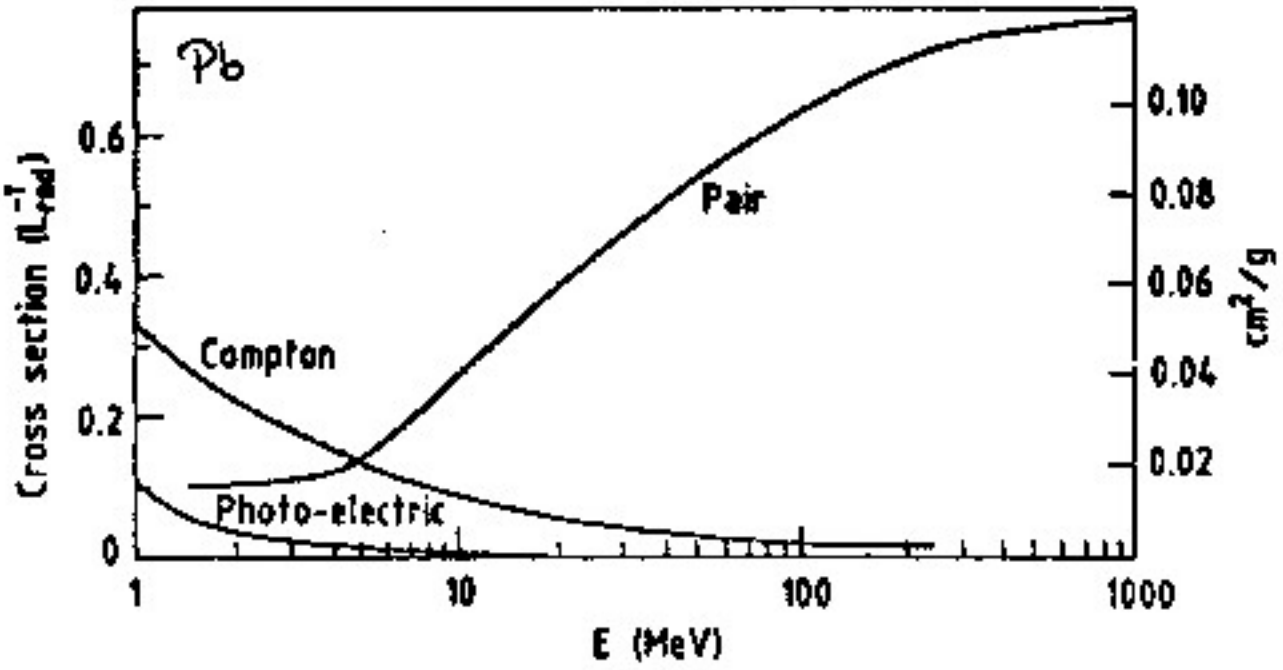

$$I = I_0 e^{-\sigma x}$$

PHOTON CROSS-SECTIONS

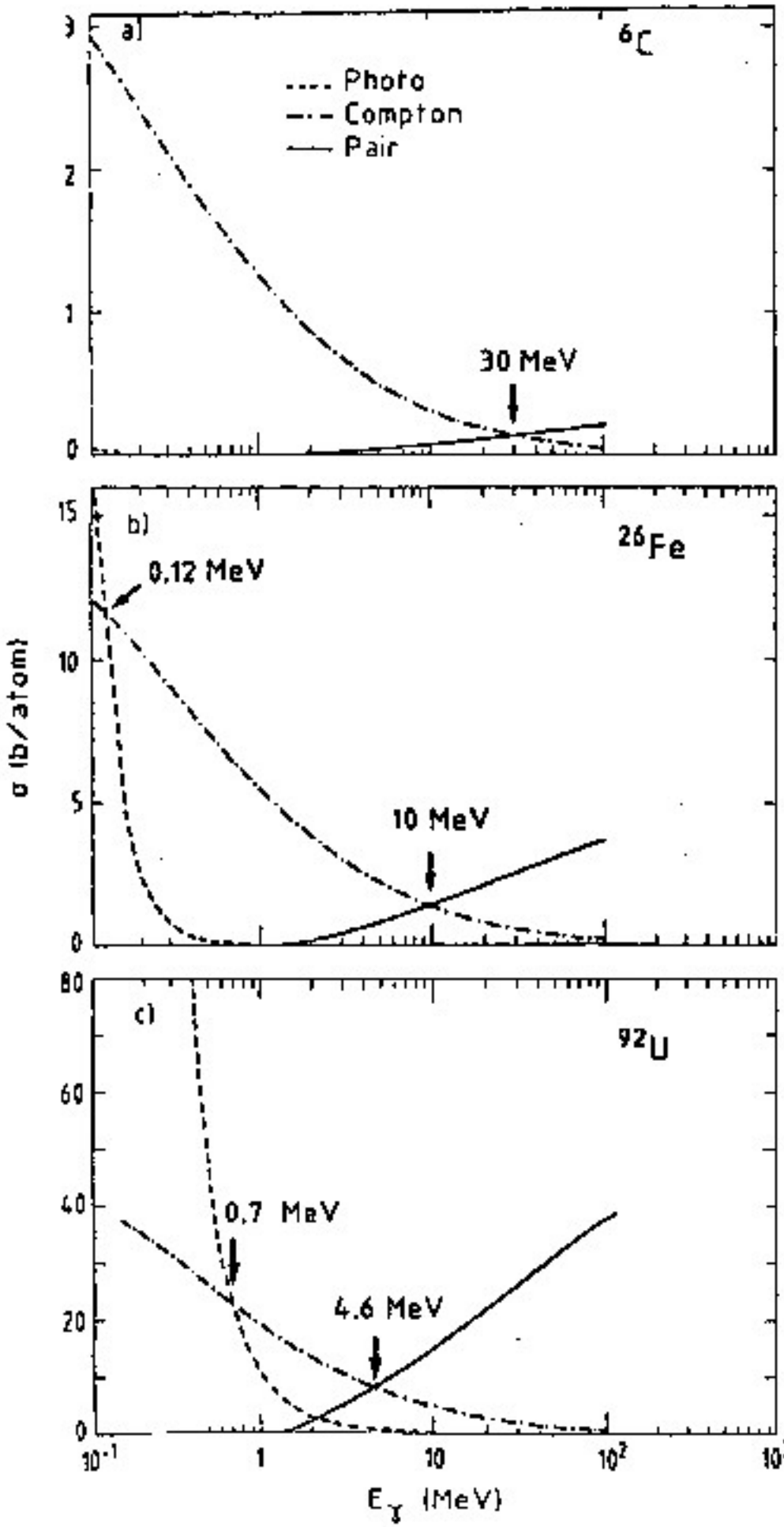

HERE ALSO:
$E_c \sim \frac{1}{Z}$

CRITICAL ENERGY E_c

AS FUNCTION OF TIME, THE SHOWER DEVELOPMENT INVOLVES AN INCREASING NUMBER OF SECONDARY PARTICLES WITH EVER DECREASING ENERGIES E_i UP TO MAXIMUM

ONE DEFINES THE CRITICAL ENERGY E_c SUCH THAT:

(2) $E_i < E_c$: IONIZATION DOMINATES AND

$e^{\pm} \longrightarrow e^{\pm}$ (ionization)
$\gamma \longrightarrow \gamma, e$ (Compton)

THE NUMBER OF PARTICLES DECREASES

(1) $E_i > E_c$: RADIATION DOMINATES AND

$\gamma \rightarrow e^+ e^-$ (pair production)
$e^{\pm} \rightarrow e^{\pm} \gamma$ (Bremsstrahlung)

THE NUMBER OF PARTICLE INCREASES

RADIATION LENGTH X_0

IT IS THE DISTANCE OVER WHICH A HIGH-ENERGY ELECTRON LOSES $1/e$ OF ITS ENERGY TO BREMSSTRAHLUNG.

$$-\left.\frac{dE}{E}\right|_{BREMS.} = \frac{dx}{X_0}$$

WHERE

$$X_0 \simeq \frac{180\,A}{Z^2} \quad [g/cm^2] \qquad (Z \geq 13: \pm 20\%)$$

OR, FOR $E > E_c$:

$$\langle E^e_{AFTER} \rangle = E^e_{BEFORE} \cdot e^{-\frac{x}{X_0}}$$

= AVERAGE ENERGY AFTER PATH "x" IN MATTER

$[g/cm^2]$ SINCE MOST ELECTROMAGNETIC PROCESSES ARE PROPORTIONAL TO THE MATERIAL DENSITY, IT IS MOST CONVENIENT TO WORK IN UNITS OF $[g/cm^2]$ AND PUT THEM IN X_0

X_0 IS FURTHERMORE, IN FIRST APPROXIMATION, MATERIAL-INDEPENDENT.

PAIR PRODUCTION

THE MEAN FREE PATH FOR PAIR PRODUCTION $\gamma \to e^+e^-$ IS GIVEN BY:

$$X_p = \frac{9}{7} X_0$$

IE. FOR $E > E_c$:

$$\langle N^{\gamma}_{AFTER} \rangle = N^{\gamma}_{BEFORE} \cdot e^{-\frac{x}{X_p}}$$

CRITICAL ENERGY

... WHEN ENERGY LOSSES THROUGH IONIZATION (COLLISIONS) AND RADIATION BECOME EQUAL:

$$-\frac{dE}{E_c}\bigg|_{IONIZATION} = -\frac{dE}{E_c}\bigg|_{RADIATION} \doteq \frac{dx}{X_0}$$

LEADING TO:

$$E_c \simeq \frac{750}{Z} \text{ [MeV]} \qquad (Z \gtrsim 13 \pm 10\%)$$

PARTICLE DATA BOOK

ATOMIC AND NUCLEAR PROPERTIES OF MATERIALS

Material	Z	A	Nuclear[a] total cross section σ_T [barn]	Nuclear[b] inelastic cross section σ_I [barn]	Nuclear[c] collision length λ_T [g/cm^2]	Nuclear[c] interaction length λ_I [g/cm^2]	$\frac{dE}{dx}\Big\|_{min}$ $\left[\frac{MeV}{g/cm^2}\right]$	Radiation length[d] X_0 [g/cm^2] () is for gas	[cm]	Density[f] [g/cm^3] () is for gas [g/ℓ]	Refractive index n[f] () is $(n-1)\times10^4$ for gas
H_2	1	1.01	0.0257	0.033	42.8	50.8	4.12	61.28	865	0.0708(0.090)	1.112(140)
D_2	1	2.01	0.073	0.061	48.7	54.7	2.07	122.6	707	0.162(0.177)	1.128
He	2	4.00	0.120	0.102	49.9	65.1	1.94	94.32	755	0.125(0.178)	1.024(35)
Li	3	6.94	0.211	0.157	64.8	79.4	1.58	82.76	154	0.534	—
Be	4	9.01	0.268	0.199	65.8	78.2	1.61	65.19	35.3	1.848	—
C	6	12.01	0.331	0.231	60.2	85.8	1.78	42.78	18.8	2.265[g]	—
N_2	7	14.01	0.379	0.265	61.4	87.8	1.82	37.99	47.0	0.806(1.25)	1.205(300)
O_2	8	16.00	0.420	0.292	63.2	92.0	1.82	34.24	30.0	1.14(1.43)	1.22(266)
Ne	10	20.18	0.507	0.347	66.1	96.6	1.73	28.94	24.0	1.207(0.90)	1.092(67)
Al	13	26.98	0.634	0.431	70.6	105.4	1.62	24.01	8.9	2.70	—
Si	14	28.09	0.666	0.440	70.9	106.0	1.66	21.82	9.36	2.33	—
Ar	18	39.95	0.868	0.566	76.4	117.2	1.51	19.55	14.0	1.40(1.78)	1.233(283)
Ti	22	47.88	0.996	0.637	79.6	124.9	1.51	16.17	3.56	4.54	—
Fe	26	55.85	1.120	0.702	82.8	131.9	1.48	13.84	1.76	7.87	—
Cu	29	63.55	1.323	0.783	86.0	134.9	1.44	12.86	1.43	8.96	—
Ge	32	72.59	1.386	0.858	88.2	140.6	1.40	12.25	2.30	5.323	—
Sn	50	118.69	1.967	1.21	100.2	163	1.26	8.82	1.21	7.31	—
Xe	54	131.29	2.130	1.29	102.9	169	1.24	8.48	2.77	3.057(5.89)	(705)
W	74	183.85	2.787	1.65	116.3	185	1.14	6.76	0.35	19.3	—
Pt	78	195.08	2.861	1.708	113.3	189.7	1.13	6.54	0.305	21.45	—
Pb	82	207.19	2.960	1.77	116.2	194	1.12	6.37	0.56	11.35	—
U	92	238.03	3.378	1.96	117.0	199	1.09	6.00	≈0.32	≈18.95	—
Air, 20°C, 1 atm. (STP in parens.)					63.0	90.0	1.82	36.66	(30420)	0.001205(1.29)	1.000273(293)
H_2O					60.1	84.8	1.93	36.08	36.1	1.00	1.33
Shielding concrete[h]					47.4	98.9	1.79	26.7	10.7	2.3	—
SiO_2 (quartz)					47.0	99.5	1.72	27.05	12.3	2.64	1.459
H_2 (bubble chamber 26°K)					43.3	50.8	4.12	61.28	≈1000	≈ 0.063[i]	1.100
D_2 (bubble chamber 31°K)					48.7	54.7	2.07	122.6	≈900	≈ 0.140[i]	1.110
H-Ne mixture (50 mole percent)[j]					65.0	94.5	1.84	29.70	73.0	0.407	1.069
Ilford emulsion G5					83.9	134	1.44	11.9	2.39	3.815	—
NaI					84.3	152	1.32	9.49	2.59	3.67	1.775
BaF_2					82.1	148	1.35	9.91	2.06	4.89	1.56
BGO ($Bi_4Ge_3O_{12}$)					97.4	186	1.27	7.98	1.12	7.1	2.15
Polystyrene, scintillator (CH)[k]					54.4	83.0	1.96	43.8	42.4	1.032	1.581
Lucite, Plexiglas ($C_5H_8O_2$)					59.2	85.6	1.96	40.56	≈34.4	1.15–1.20	≈ 1.49
Polyethylene (CH_2)					56.9	78.9	2.00	44.8	≈47.9	0.92–0.96	—
Mylar ($C_5H_4O_2$)					60.2	88.7	1.88	39.95	28.7	1.39	—
Borosilicate glass (Pyrex)[l]					86.2	97.8	1.73	28.3	12.7	2.23	1.474
CO_2					62.4	90.5	1.83	36.2	(18310)	(1.977)	(410)
Dibase C_2H_6					55.73	76.71	2.25	45.68	(34035)	0.509(1.356)[m]	(1.036)[m]
Methane CH_4					54.7	74.6	2.41	46.5	(54850)	0.423(0.717)	(444)
Isobutane C_4H_{10}					56.3	77.4	2.23	45.3	(16930)	(2.67)	(1270)
NaF					68.78	97.57	1.89	29.87	11.68	2.558	1.336
LiF					62.00	88.34	1.86	39.25	14.91	2.632	1.392
Freon 12 (CCl_2F_2) gas, 20°C, 1 atm.[n]					70.6	108	1.82	23.7	4618	(4.63)	1.001030
Silica Aerogel[o]					65.5	95.7	1.83	29.85	≈130	0.1–0.3	1.0+0.25ρ
NEMA G10 plate[p]					62.8	90.2	1.87	35.0	19.4	1.7	—

10 GeV ELECTRON SHOWER

A COMPOSITE OF NUMEROUS LOW-ENERGY PROCESSES

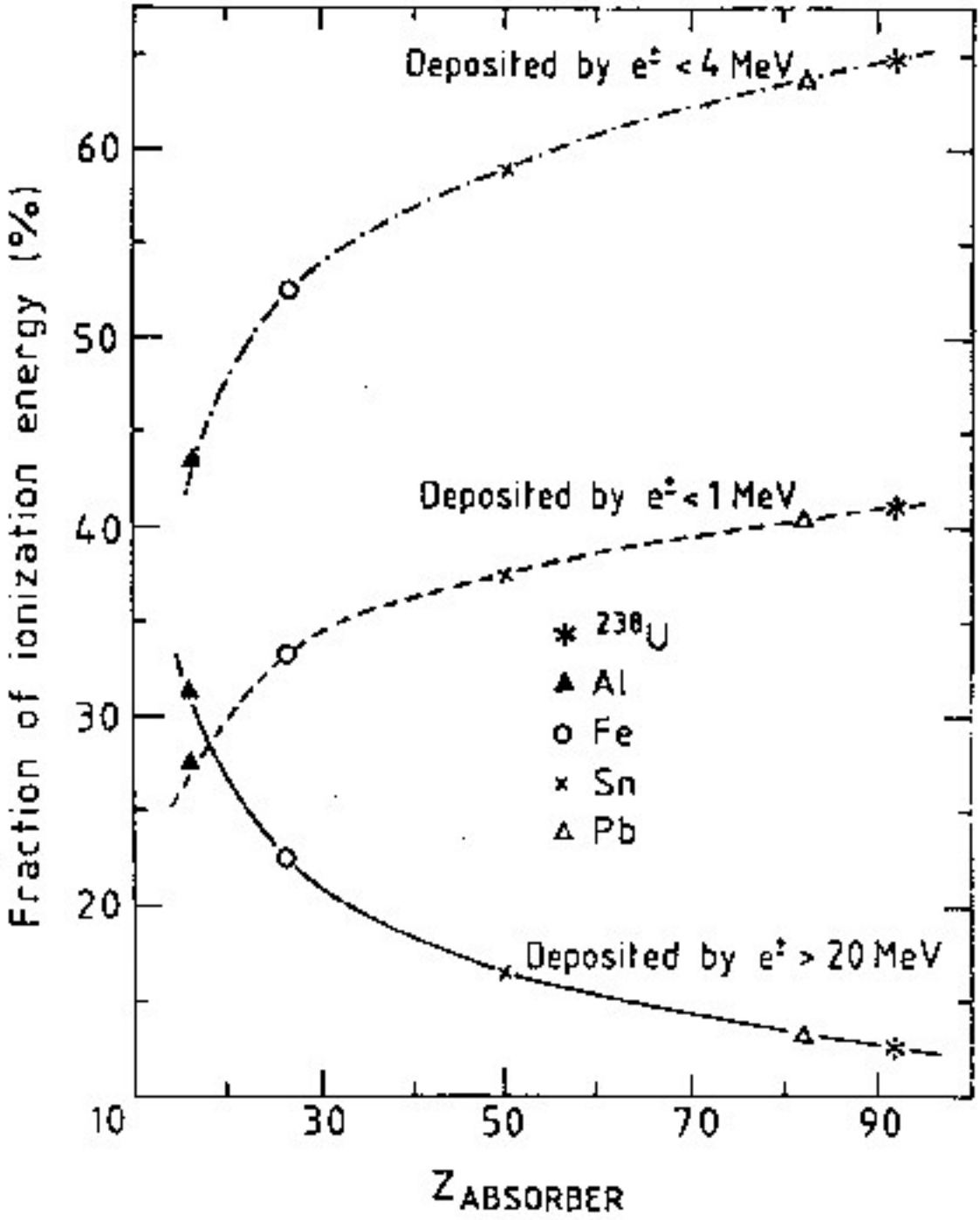

E.M. SHOWER MODEL #1

(Rossi, 1952)

- ASSUME THE IONIZATION CROSS-SECTION TO BE ENERGY-INDEPENDENT :

$$\left.\frac{dE}{dx}\right|_{ion.} = -\frac{E_c}{X_0}$$

- NEGLECT MULTIPLE AND COMPTON SCATTERING
- DEFINE $t \doteq x/X_0$

$y \doteq E/E_c$

- CONSIDER

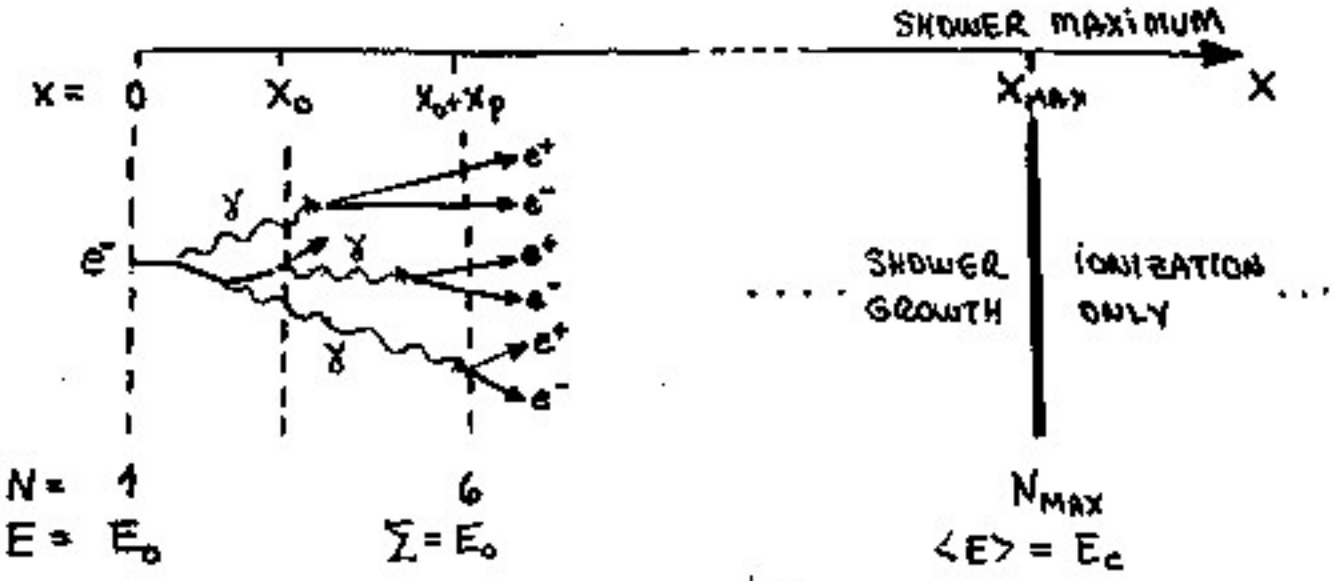

- EXPONENTIAL GROWTH: $N(x) = e^{kx}$

SOLVE FOR $N(X_0+X_p) = 6 \longrightarrow k = 0.78/X_0$ $\quad (X_p = \frac{9}{7}X_0)$

- AT SHOWER MAXIMUM, e^+, e^-, γ SHARE ENERGY EQUALLY

I.E. $N_{MAX} \doteq E_0/\beta E_c = e^{k X_{max}}$

$$\longrightarrow t_{MAX} = \frac{1}{0.78} \times \ln\left(\frac{y_0}{3}\right) \approx 1.3\,(\ln y_0 - 1.1)$$

E.M. SHOWER MODEL #2

(Rossi, revisited, 1964)

INITIAL PARTICLE:	e^-	γ
t_{MAX}	$\ln y - 1.0$	$\ln y - 0.5$
$\langle t \rangle$	$t_{MAX} + 1.4$	$t_{MAX} + 1.7$
N_{MAX}	$\frac{0.3y}{(\ln y - 0.37)^{1/2}}$	$\frac{0.3y}{(\ln y - 0.31)^{1/2}}$
total track length	y	y

E.M. SHOWER MODEL #3

(Longo + Sestili, 1985)

t_{MAX}	$\ln y - 0.5$	$\ln y + 0.5$

ANALYTICAL FORM:

$$\frac{dE}{dt} = E_0 b \frac{(bt)^{a-1} e^{-bt}}{\Gamma(a)}$$

E.M. SHOWER MODEL #4

(Nelson et al., 1985)

THE EGS4 CASCADE SIMULATION

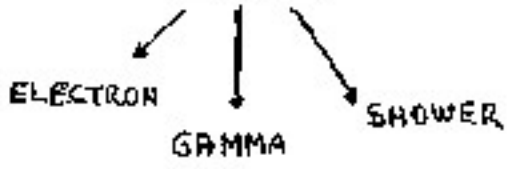

EXTREMELY SUCCESSFUL

ELECTROMAGNETIC SHOWER

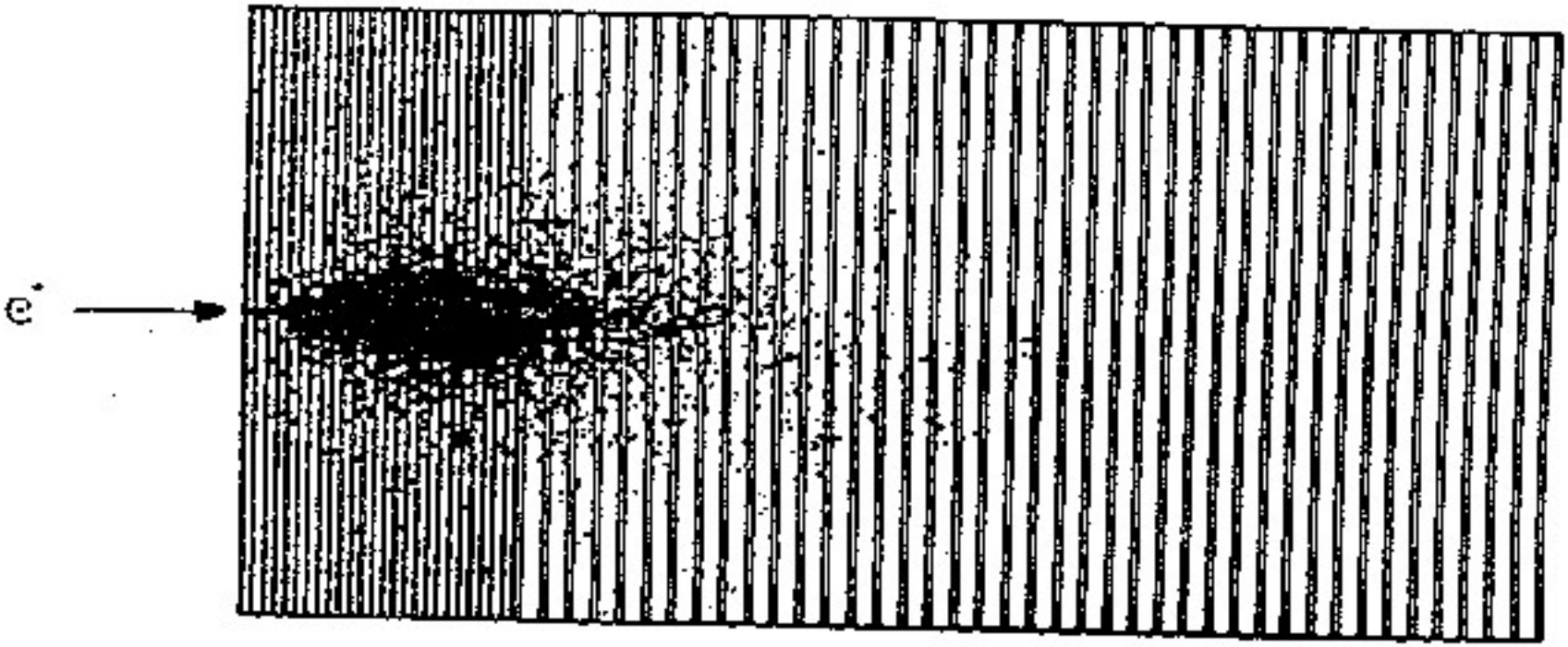

STARTS IN AVERAGE ($1/e$) AT $x = X_0$

LONGITUDINAL SHOWER DEVELOPMENT

DATA FOR 6 GeV ELECTRONS

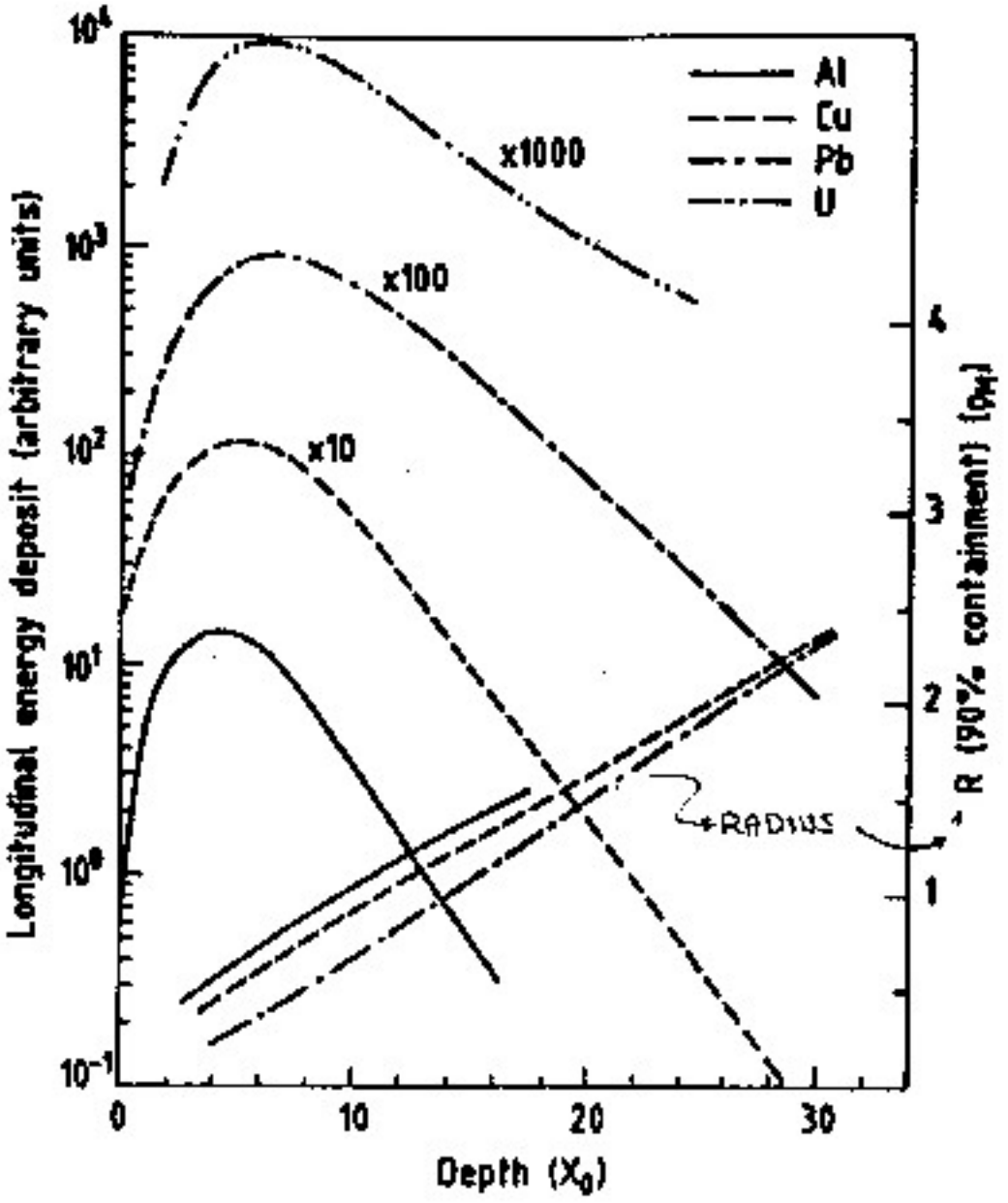

→ VERY SIMILAR SHAPES

LONGITUDINAL SHOWER DEVELOPMENT :

DATA vs MONTE CARLO SIMULATION (EGS4)

10 GeV ELECTRONS

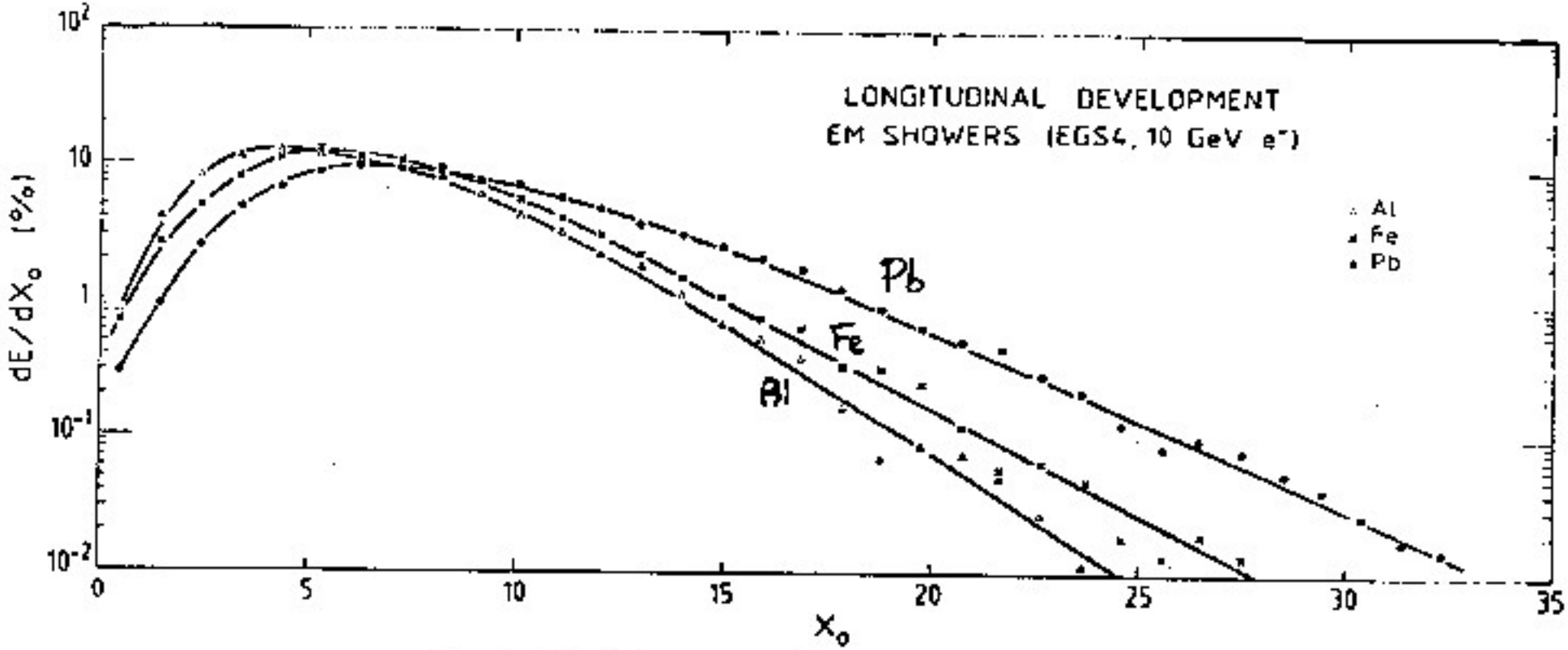

REMARKS :

- X_0 - SCALING IS APPROXIMATE
- SHOWER MAXIMUM IS SHIFTED DEEPER WITH HIGHER Z
- SHOWER DECAY IS SLOWER AFTER MAX. " " "

MORE LOW-ENERGY PROCESSES

LATERAL ENERGY DEPOSITION

FIRST DETERMINED BY : $\theta_{\text{BREMSSTRAHLUNG}} \sim \frac{p_s}{m_e}$

MULTIPLE SCATTERING

LATER, AFTER SHOWER MAXIMUM: " " ONLY

1 GeV e.m. SHOWER IN LEAD

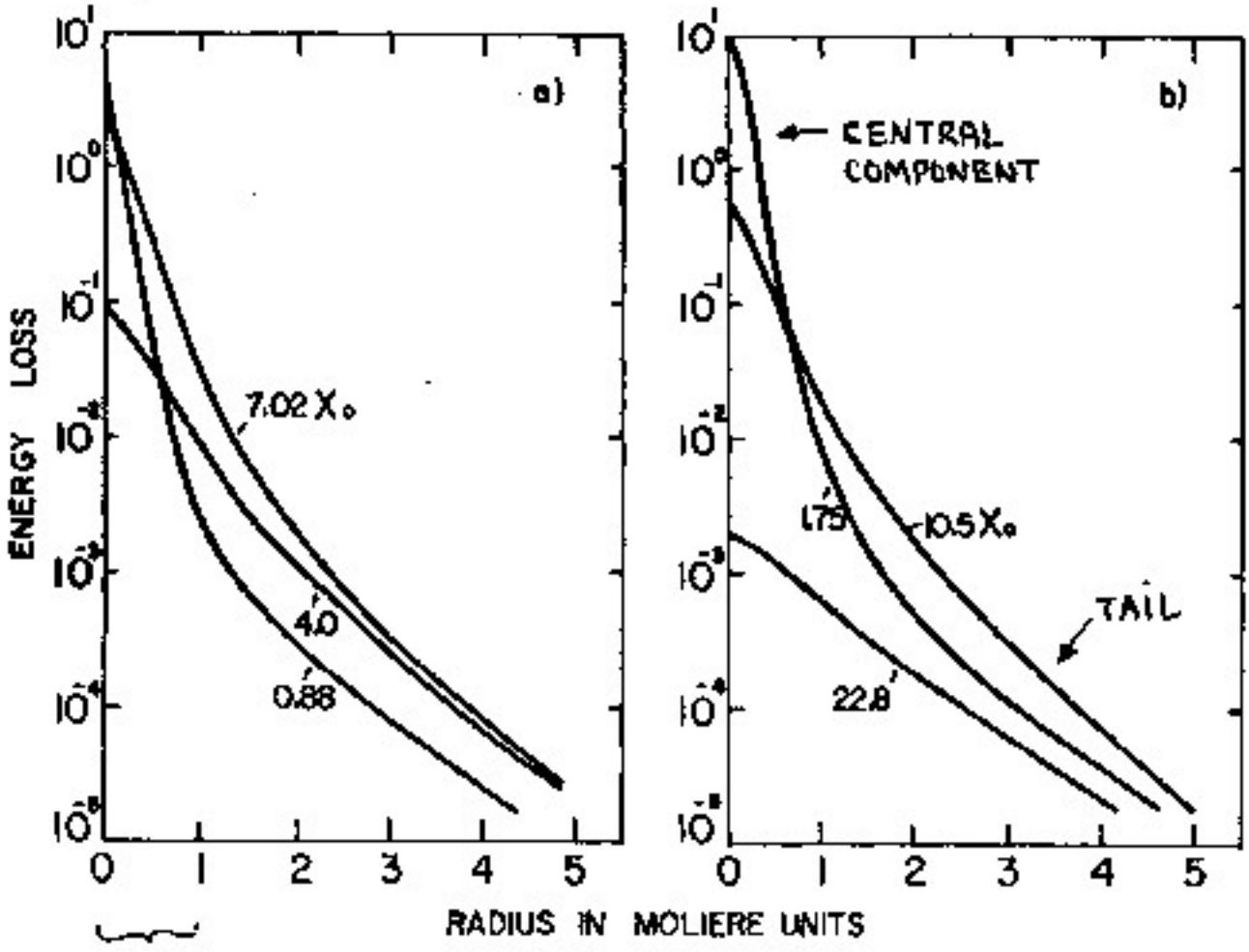

~90 % CONTAINMENT

~99 % CONTAINMENT

SCALING VARIABLE R_M

$$= \frac{21\ X_0}{E_{c\,[\text{MeV}]}} \approx \frac{7A}{Z}\ \left[\text{g/cm}^2\right]$$

LATERAL ENERGY DEPOSITION

6 GeV ELECTRON SHOWER

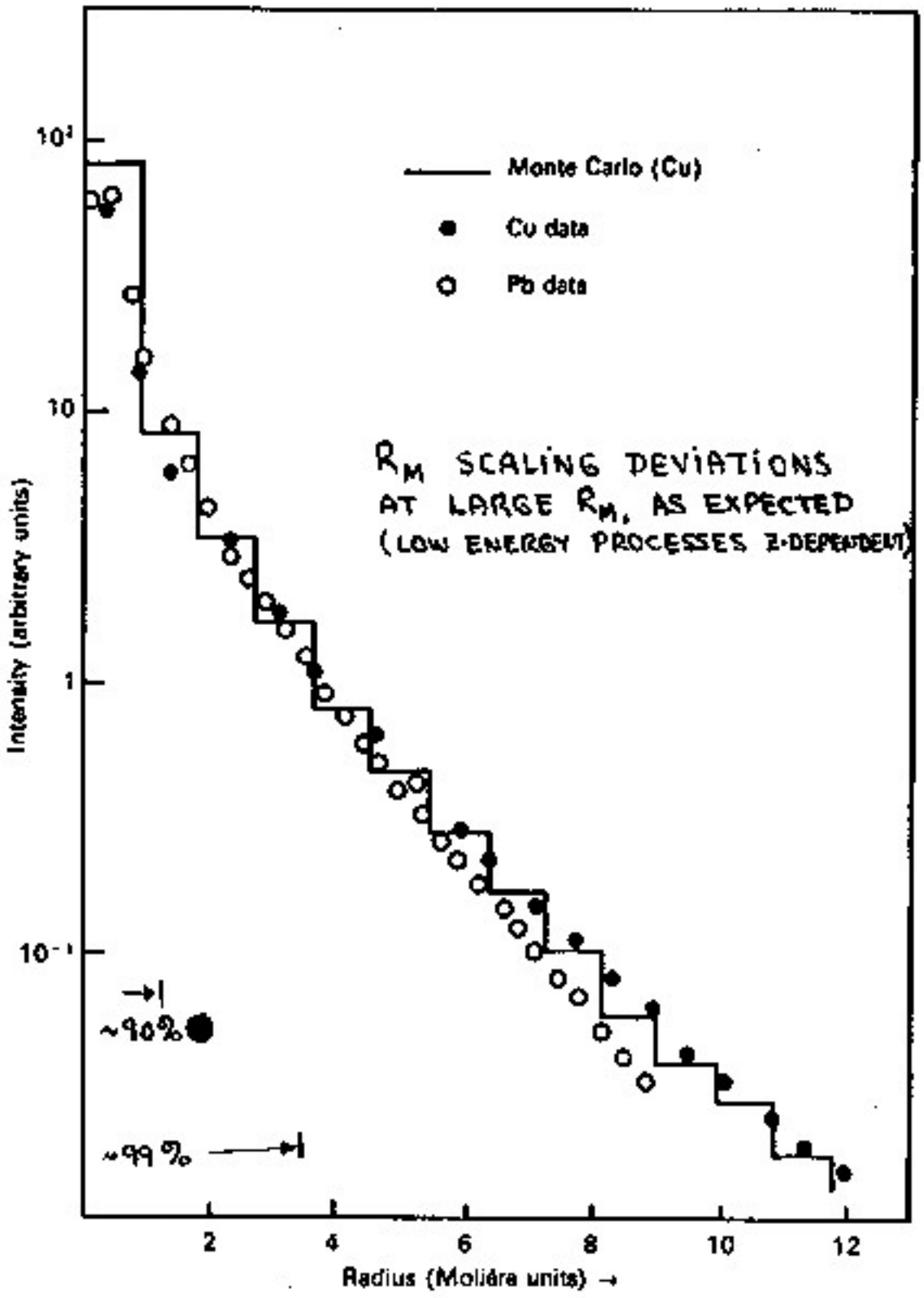

SHOWER ENERGY MEASUREMENT

- AT SHOWER MAXIMUM, THE N_{MAX} PARTICLES OF ENERGY $\langle E \rangle \approx E_c$ REPRESENT A TOTAL TRACK LENGTH $L \approx E_0 / E_c$

- ALL OF THIS ENERGY IS EVENTUALLY CONVERTED INTO LOW ENERGY IONIZING ELECTRONS. NUCLEAR ABSORPTION EFFECTS CAN BE NEGLECTED.

> A CALORIMETER SAMPLES THOSE ELECTRONS ABOVE SOME THRESHOLD η

- THE DETECTABLE TRACK LENGTH L_D IS GIVEN BY

$$L_D = \underbrace{f(\eta/E_c)}_{f(0) \doteq 1} \cdot L \cdot \text{Sampling}$$

- FOR MOST DETECTORS, $\eta \ll E_c$, HENCE

$$L_D \sim E_0$$

E.M. CALORIMETERS

FULLY ACTIVE DEVICES

THE ABSORBER MEDIUM IS THE SAME THAT PRODUCES AND PROPAGATE THE LIGHT SIGNAL TO BE MEASURED.

e.g.: SCINTILLATION LIGHT FROM INORGANIC CRYSTALS such as CsI (Tl) $\eta \sim 20$ eV

CERENKOV LIGHT FROM LEAD GLASS $\eta \sim 0.7$ MeV

SAMPLING DEVICES

THE ABSORBER IS PASSIVE, CAN THEREFORE BE DENSER FOR A MORE COMPACT DEVICE.

ONLY A FRACTION OF THE IONIZATION SIGNAL CAN BE DETECTED BY THE ACTIVE MEDIUM.

PASSIVE DEVICES

THESE ARE NOT REALLY CALORIMETERS BUT IN FACT BEAM DUMPS: ONLY LEAKAGE IS OF INTEREST.

	Parameters of Scintillation Materials					
	BGO	CsI(Tl)	BaF2	NaI(Tl)	Scintillating Glass	Plastic Scintillator
Density (g/cc)	7.13	4.5	4.88	3.7	4.8	1
Radiation Length (cm)	1.13	1.85	2.05	2.6	4.35	43
Interaction Length (cm)	21.9	34	29.9	41.1	44	82
Critical Energy (MeV)	8.8	10.2	12	12.5		
Moliere Radius (cm)	2.7	3.8	4.3	4.3		
dE/dx (MeV/cm)	8.07	5.1	5.72	4.13		1.72
Wavelength (nm)	480	550	325,225	410	440	400
Photons/MeV	1.0E+04	5.3E+04	1.5E+04	4.0E+04	1.5E+03	1.0E+04
Mechanical Stability	good	very good	good, cleaves	fair, cleaves	excellent	good
Hygroscopicity		weak		strong		
Radiation Resistance	medium	fair	good	fair	good	
Price ($/cc)	7-13	2-3.5	3-5	1-2	0.23-0.5	0.05

Characteristic Dimensions and Price Comparisons for e.m. Calorimeters

Material Quantity	NaI	BGO	U/Si sampling calorimeter
X_0 (mm)	26	11	4
ϱ_M (mm)	44	23	11
Reference volume (cm^3) for 95% containment of ~ 5 GeV electrons	1600	180	15
Approx. price/Ref. vol. (arbitrary units)	1	1	0.1

ENERGY RESOLUTION

$$\left(\frac{\sigma_E}{E}\right)^2 = \left(\frac{a_0}{E}\right)^2 + \left(\frac{a_1}{\sqrt{E}}\right)^2 + b^2$$

WHERE:

a_0 = ELECTRONIC NOISE { LIMITATION FOR SMALL ENERGIES

a_1 = PHOTOELECTRON STATISTICS

b = SYSTEMATIC ERRORS { LIMITATION FOR HIGH ENERGIES

SYSTEMATIC CONTRIBUTION MAY INCLUDE:

- GEOMETRY EFFECTS : SHOWER LEAKAGE
  INACTIVE MATERIAL
  CONSTRUCTION DEFECTS
  ...
- PHYSICS NOISE : SIGNAL DISTORSIONS ($\propto E$)
  ...
- INTERCALIBRATION ERRORS BETWEEN UNITS

QUALITATIVE EXAMPLE OF RESOLUTION VS ENERGY

$$\frac{\delta E}{E} = \frac{2.5}{E} \oplus \frac{0.8}{\sqrt{E}} \oplus 0.05$$

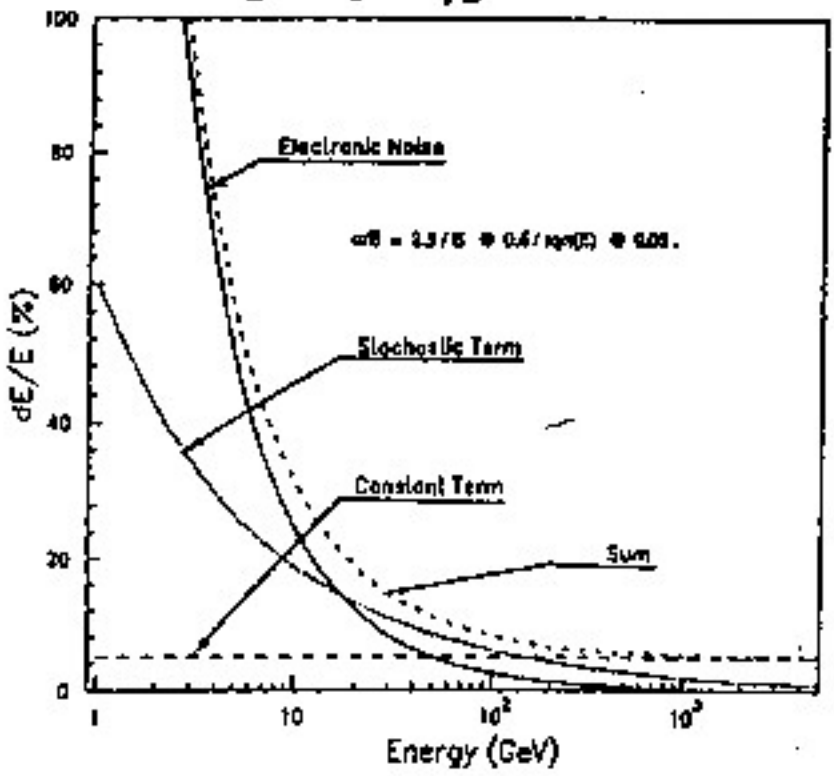

COUNTING STATISTICS

a_1 : THIS IS USUALLY THE MAIN TERM IN THE RESOLUTION. THE SOURCES CAN BE SEEN AS:

- TRACK LENGTH FLUCTUATIONS

  THE NUMBER OF DETECTABLE TRACK SEGMENTS ABOVE THE CUTOFF ENERGY η IS $N_{TS} = E_0/\eta$

  $$\rightarrow \frac{\sigma_E}{E} = \frac{\sigma(N_{TS})}{N_{TS}} = \frac{1}{\sqrt{N_{TS}}} \sim \frac{1}{\sqrt{E}}$$

- PHOTOELECTRON COUNTING STATISTICS

  THE NUMBER OF PHOTOELECTRONS BY DEPOSITED ENERGY IS

  $$N_{PE/MeV} = N_{\gamma/MeV} \times \epsilon_\gamma \times QE$$

  $N_{PE/MeV}$: DETECTED
  $N_{\gamma/MeV}$: PHOTONS
  ϵ_γ: COLLECTION EFFICIENCY
  QE: QUANTUM EFFICIENCY (PHOTOCATHODE)

  $$\rightarrow \frac{\sigma_E}{E} = \frac{\sigma(N_{PE})}{N_{PE}} = \frac{1}{\sqrt{N_{PE}}} \sim \frac{1}{\sqrt{E}}$$

FULLY ACTIVE CAL.

EXAMPLES OF E.M. CALORIMETER ENERGY RESOLUTIONS:

1. CsI (Tl)

THRESHOLD $\eta \approx 0$

γ-production $\sim 5\times10^{4}/\text{MeV}$ $\Big\}$ $\frac{\sigma_E}{E} \approx \frac{0.4\,\%}{\sqrt{E}}$ [GeV]

PE-YIELD $\sim 5\times10^{3}/\text{MeV}$ $\Big\}$ $\frac{\sigma_E}{E} \approx \frac{1.4\,\%}{\sqrt{E}}$ [GeV] $\Big\}$ $\frac{1.5\,\%}{\sqrt{E}}$

2. LEAD GLASS

THRESHOLD $\eta \approx 0.7$ MeV $\Big\}$ $\frac{\sigma_E}{E} = \frac{2.6\,\%}{\sqrt{E}}$ [GeV]

PE-YIELD $\sim 1\times10^{3}/\text{MeV}$ $\Big\}$ $\frac{\sigma_E}{E} = \frac{3.2\,\%}{\sqrt{E}}$ [GeV] $\Big\}$ $\frac{4.1\,\%}{\sqrt{E}}$ [GeV]

3. NaI (Tl)

„NOT LIMITED BY PE-YIELD! $\frac{\sigma_E}{E} \gtrsim \frac{0.9\,\%}{\sqrt[4]{E}}$ [GeV]

BUT NON-UNIFORMITIES, ETC.. COME IN

CRYSTAL BALL DETECTOR

e^+e^- AT SPEAR Doris at SLAC at DESY

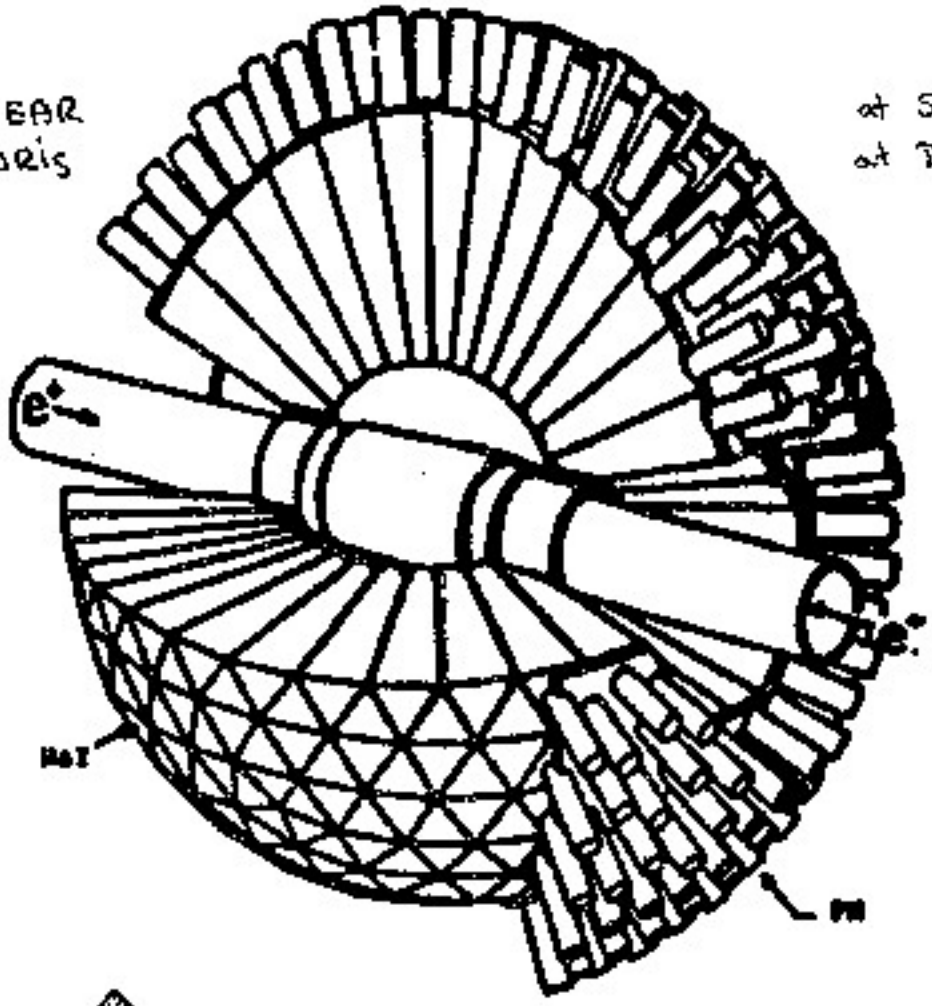

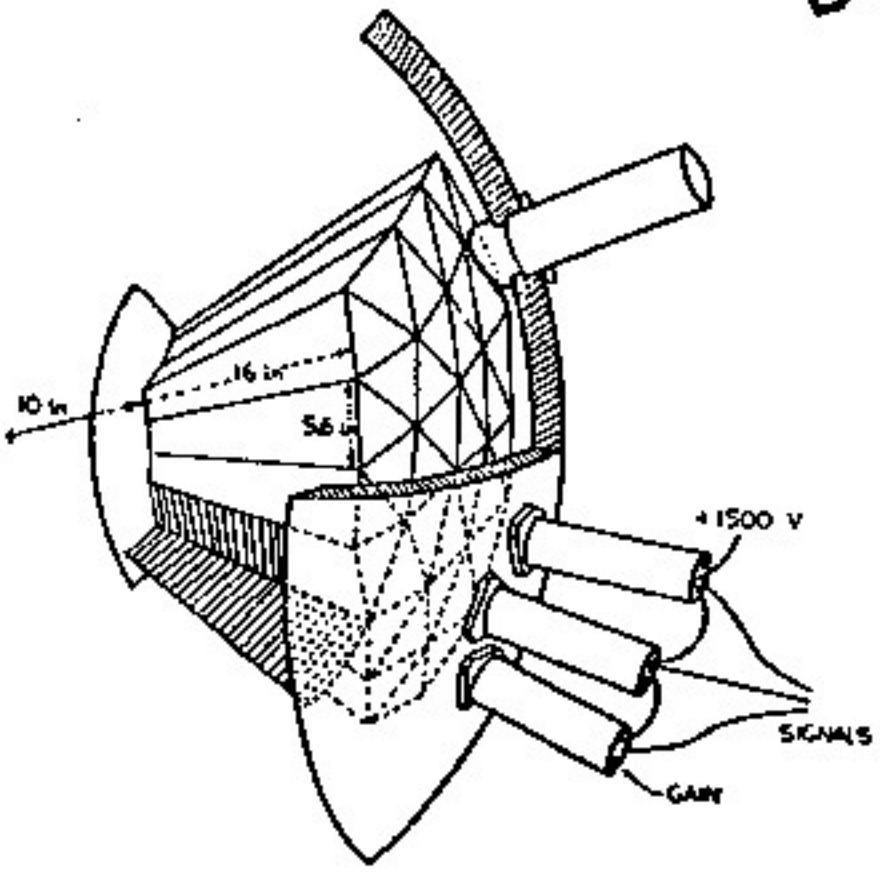

~ 672 NaI ELEMENTS

~ 4π COVERAGE

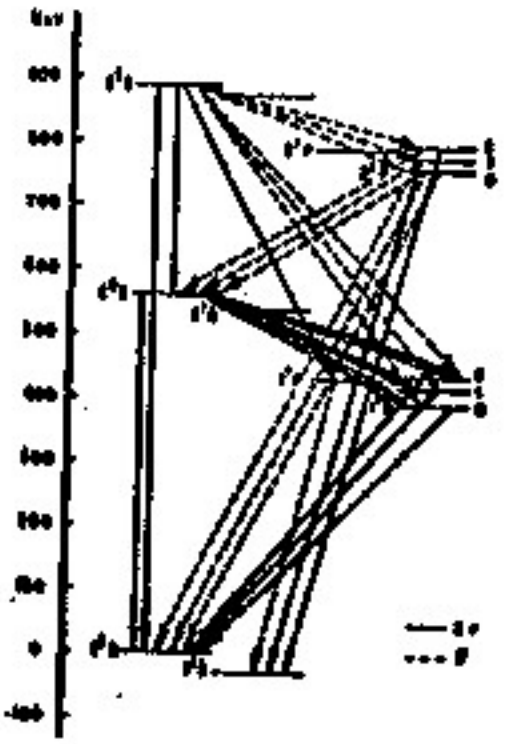

SEARCH FOR

$\Upsilon(2s) \to \Upsilon_b \gamma$

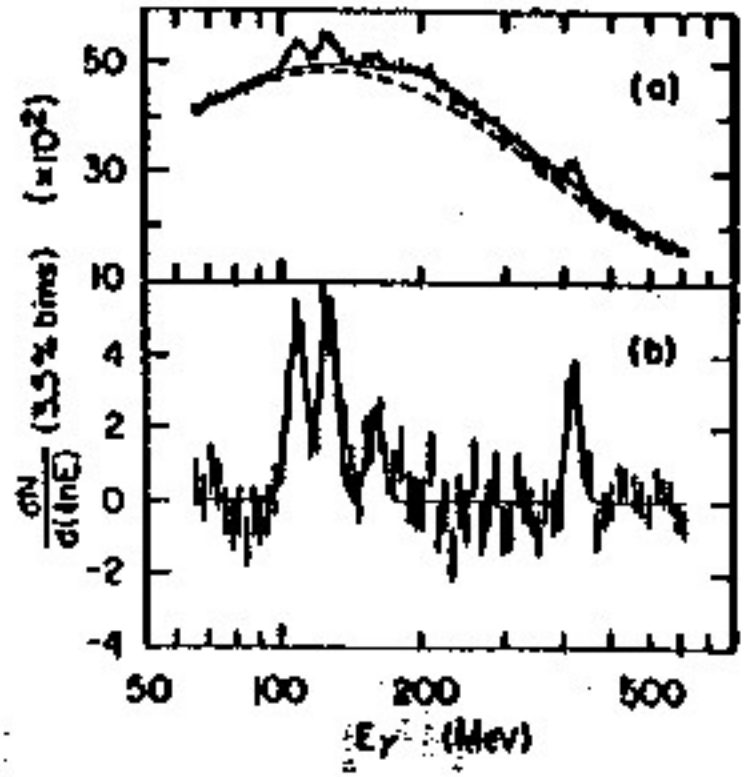

$\frac{\sigma_E}{E} \approx \frac{2.8\,\%}{\sqrt[4]{E}}$

E [GeV]

CLEO

e^+e^- AT CESR

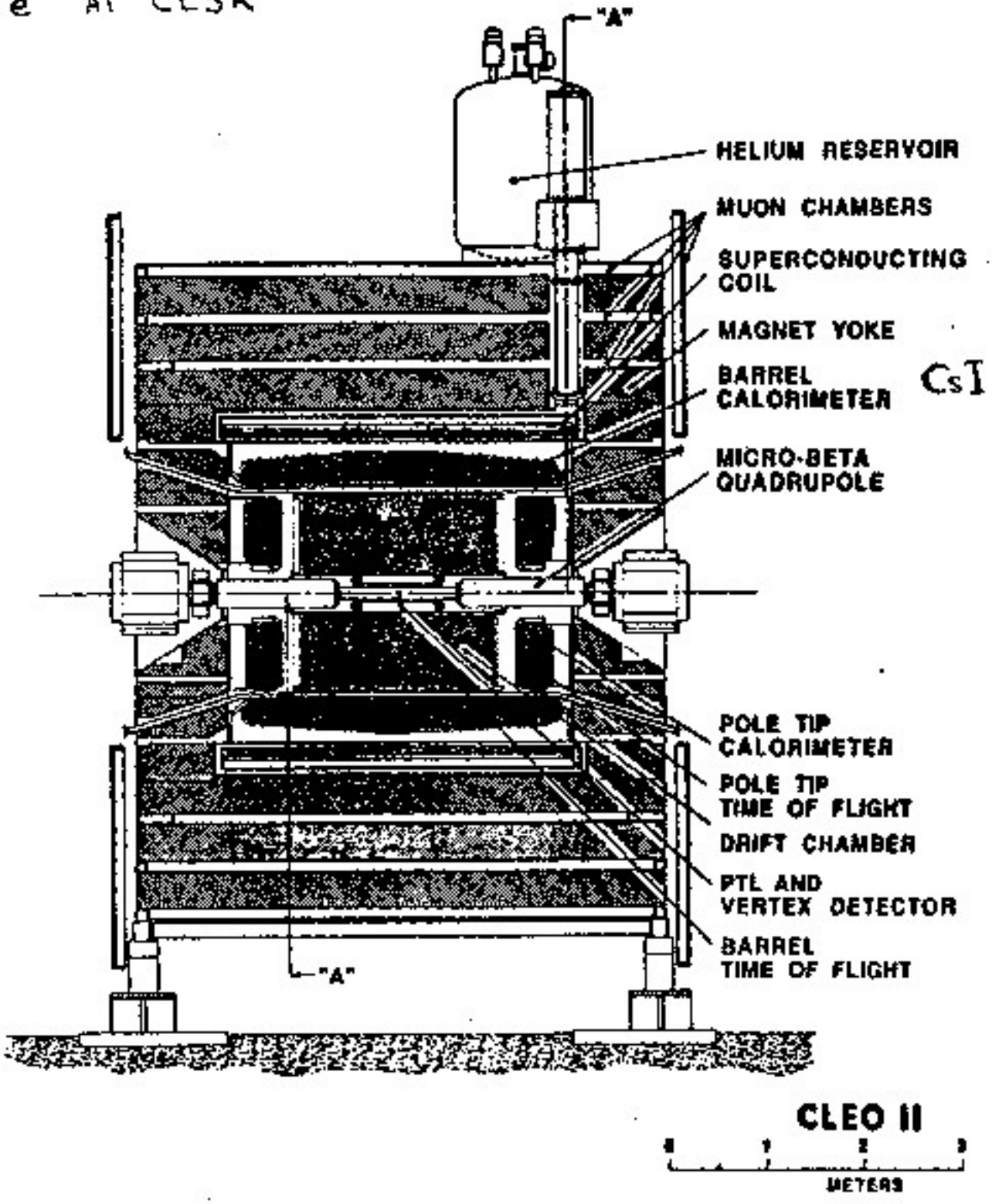

$J/\psi \rightarrow e^+e^-$, $\mu^+\mu^-$

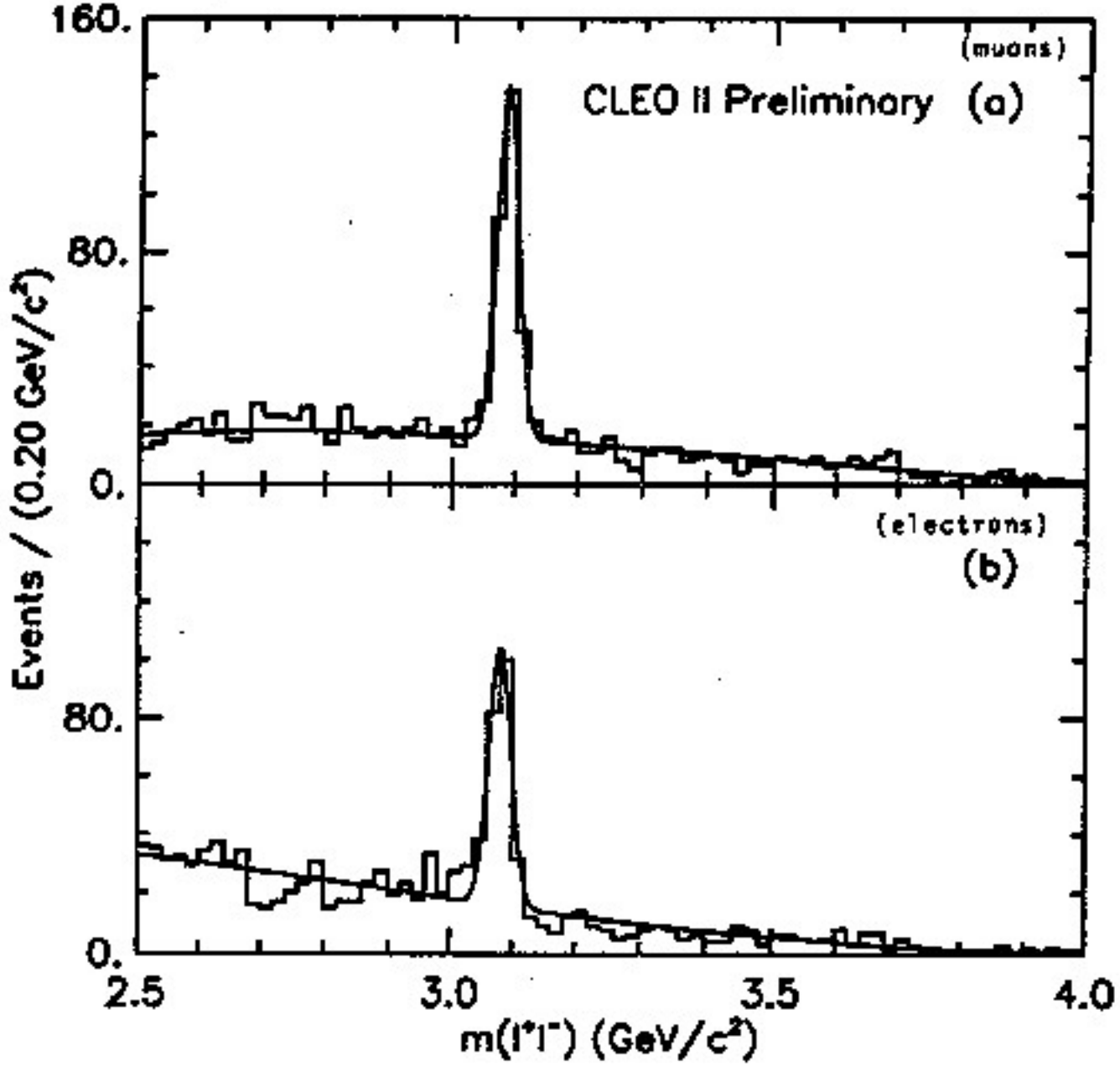

$\eta \rightarrow \gamma\gamma$

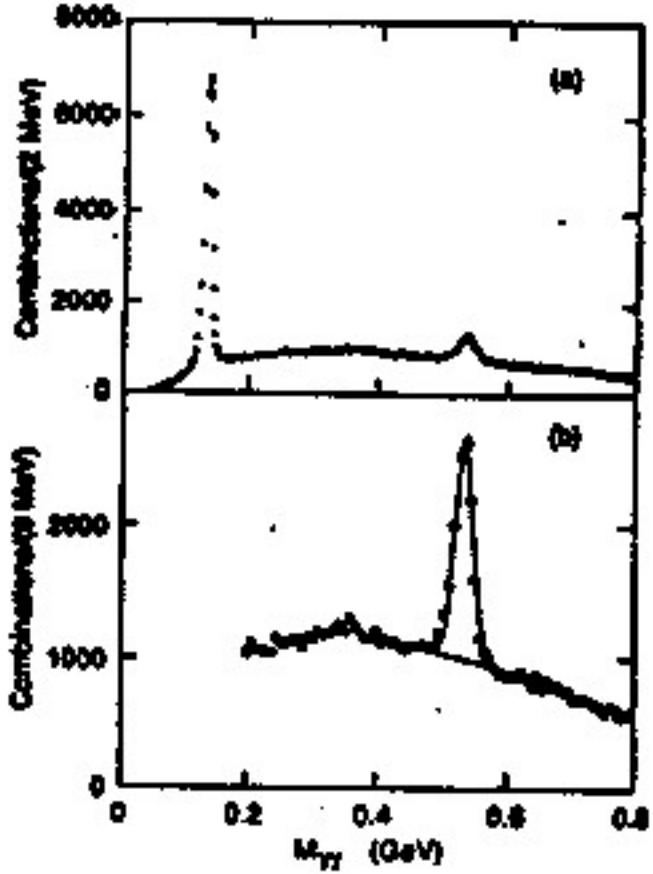

CLEO MASS SPECTRA WITH CsI CALORIMETER

BaF_2 CALORIMETER

GEM AT SSC†

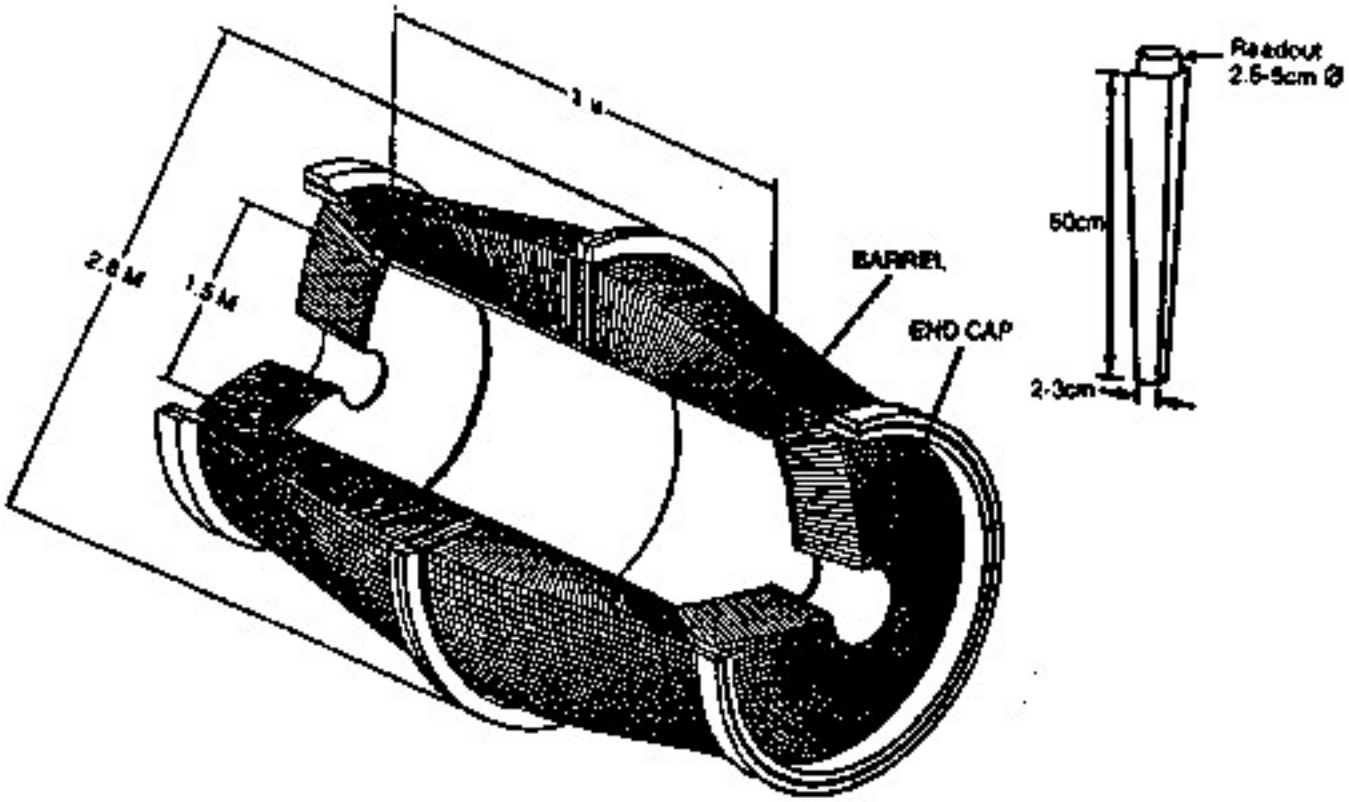

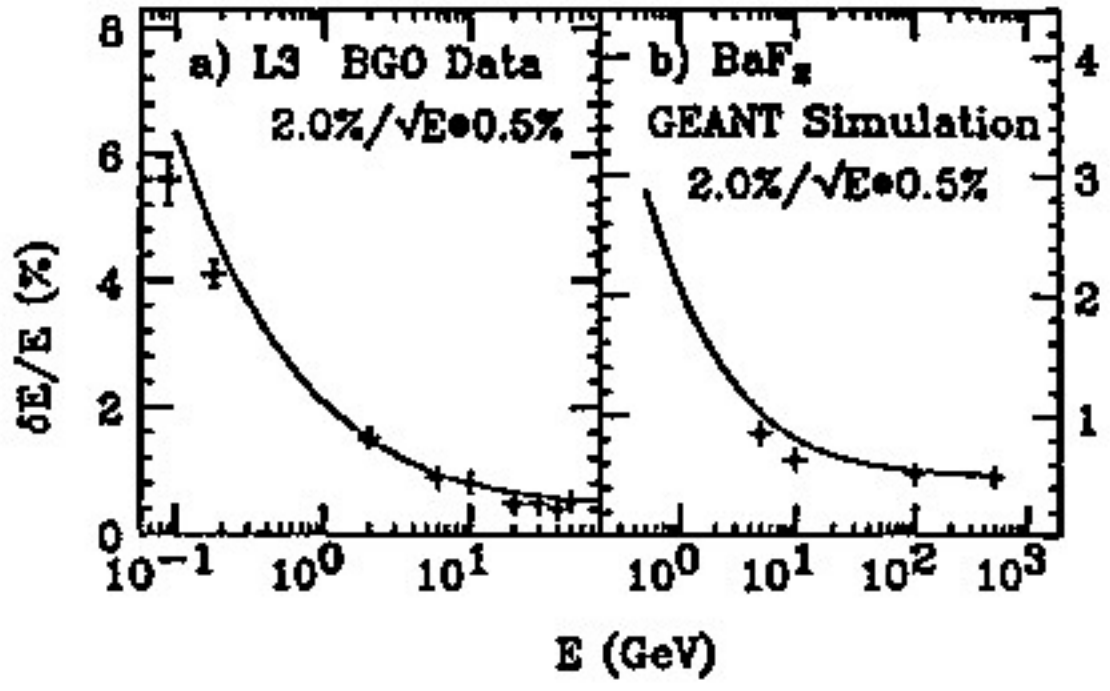

SHOWER LEAKAGE

THE LONGITUDINAL CONTAINMENT CAN BE PARAMETRIZED AS

$$L(98\%) = t_{MAX} + 4\,\lambda_{ATT}$$

λ_{ATT} = $\underset{\text{MINIMUM}}{\text{ATTENUATION}}$ LENGTH FOR γ's $\approx (3.4 \pm 0.5)\,X_0$

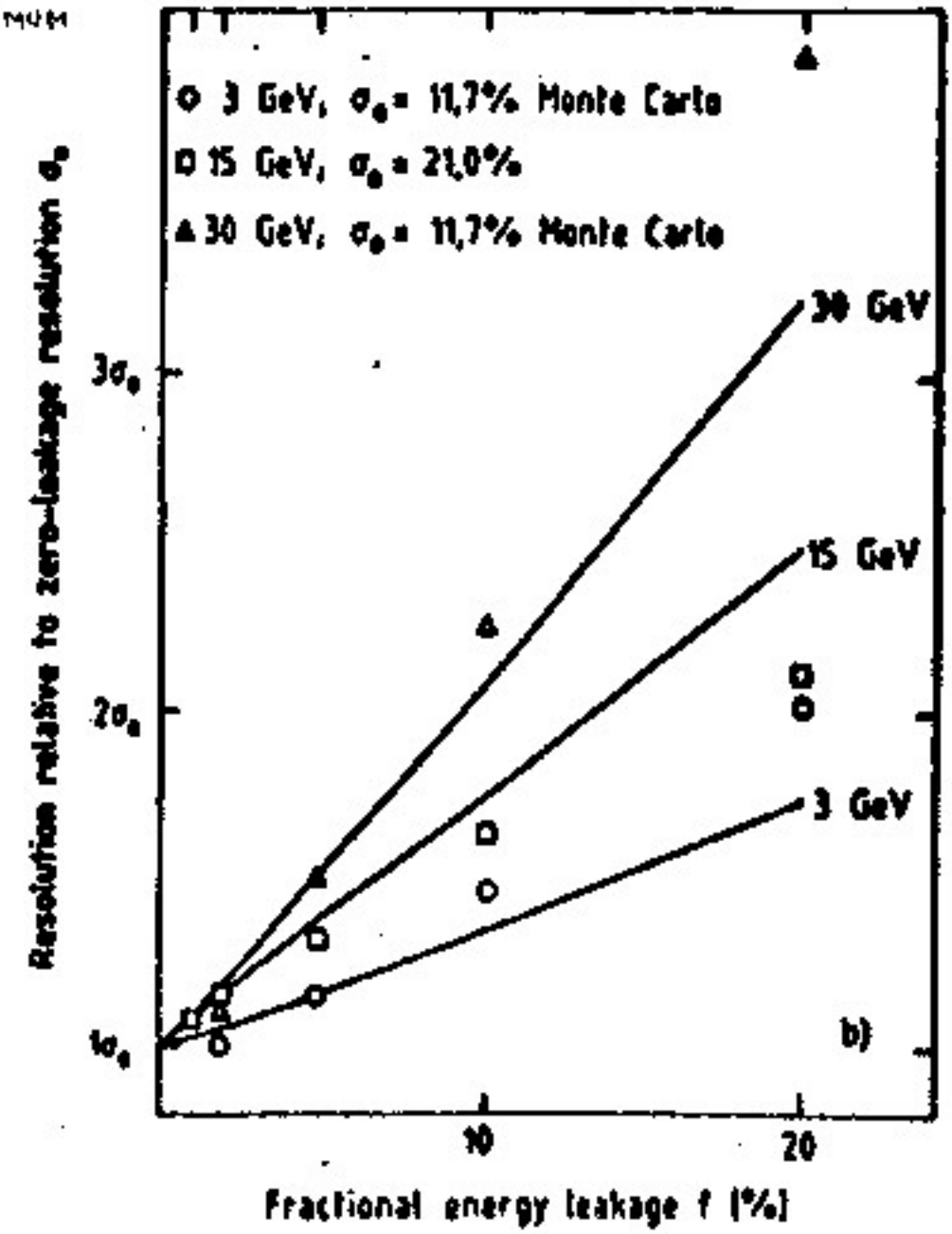

CHANGE IN RESOLUTION: $\dfrac{\sigma_E}{E} \approx \left.\dfrac{\sigma_E}{E}\right|_{f=0} \cdot \left[1 + 2\sqrt{E}\,f\right]$

Properties and Performances of Homogeneous e.m. Shower Detectors

Detector type	NaI(Tl)	CsI(Tl)	BaF_2	$Bi_4Ge_3O_{12}$	Scintillating glass	Lead glass 55% PbO + 45% SiO_2	$Tl(HCO_2)$-liquid 'Heliums'	Liquid argon
Radiation length (cm)	2.59	1.86	2.1	1.12	~ 4	2.36	~ 1.9	14
Density (g/cm^3)	3.7	4.51	4.9	7.13	~ 3.5	4.08	~ 4.3	1.4
Detection mechanism	Scintillation	Scintillation	Scintillation (20% around 210 nm, 80% around 310 nm)	Scintillation	Scintillation	Cherenkov light	Cherenkov light	Ionization charge
Energy resolution (E in GeV)	$\sim 0.015\ E^{-1/2} \oplus 1$ $\oplus\ 0.015\ E^{-1/4} \oplus 1$	Comparable to NaI(Tl)	Comparable to NaI(Tl)	Comparable to NaI(Tl)	$\sim 0.002\ E^{-1/2}$	$\sim 0.04\ E^{-1/2}$	Comparable to lead glass	$\geq 0.02\ E^{-1/2}$
Principal limitation to $\sigma(E)$	Shower fluctuations optically non-uniform	Similar to NaI(Tl)	Light collection non-uniformities	Similar to NaI(Tl)	Photon statistics	Photon statistics	Photon statistics	Effect of shower fluctuation on electron collection
Signal[a] (photo-el/GeV)	$\sim 10^7$	$\sim 5 \times 10^6$	$\sim 10^6$	$\sim 10^6$	Few $\times 10^5$	10^5	$\leq 10^5$ (?)	$\leq 2 \times 10^6$
Characteristic time (ns)	250	900	0.6 ; 300	300	~ 70	~ 20	~ 20	≥ 100
Rad. damage at appr. dose[b] (Gy)	< 10	< 10	$\sim 10^2$	~ 10	$\sim 10^2$	$\sim 10^2$	$\geq 10^4$	Not measured: expected to be very large
Mechanical stability	Hygroscopic, fragile	Very good	Good	Good	Very good	Very good	Toxic liquid	Cryogenic liquid
References	[54, 55, 57]	[72]	[73, 74]	[61–63]	[64, 65]	[66–69]	[75]	[76–79]

a) Values are approximate, and depend on spectral matching between light source and photon detector.
b) Values are guidelines only and very substantially depending on experiment and monitoring conditions.

SAMPLING CALORIMETERS

ONLY A FRACTION OF THE DEPOSITED ENERGY IS ACTUALLY DETECTED, HENCE A LOSS IN ENERGY RESOLUTION

$\frac{\sigma_E}{E} \approx (10\text{-}20)\%/\sqrt{E}$

But!

THERE ARE GAINS IN

COSTS
SIZES
RATES
GRANULARITY
RADIATION HARDNESS
⋮

IONIZATION TECHNIQUES

FOR SAMPLING CALORIMETERS

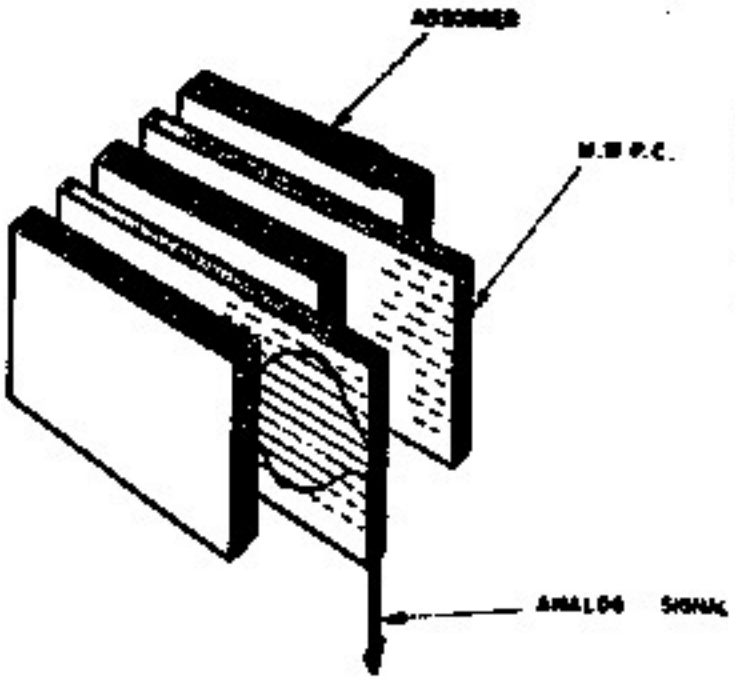

MULTI-WIRE PROPORTIONAL COUNTER

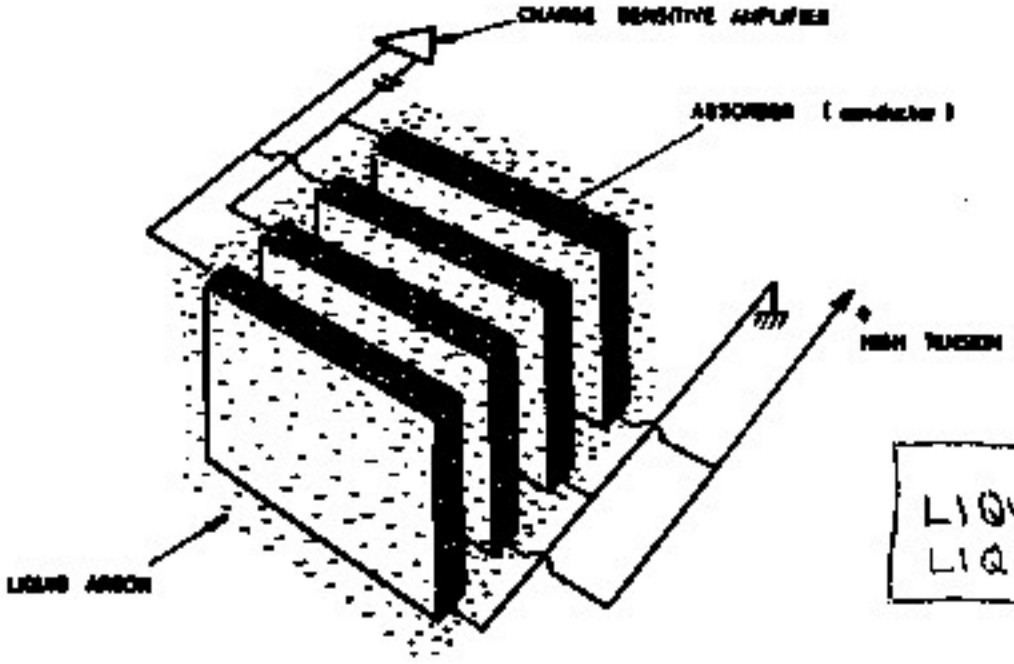

LIQUID ARGON
LIQUID KRYPTON

INTRINSIC SAMPLING FLUCTUATIONS

CONSIDER NOW THE NUMBER OF CROSSINGS, GIVEN THE DISTANCE d BETWEEN ACTIVE LAYERS:

$$N_x = \frac{L}{d} = \frac{E}{E_c d} = \frac{E}{\Delta E}$$

ΔE → LOST PER LAYER

FROM WHICH ONE MAY DERIVE

$$\left.\frac{\sigma_E}{E}\right|_{\text{SAMPLING}} = \frac{\sigma(N_x)}{N_x} = \frac{1}{\sqrt{N_x}} = 3.2\% \cdot \left(\frac{\Delta E\,[\text{MeV}]}{E\,[\text{GeV}]}\right)^{\frac{1}{2}}$$

ADDING IN MULTIPLE SCATTERING, η-CUTOFF:

$$\left.\frac{\sigma_E}{E}\right|_{\text{SAMPLING}} \gtrsim 3.2\% \cdot \left(\frac{\Delta E\,[\text{MeV}]}{F(\gamma_{E_c}) \cos\left(\frac{24}{\pi E_c}\right) E\,[\text{GeV}]}\right)^{\frac{1}{2}}$$

AND LANDAU FLUCTUATIONS FOR THIN DETECTORS

$$\left.\frac{\sigma_E}{E}\right|_{\text{LANDAU}} \approx \frac{3}{\sqrt{N_x \cdot \ln\left(1.3 \times 10^4 \cdot \Delta E\,[\text{MeV}]\right)}}$$

IONIZATION TECHNIQUES EXAMPLES

1 GeV ELECTRONS

Pb / MWPC CALORIMETER

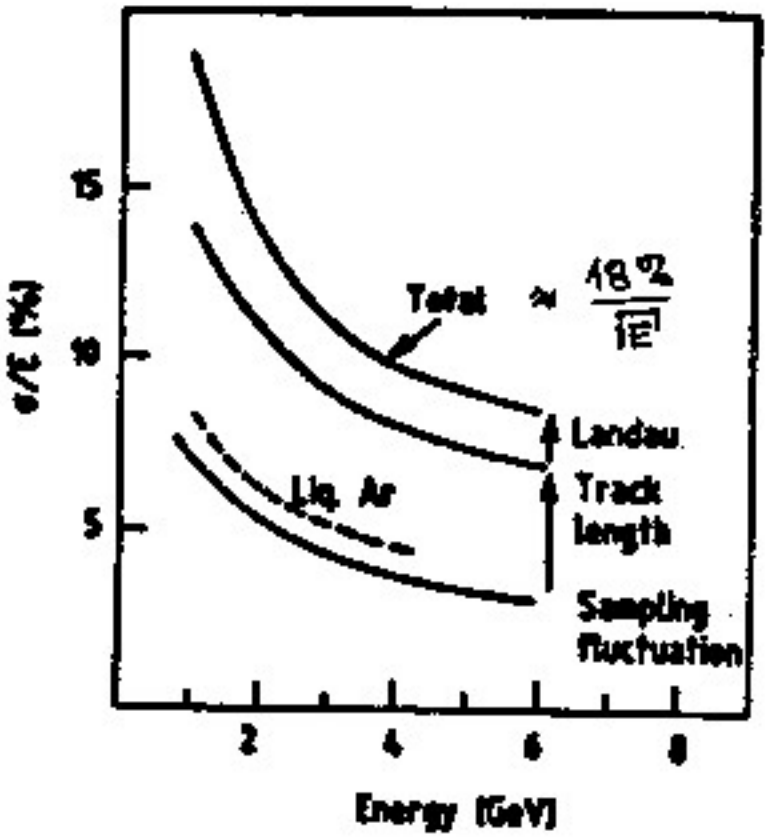

Fe / L.Ar CALORIMETER

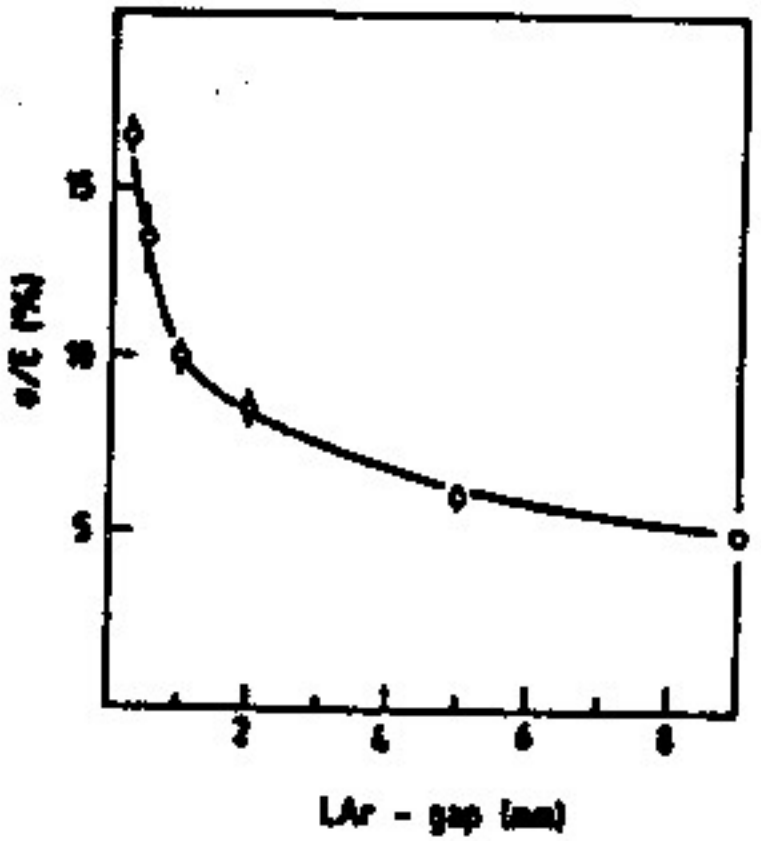

Measured and Estimated Performance of Electromagnetic Sampling Calorimeters

Device passive/active (mm)	Al/scint. 89/30	Fe/LAr 1.5/2.0	Cu/scint. 5/2.5	W/Si detector 7.0/0.2	Pb/Ar/CO_2 at NTP 2.0/10.0	U/scint. 1.6/2.5
Energy resolution measured at 1 GeV(%)	20	7.5	13.0	25.0	≤ 20.0	11.0
η (MeV)	3.0	0.7 (?)	0.7 (?)	0.7 (?)	≤ 0.6 (?)	0.7 (?)
$F(\xi)^{-1/2}$	1.16	1.10	1.10	1.18	1.18	1.20
$(\cos\theta)^{-1/2}$	1.00	1.03	1.03	1.27	1.36	1.51
σ^{sample}	23	4.8	9.2	19.1	8.2	10.6
σ_{Landau}	3.8	1.0	1.0	4.5	8.70	1
$\sigma_{path\ length}$		5.7	6	17.5	13.0	6 (?)
$\sigma_{estimated}$	23	7.5	10.0	25.9	17.7	12.2

SCINTILLATION TECHNIQUES

FOR SAMPLING CALORIMETERS

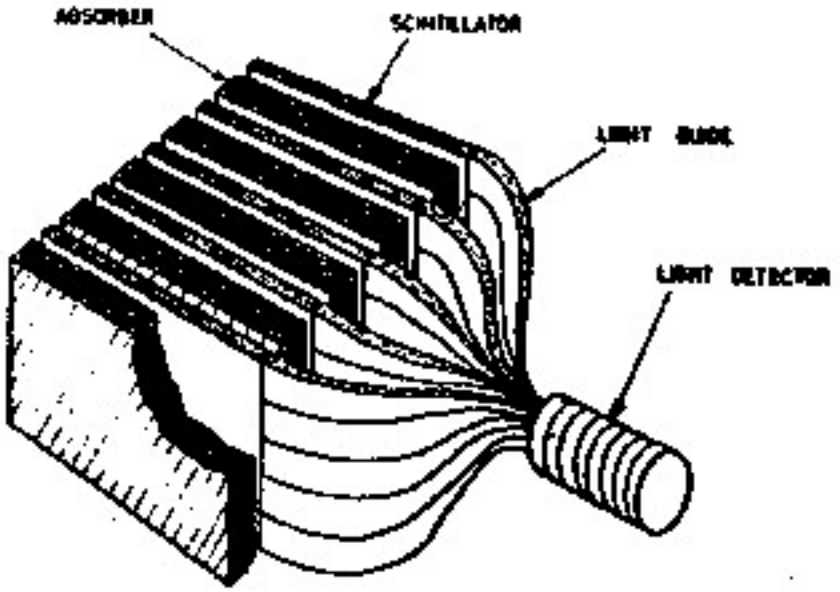

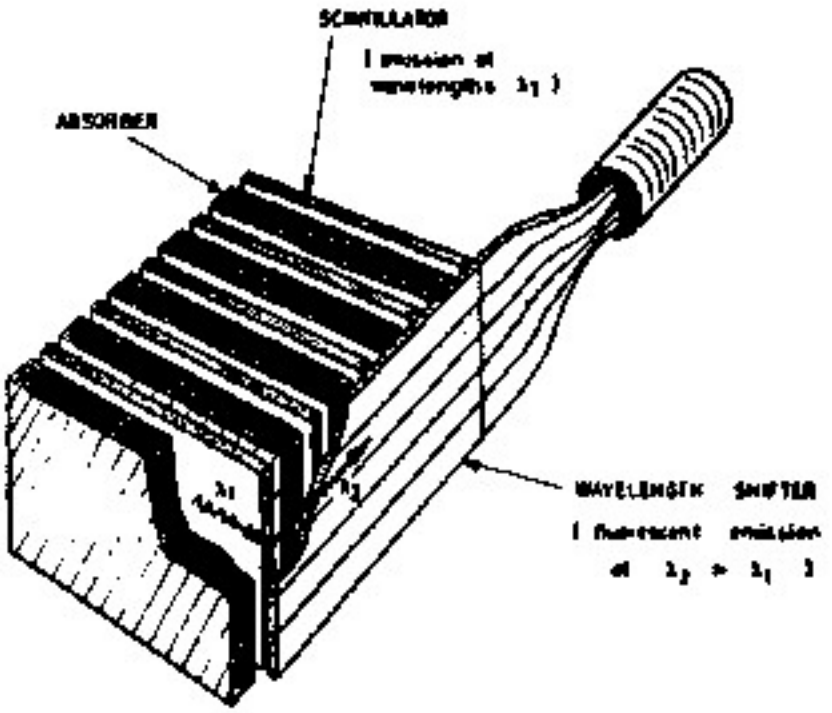

WLS = WAVELENGTH SHIFTER READOUT

ARGUS CASE

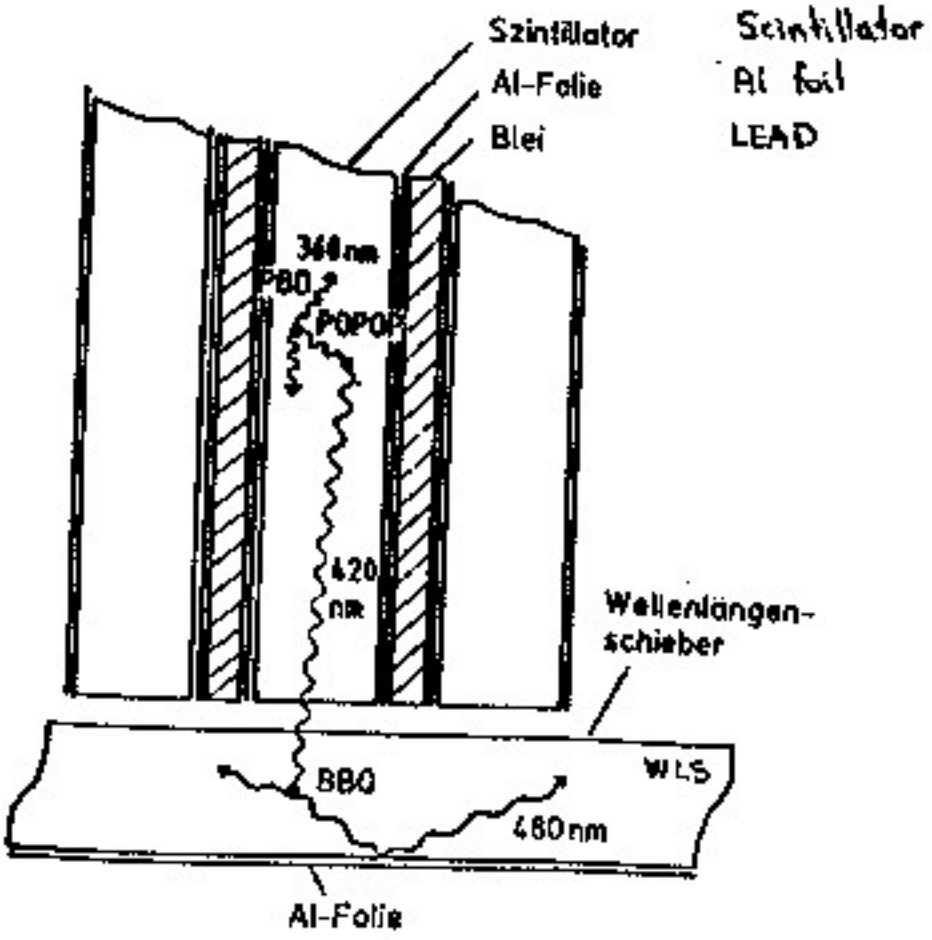

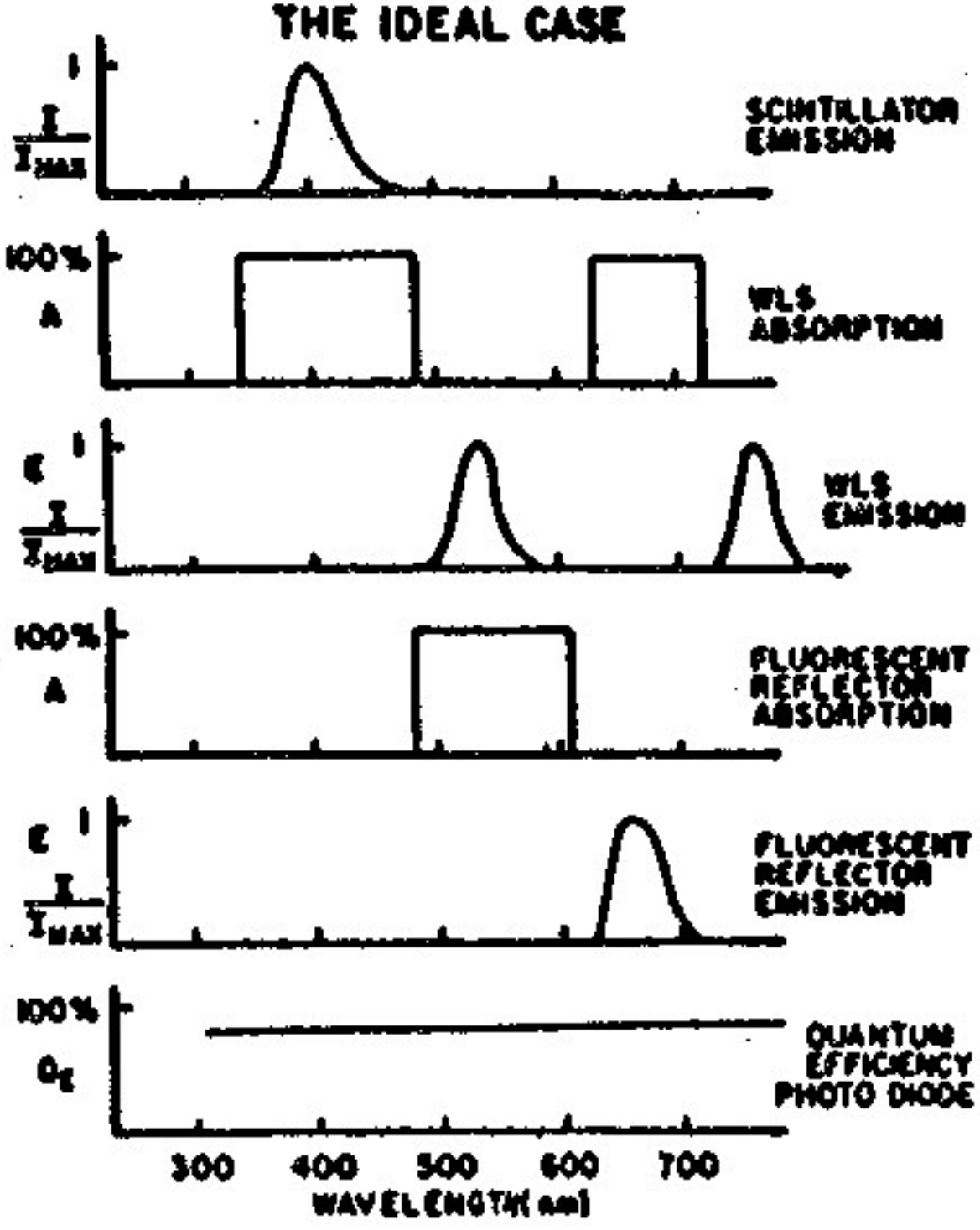
THE IDEAL CASE
I
I/I MAX
SCINTILLATOR EMISSION
100%
A
WLS ABSORPTION
ε
I
I/I MAX
WLS EMISSION
100%
A
FLUORESCENT REFLECTOR ABSORPTION
ε
I
I/I MAX
FLUORESCENT REFLECTOR EMISSION
100%
Qε
QUANTUM EFFICIENCY PHOTO DIODE
300
400
500
600
700
WAVELENGTH(nm)

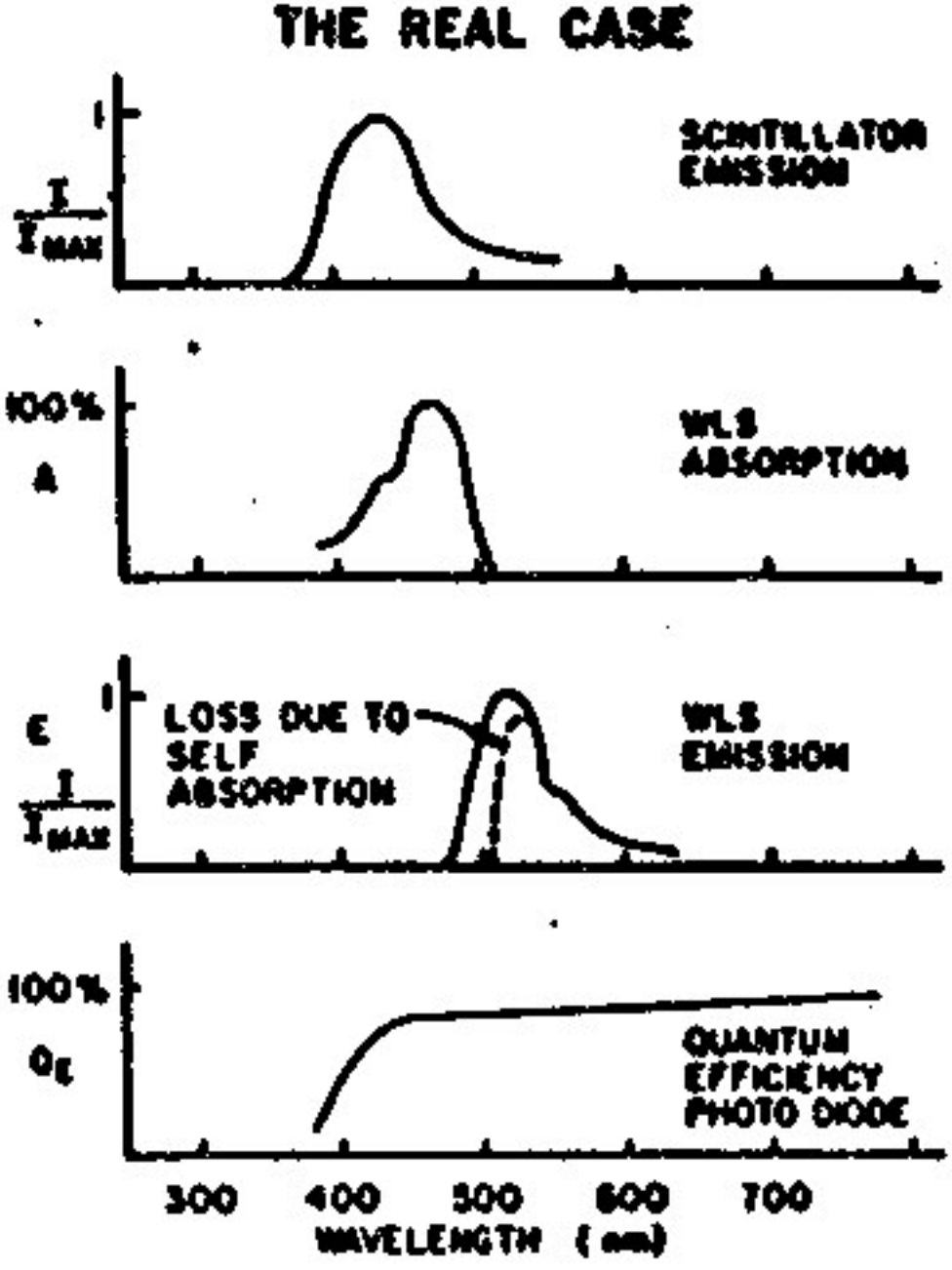
THE REAL CASE
I
I/I MAX
SCINTILLATOR EMISSION
100%
A
WLS ABSORPTION
ε
I
I/I MAX
LOSS DUE TO SELF ABSORPTION
WLS EMISSION
100%
Qε
QUANTUM EFFICIENCY PHOTO DIODE
300
400
500
600
700
WAVELENGTH (nm)

Temporal Response of Readout Systems

Calorimeter system	Occupation time (ns)	Pulse width (integration) (ns)	Timing resolution σ (ns)	Radiation resistance
Metal/scintillator with WLS readout	50	50	2.5 for few-GeV deposit; better at higher energy, if not limited by PM	Depends on scintillator, dose rate, environment; $> 10^3$ Gy appear achievable [10Z].
^{238}U/scintillator with fast WLS readout	~ 100	100	2.5	As above
Metal/fast scintillator with fast WLS readout	$\leq$ 20	$\leq$ 20	< 2 (?)	
Metal/proportional or saturated gas-gain readout	50–100	100–200 bipolar shaping	$\leq$ 10	Adequate for chamber; lifetime of on-detector electronics may be a limitation; readout elements need to be shielded from U radioactivity.
^{238}U/proportional or saturated gas-gain readout	$\geq$ 100	$\geq$ 200 bipolar shaping	$\leq$ 10	
Metal/LAr ion chamber	~ 200 per 1 mm gap	2λ = 400 bipolar shaping	~ 2 for few-GeV deposit	Lifetime of on-detector electronics may be a limitation
Metal/LAr–CH_4 ion chamber	~ 100 per 1mm gap	$2\lambda \leq$ 200	$\leq$ 2 for few-GeV deposit	NB: shorter pulse width (2λ) possible the expense of signal/noise $\propto \lambda^{\alpha}$, at $\alpha \sim 1$.

CALORIMETER TRIGGER SIGNAL EXTRACTION

SPLITTING THE UCAL PM ANODE SIGNAL

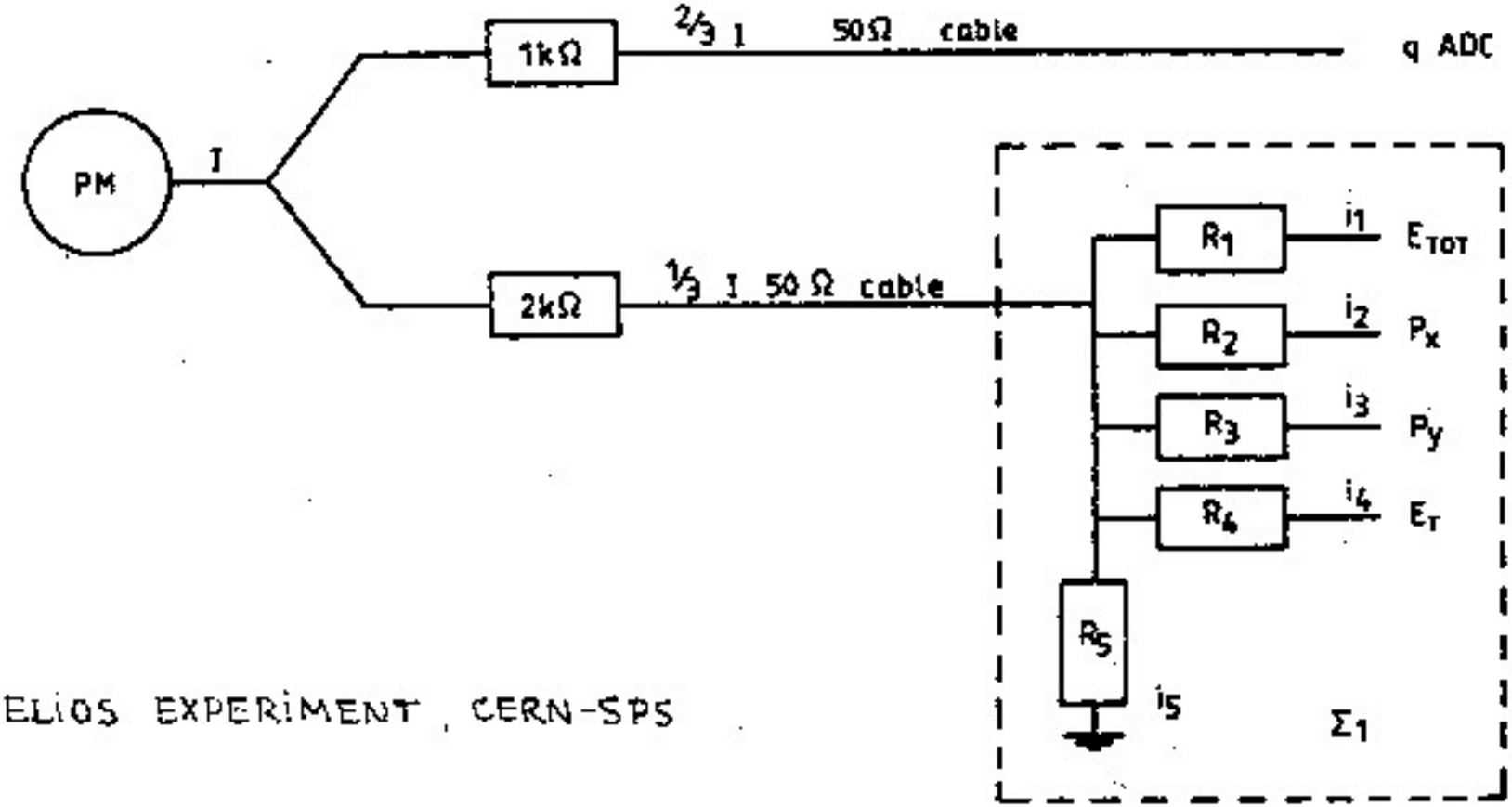

HELIOS EXPERIMENT, CERN-SPS

CALORIMER TIME INFORMATION

IT IS USE FUL IN THE TRIGGER TO REJECT BACKG

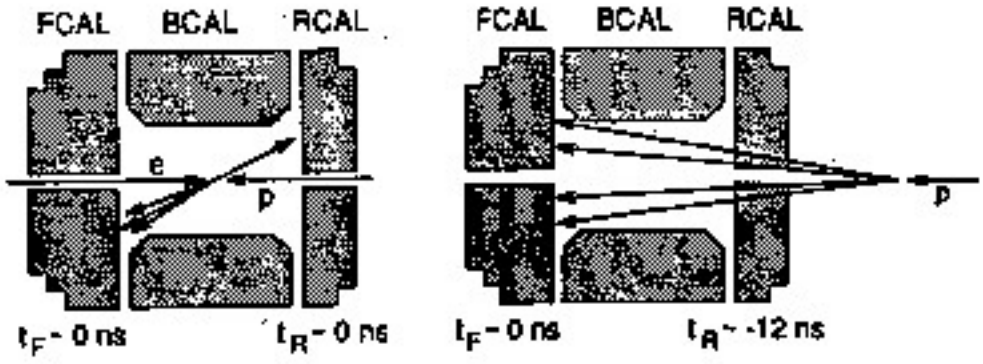

e-p EVENT

BACKGROUND EVENT

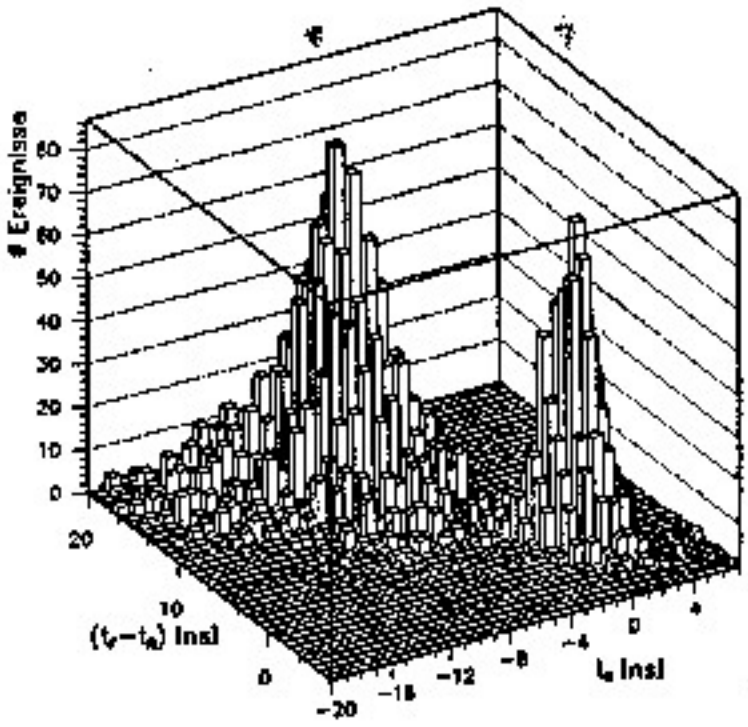

CALORIMETER INFORMATION

CLUSTERING

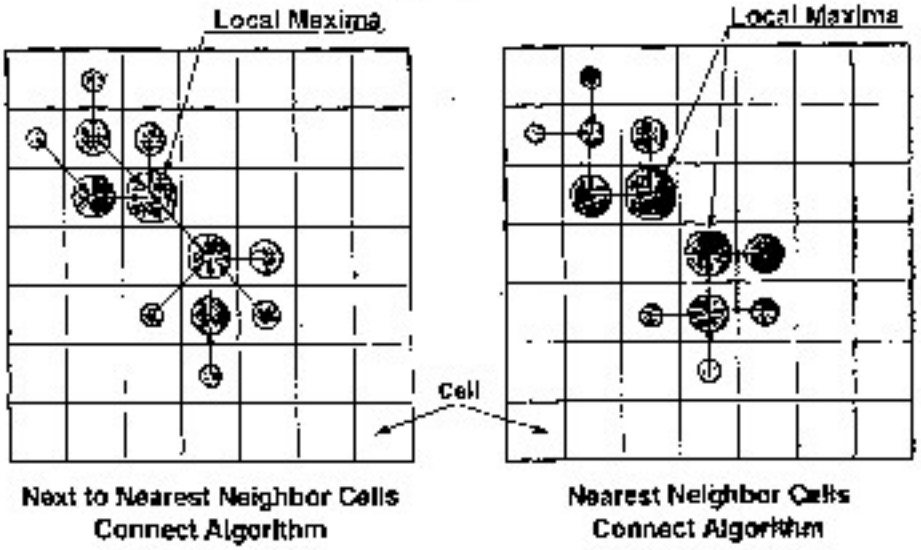

MATCHING

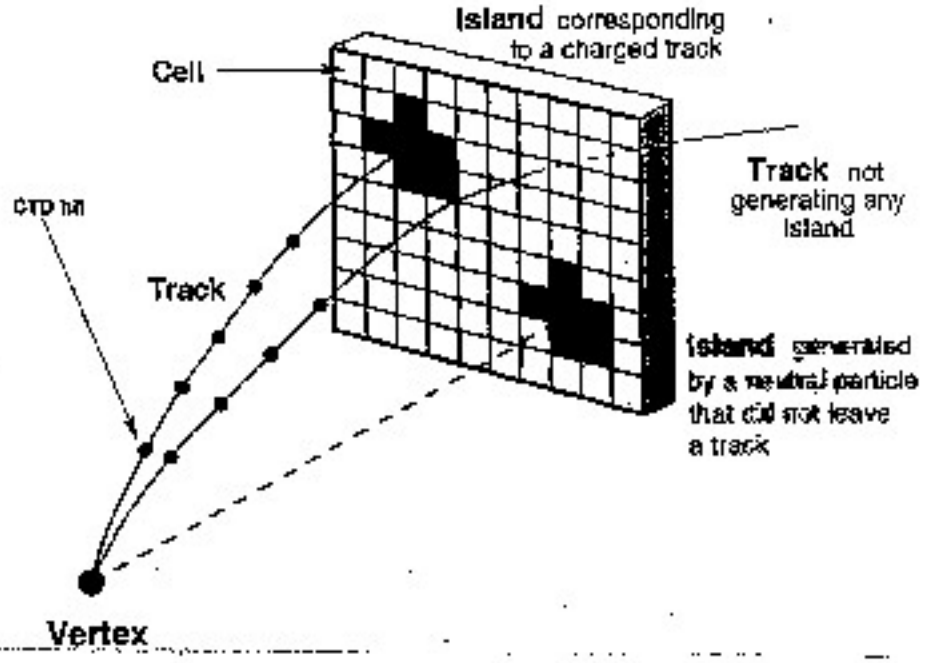

CONSIDERABLE IMPROVEMENT ON TRACKING ALONE

HADRONIC SHOWERS

THE STRONG INTERACTION IS HEAVILY INVOLVED IN THE HADRONIC CASCADE PROCESSES:

- THERE ARE MANY MORE TYPES OF SECONDARY PARTICLES PRODUCED
- THROUGH THEIR FAST ELECTROMAGNETIC DECAY MODES, π^0 AND η MESONS (THE LIGHTESTS) PRODUCE ELECTROMAGNETIC SHOWERS WITHIN THE PURELY HADRONIC ONE.
- DISRUPTION OF NUCLEI LEADS TO "INVISIBLE" LOSSES IN BINDING ENERGIES AND GENERATION OF LARGE NUMBERS OF LOW-ENERGY NUCLEONS

THE SCALING VARIABLE FOR THE HADRONIC SHOWER SIZES IS THE INTERACTION LENGTH λ, PARAMETRIZING THE AVERAGE ENERGY LOSSES (as X_0 for e.m. showers)

'ELEMENTARY PROCESS' IN A HADRON SHOWER

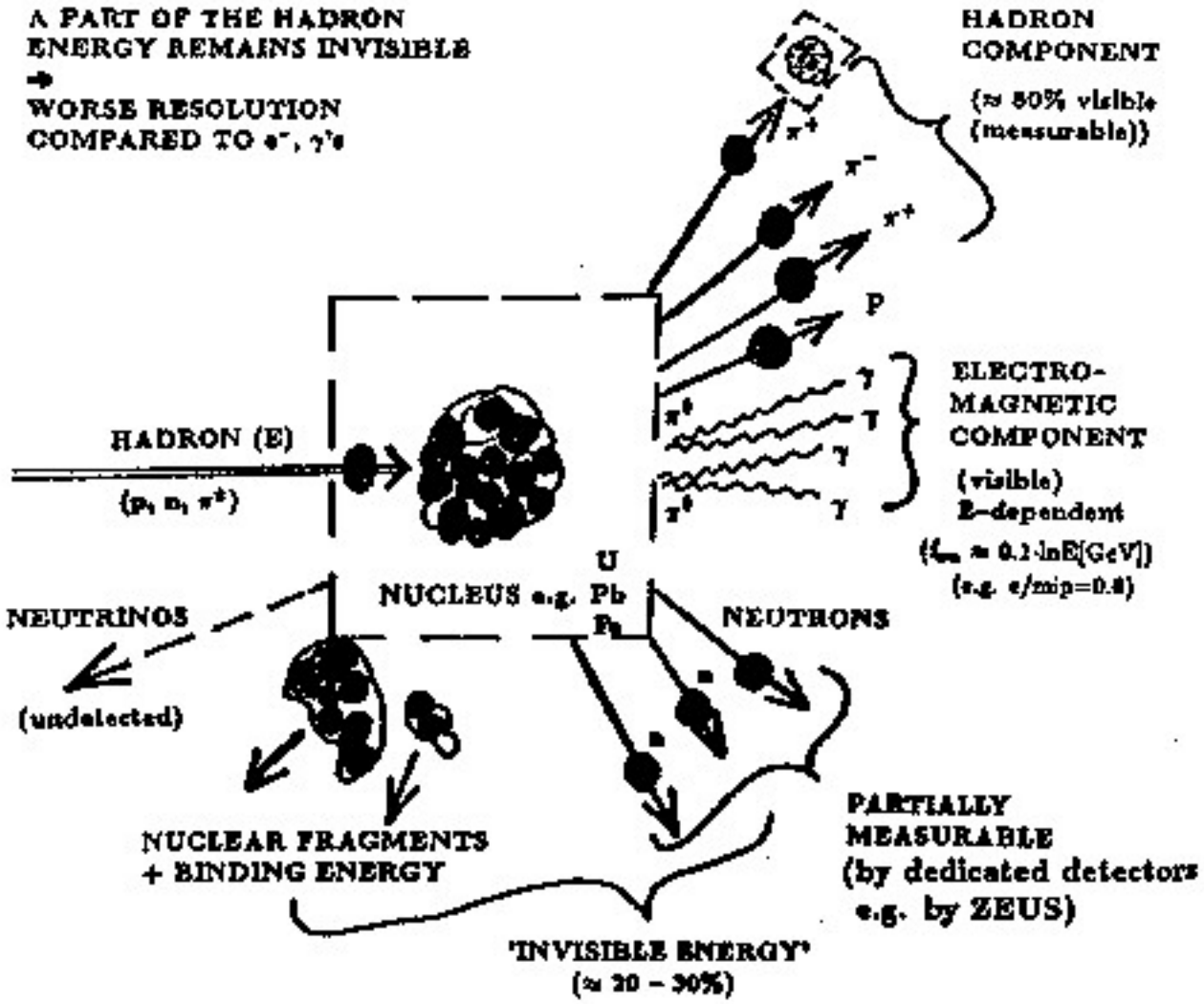

'Elementary physical process' in a hadron shower.

Reaction	Properties	Influence on energy resolution	Characteristic time (s)	Characteristic length (g/cm²)
Hadron production	Multiplicity ≈ $A^{0.1} \ln s$	π^0/π^+ ratio Binding energy loss.	10^{-23}	Abs. length $\lambda = 35A^{1/3}/\rho$
Nuclear de-excitation	Evaporation energy ≈ 10% Binding energy ≈ 10% Fast neutrons ≈ 40% Fast protons ≈ 40%	Binding energy loss. Poor or different response to n, charged particles, and γ's.	10^{-16}–10^{-13}	Fast neutrons $\lambda_n \approx 100$ Fast protons $\lambda_p \approx 20$
Pion and muon decays	Fractional energy of μ's and ν's ≈ 5%	Loss of ν's partial loss of μ's	10^{-8}–10^{-6}	$\gg \lambda$
Decay of c, b particles produced in multi-TeV cascades	Fractional energy of μ's and ν's at percent level	Loss of ν's, part. μ's Tails in resolution function.	10^{-12}–10^{-10}	$\ll \lambda$

MEASUREMENT OF LONGITUDINAL SHOWER PROFILE

FOR THE WA78 - ZEUS - H1 TESTS

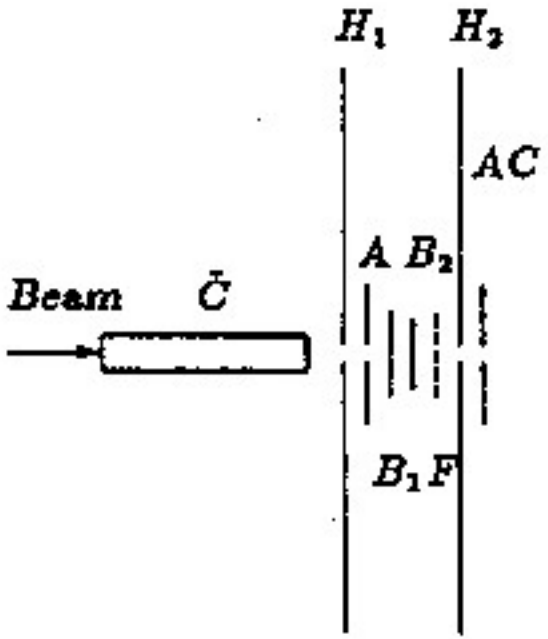

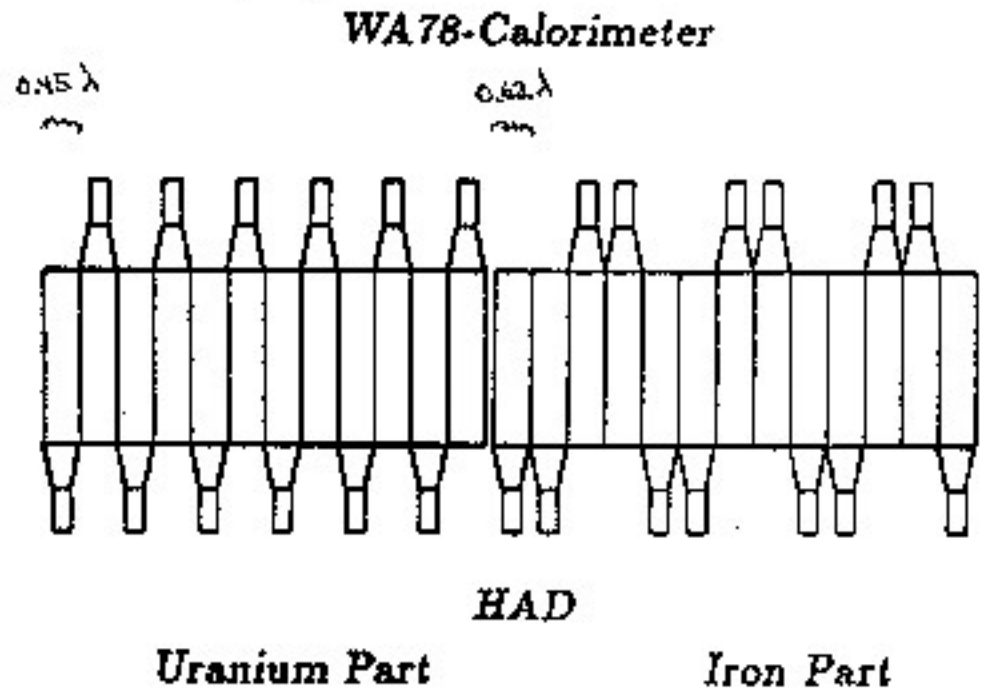

ENERGY DEPOSITION IN SINGLE MODULES

WA78-ZEUS-H1 TESTS

20 GeV

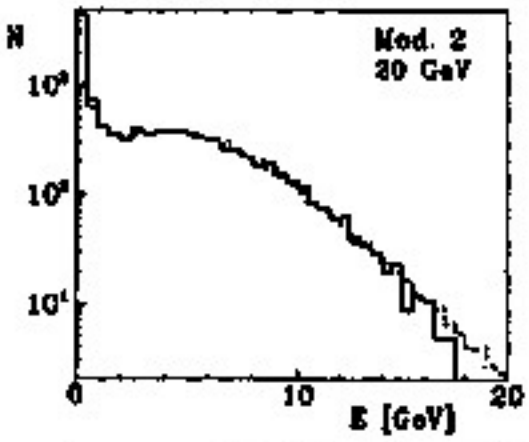

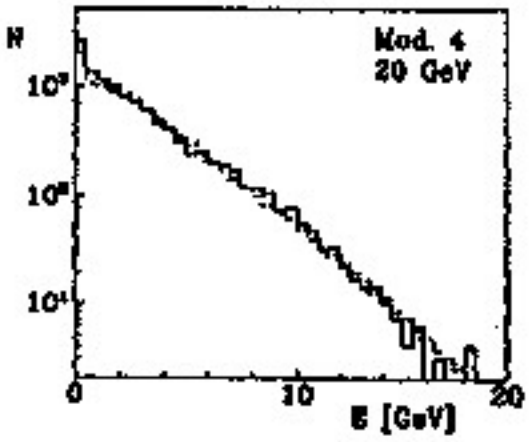

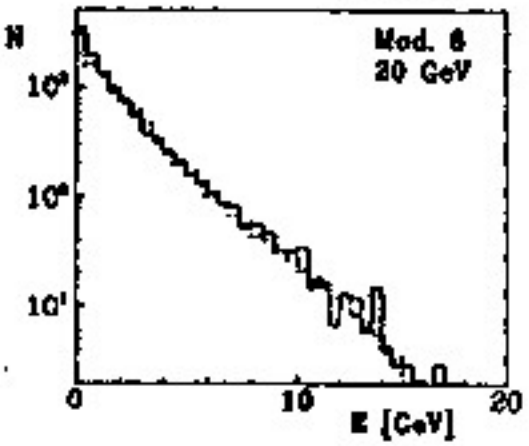

210 GeV

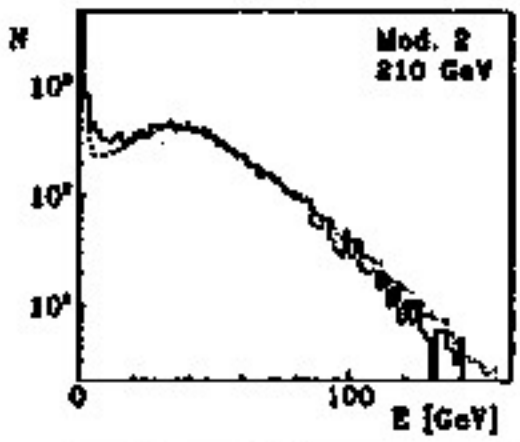

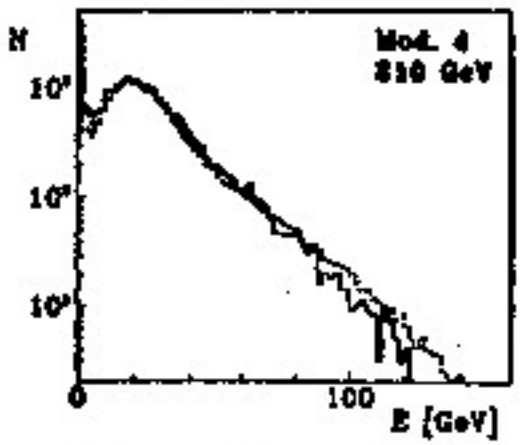

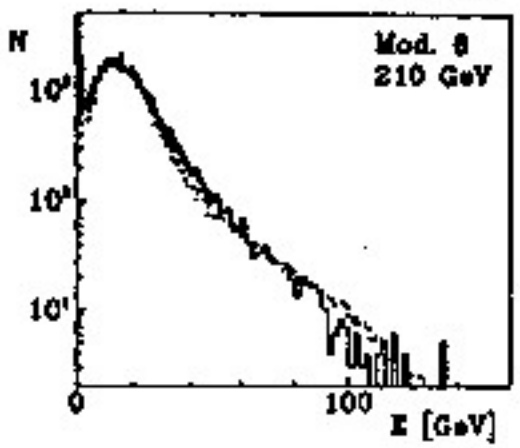

TOTAL ENERGY DEPOSITION

WA78 - ZEUS - H1 TESTS

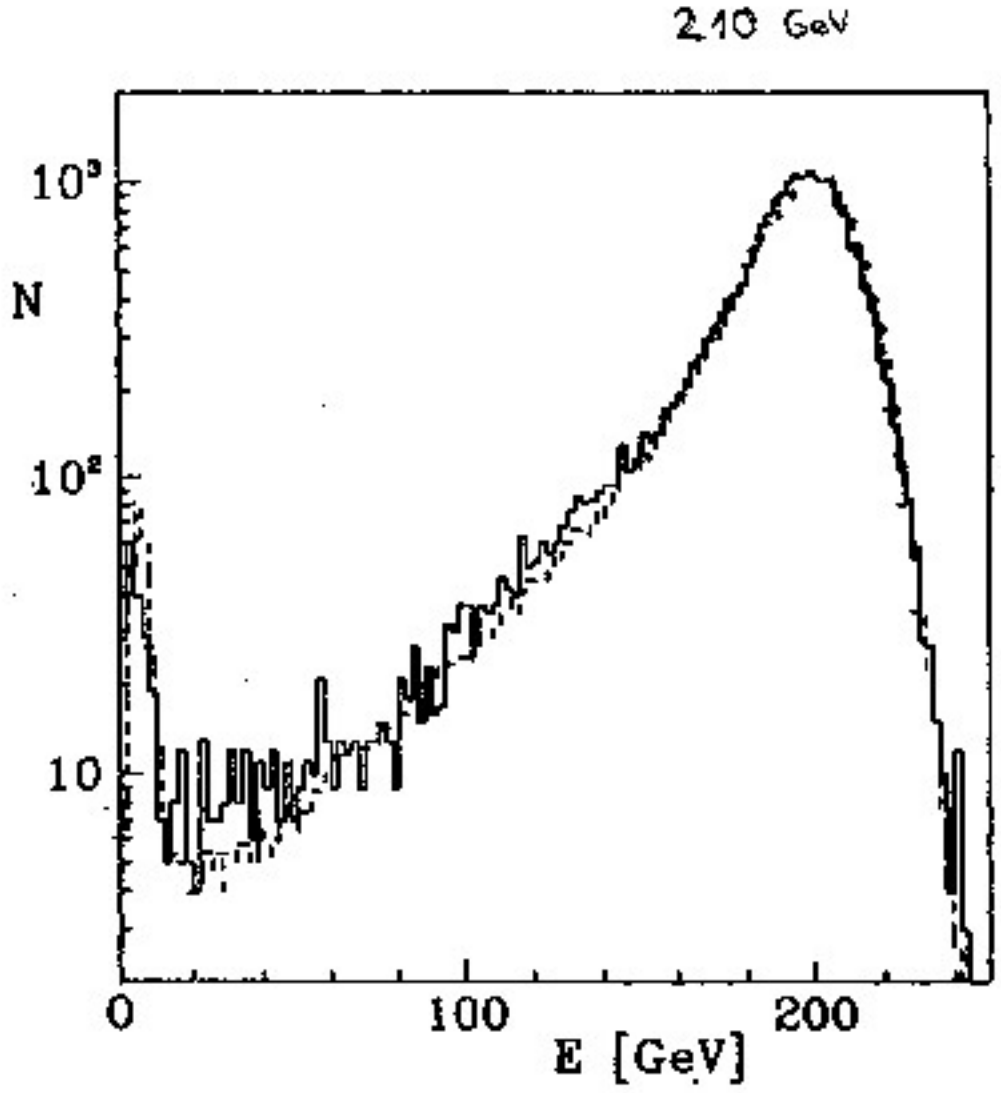

LONGITUDINAL SHOWER PROFILE FOR HADRONIC CASCADES

(VISIBLE ENERGY)

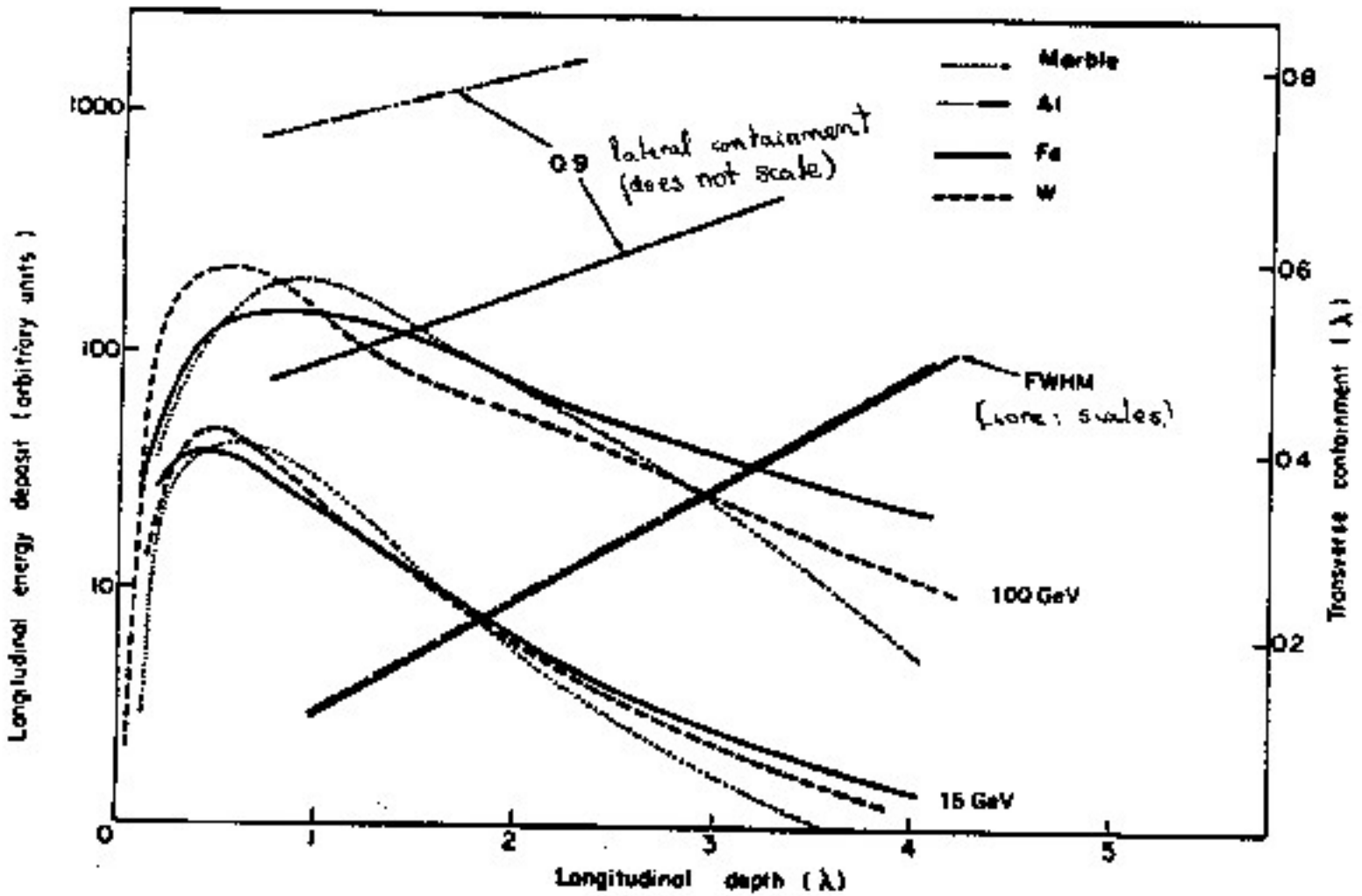

λ : GOOD APPR. SCALE LONGITUDINALLY BUT NOT LATERALLY (EXCEPT FOR SHOWER CORE)

LONGITUDINAL HADRONIC SHOWER PROFILES IN URANIUM

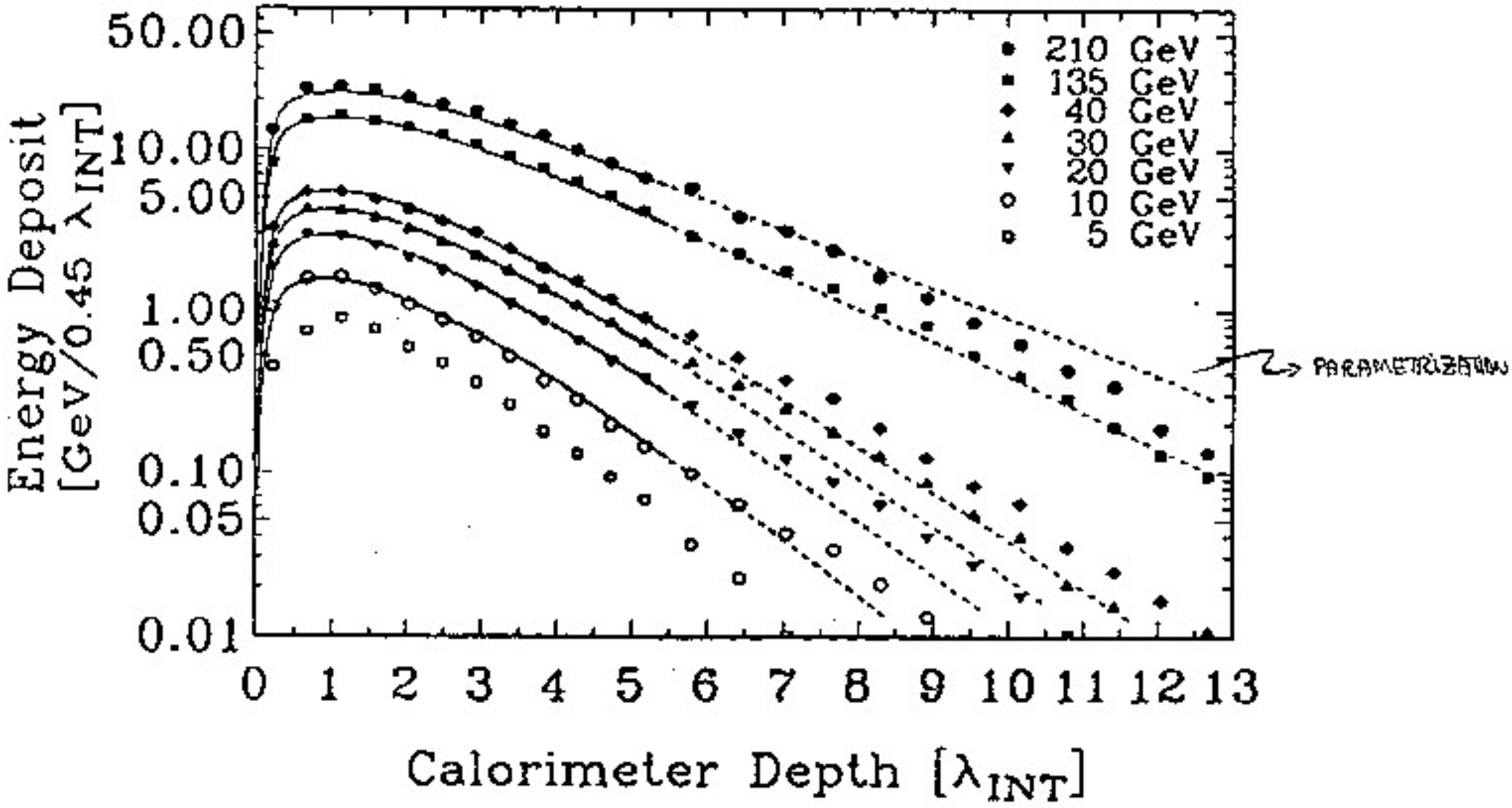

HAD. SHOWER MODEL

TO THE FIRST ORDER, TAKE A PARAMETRIZATION OF THE TYPE USED FOR E.M. SHOWERS, BUT WITH TWO TERMS:

- E.M. COMPONENT (π^0)
- PURELY HADRONIC COMPONENT

with $t_E \doteq x/X_0$ and $t_H \doteq x/\lambda$

$$\frac{dE}{dx} = E_0 \left\{ c \, \frac{(b_E t_E)^{a_E - 1} e^{-b_E t_E}}{\Gamma(a_E)} + (1-c) \, \frac{(b_H t_H)^{a_H - 1} e^{-b_H t_H}}{\Gamma(a_H)} \right\}$$

EM. PART — HAD. PART

EXAMPLE: $a_E = 0.6165 + 0.3193 \ln E$, $a_H = a_E$

$(1 \leq E_0 \leq 1000 \text{ GeV})$ $b_E = 0.2198$, $b_H = 0.9641 - 0.0237 \ln E$

$c = 0.4634$ (also called f_{π^0})

SHOWER MAXIMUM

$$t_{MAX}[\lambda] \approx 0.2 \ln(E[\text{GeV}]) + 0.7 \qquad \sim 1.6 \quad (100 \text{ GeV in } {}^{238}U)$$

CONTAINMENT

$$t_{98\%}[\lambda] \approx 1.6 \ln(E[\text{GeV}]) + 1.2 \qquad \sim 8.6$$

LONGITUDINAL SHOWER PROFILE FROM INDUCED RADIOACTIVITY

300 GeV π^- in U/Scint. CALORIMETER

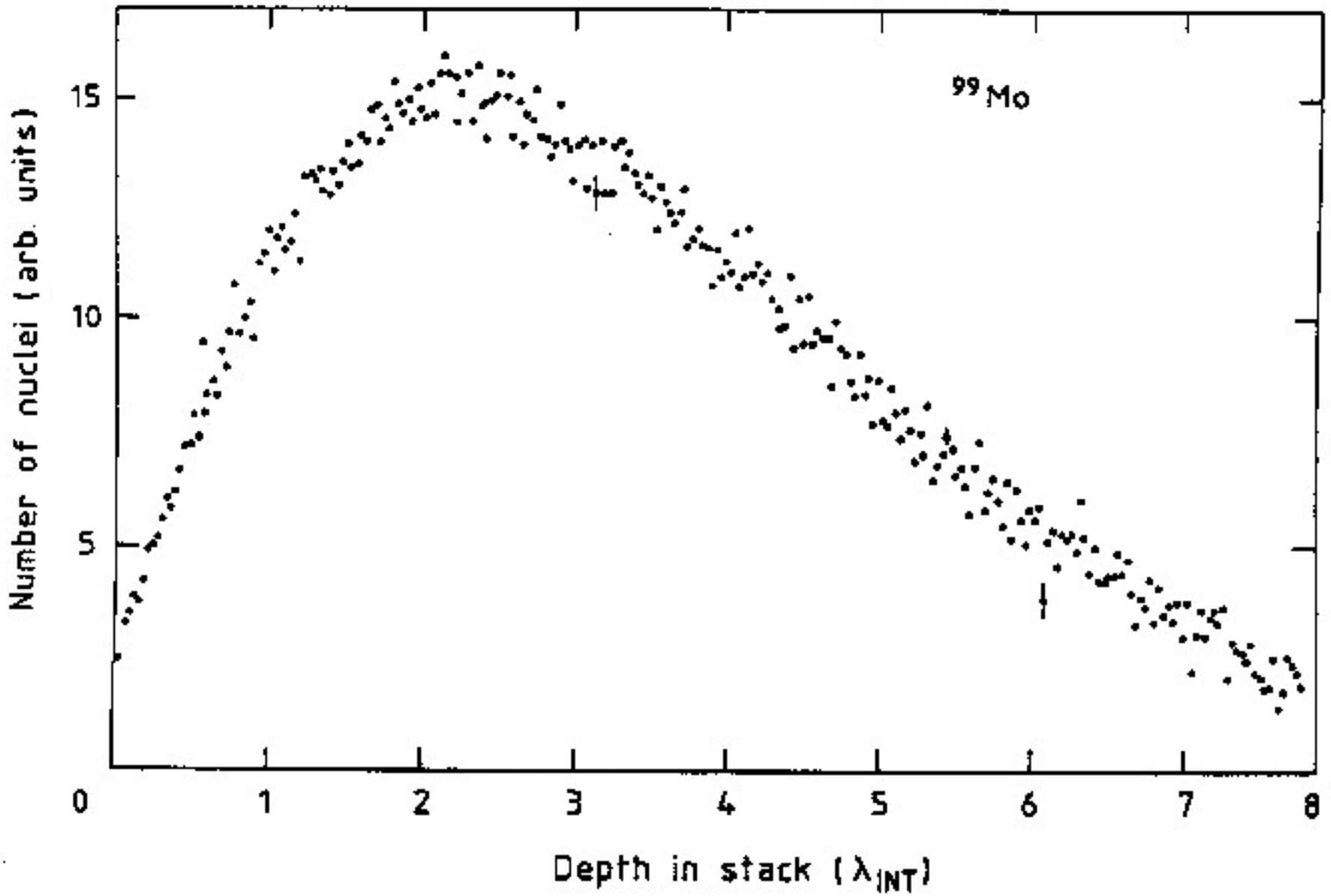

LATERAL SHOWER PROFILE FROM INDUCED RADIOACTIVITY

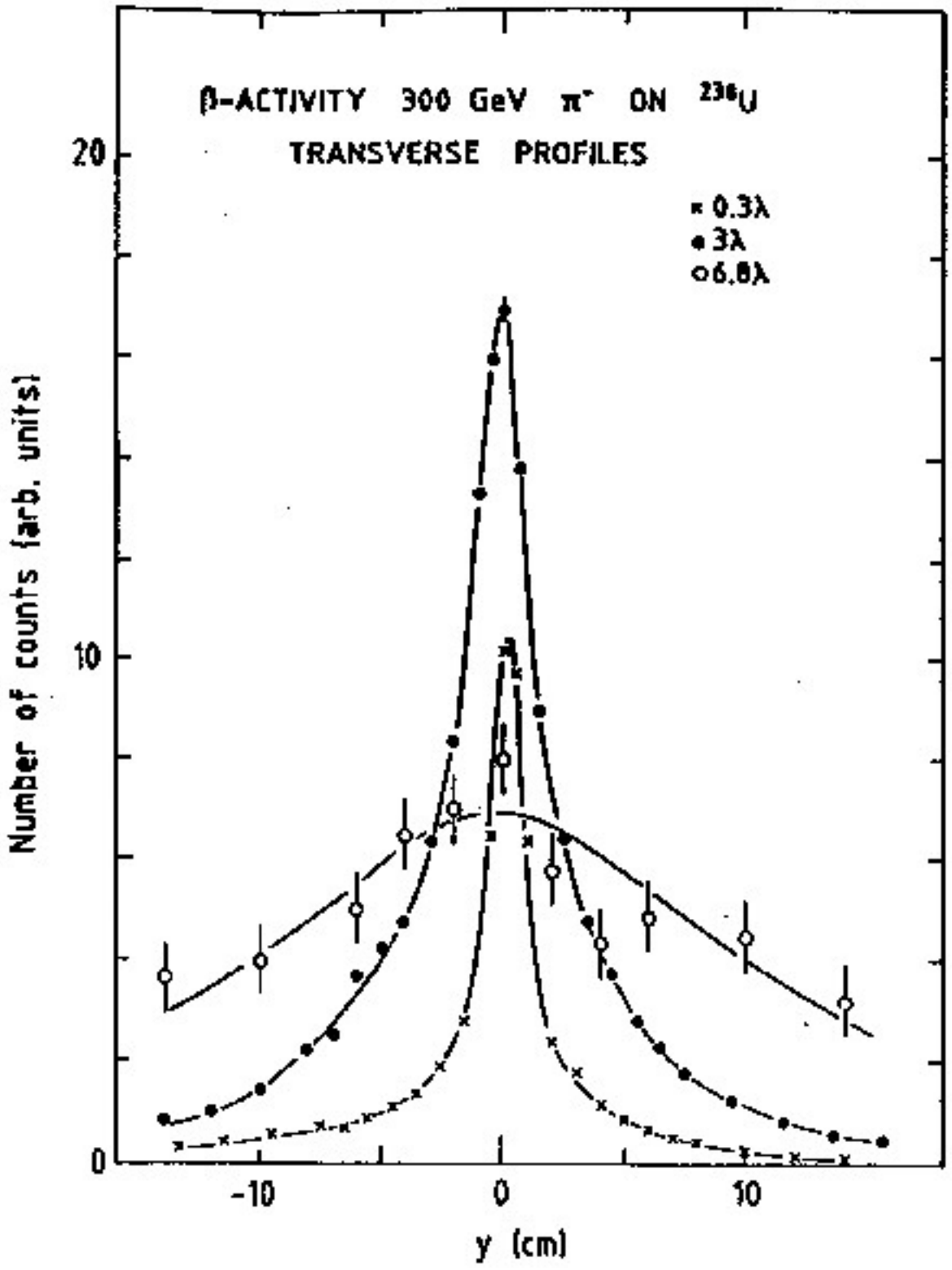

I.R. IS AN IMPORTANT TOOL TO UNDERSTAND PROCESSES IN DETAILS

TRANSVERSE PROFILE

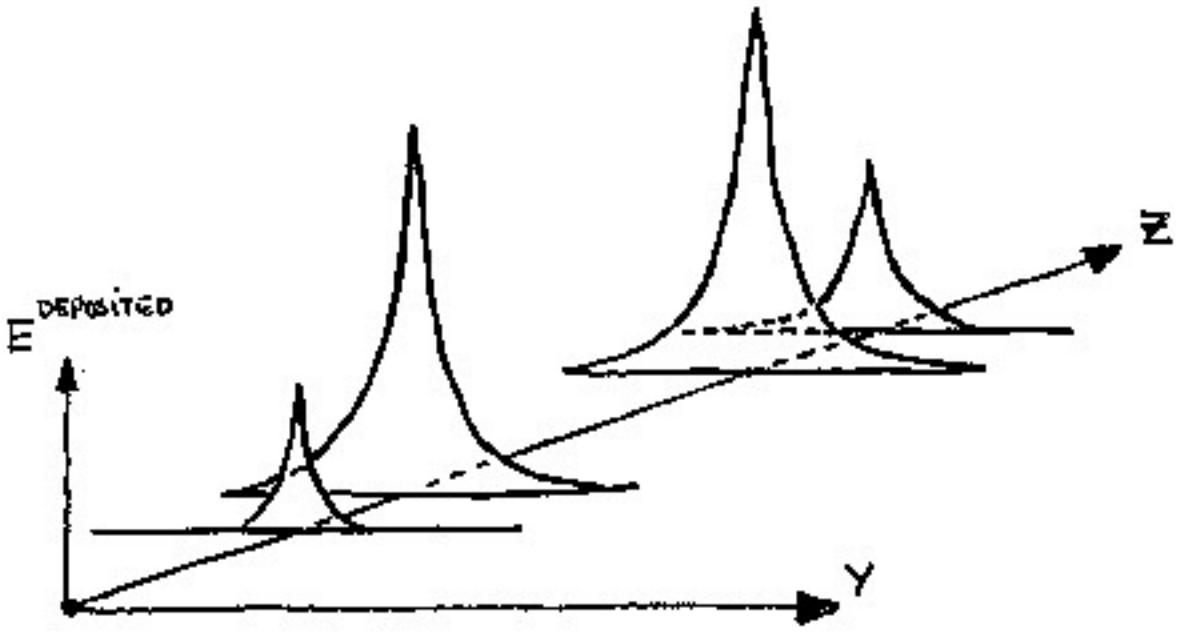

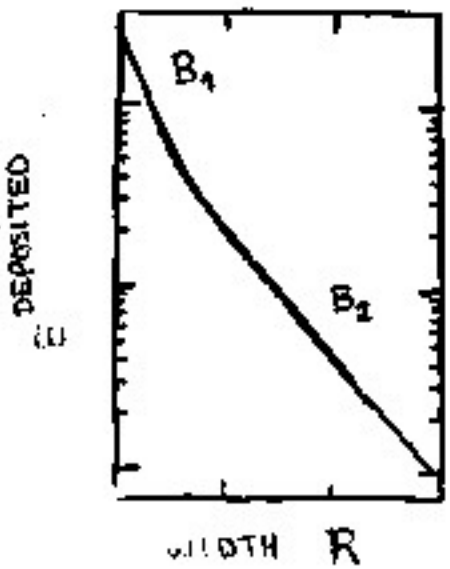

A CORE $(R < \frac{\lambda}{2})$ AND
A HALO $(R \sim \lambda)$ ARE OBSERVED

→ USE A PARAMETRIZATION OF THE TYPE

$$\frac{dE}{dR} = A_1 e^{-RB_1} + A_2 e^{-RB_2}$$

→ HERE: $\frac{A_1}{A_2} \sim 2$ $\frac{B_2}{B_1} \sim \frac{1}{3}$

LATERAL SHOWER CONTAINMENT GOES AS $R \approx 0.5 + 0.03 \ln E$

$[\lambda]$ $[GeV]$

HADRONIC SHOWERS

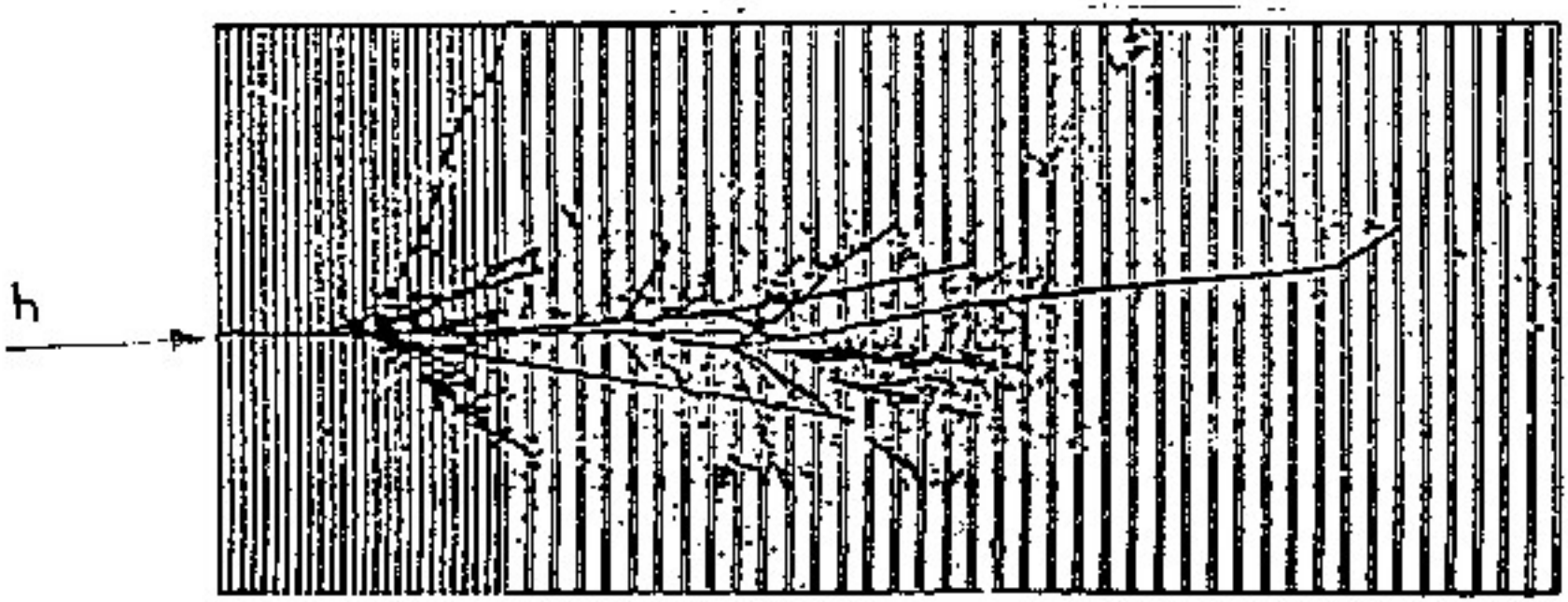

STARTS IN AVERAGE ($1/e$) AT $x = \lambda$

SIMULATION OF HADRONIC CASCADE

——— 100 GeV π^- in Fe

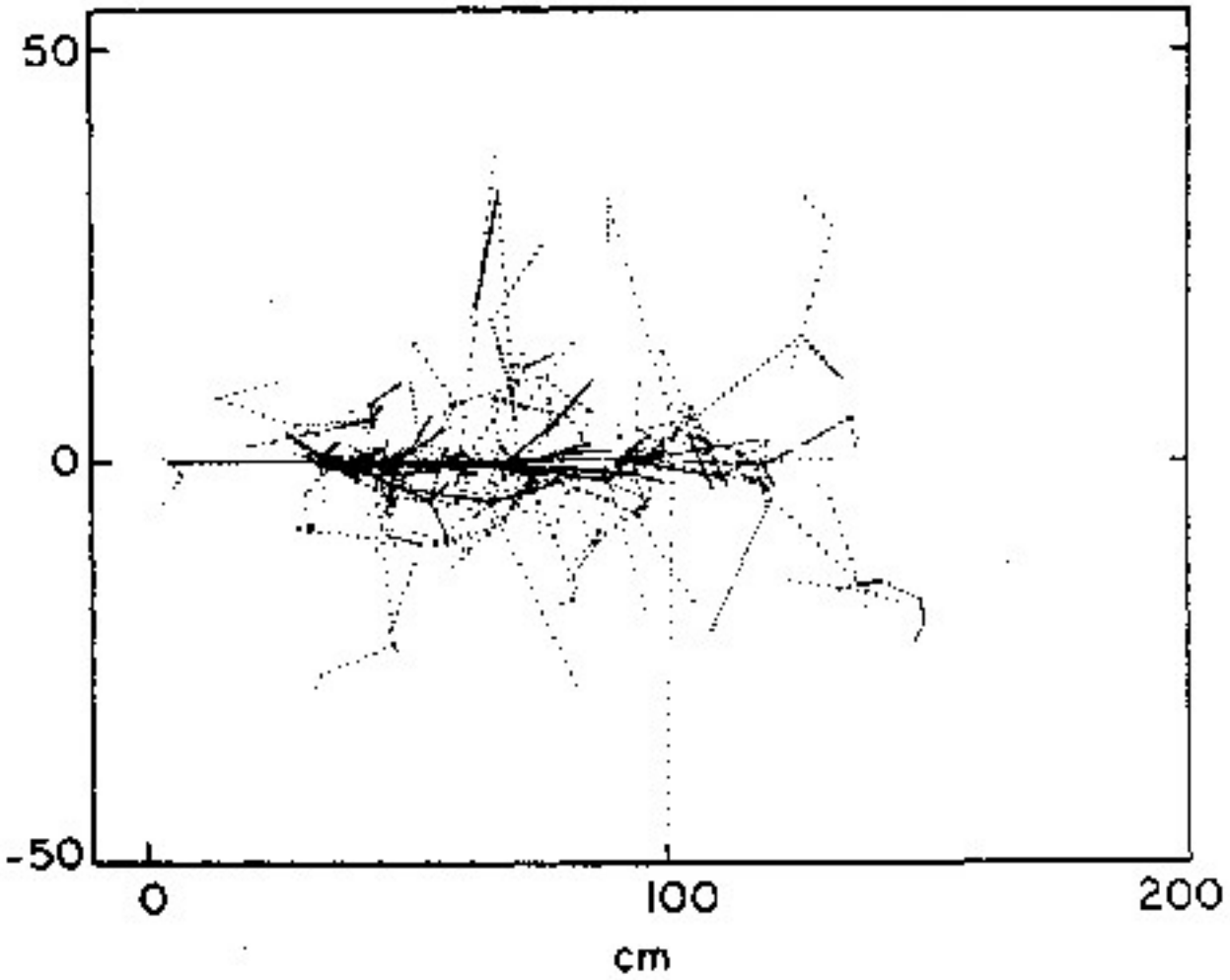

NEUTRONS ARE SEEN TO DEVIATE CONSIDERABLY FROM MAIN SHOWER AXIS.

HADRONIC SHOWER COMPONENTS

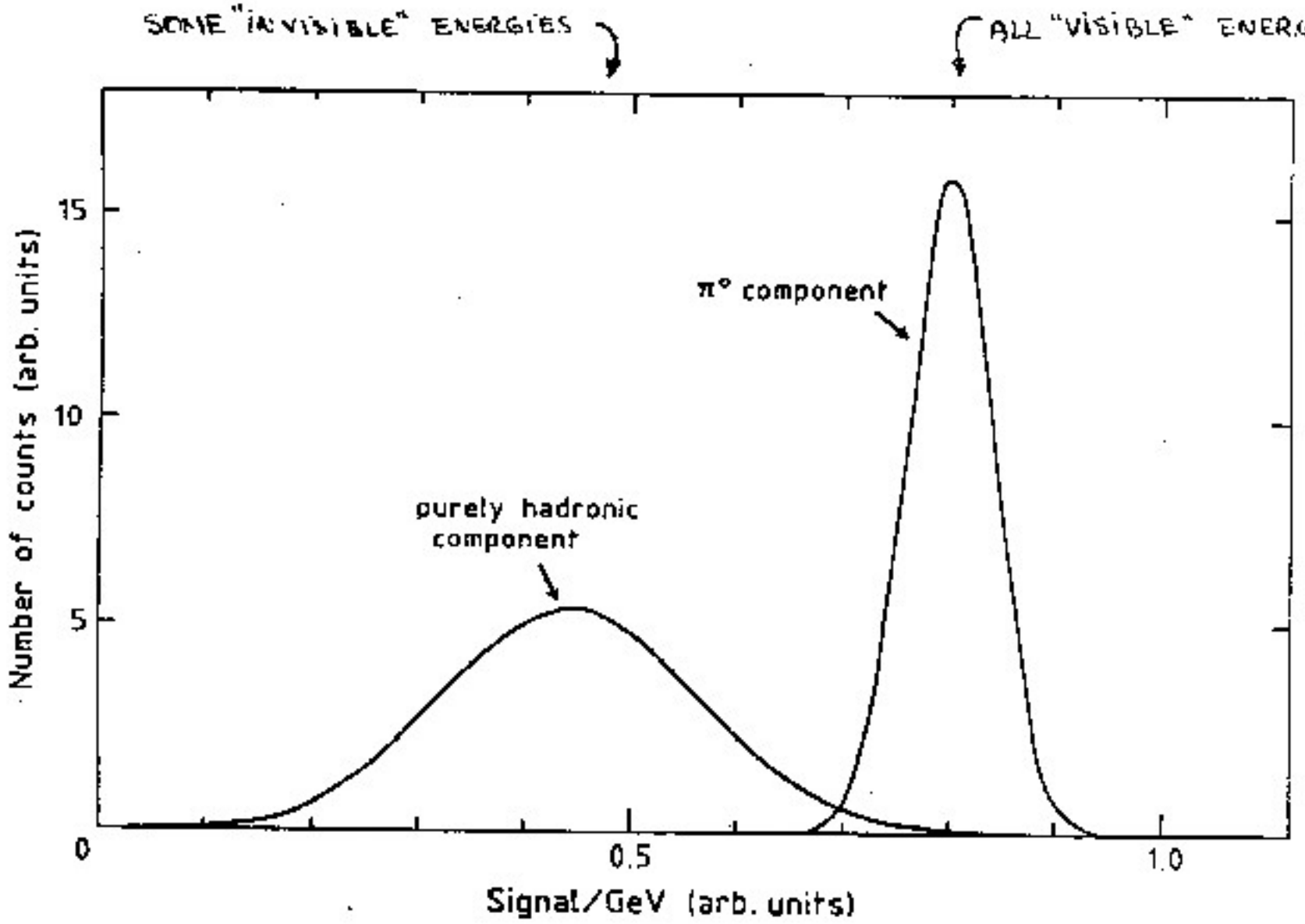

e/h RATIO (INTRINSIC)

SINCE THE HADRONIC SIGNAL IS PARTLY INVISIBLE, THE ENERGY RESPONSE WILL BE BROADER. ONE DEFINES :

$$\frac{e}{h} \doteq \frac{\text{PURE E.M. RESPONSE}}{\text{PURE HAD. RESPONSE}}$$

WITH: $e/h > 1$ IN GENERAL, BECAUSE OF MISSING ENERGY

$= 1$ FOR A "COMPENSATING" CALORIMETER

< 1 FOR AN OVER-COMPENSATING CAL.

THE CALORIMETER RESOLUTION WILL THEREFORE BE A FUNCTION OF THE e/h RATIO :

$$\frac{\sigma_E}{E} = \frac{k_1}{\sqrt{E}} + k_2 \cdot \left| \frac{e}{h} - 1 \right|$$

where $k_i > 0$

WITH MINIMUM VALUE FOR $e/h = 1$ (COMPENSATING)

$e/h > 1$

RANDOM EVENT

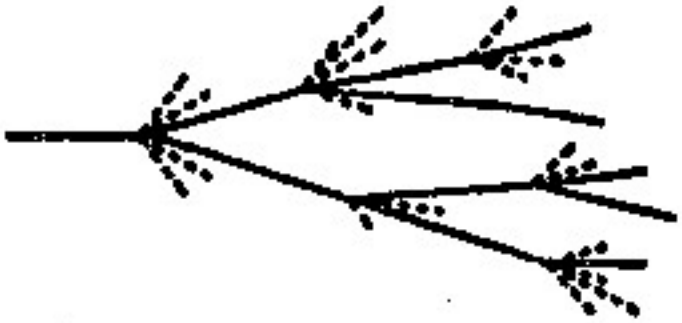

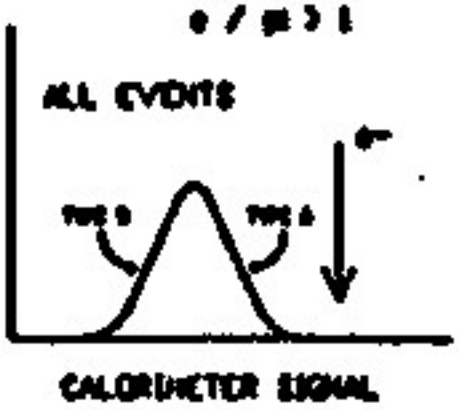

EXTREME EVENT: TYPE A

'small' EM loss
mostly EM energy

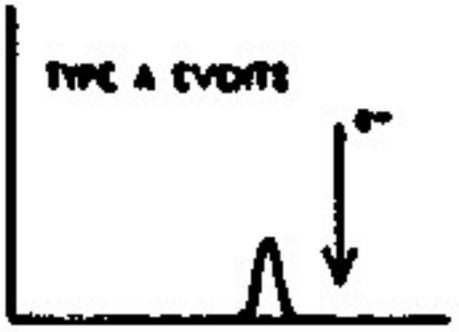

EXTREME EVENT: TYPE B

large EM loss
little EM energy

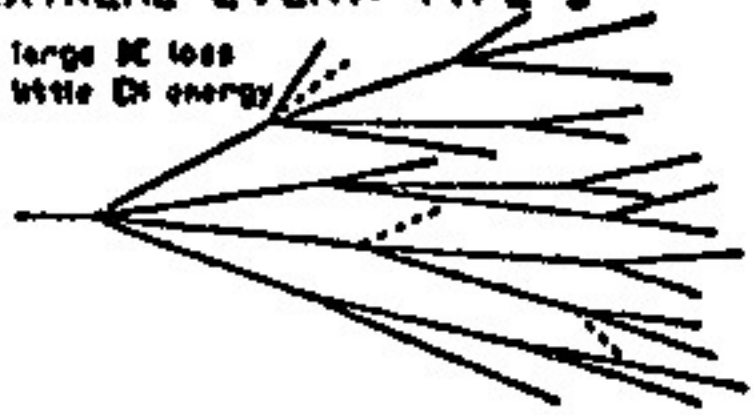

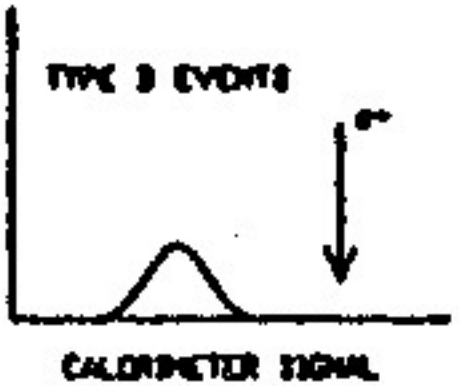

$e/h = 1$

RANDOM EVENT

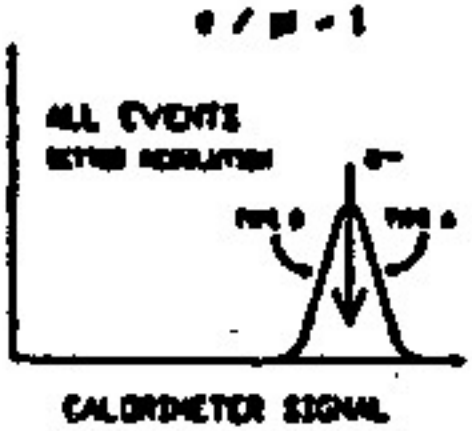

EXTREME EVENT: TYPE A

"small" EM loss

mostly CH energy

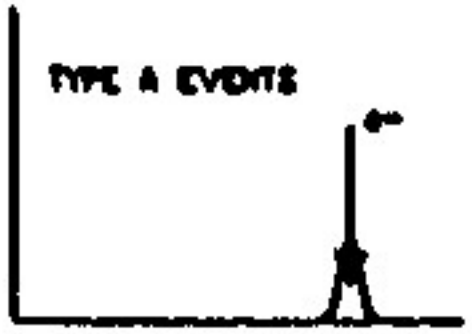

EXTREME EVENT: TYPE B

large EM loss

little CH energy

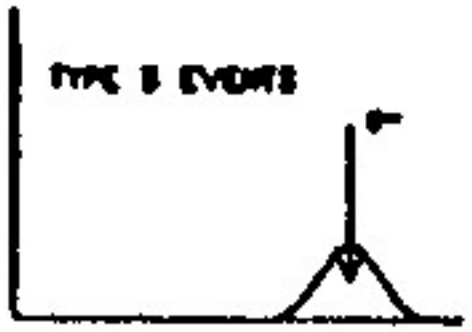

CALORIMETER RESPONSE WITHOUT & WITH COMPENSATION

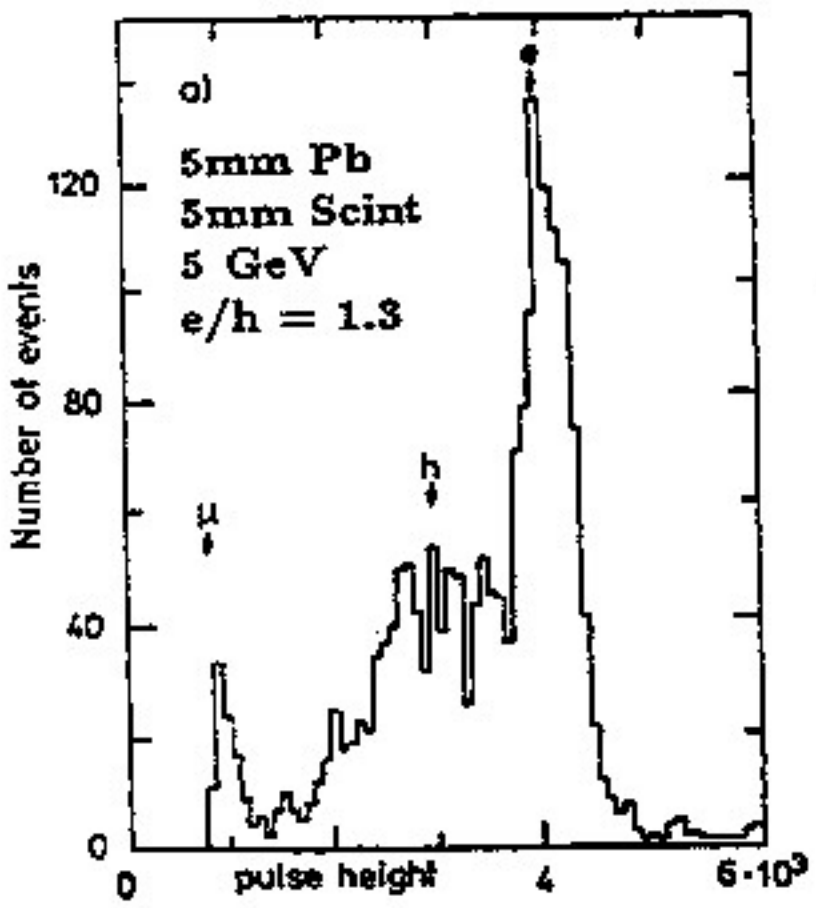

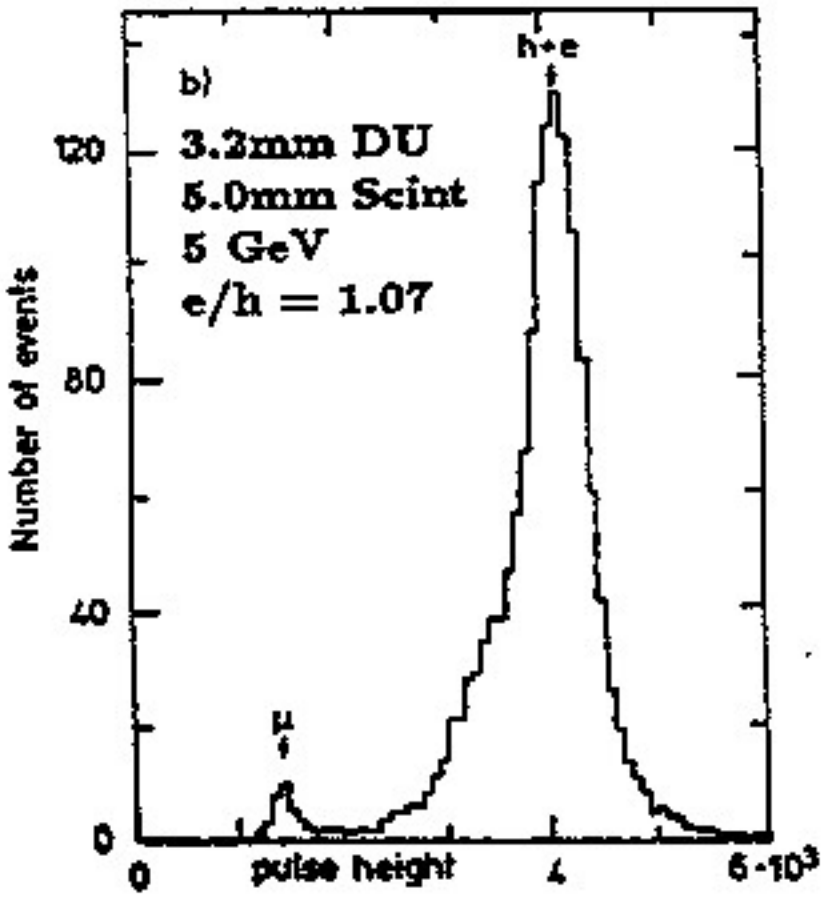

HADRONIC RESOLUTION

HADRONIC SHOWERS ARE COMPOSED OF PURELY HADRONIC AND PURELY ELECTROMAGNETIC PARTS.

SUBJECT TO LARGE FLUCTUATIONS, THE FRACTION OF THE E.M. TERM IN THE SHOWER CAN BE PARAMETRIZED AS:

$$f_{em} \approx 0.12 \ln E \ [\text{GeV}]$$

SEVERAL FACTORS CONTRIBUTE TO THE DEGRADATION OF THE ENERGY RESOLUTION:

1) INVISIBLE PARTS OF THE HADRONIC ENERGY

- LOST IN EXCITATION / BREAKUP OF NUCLEI
- LOST BY RUNAWAY NEUTRINOS OR SOME NEUTRONS

2) DIFFERENT CALORIMETER RESPONSES TO THE DIFFERENT TYPES OF SECONDARY PARTICLES (e, m, p, etc...)

- SIGNAL SATURATION FOR HIGHLY IONIZING PROTONS
- DETECTION OF THERMAL NEUTRONS

e/h ENERGY DEPENDENCE

$$\left(\frac{e}{h}\right)_{MEASURED} = \frac{\text{E.M. RESPONSE}}{\text{HAD. RESPONSE} + \pi^0 \text{ RESPONSE}}$$

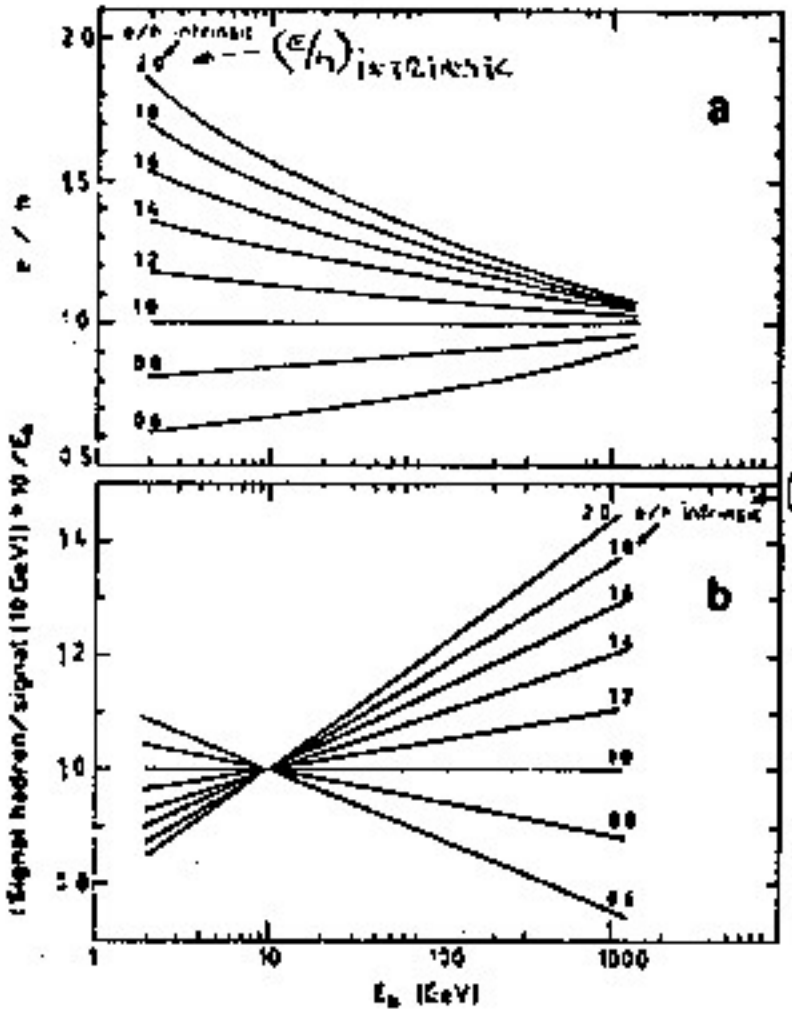

f_{π^0} IS ENERGY DEPENDENT, HENCE $(e/h)_{MEAS} \neq (e/h)_{INT.}$ (IN GENERAL)

CALORIMETER SIGNALS ARE PROPORTIONAL TO ENERGY ONLY WHEN

$$\left(\frac{e}{h}\right)_{INT.} = 1$$

RESOLUTION vs e/h

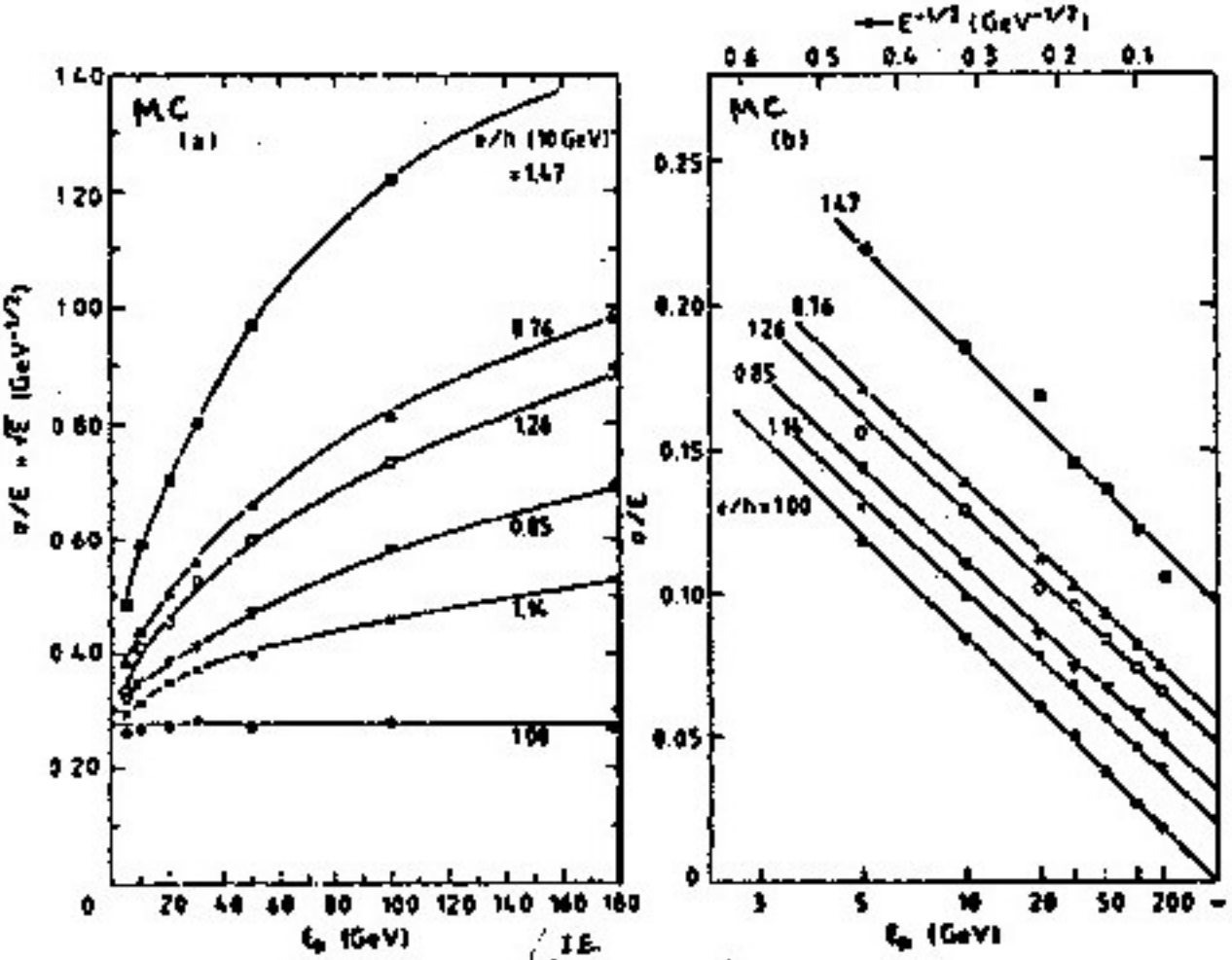

↳ i.e. VERY IMPORTANT AT HIGH ENERGIES

CONSTANT TERM vs e/h

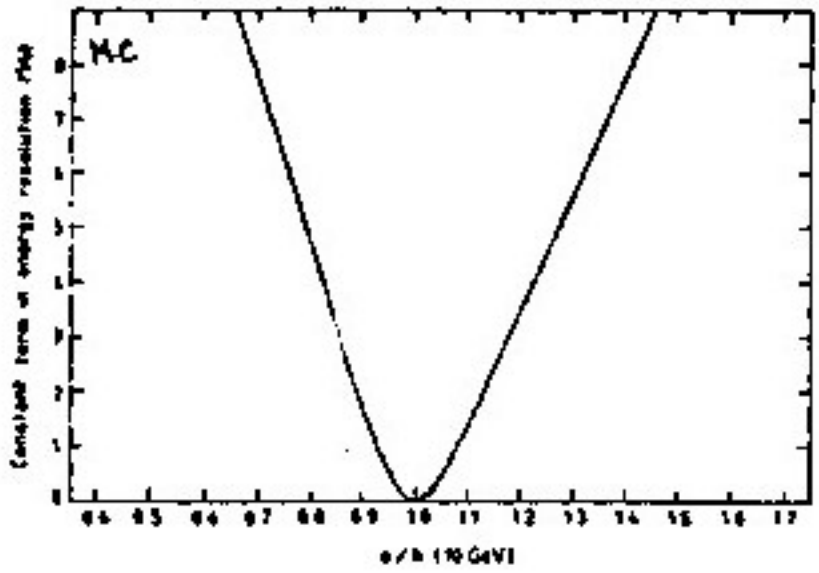

DISSIPATION OF ENERGY IN HAD. SHOWERS

3 MONTE-CARLO CALCULATIONS ('81)

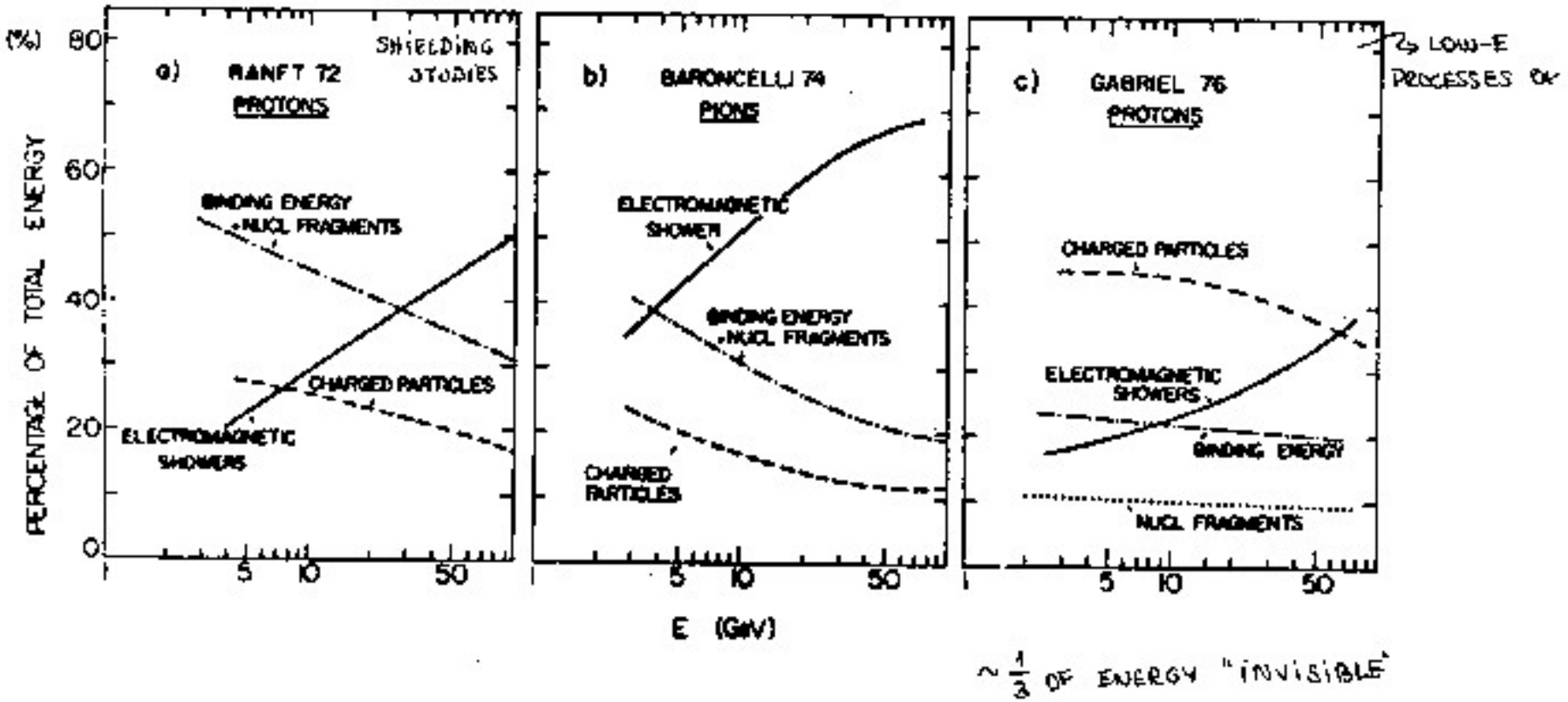

mip

m.i.p. ≐ MINIMUM IONIZING PARTICLE

IS USED AS A SCALE STANDARD FOR ENERGY DEPOSITION IN DETECTOR.

IN PRACTICE, MUONS ARE USED TO FULFILL THAT ROLE:

mip ≐ muon response

THIS IS NOT QUITE TRUE, SINCE THE RESPONSE IN FACT INCREASES WITH ENERGY ("RELATIVISTIC RISE"), DUE TO:

- BREMSSTRAHLUNG
- PAIR PRODUCTION
- δ- RAYS

...BUT THESE EFFECTS CAN BE CORRECTED FOR.

ONE CAN THEN COMPARE OR COMPUTE QUANTITIES LIKE

$e/\mu \doteq e/mip \leftrightarrow e/h \leftrightarrow h/mip$ etc... (AT SAME ENERGY)

e/mip

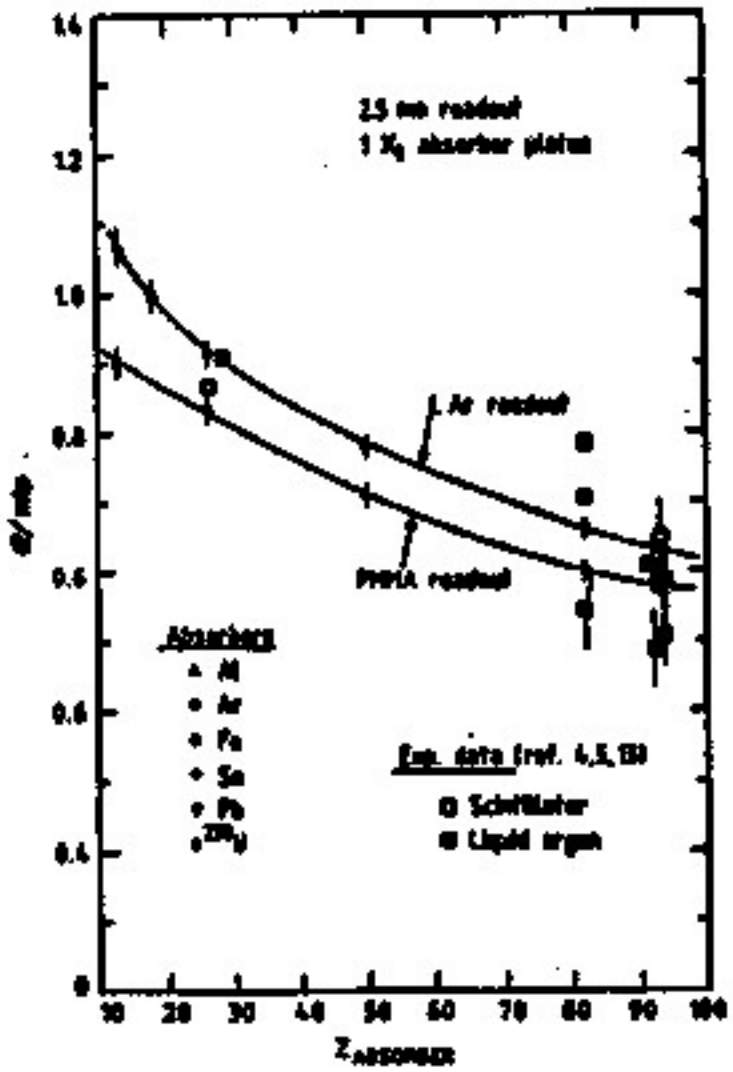
2.5 mm readout
1 X_0 absorber plates
Ar readout
PWC readout
Absorber
Al
Ar
Fe
Sn
Pb
^{238}U
Exp. data (ref. 4,5,19)
Schiltkamp
Liquid argon
e/mip
$Z_{ABSORBER}$

HIGH ENERGY ELECTRONS

THE FIRST EXPECTATION WOULD BE $e/_{mip} = 1$

BUT THE OBSERVATION IS: < 1 !

AND $e/_{mip}$ DECREASES AS $\underbrace{Z_{ABS} - Z_{ACT}}_{\doteq \Delta Z}$ INCREASES

THIS IS CONFIRMED BY DETAILED EGS4 CALCULATIONS.

EXAMPLE: HELIOS EXPT. (U/Scint.)

$e/_{mip} = 0.\overset{70}{\blacksquare} \pm 0.05$ (E-INDEPENDENT)

THE EFFECT IS TRACED DOWN TO DIFFERENT RESPONSES TO LOW ENERGY PHOTONS

... ITSELF FROM THE FACT THAT THE PHOTON ATTENUATION COEFFICIENTS FOR ABSORBER AND ACTIVE LAYERS ARE NOT PROPORTIONAL FOR $E_\gamma \lesssim$ MeV

e/mip

(HELIOS EXPERIMENT)

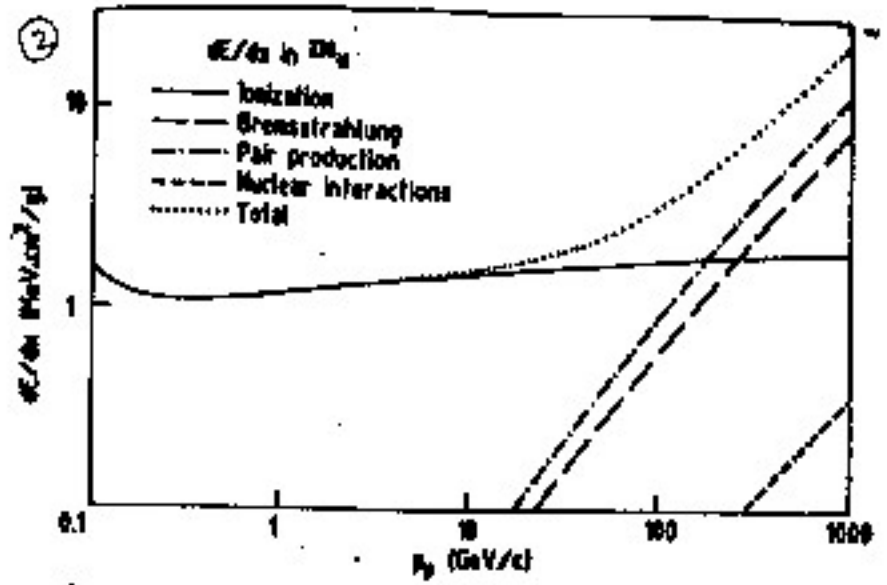

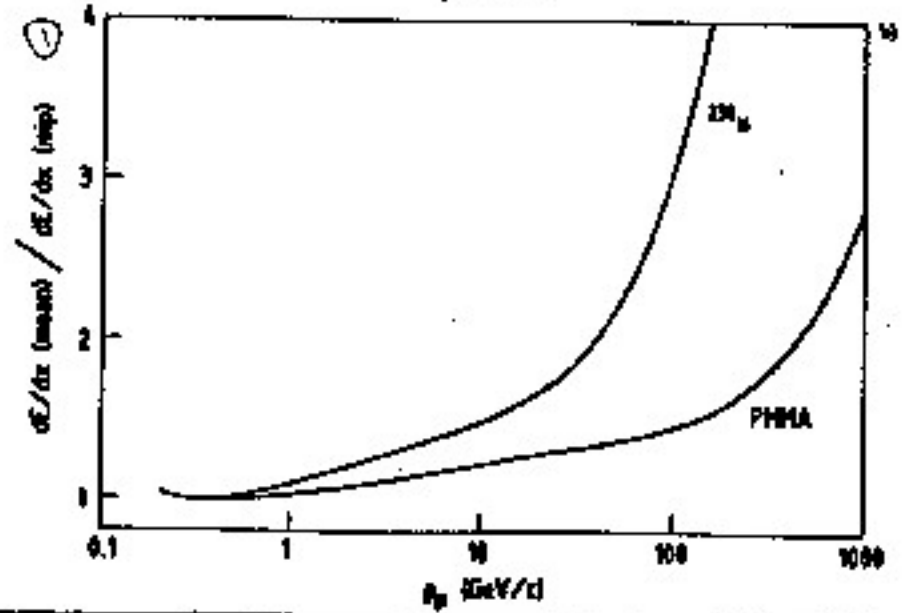

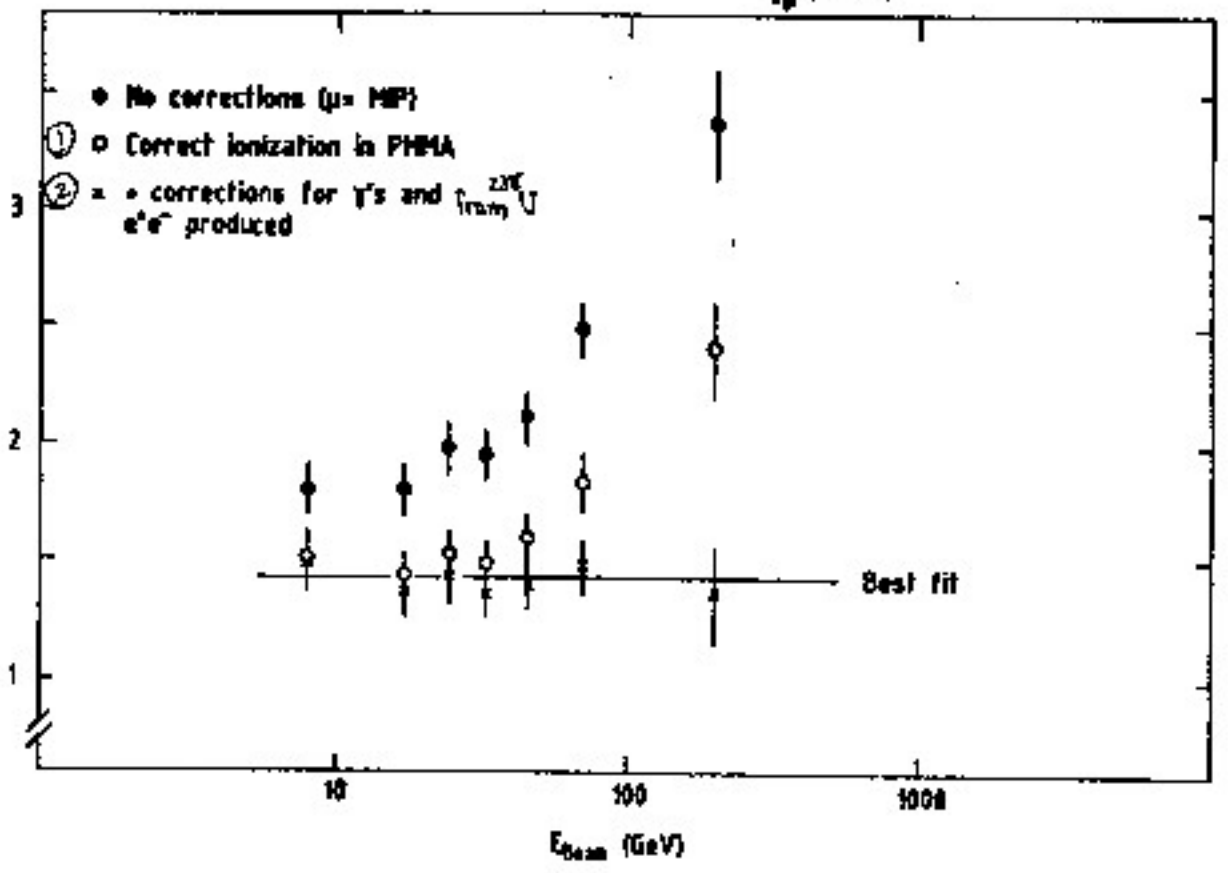

e/mip VARIATIONS

vs EGS4 CALCULATIONS

$\Delta z = z_{\text{max}}^{\text{PEC}} - z_{\text{max}}^{\text{ACT}}$

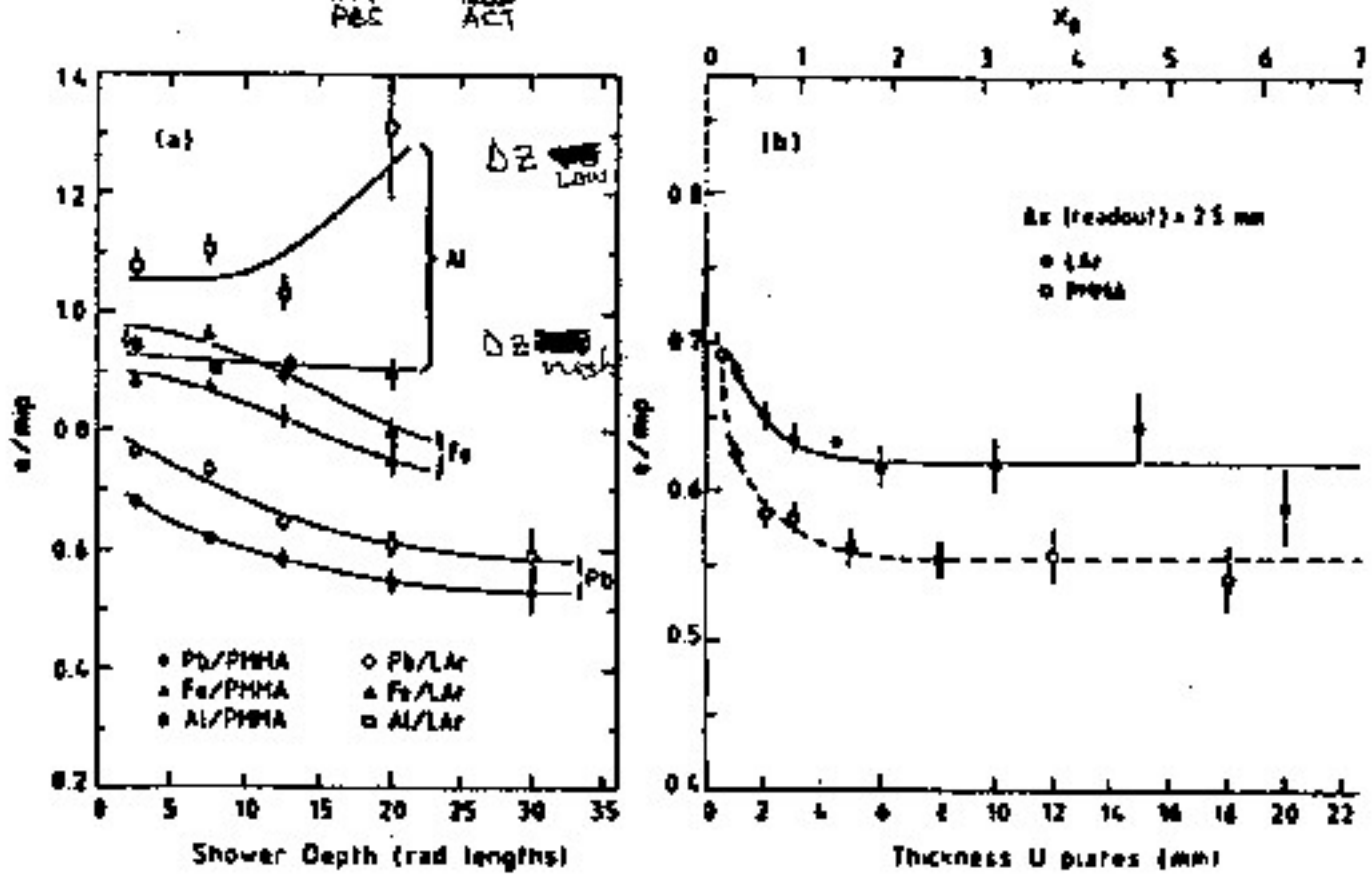

LOWER ENERGY γ'S

COMPTON ELECTRONS CAN ESCAPE AND BE DETECTED (OR PHOTOELECTRONS)

γ/mip PROMPT γ's FROM ^{238}U FISSION

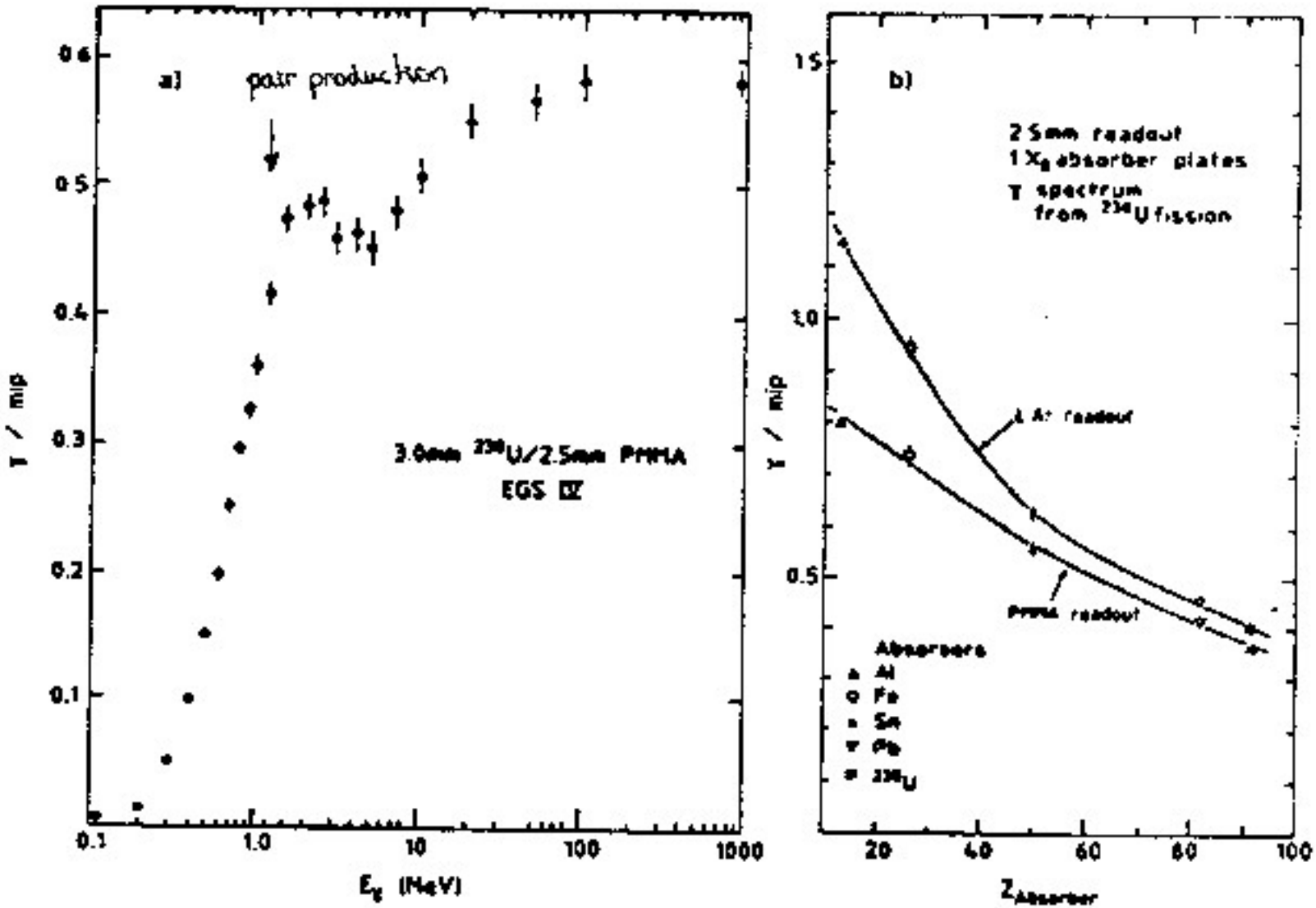

OTHER LOW-E γ's MAY COME FROM INELASTIC n-SCATTERING
EXCITED NUCLEI
U FISSION PRODUCTS, etc...

HADRONIC SHOWER PROCESSES

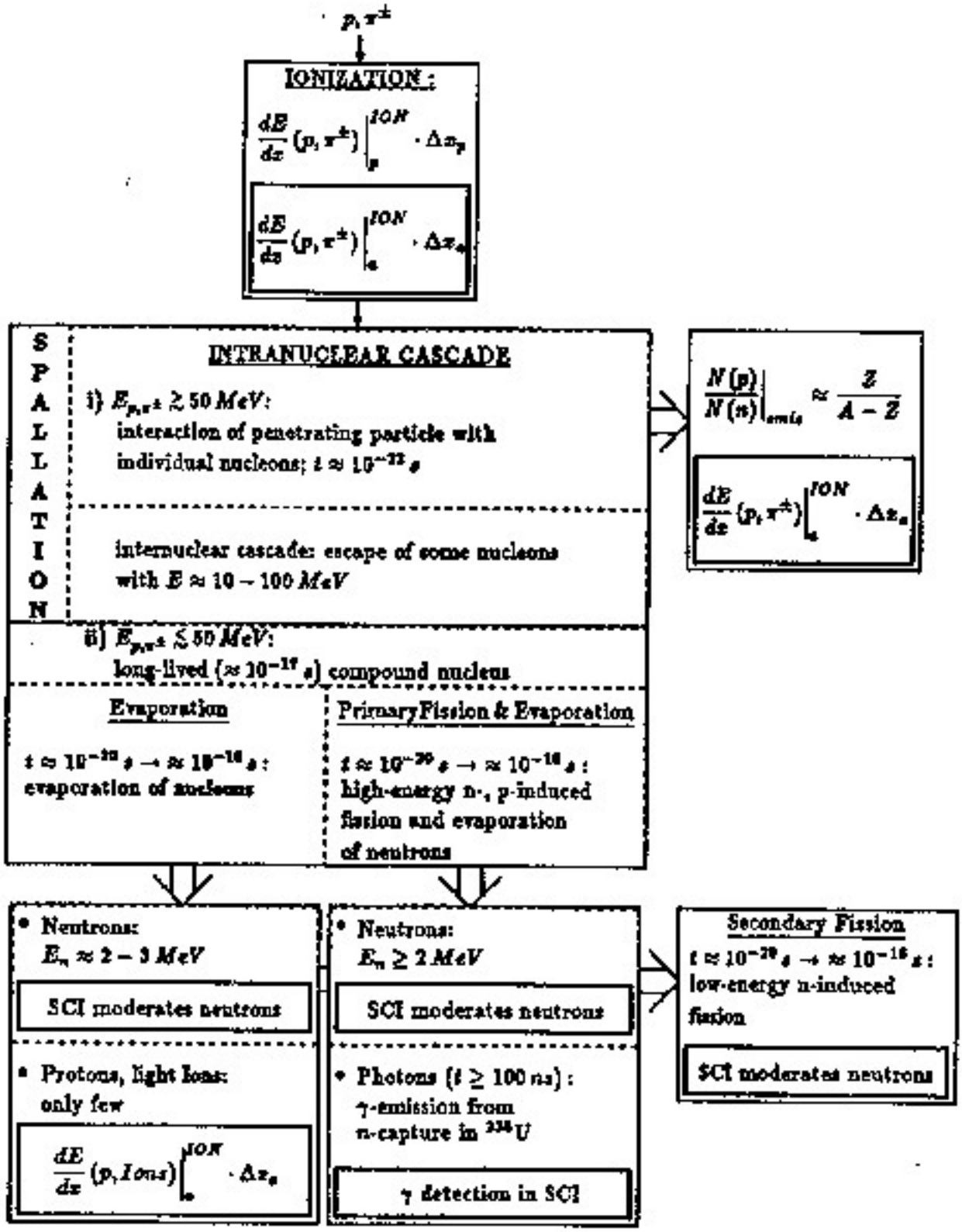

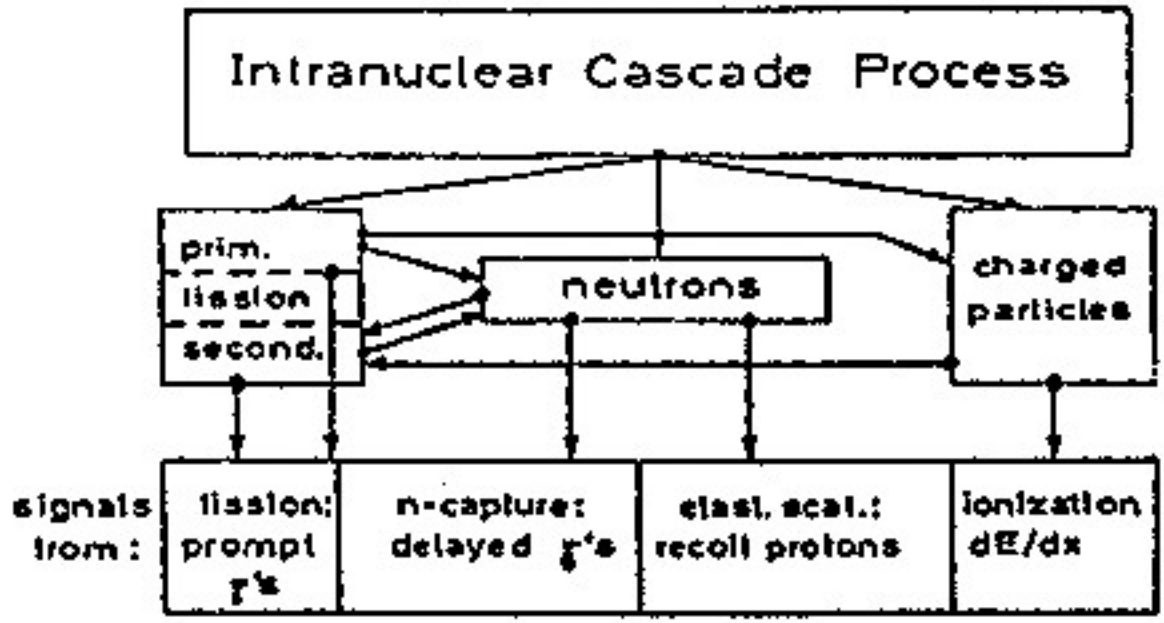
Intranuclear Cascade Process
prim.
fission
second.
neutrons
charged particles
signals from :
fission: prompt γ's
n-capture: delayed γ's
elast. scat.: recoil protons
ionization dE/dx

Characteristic Properties of the Hadronic Cascade

Reaction	Properties	Influence on energy resolution	Characteristic time (s)	Characteristic length (g/cm^2)
Hadron production	Multiplicity $\propto A^{0.1} \ln s$ Inelasticity $= 1/2$	π^0/π^+ ratio Binding energy loss.	10^{-22}	Abs. length $\lambda \simeq 35A^{1/3}$
Nuclear de-excitation	Evaporation energy $\simeq 10\%$ Binding energy $\simeq 10\%$ Fast neutrons $\simeq 40\%$ Fast protons $\simeq 40\%$	Binding energy loss. Poor or different response to n, charged particles, and γ's.	10^{-18}–10^{-13}	Fast neutrons $\lambda_n = 100$ Fast protons $\lambda_p = 20$
Pion and muon decays	Fractional energy of μ's and ν's $\simeq 5\%$	Loss of ν's	10^{-8}–10^{-6}	$\gg \lambda$
Decay of c, b particles produced in multi-TeV cascades	Fractional energy of μ's and ν's at percent level	Loss of ν's. Tails in resolution function.	10^{-12}–10^{-10}	$\ll \lambda$

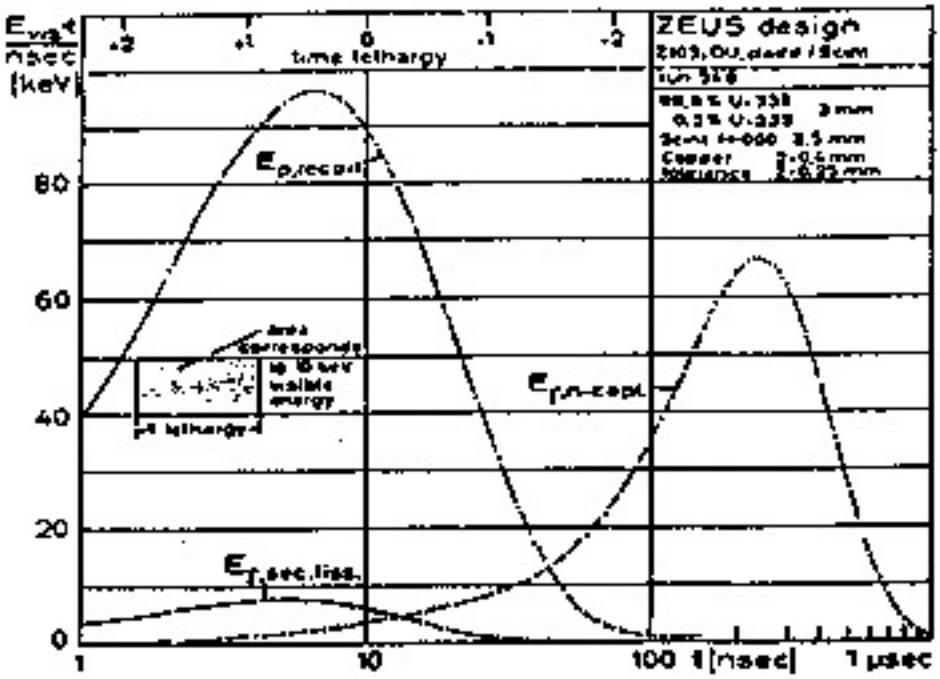

Contributions to 'visible' (measurable) energy from proton recoils and from nuclear processes in a uranium scintillator calorimeter (3mm DU, 2.5mm Scint) calculated from HERMES Monte Carlo simulations.

→ e/h will be gate time dependant !

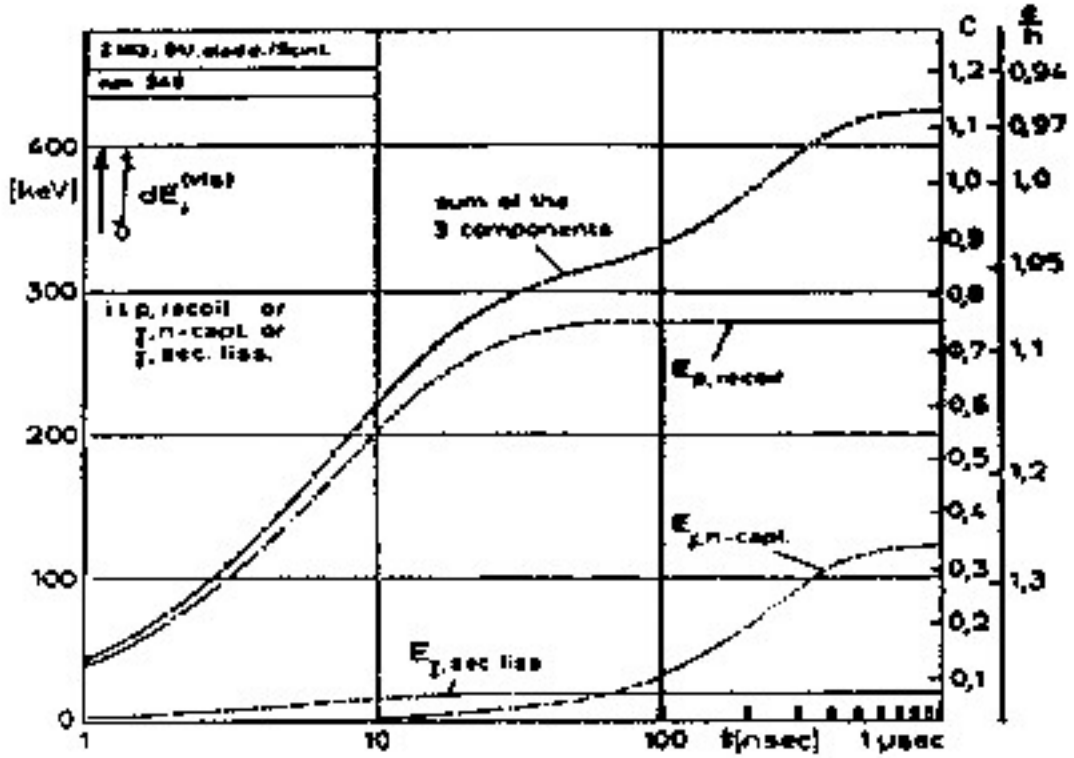

The visible energies from Fig. 3.19 integrated over time. The contributions to compensation can be read at the right ordinate versus gate time [BRÜ86]. An e/mip = 0.6 was taken from an EGS calculation including the cladding.

NUCLIDE CROSS SECTIONS BY SPALLATION OF ^{238}U

ΔZ } NUMBER OF PROTONS
ΔN } " " NEUTRONS } OF ESCAPING NUCLIDE

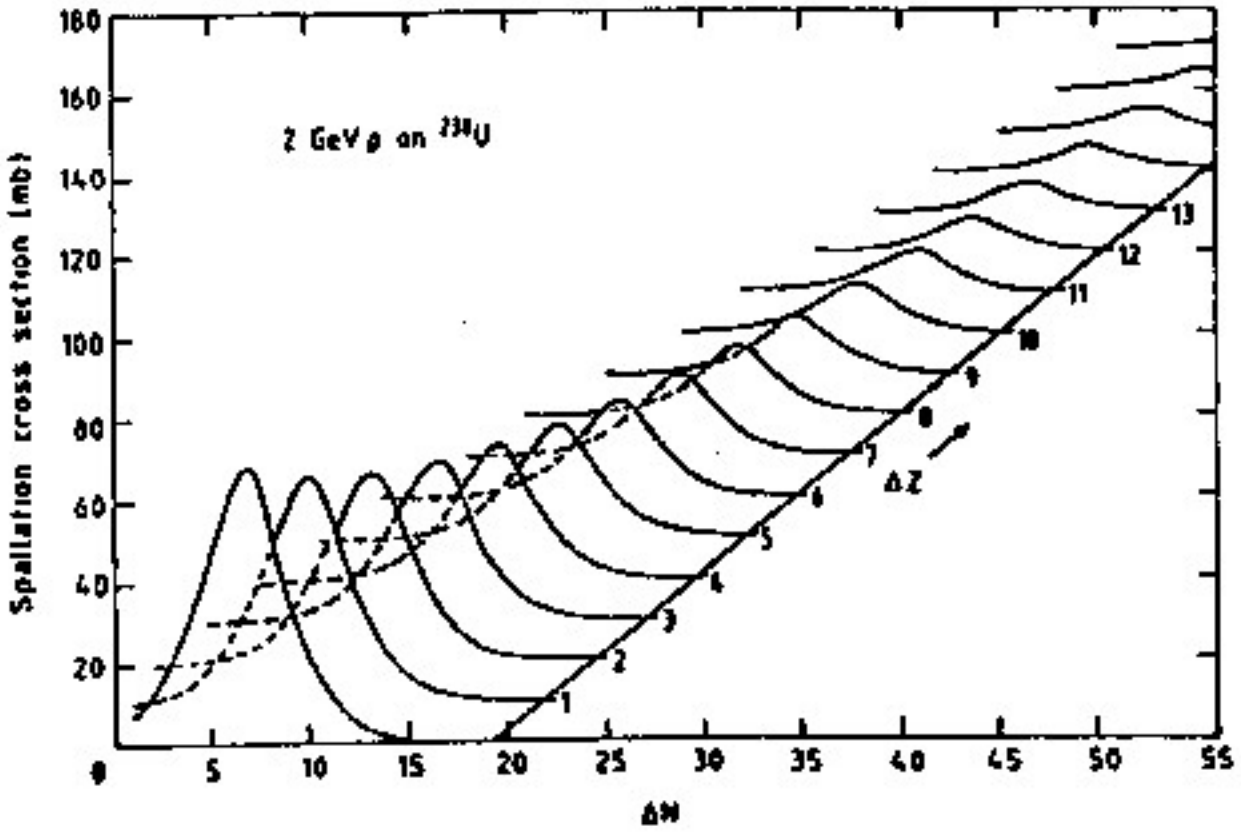

CALORIMETER RESPONSE TO PROTONS

...BEFORE INTERACTION WITH ^{238}U

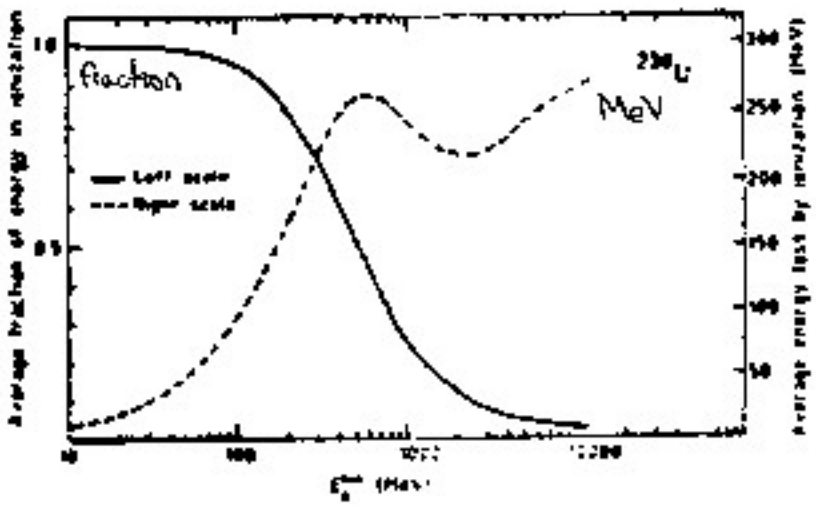

... RESPONSE TO SPALLATION PROTONS

SATURATION EFFECT

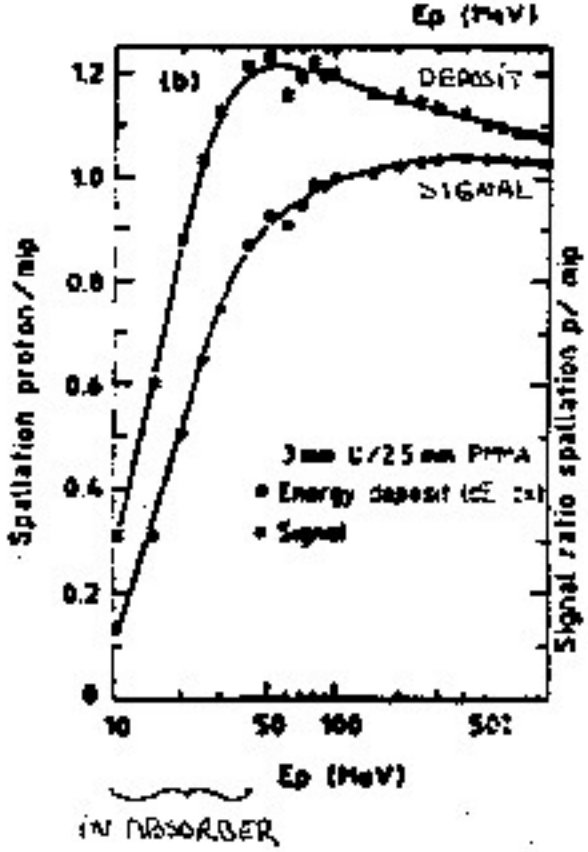

IN ABSORBER

PLATE THICKNESS EFFECT ON P/mip

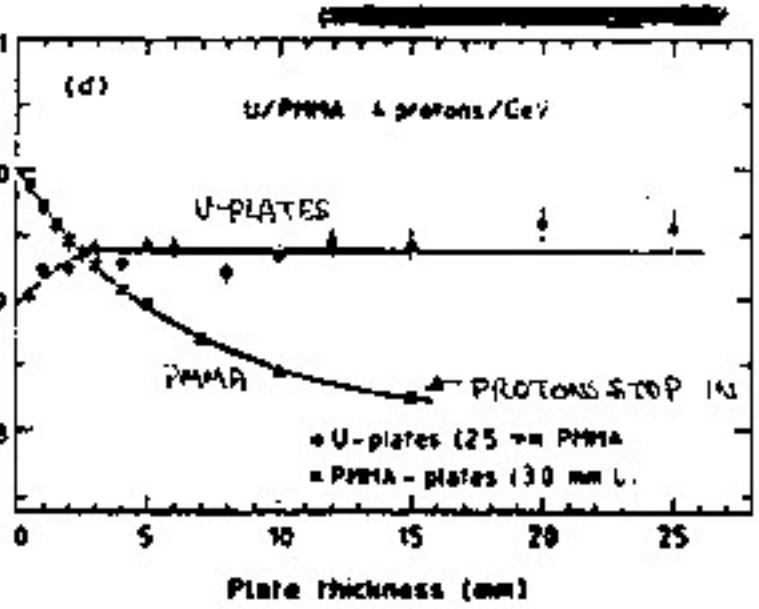

HADRON ENERGY SPENT ON ...

→ BINDING ENERGY LOSS
TARGET RECOIL
} INVISIBLE

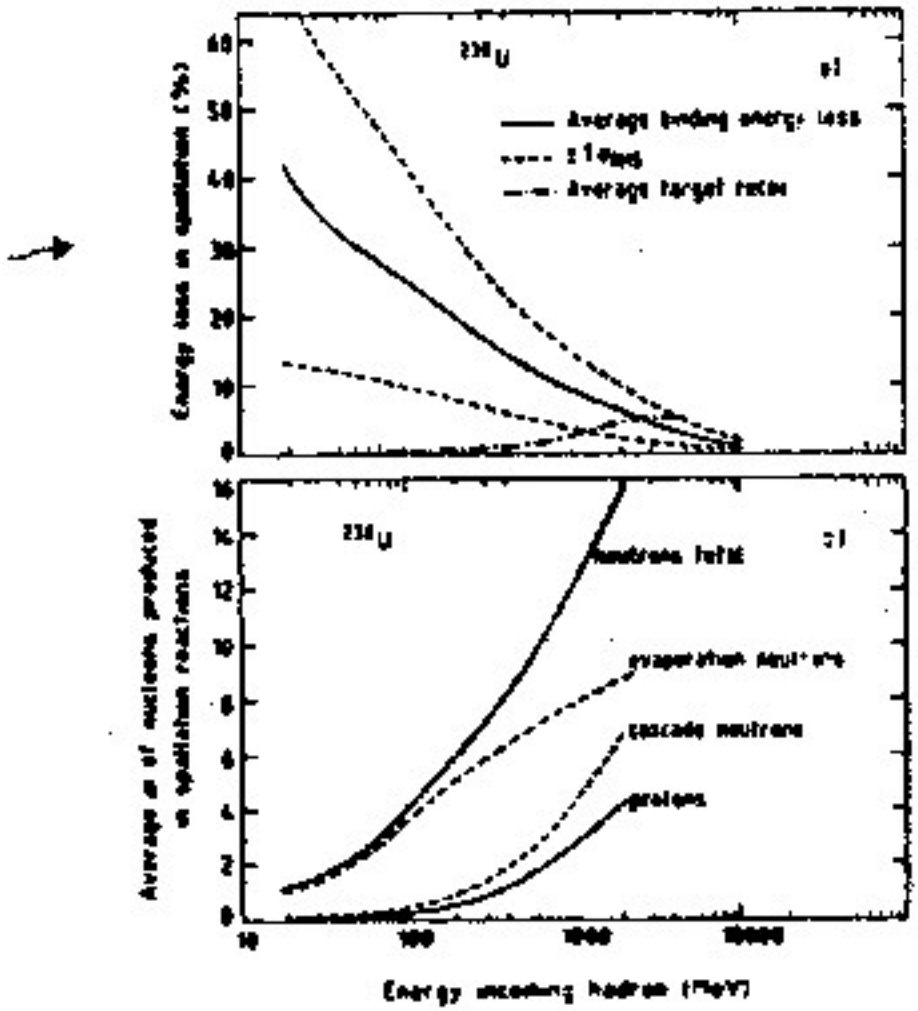

BINDING ENERGY OF LAST ("OUTERMOST") NUCLEON :

U 6.4 MeV = 32% OF E_{loss} DUE TO NEUTRONS

Pb 7.6 MeV = 28% " " " " "

Fe 10.5 MeV = 22% " " " " "

DE-EXCITATION OF NUCLEI (AFTER SPALLATION)

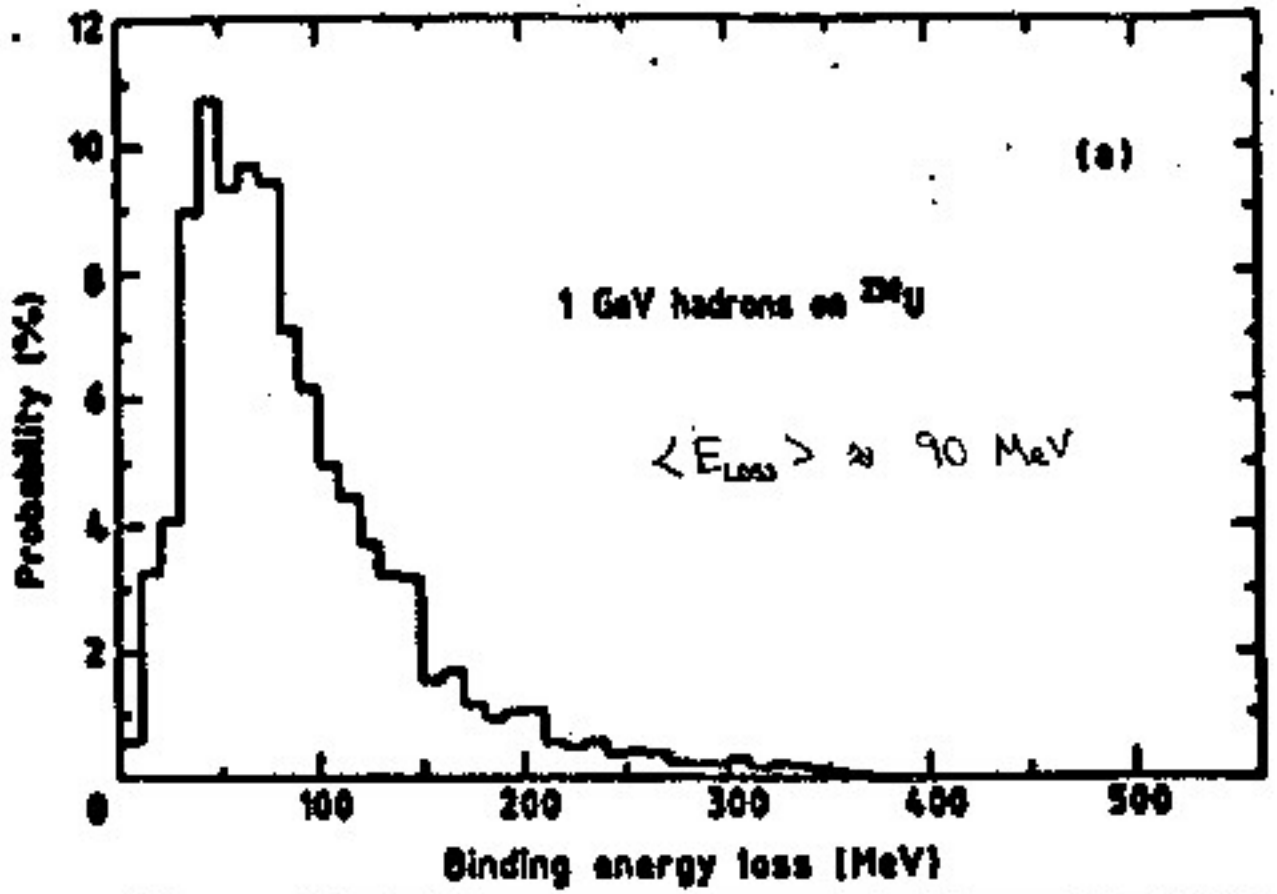

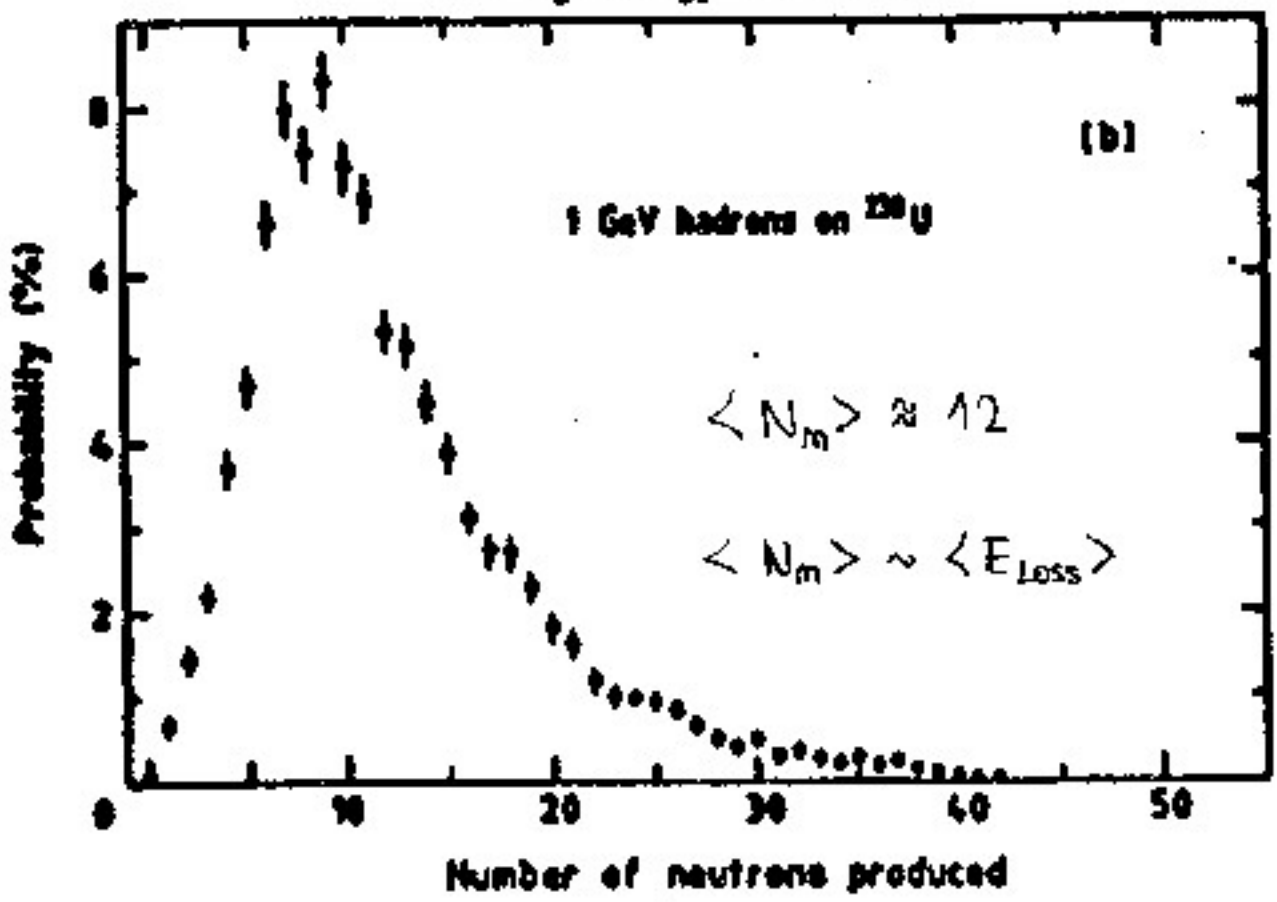

FLUCTUATIONS ARE LARGE

NEUTRON-INDUCED REACTIONS

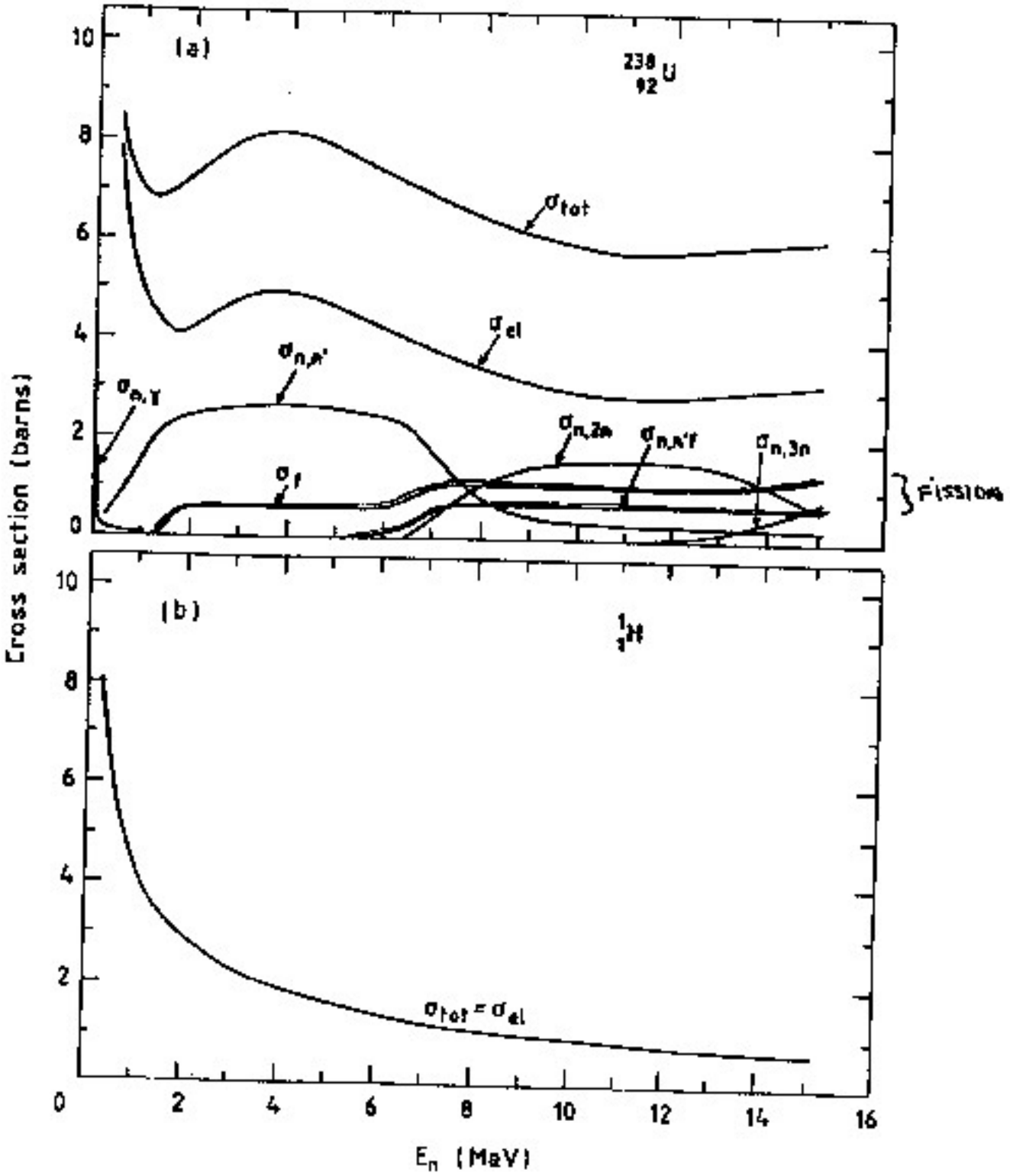

NEUTRON CROSS-SECTION IN URANIUM & HYDROGEN

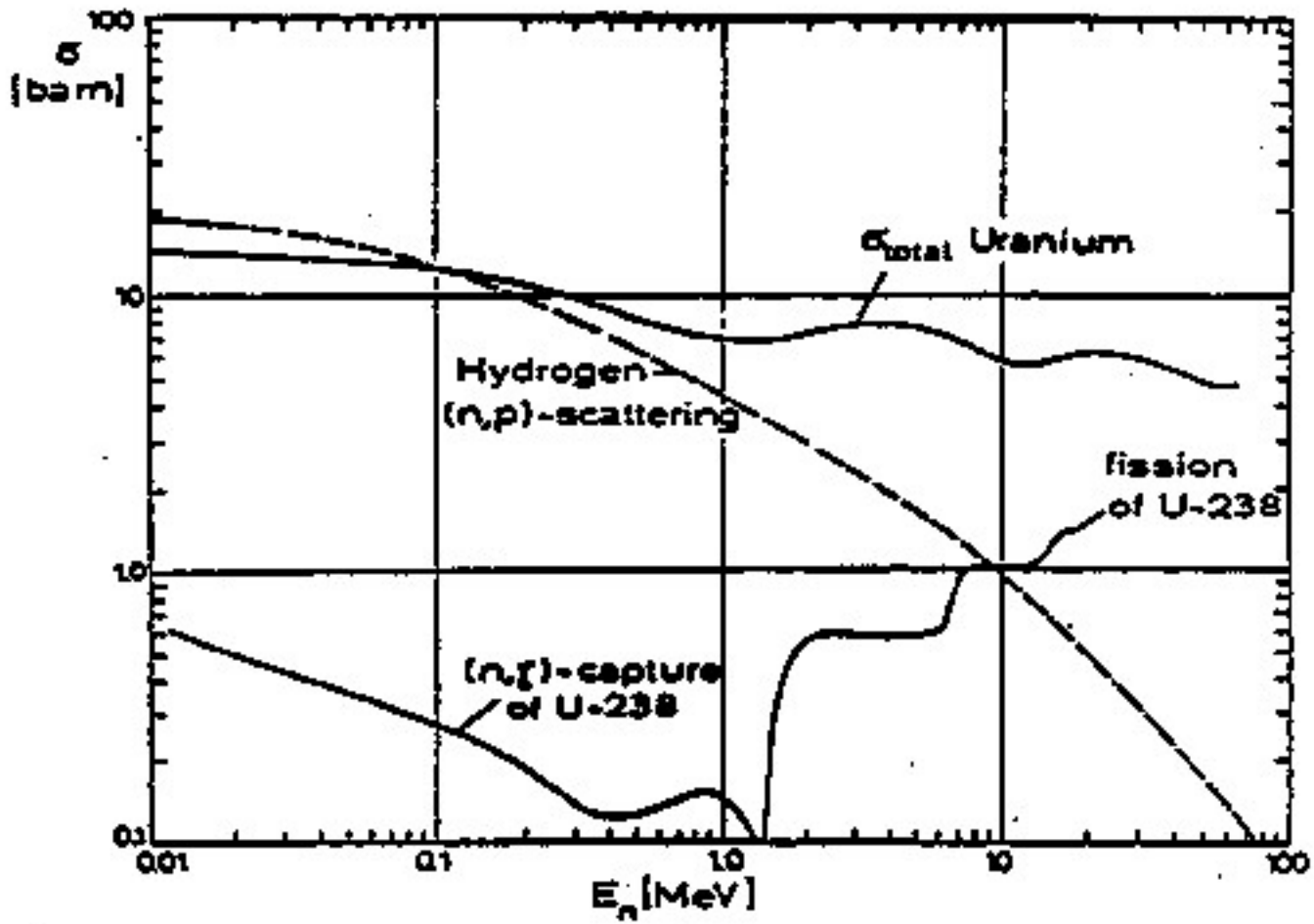

SPALLATION $\xrightarrow{\text{(PART)}}$ FISSION $\xrightarrow{n's}$ CAPTURE $\xrightarrow{\gamma's}$

THE NET RESULT OF THIS CHAIN IS AN AMPLIFICATION OF SIGNAL FROM:

- KINETIC NEUTRONS
- SOFT PHOTON ENERGY

SHOWER PROFILE IN ^{238}U

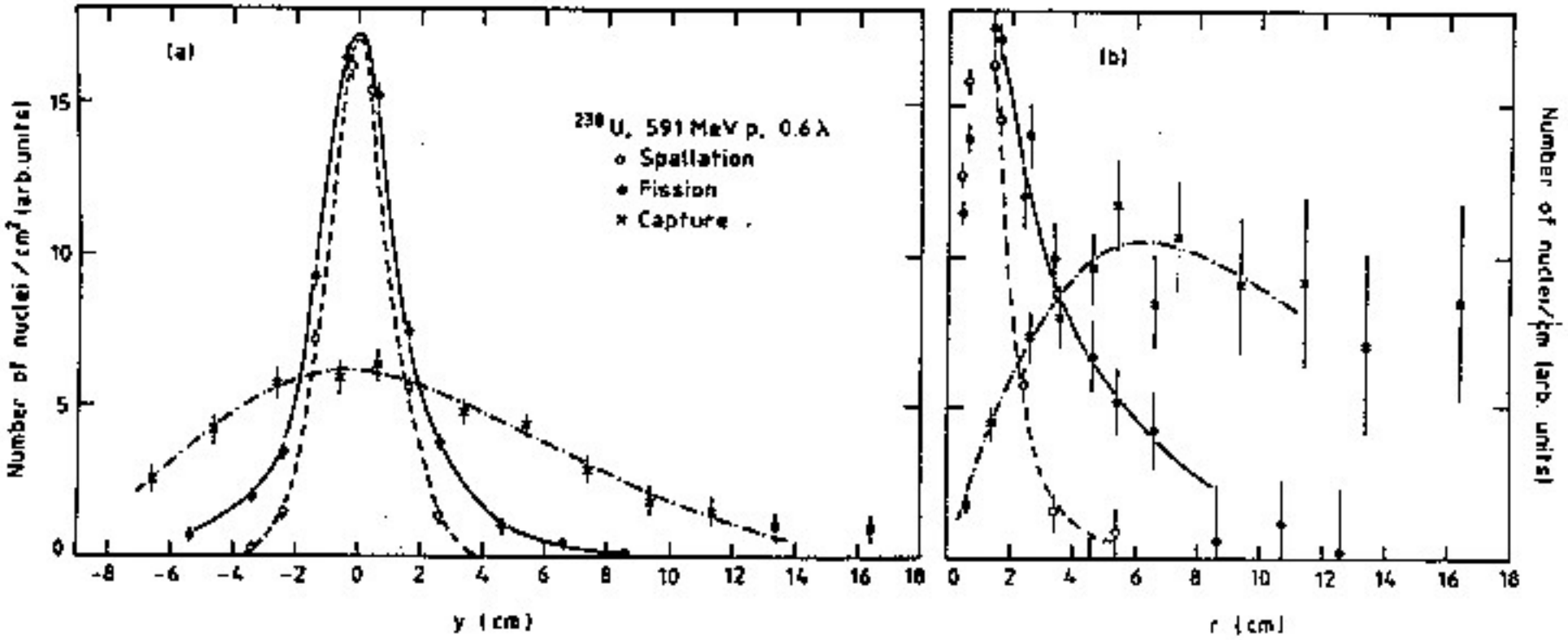

TUNING e/h

GENERALLY, $e/h > 1$

SEVERAL SCENARIOS CAN BE CONSIDERED TO GET $e/h = 1$

- SUPPRESSION OF E.M. RESPONSE:

  FOR $E_\gamma < 1$ MeV, THE PHOTOELECTRIC EFFECT DOMINATES AS $\sigma_{PE} \sim Z^5$, SO THAT HIGH-Z ABSORBERS WILL HELP REDUCE THE SIGNAL IN ACTIVE MATERIAL (CHANGE THICKNESSES, TOO)

  FOR E_e SMALL, HIGH-Z ABSORBERS WILL ALSO INCREASE MULTIPLE SCATTERING AND REDUCE THE NUMBER OF PARTICLES REACHING ACTIVE LAYER.

- BOOST NEUTRON FRACTION THROUGH FISSION (SELECT MATERIAL)

- TUNE NEUTRON RESPONSE:

  USE HYDROGENOUS MATERIAL IN ACTIVE LAYER TO TRANSFER MORE E_n^{kin} TO RECOIL PROTONS

  CHANGE RATIO R_d OF ACTIVE TO PASSIVE THICKNESSES

  CHANGE SIGNAL INTEGRATION TIME

  ... ENERGY FRACTION IN SOFT NEUTRONS

  ... SIGNAL SATURATION FOR SLOW PROTONS

SATURATION

L = LIGHT PRODUCED
E = PARTICLE ENERGY

$\frac{L}{E} = 1$ FOR MIP

BIRK'S LAW:

$$\frac{dL}{dx} = \frac{dE/dx}{1 + kB\ dE/dx}$$

OR:

$$\frac{L}{E} = \left[\int_0^{x_{source}} \left(1 + kB \frac{dE}{dx}\right) dx \right]^{-1}$$

L/E IN SCINTILLATOR

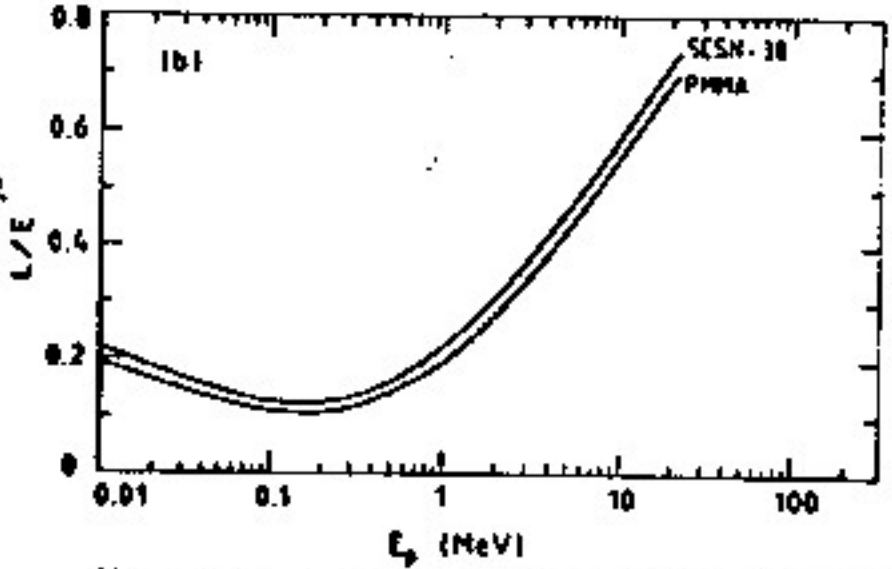

→ FACTOR 4-5 AT LOW E_p

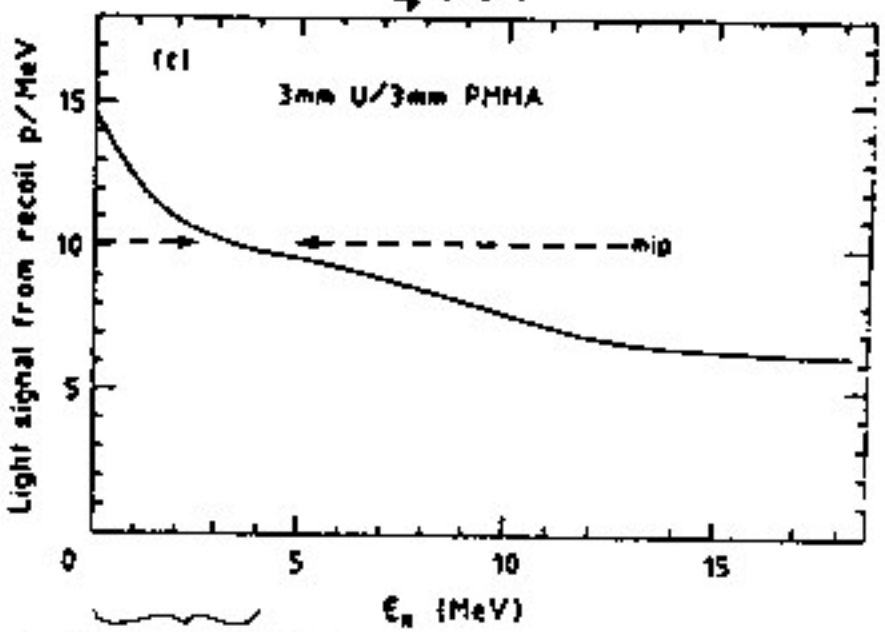

SATURATION FROM LOW-E PROTONS

NEUTRON RESPONSE

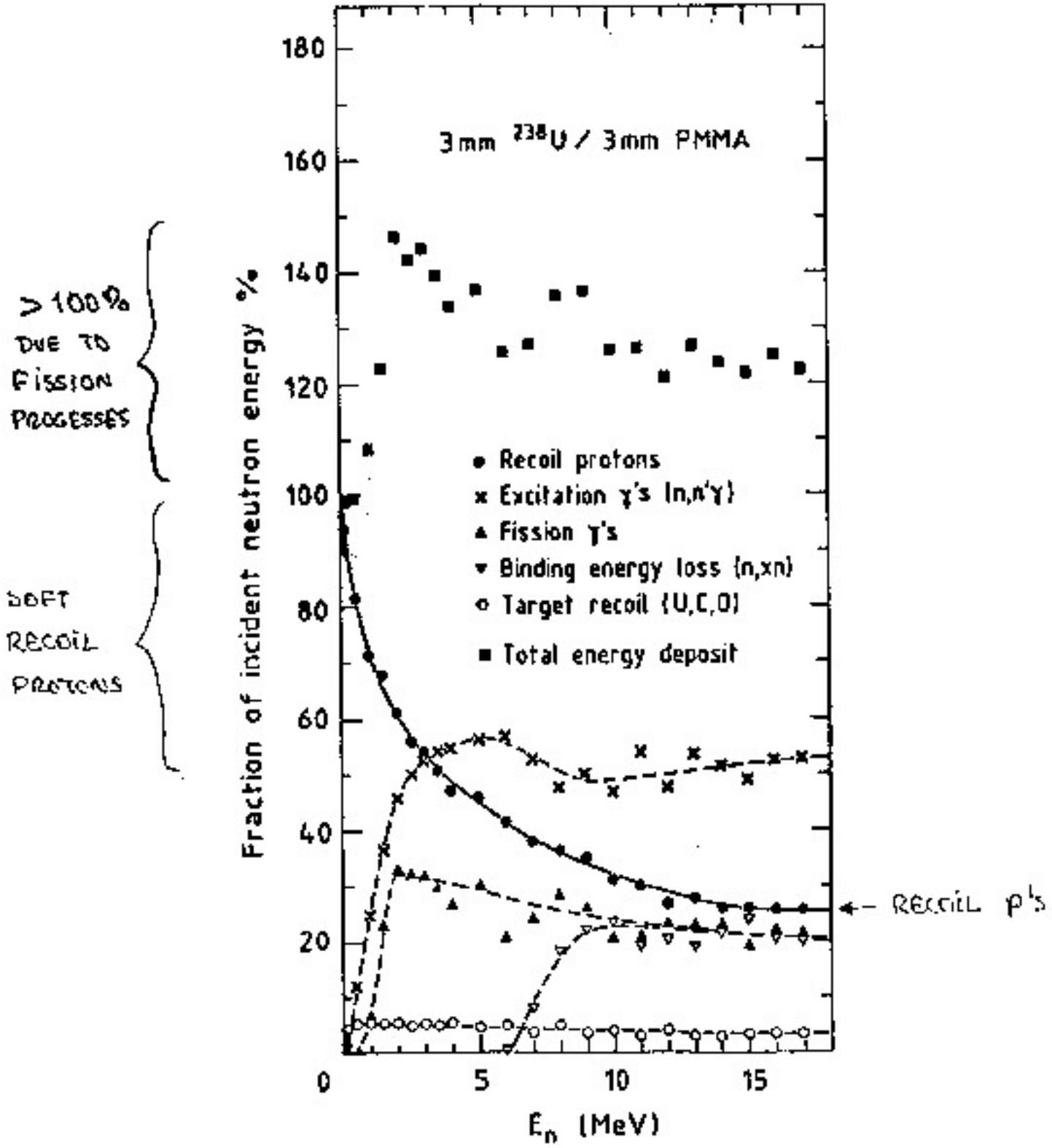

A THICK SCINTILLATOR MEANS THAT SOFT RECOIL PROTONS ARE WITHIN RANGE AND THAT ALL THEIR ENERGY IS DETECTED.

SAMPLING FRACTION

THE NEUTRON ENERGY DEPOSITION (VIA RECOIL PROTONS) IS NOT SAMPLED SINCE THE NEUTRON CONTRIBUTION DECREASES WITH INCREASING SAMPLING FRACTION, BUT m/mip INCREASES " " " " ⇒ TUNING!

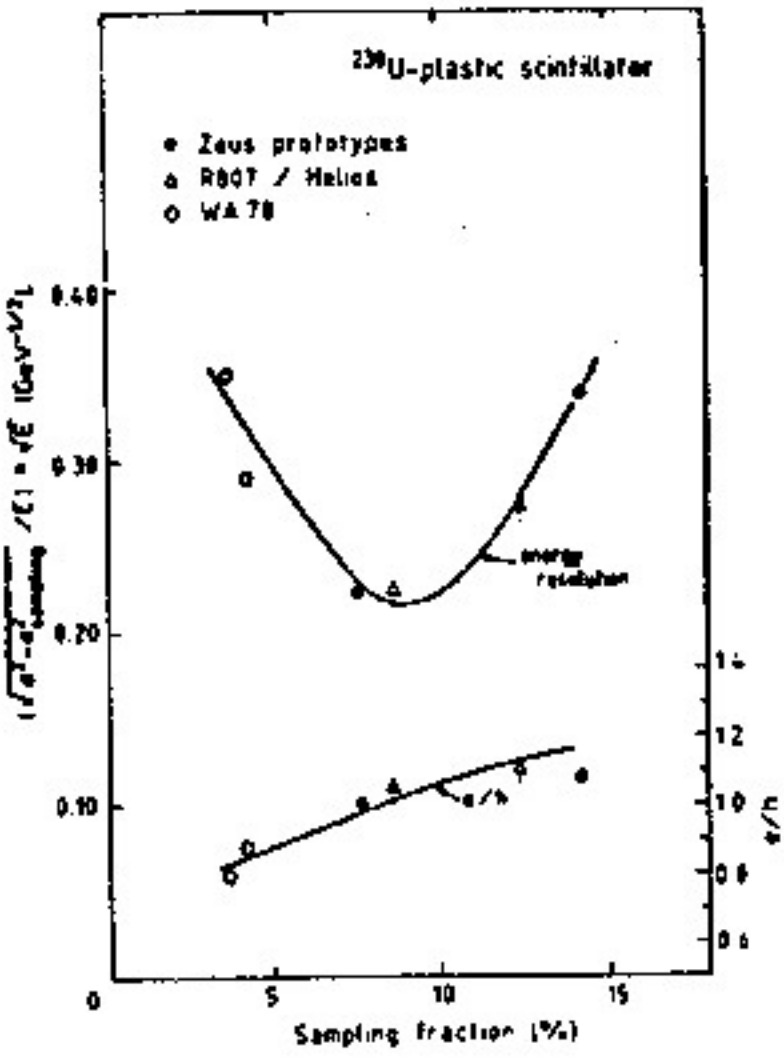

NONSAMPLING PART OF σ/E

e/h

MINIMUM RESOLUTION DOES NOT NECESSARILY OCCUR AT $e/h = 1$ FOR ALL ENERGIES SIMULTANEOUSLY. THIS ALSO DEPENDS ON THE RESPECTIVE THICKNESSES.

n/mip

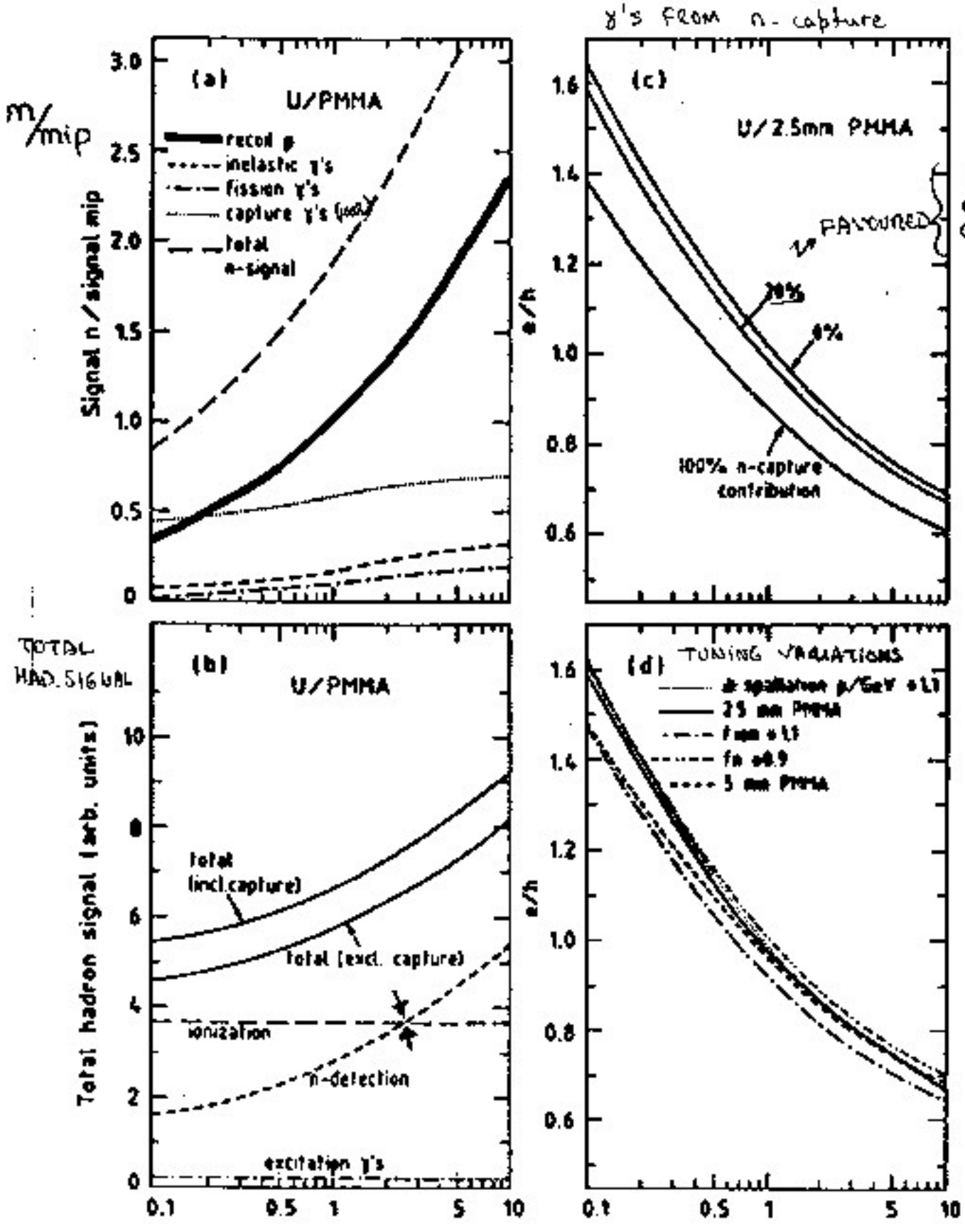

γ's from n-capture

μsec PROCESS CUT BY THE GATE WIDTH

TOTAL HAD. 516 MIP

$$R_d = \frac{\text{ABSORBER}}{\text{ACTIVE}} \text{ (THICKNESSES)} \qquad R_d$$

U + DIFFERENT READOUT MATERIALS

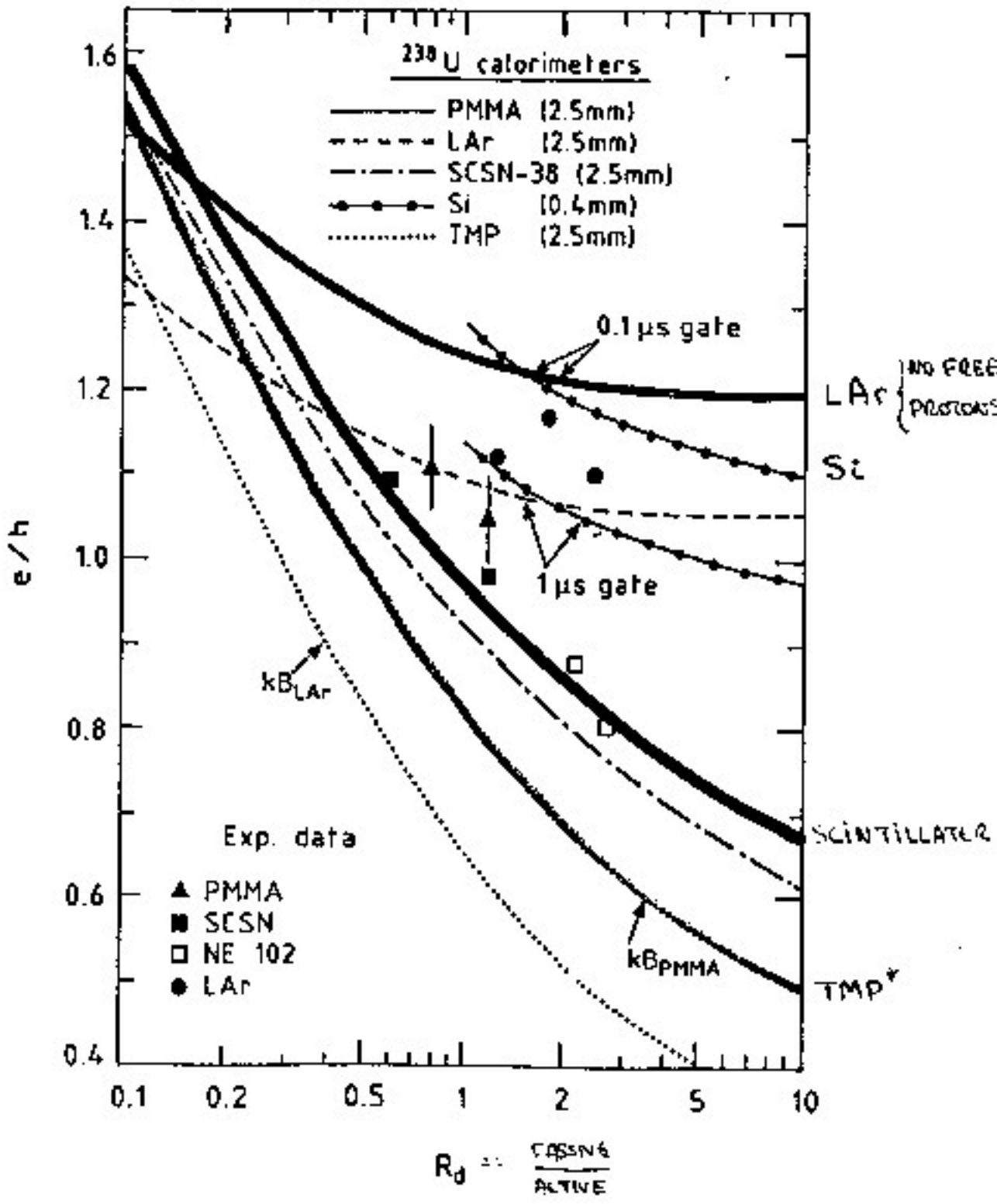

* TMP = TETRAMETHYLPROPYLTHANE

Pb + DIFFERENT READOUT MATERIALS

WITH SCINTILLATOR: $R_D^{Pb} \approx R_D^{T} \times 4$ (to get $e/h = 1$)

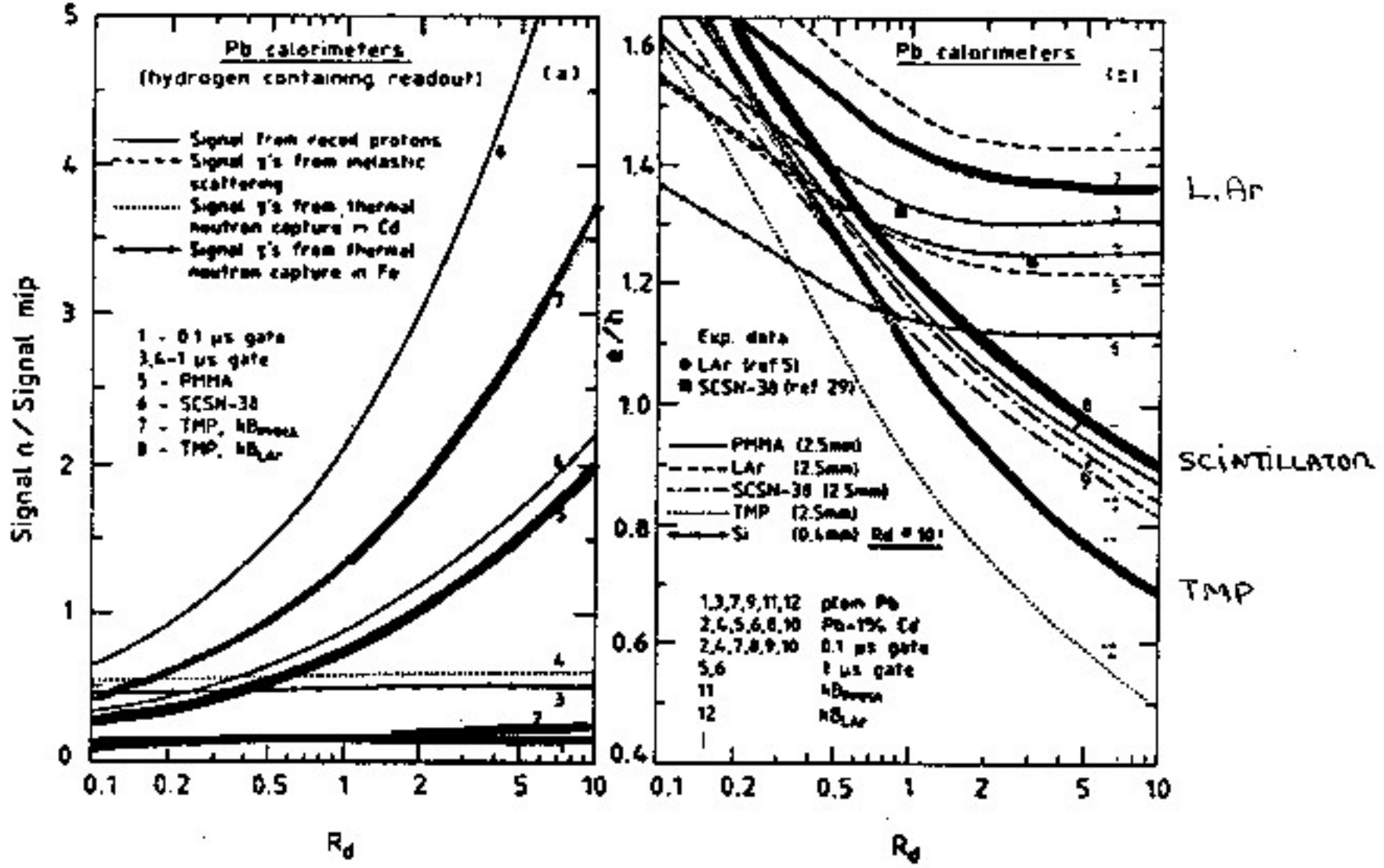

Fe + DIFFERENT READOUT MATERIALS

WITH SCINTILLATOR: NEXT TO IMPOSSIBLE TO GET REASONNABLE e/h EXCEPT FOR EXTREMELY HIGH ENERGIES

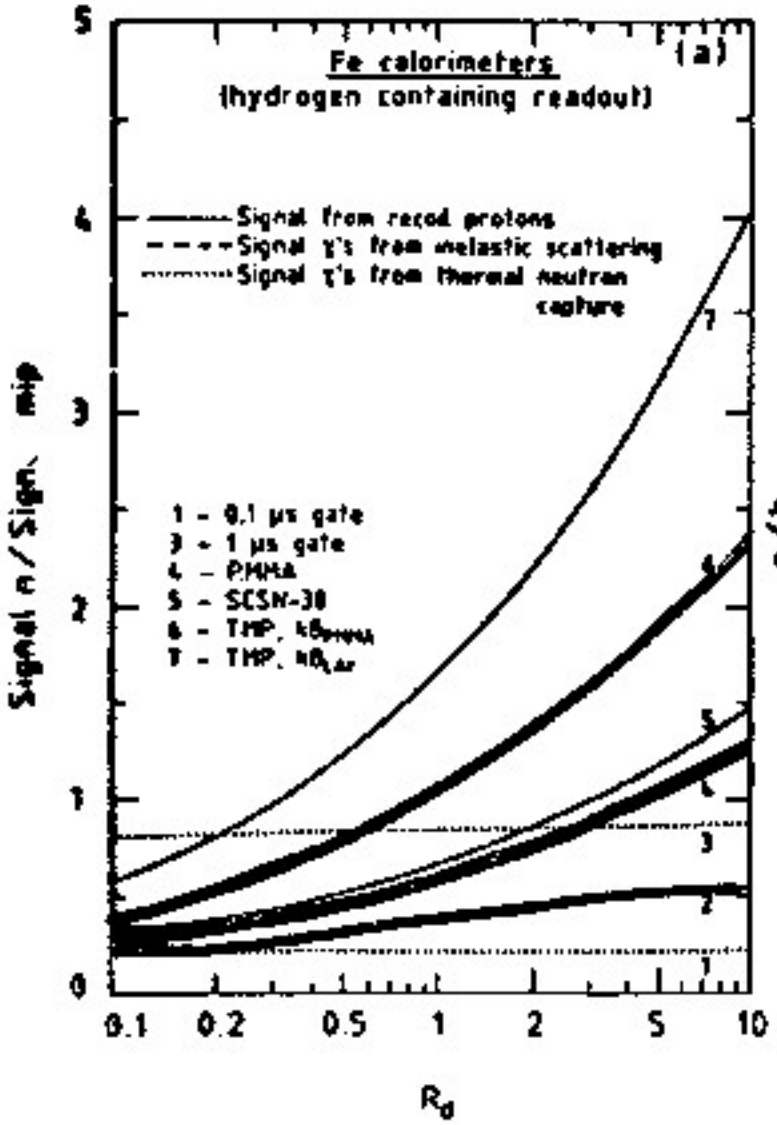

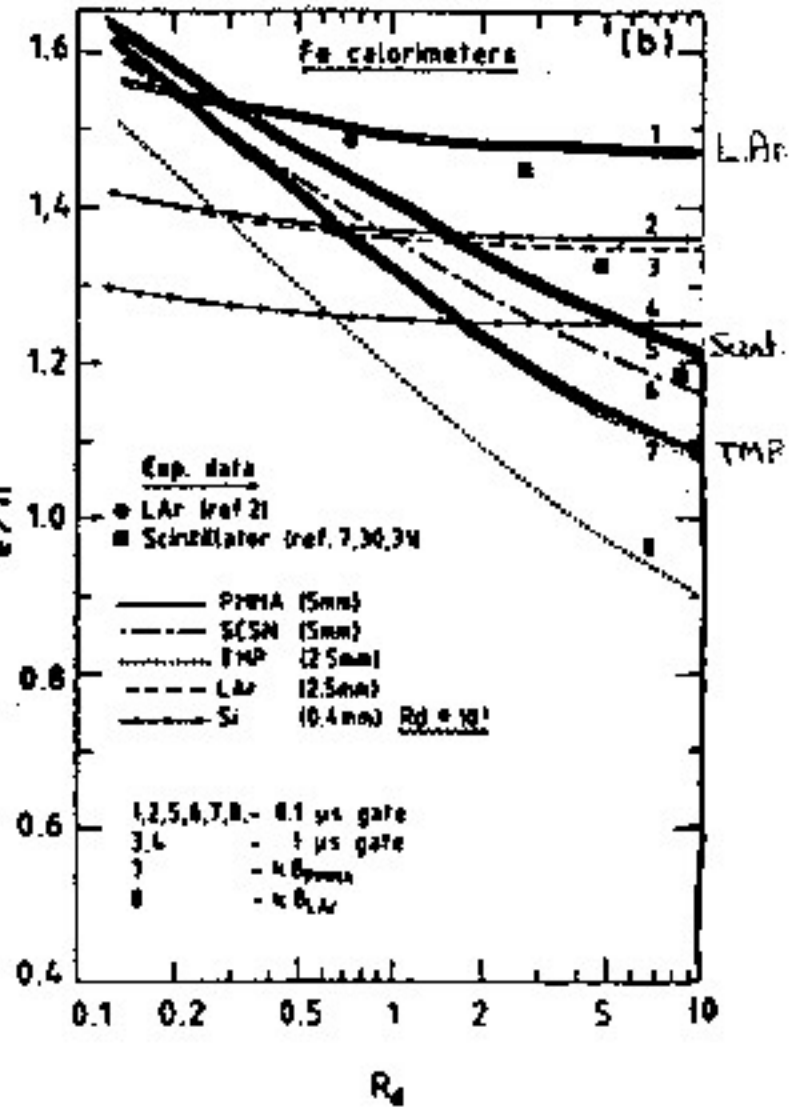

HADRONIC ENERGY RESOLUTION

- SAMPLING FLUCTUATIONS

  ΔE = LOST IN 1 ABSORBER LAYER

$$\frac{\sigma_{\text{SAMPLING}}}{E} \approx 0.09 \left\{ \frac{\Delta E\,[\text{MeV}]}{E\,[\text{GeV}]} \right\}^{1/2}$$

- DEVIATIONS FROM $e/h = 1$

$$\frac{\sigma_{\text{DEVIATIONS}}}{E} \approx 0 \quad \text{FOR} \quad e/h = 1$$

- DETECTOR IMPERFECTIONS { CONTAINMENT, UNIFORMITIES, ...

$$\frac{\sigma_{\text{DETECTOR}}}{E} \approx 1\% \quad \text{POSSIBLE?}$$

- INTRINSIC ENERGY RESOLUTION

$$\frac{\sigma_{\text{INTRINSIC}}}{E} \approx \frac{30\text{-}35\%}{\sqrt{E}}$$

LARGE EVENT-BY-EVENT FLUCTUATIONS

- BINDING ENERGY LOSSES
  - → UP TO ~40% IN HIGH-Z MATERIALS
  - → CORRELATED TO NEUTRON ENERGIES
- LOW-ENERGY PROCESSES
  - ⇒ ENERGY RESOLUTION FOR NEUTRONS
  - ⇒ IDEM FOR γ'S

} AT LOW ENERGIES

π AND γ ENERGY RESOLUTIONS

in the MeV range

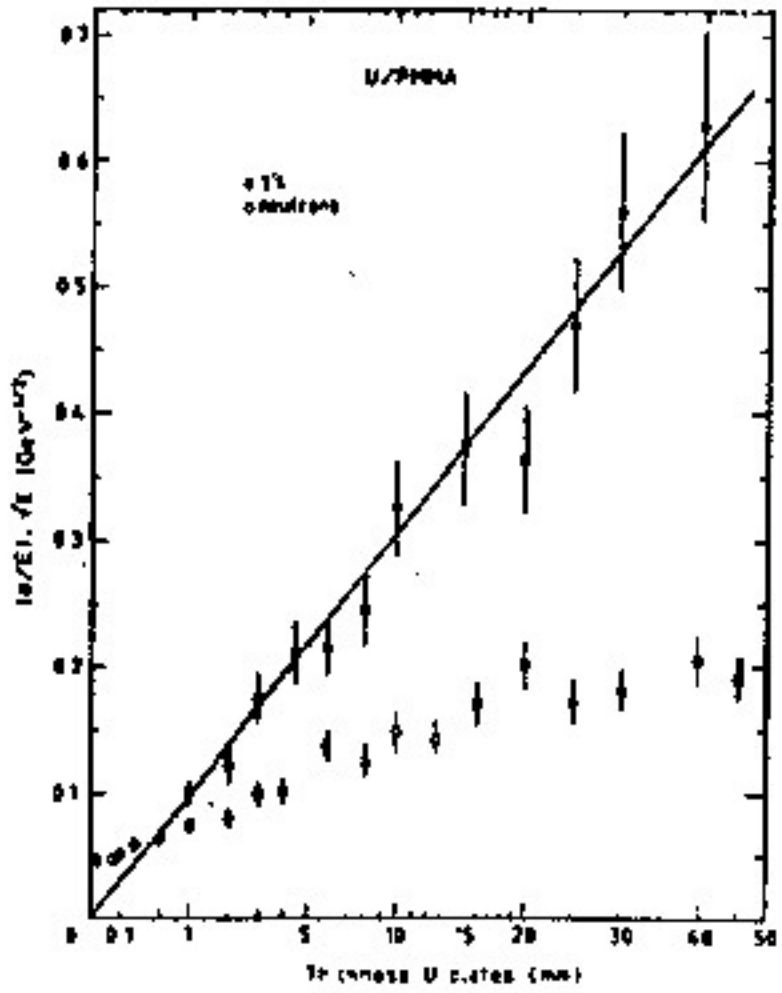

γ's

π's

BINDING ENERGY LOSSES AND INTRINSIC RESOLUTION

via n-capture

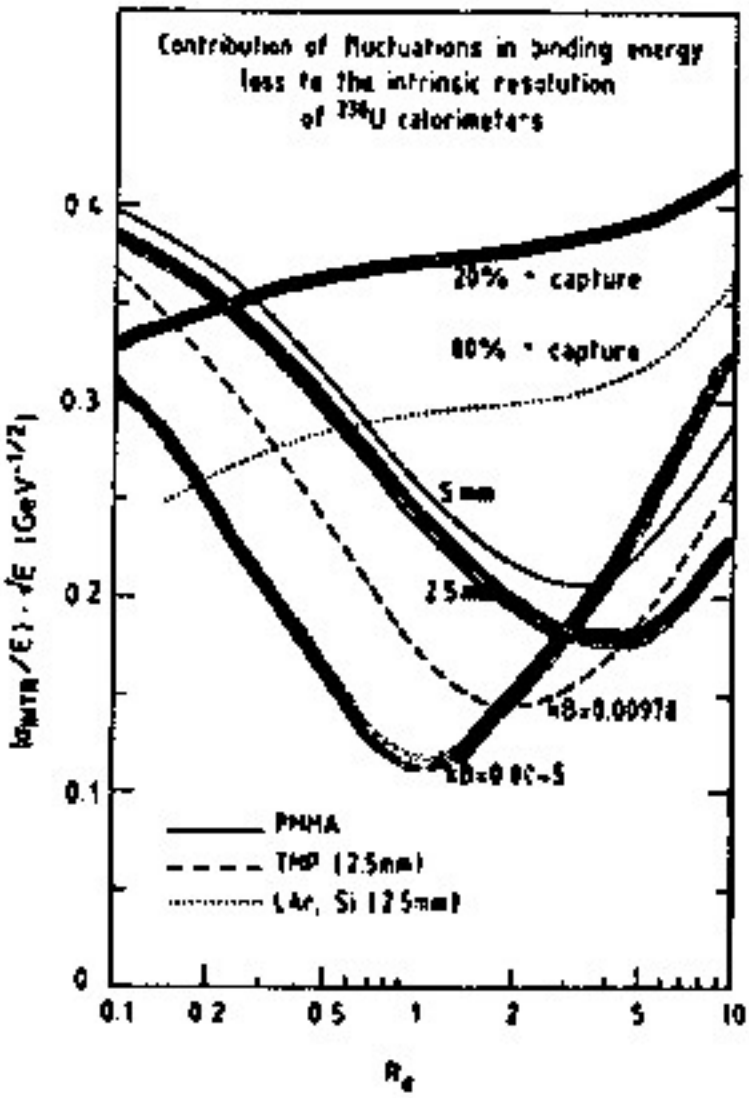

LAr

TMP

Scint.

U + SCINTILLATOR : ENERGY RESOLUTION

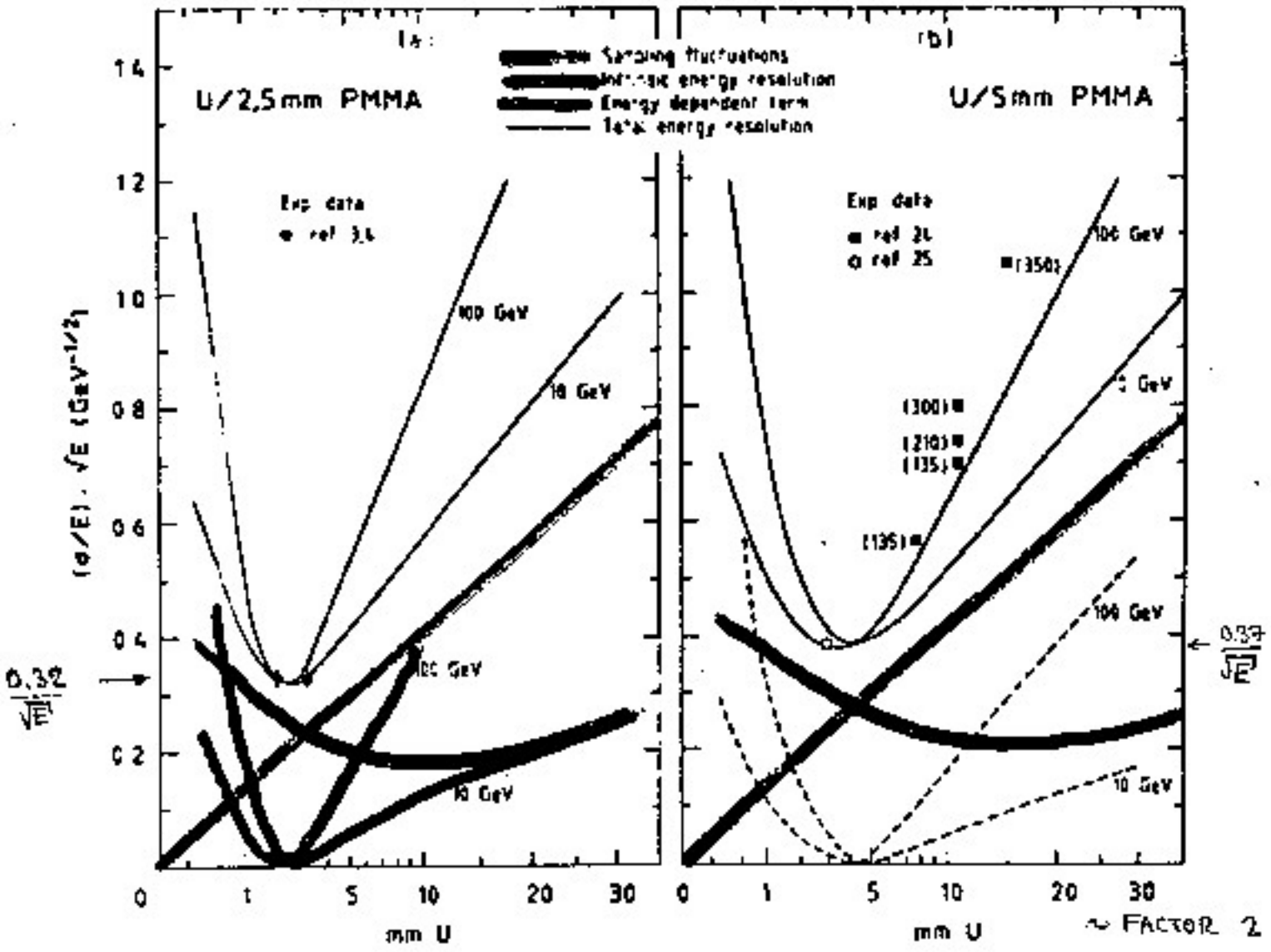

INTRINSIC (BINDING ENERGY LOSS)

SAMPLING

ENERGY DEPENDENT (FROM $e/h \neq 1$)

U + LIQUID ARGON : ENERGY RESOLUTION

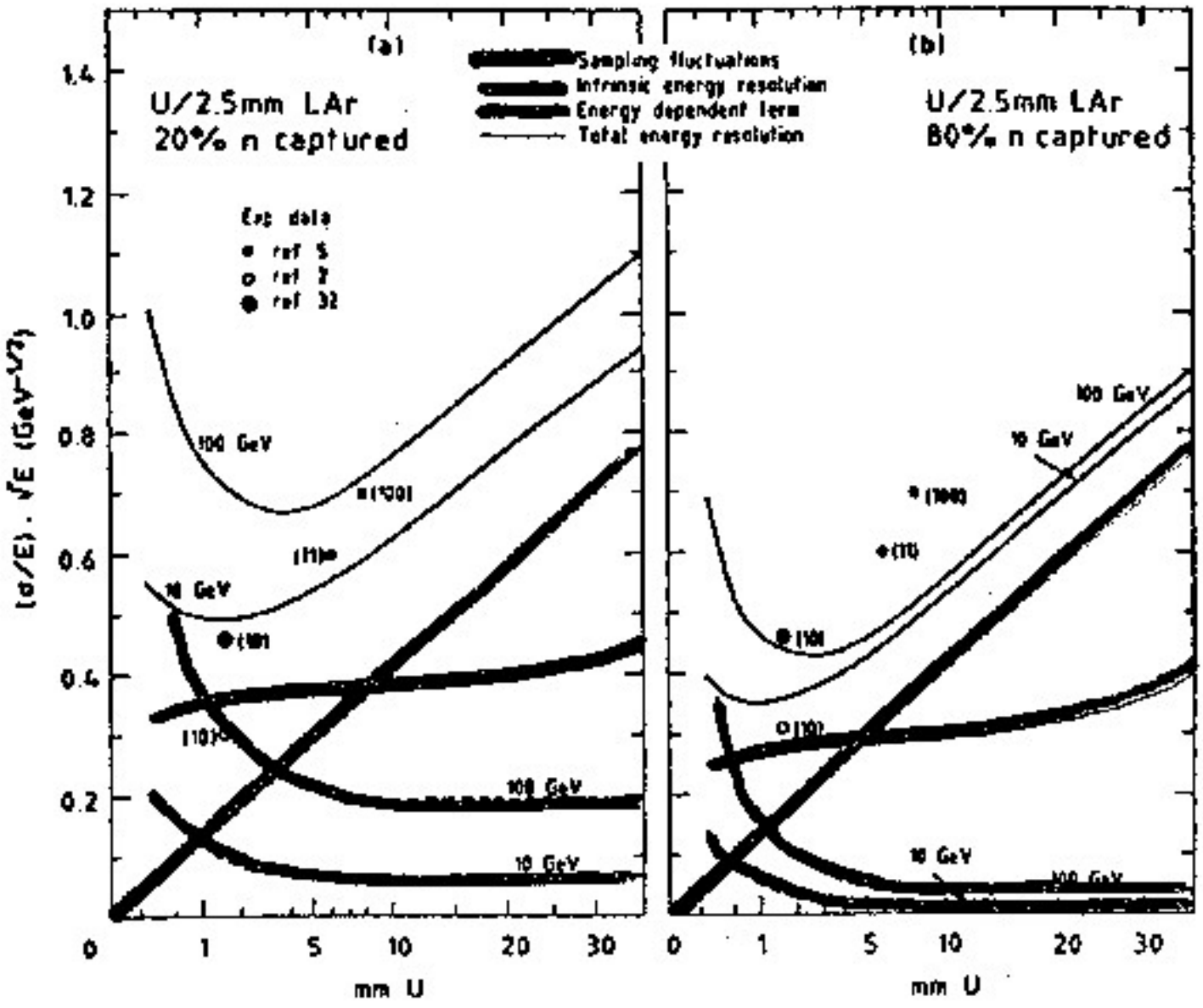

$\frac{\sigma_E}{E}$ NOT PROPORTIONAL TO $\frac{1}{\sqrt{E}}$

Pb + SCINTILLATOR : ENERGY RESOLUTION

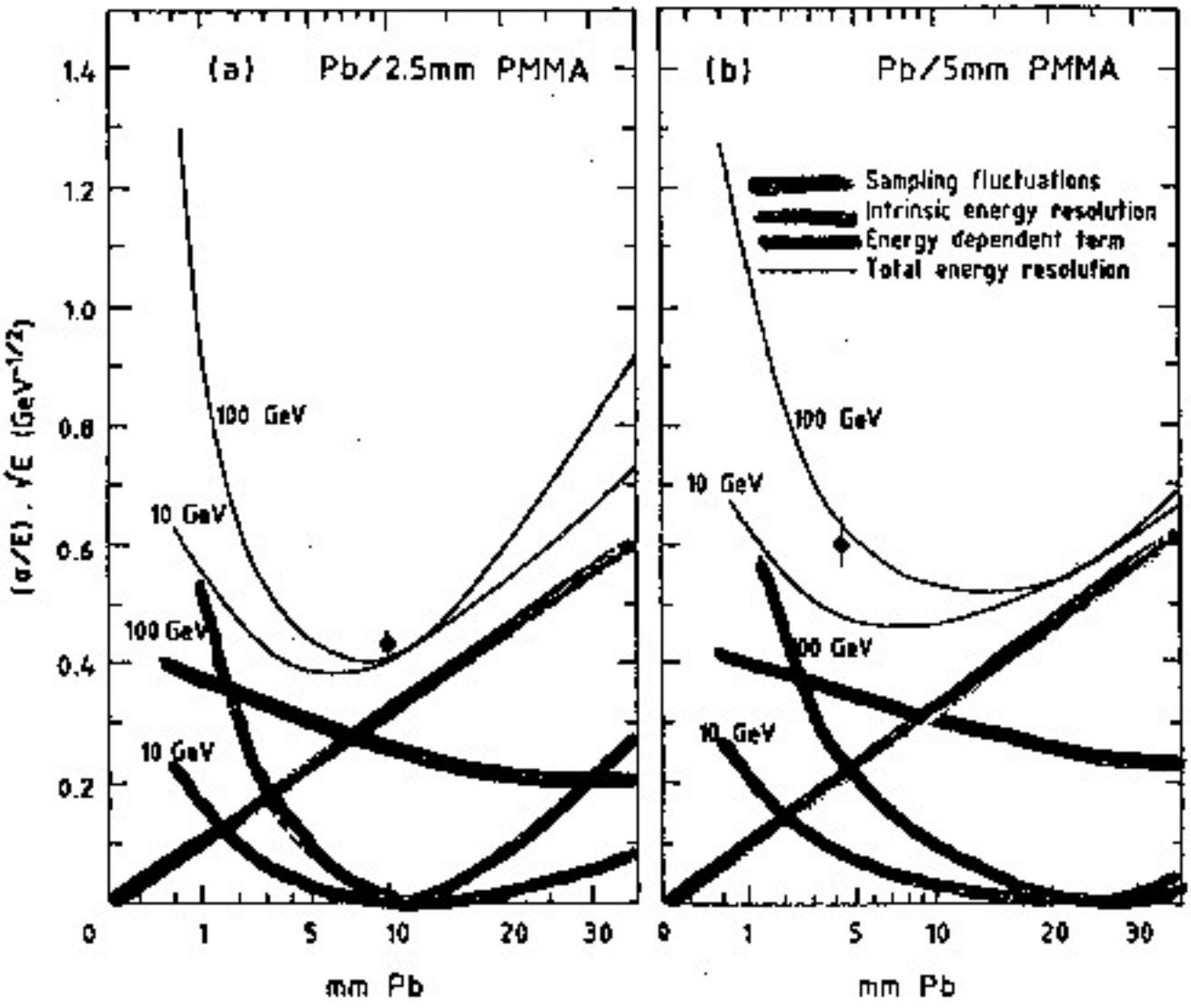

↳ ~ 4 TIMES THICKER ABSORBER WRT U + SCINTILLATOR

Fe + SCINTILLATOR : ENERGY RESOLUTION

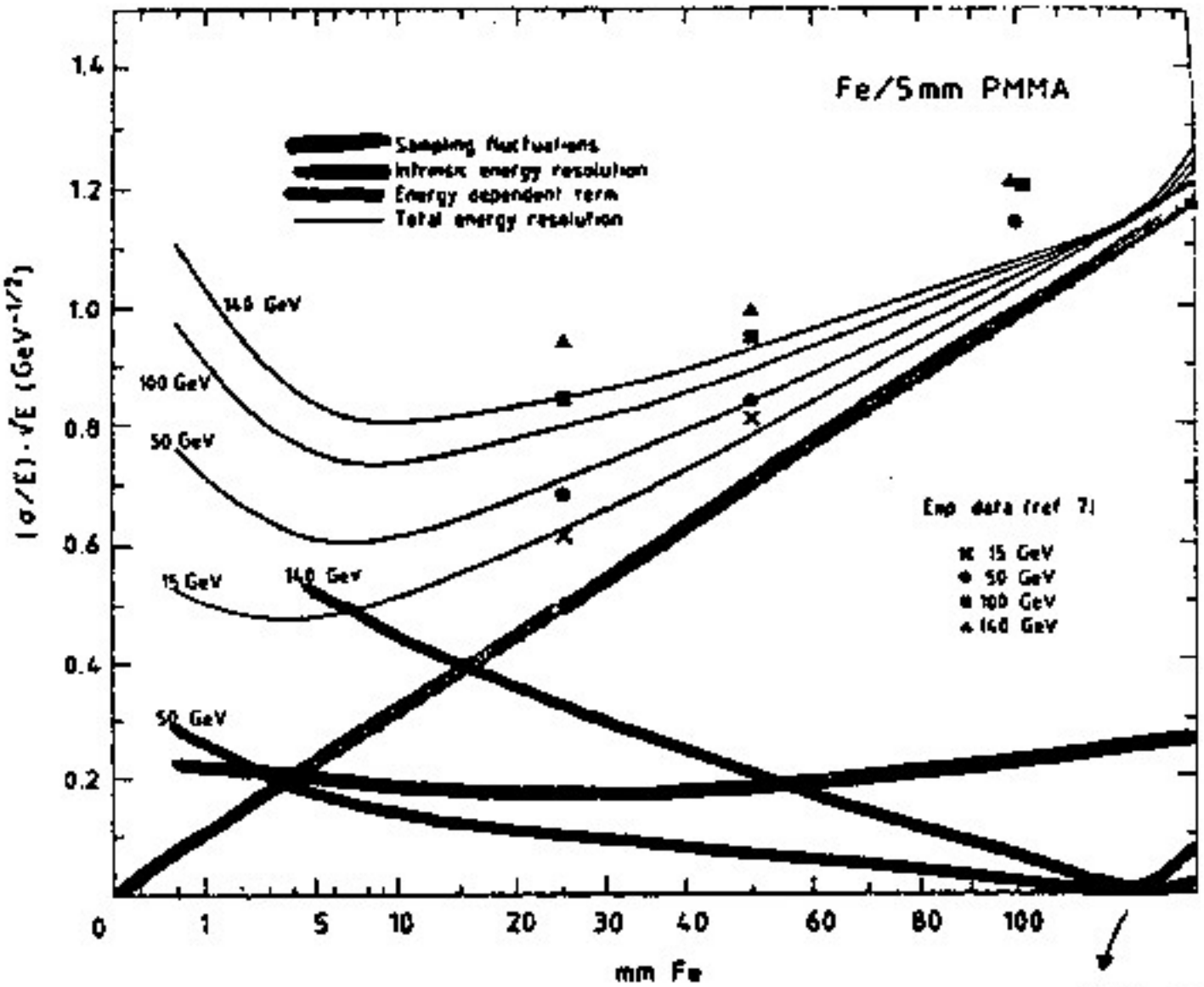

I.E. ONLY FOR VERY HIGH ENERGIES

CONTRIBUTIONS TO RESOLUTION

Mechanisms (add in quadrature)	Electromagnetic showers	Hadronic showers
Intrinsic shower fluctuations	Track-length fluctuations: $\sigma/E \geq 0.005/\sqrt{E}$ (GeV).	Fluctuations in the energy loss: $\sigma/E \simeq 0.45/\sqrt{E}$ (GeV). Scaling weaker than $1/\sqrt{E}$ for high energies. With compensation for nuclear effects: $\sigma/E \simeq 0.22/\sqrt{E}$ (GeV).
Sampling fluctuations	$\sigma/E \simeq 0.04\sqrt{\Delta E/E}$. Nature of readout may augment sampling fluctuations.	$\sigma/E \simeq 0.09\sqrt{\Delta E/E}$
Instrumental effects	Noise and pedestal width: $\sigma/E \sim 1/E$ – determine minimum detectable signal; – limit low-energy performance.	
	Calibration errors and non-uniformities: $\sigma/E \sim$ constant and therefore limits high-energy performance.	
Incomplete containment of shower	$\sigma/E \sim E^{-\alpha}$, $\alpha < 1/2$ (see subsec. 2.2, resp. 3.4). For leakage fraction $\geq$ few %: non-linear response and non-Gaussian 'tail'.	

a) ΔE = energy loss of a minimum ionizing particle in one sampling layer, measured in MeV; E = total energy, measured in GeV.

LEAKAGE

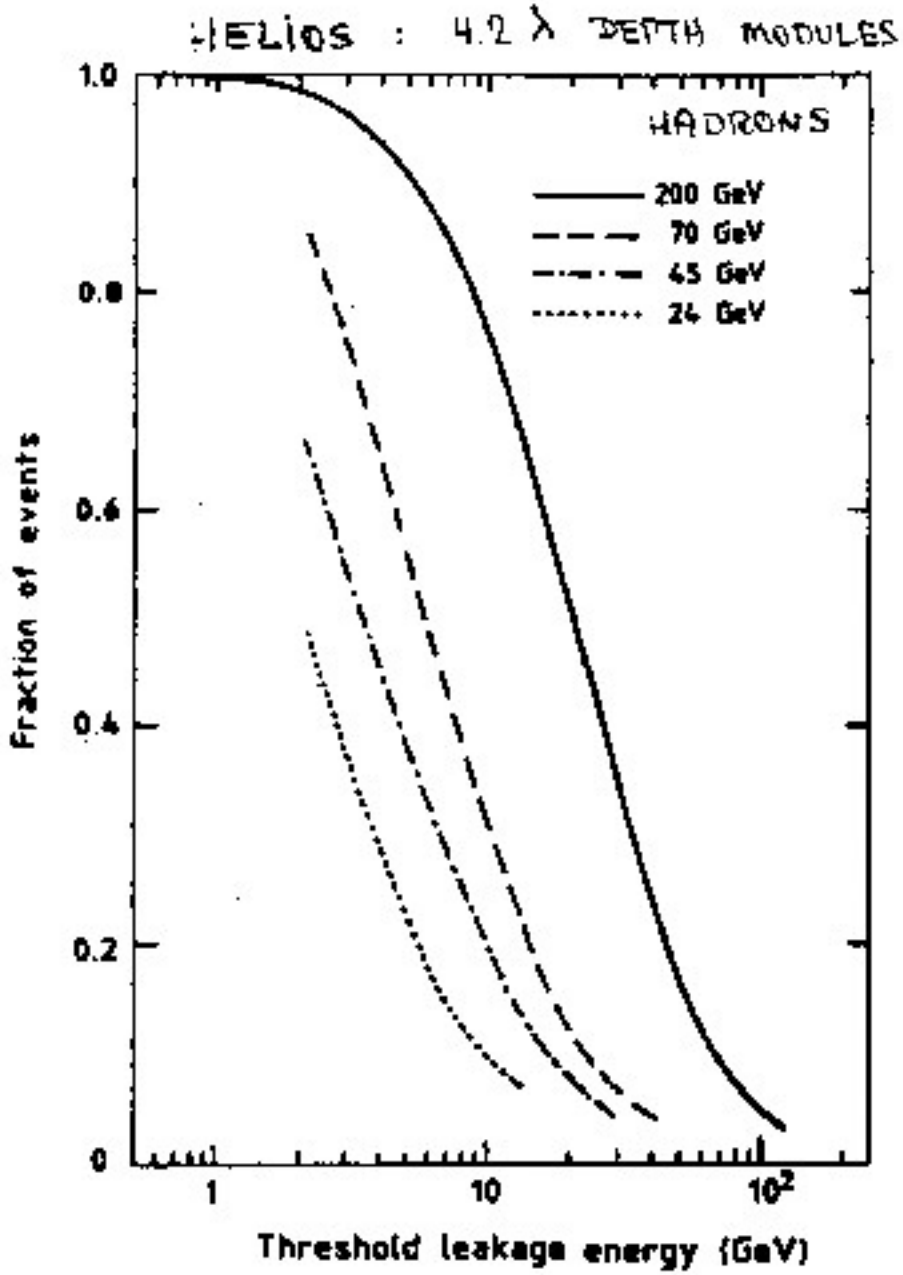

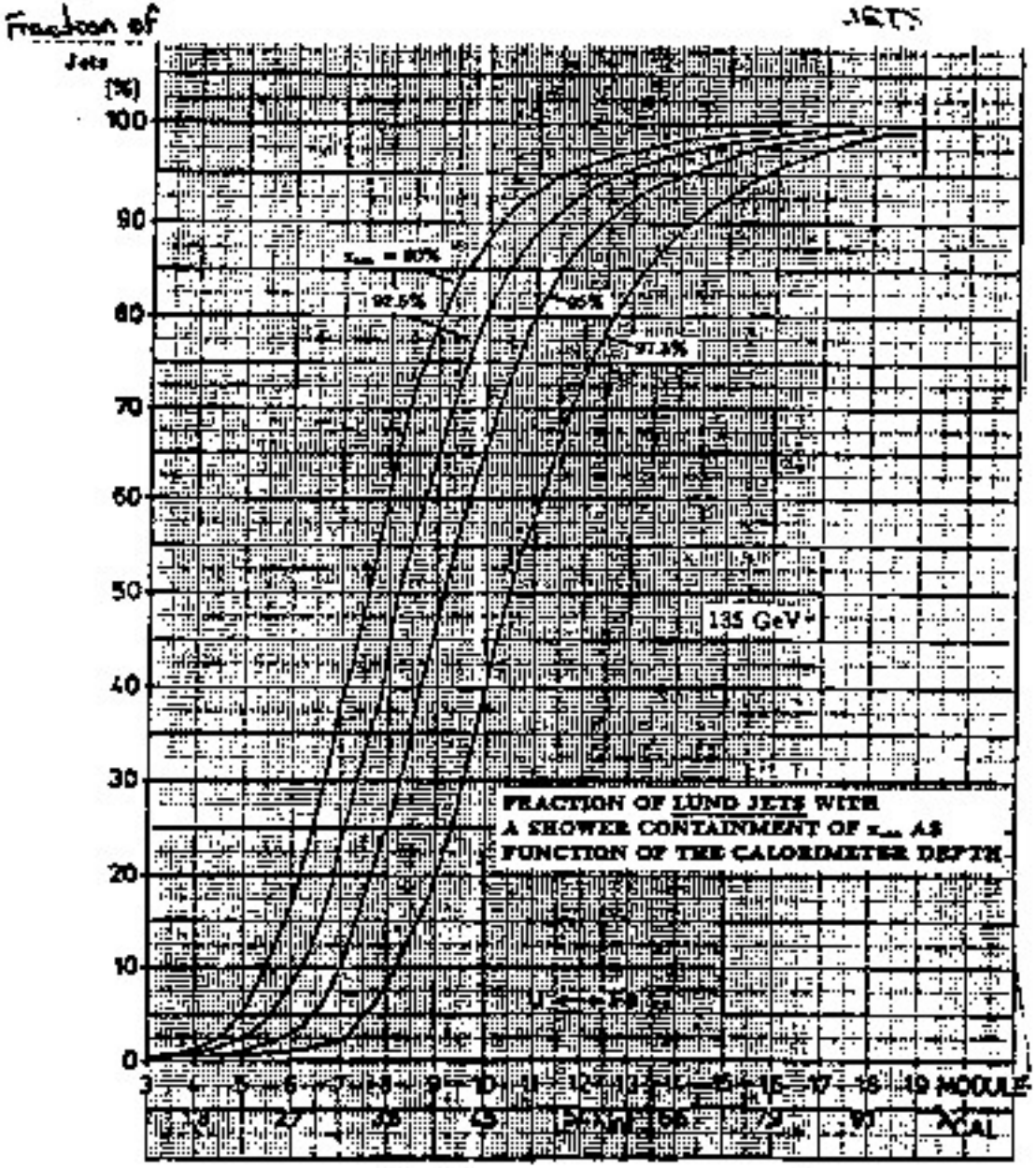

Fraction of LUND jets with a shower containment of x_{cont} as function of the calorimeter depth λ_{CAL} for 135 GeV.

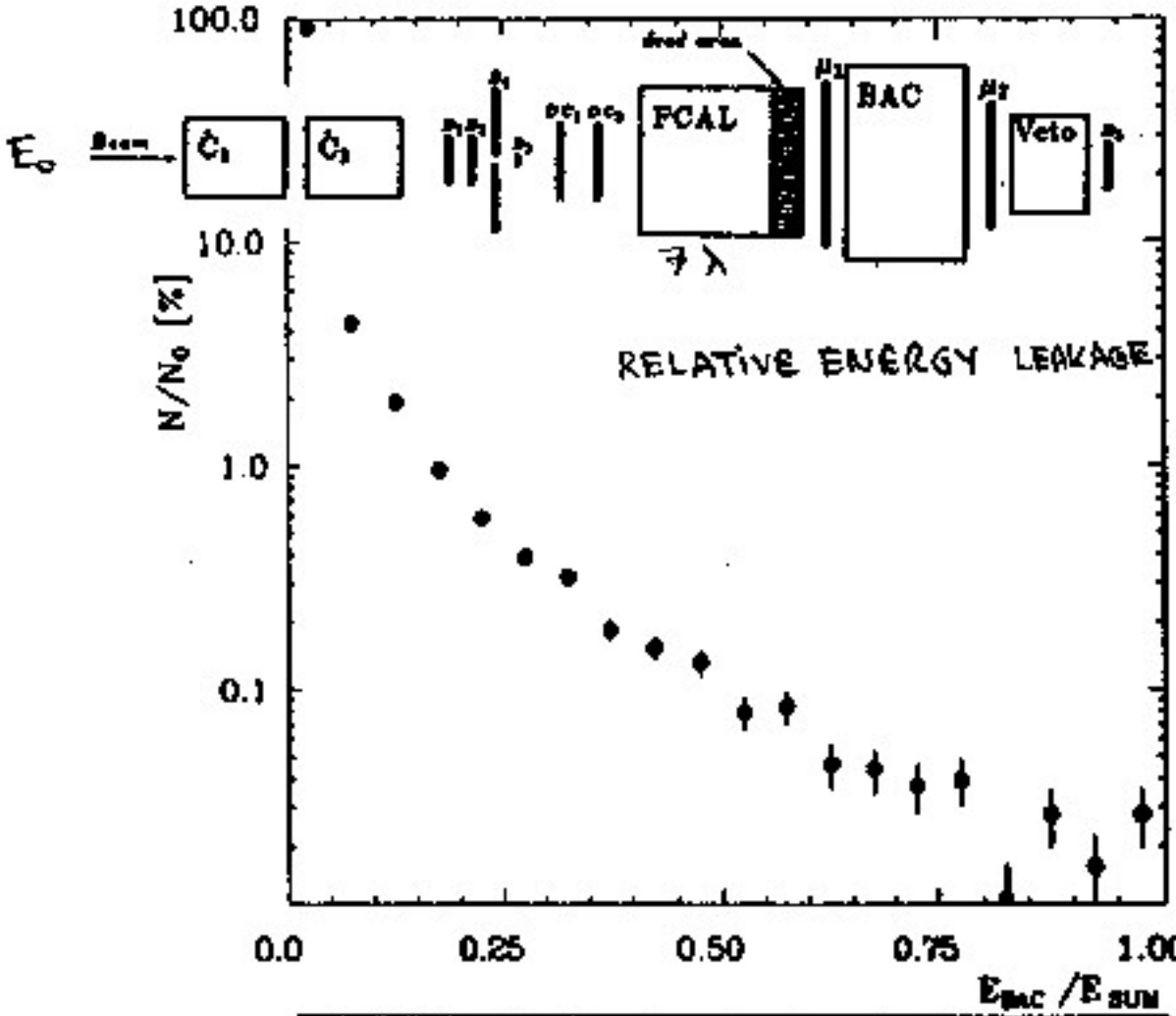

MEASURE LEAKAGE TO RECONSTRUCT SHOWER

$E_{DU} + E_{BAC} \rightarrow E_0$

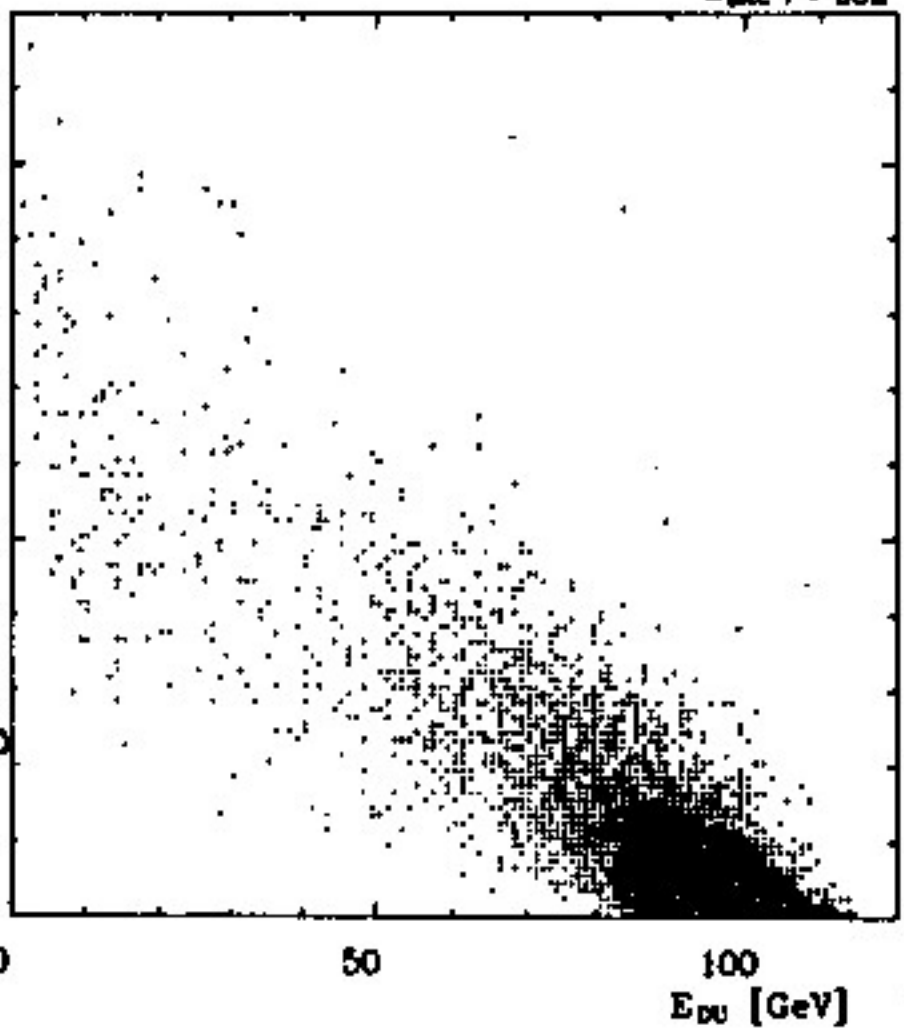

EVEN THOUGH THE "BACKING" CALORIMETER RESOLUTION MIGHT BE POORER, MUCH OF THE GLOBAL ENERGY RESOLUTION IS RECOVERED

RADIATION DAMAGE

LIGHT YIELD LOSS

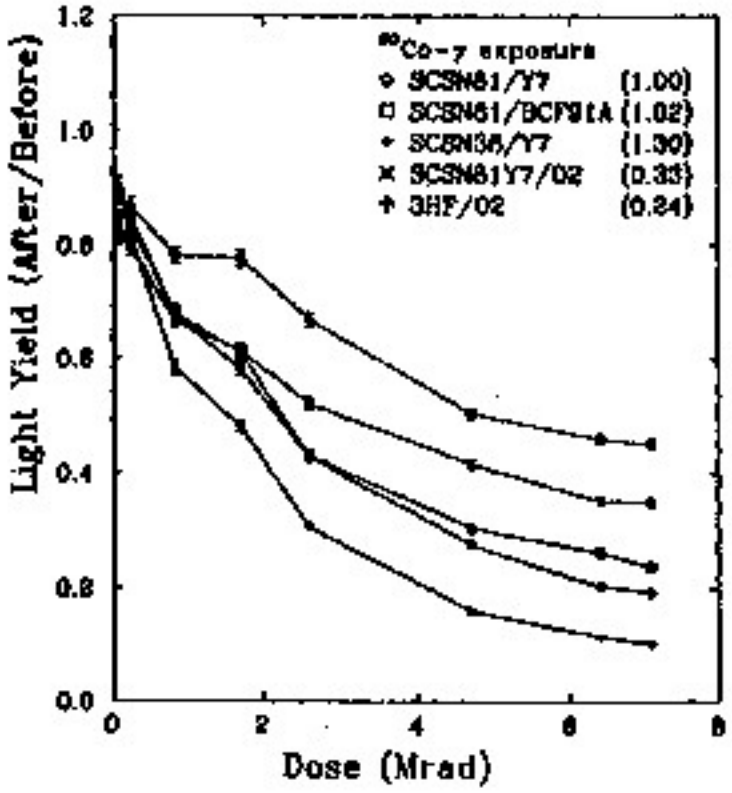

ENERGY RESOLUTION LOSS

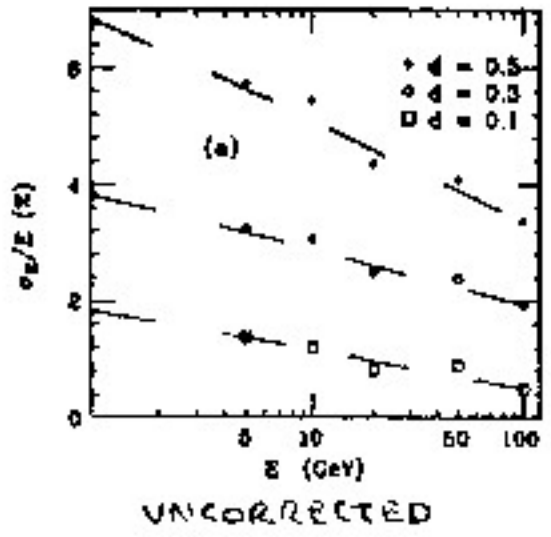

FRACTION DAMAGE

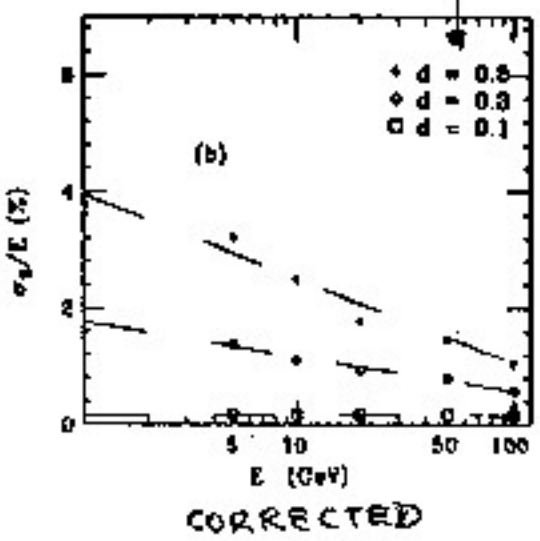

PARTICLE ID

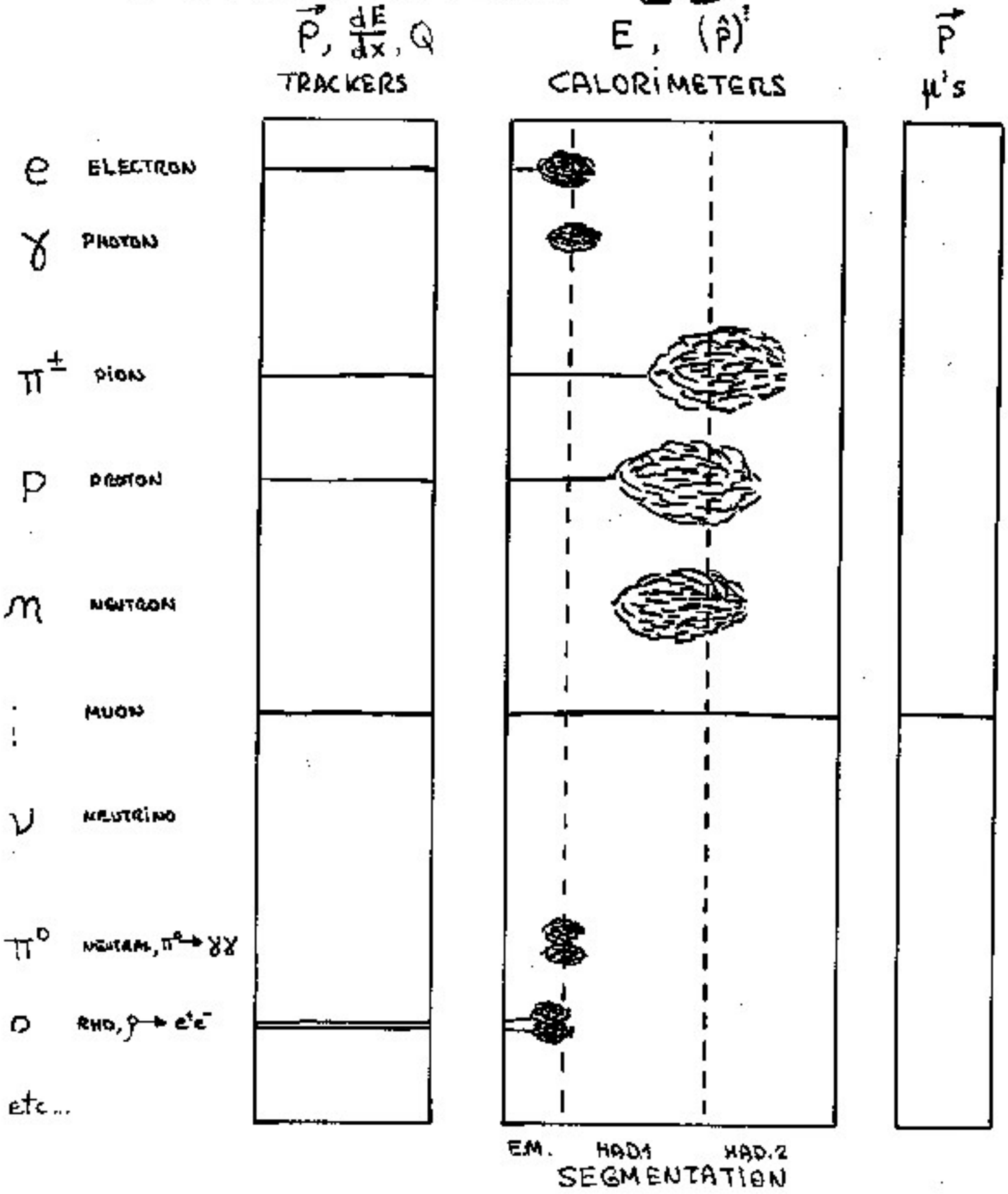
$\vec{p}, \frac{dE}{dx}, Q$
TRACKERS
$E, (\hat{p})^2$
CALORIMETERS
$\vec{p}$
μ's
e ELECTRON
γ PHOTON
$\pi^{\pm}$ PION
p PROTON
n NEUTRON
MUON
ν NEUTRINO
π^0 NEUTRAL, $\pi^0 \to \gamma\gamma$
ρ RHO, $\rho \to e^+e^-$
etc...
EM.
HAD1
HAD.2
SEGMENTATION

PARTICLE IDENTIFICATION

Particle Identification with Calorimeters

Particle produced	Calorimeter technique	Comment
Electron, e	Charged particle initiating the electromagnetic shower	Background from charge exchange $\pi^- N \to \pi^0 + X$ in calorimeter; π discrimination of $\sim$ 10–1000 possible
Photon, γ	Neutral particle initiating the electromagnetic shower	Background from photons from meson decays
$\pi^0, \eta, \ldots \to \gamma\gamma$ $\varrho, \phi, J/\psi, \Upsilon, \ldots$ $\to e^+e^-$	Invariant mass obtained from measurement of energy and angle	Classical application for electromagnetic calorimeters;
Protons, deuterons, tritons, ... and their antiparticles	Comparison of visible energy E_{vis} in calorimeter with momentum of particle	$E_{vis}^{b(\bar{b})} = (\vec{p}_b^{\,2} + m_b^2)^{1/2} - (+)\, m_b$ Protons (antiprotons) identified up to 4 (5) GeV/c; deuterons (antideuterons) correspondingly higher
(Anti)neutrino	Visible energy E_{vis} in calorimeter compared with missing momentum	Important tool for $e^+e^- \to \nu(\bar{\nu}) + X$ and at CERN Collider (FNAL $p\bar{p}$ collider, $pp(p\bar{p}) \to \nu(\bar{\nu}) + X$
Muon	Particle interacting only electromagnetically (range). E_{vis} compared to $\vec{p}$.	Background from non-interacting pions
Neutron or $K_L^0(\bar{n}, \bar{K}_L^0)$	Neutral particle initiating hadronic shower	Some discrimination perhaps possible based on detailed (longitudinal) shower information

PARTICLE IDENTIFICATION

USING LONGITUDINAL SEGMENTATION :

ENERGY DEPOSITION IN THE ELECTROMAGNETIC PART OF THE CALORIMETER

USING ONLY THE CALORIMETERS : 'FAIRLY' EFFICIENT

... COMBINED TO TRACKING INFORMATION: VERY EFFICIENT

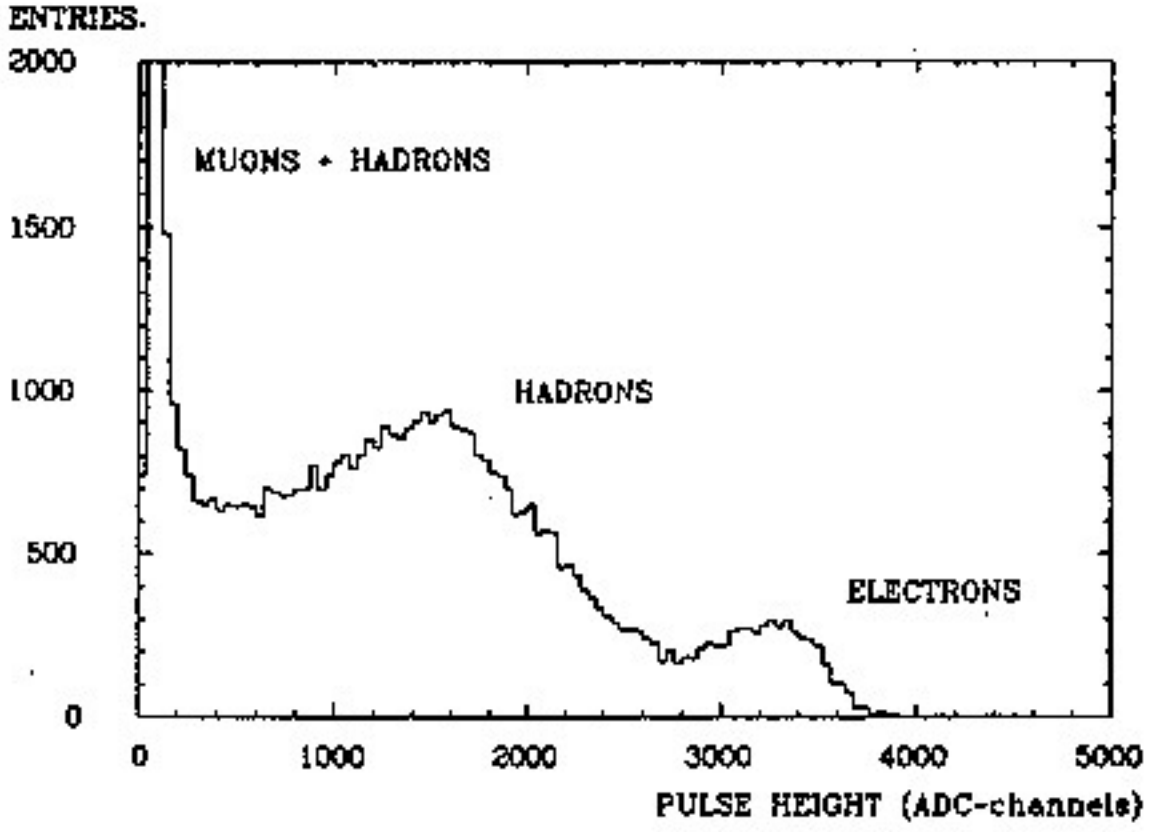

SIGNAL SEPARATION USING ČERENKOV's

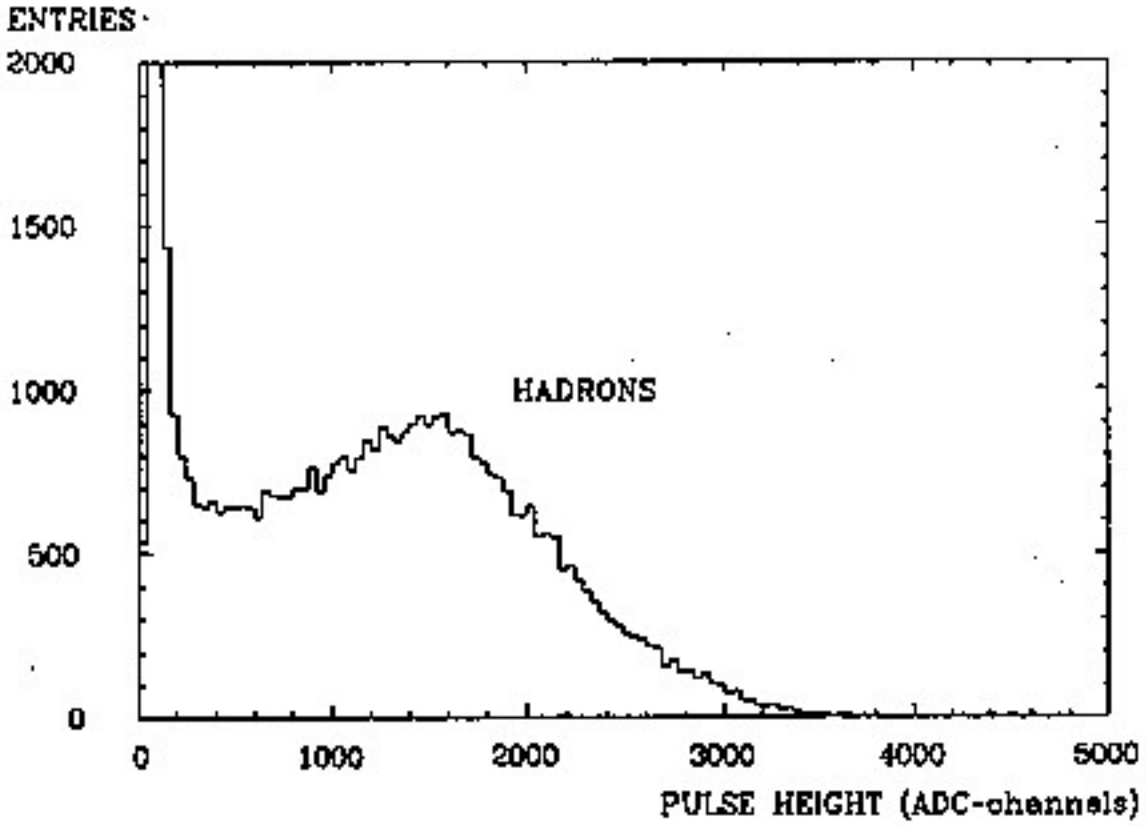

Hadronen im elektromagnetischen Kalorimeter

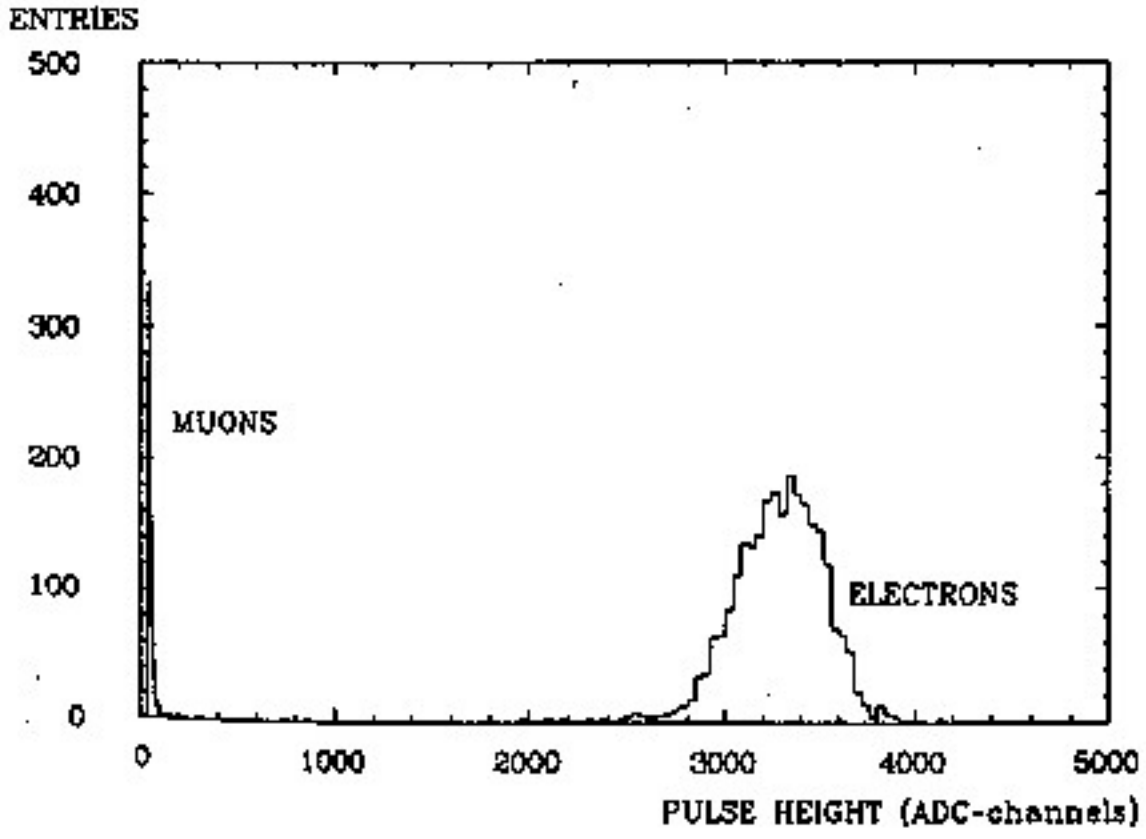

PARTICLE IDENTIFICATION

USING SILICON DIODES LOCATED AT THE EXPECTED (AVERAGE) MAXIMUM OF ELECTROMAGNETIC SHOWERS. $\sim 3.3 X_0$

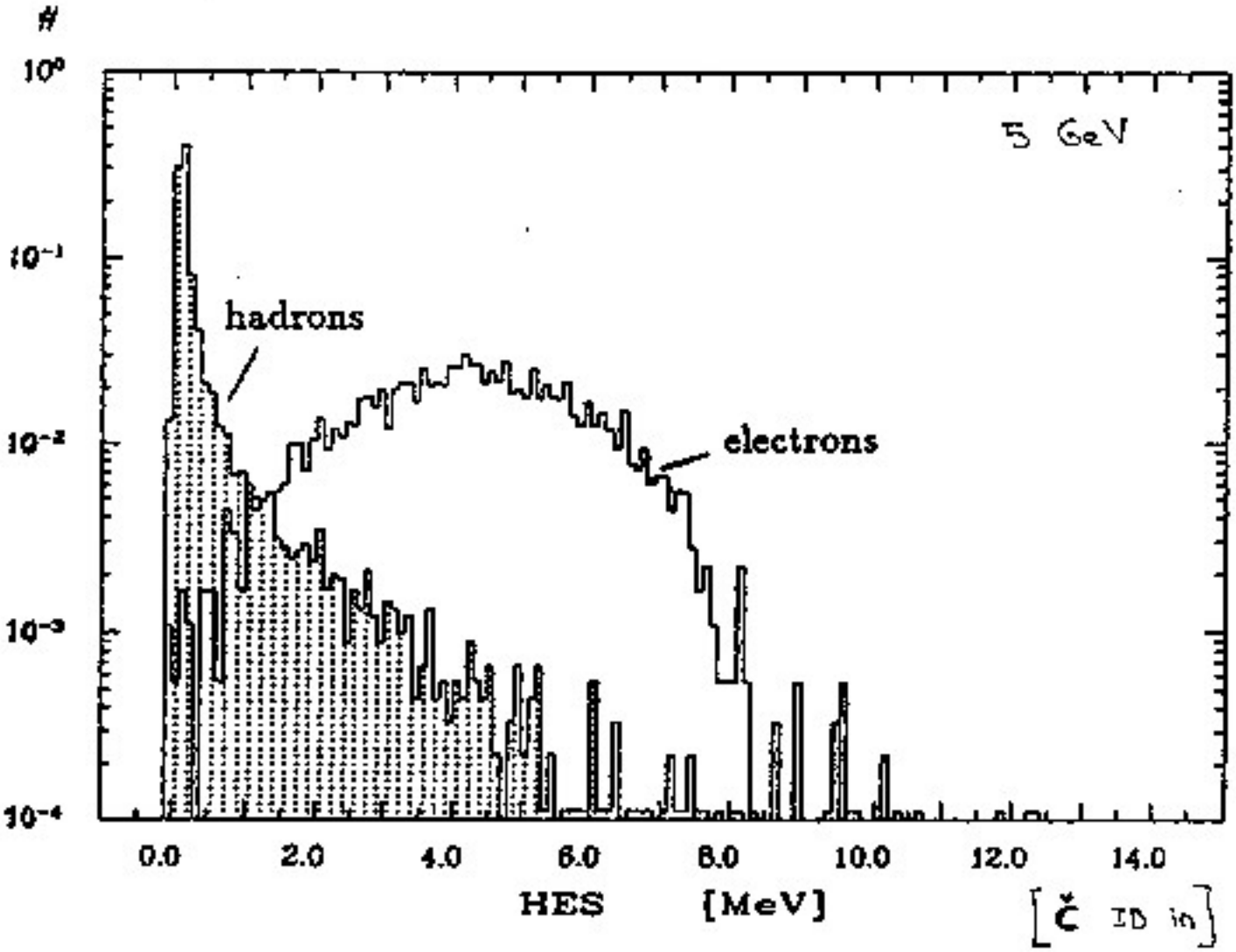

→ IMPROVED SEPARATION BETWEEN ELECTRONS & HADRONS

PARTICLE IDENTIFICATION

USING LATERAL SEGMENTATION

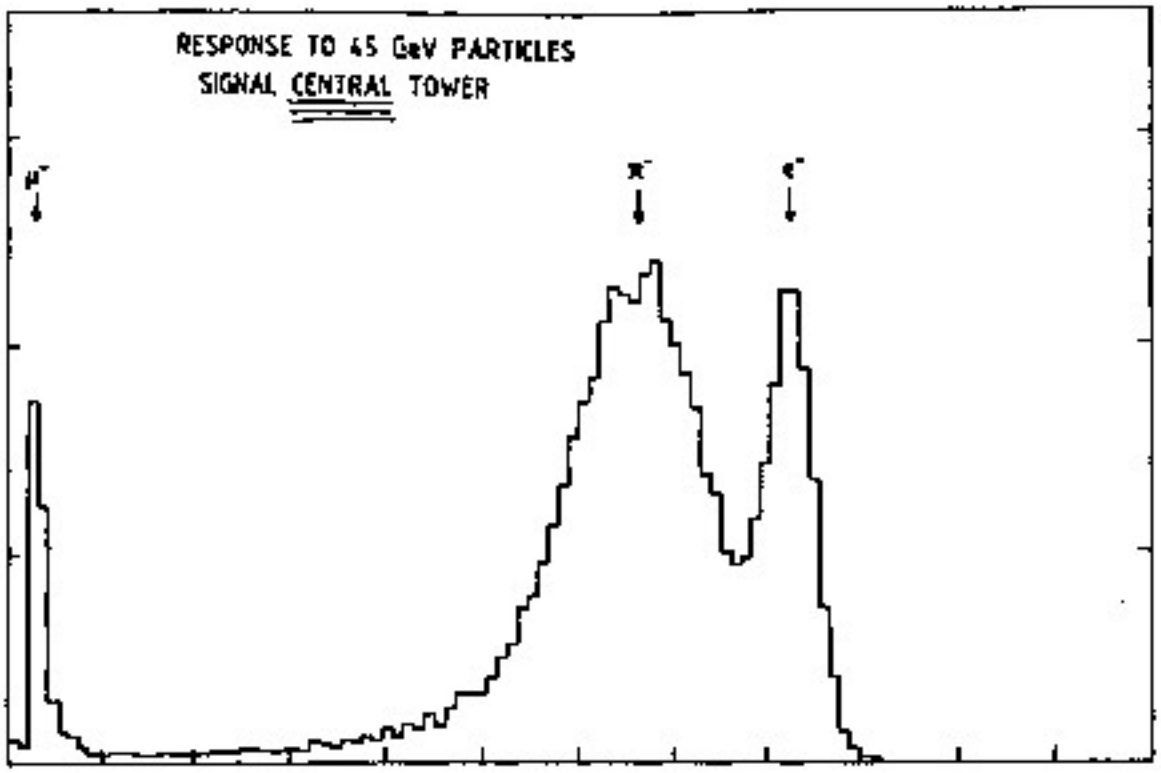

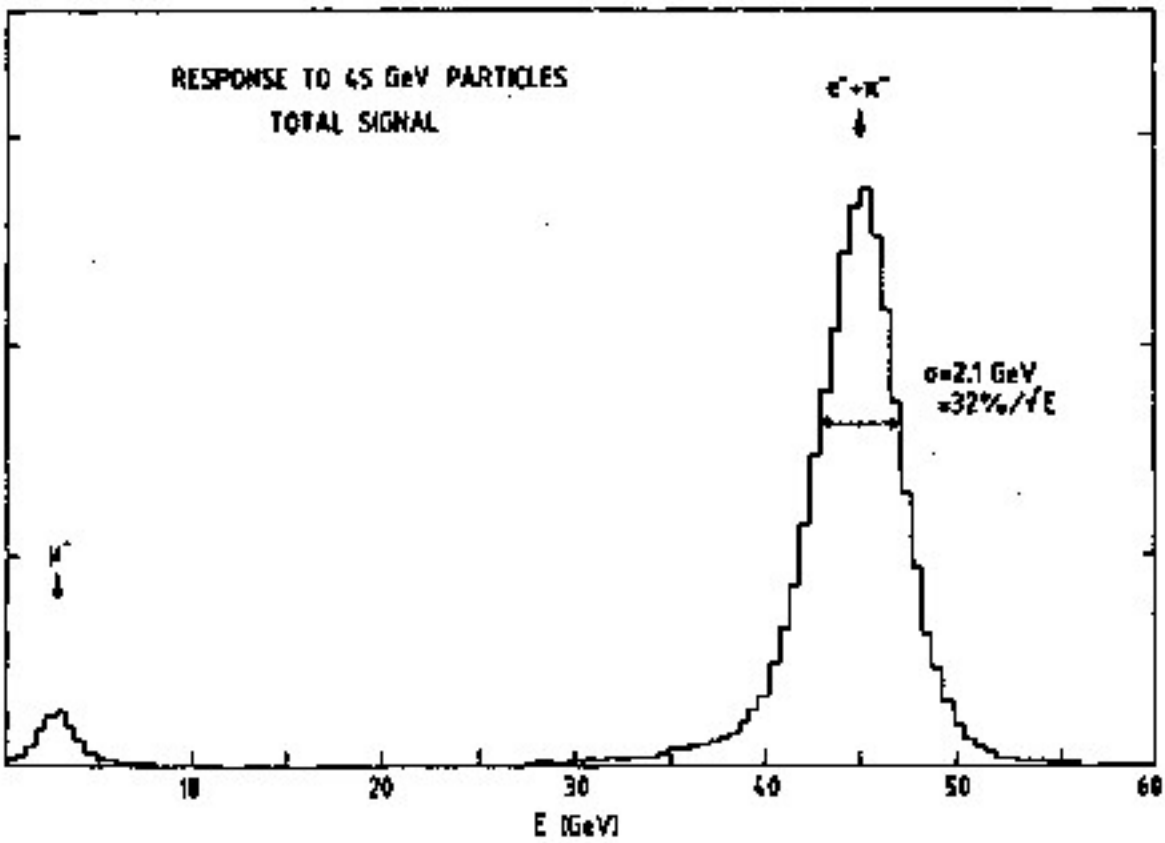

"HELIOS" TEST DATA, $e/h \approx 1$

LiQuiD ARGON : DØ

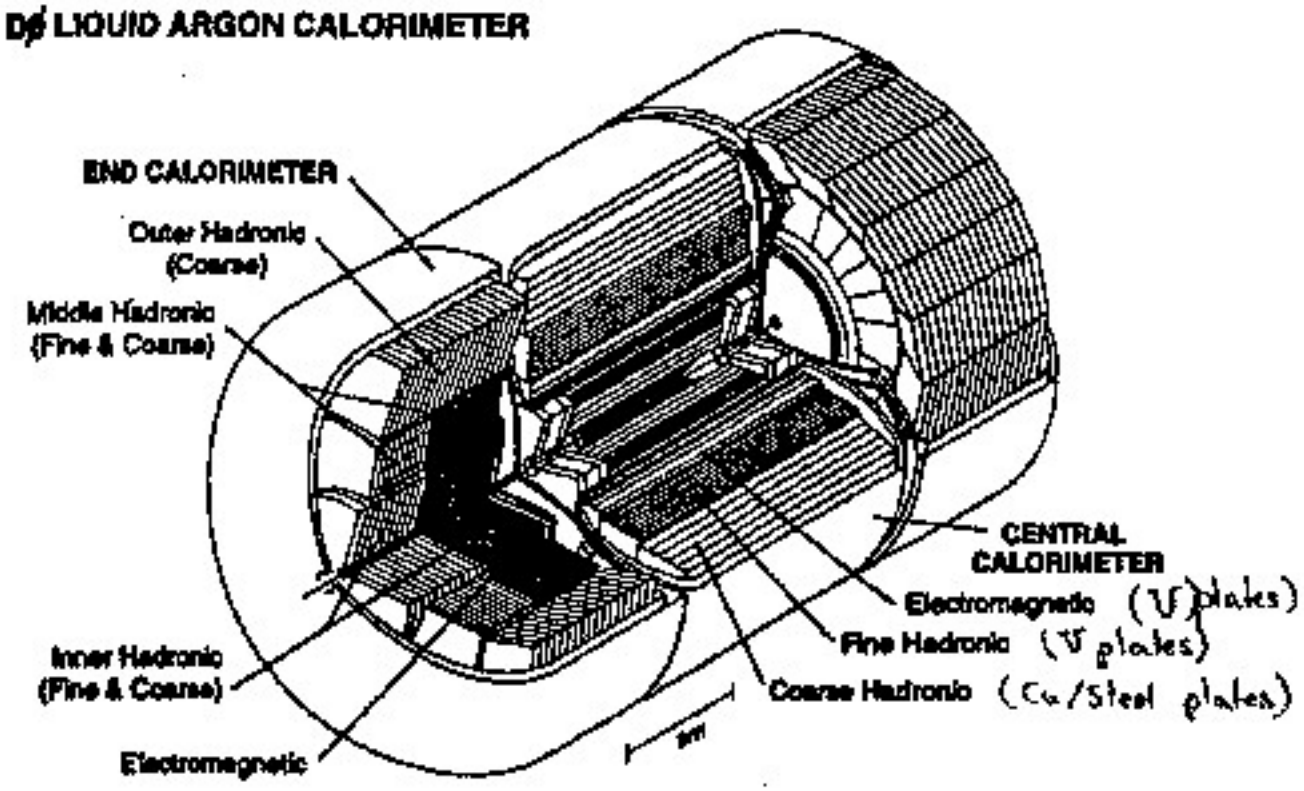

ENERGY RESOLUTION

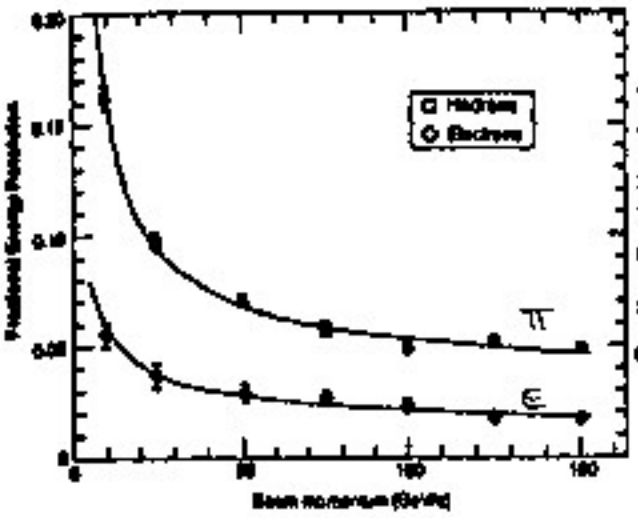

POSITION RESOLUTION !

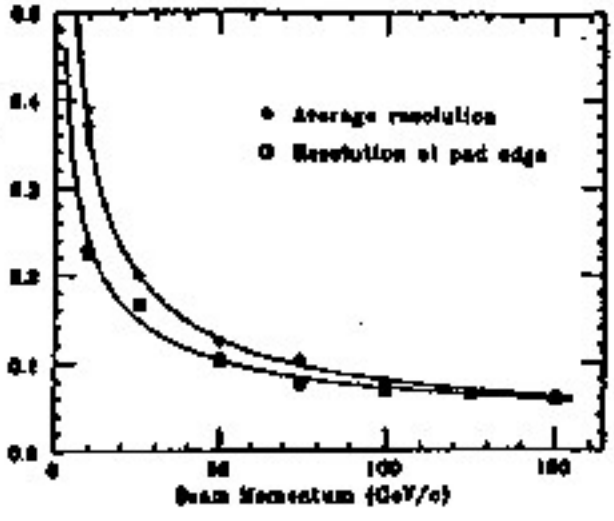

DØ

PION REJECTION VS MOMENTUM

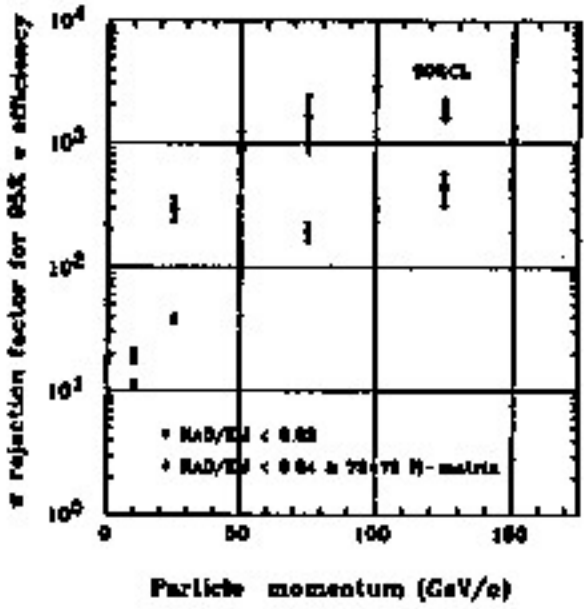

ENERGY DISTRIBUTION 100 GeV π's

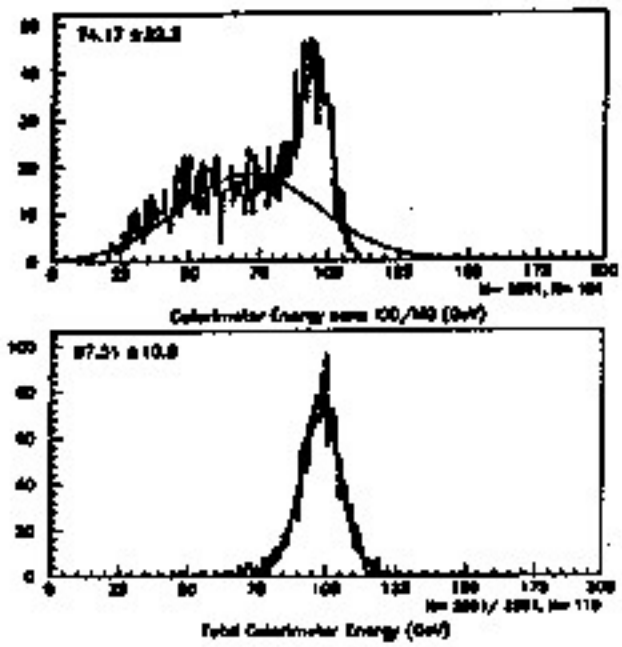

UNCORRECTED

CORRECTED

I.E. + MASSLESS GAPS
+ LIQUID-CONSTANT DETECTOR

LIQUID ARGON : H1

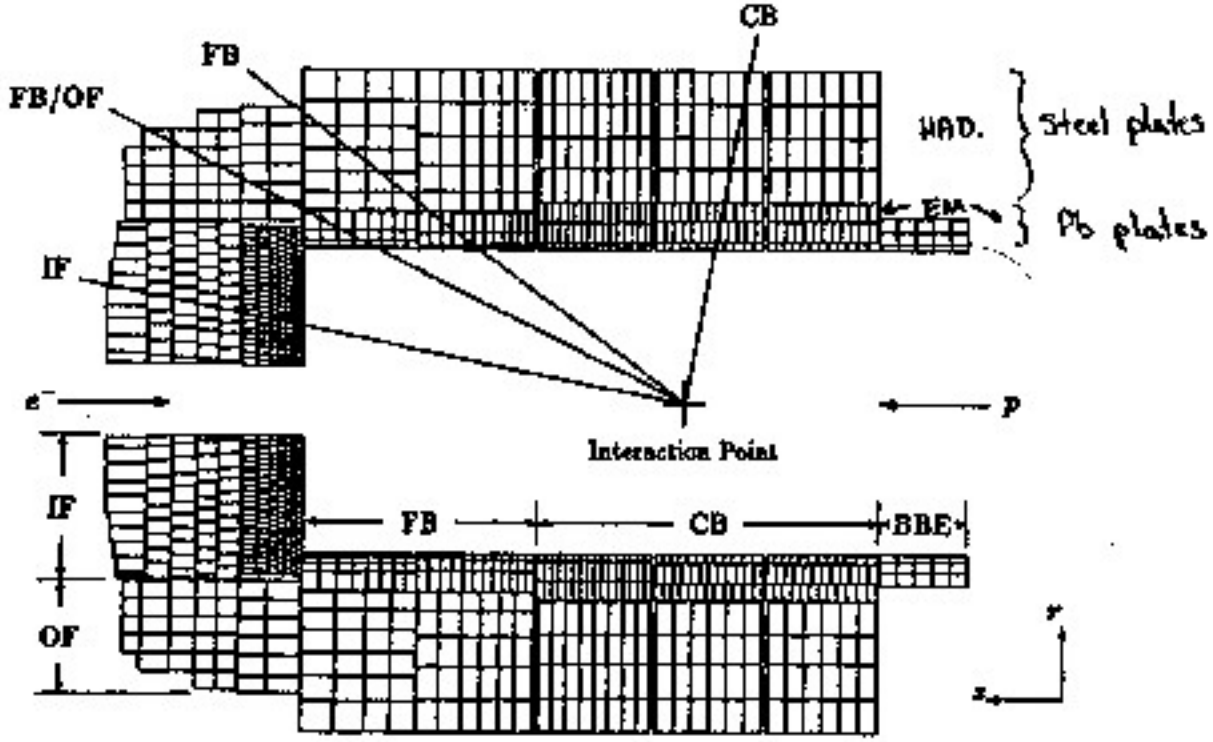

THE MODULES ARE LOCATED INSIDE THE MAGNETIC FIELD

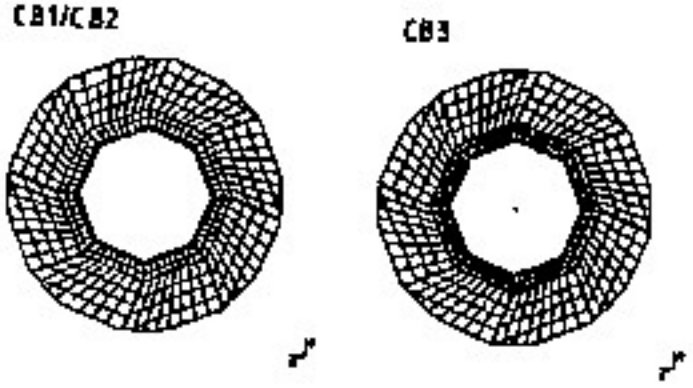

ISO- X_0 & ISO-λ LINES

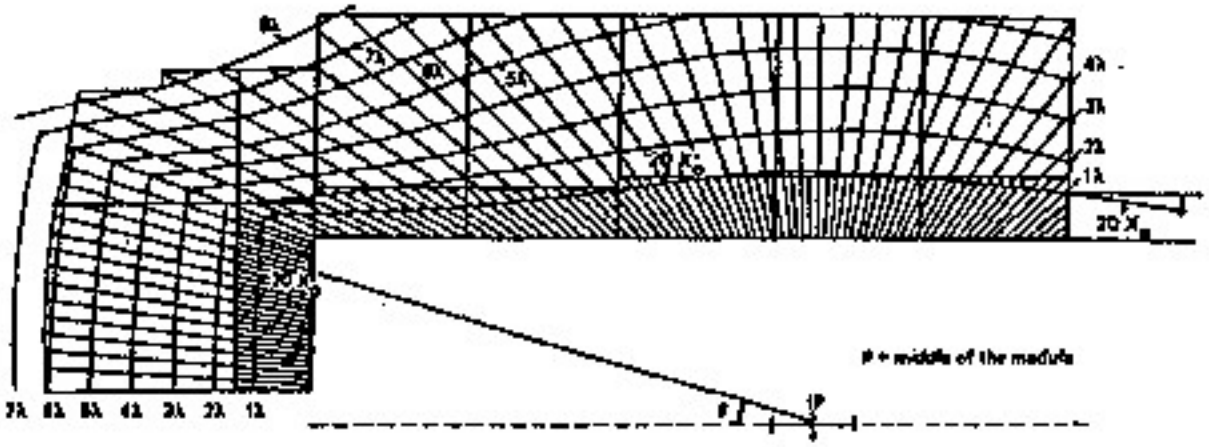

Run 54637 Event 380f Class: 6 9 14 22 28 Date 25/04/19

DIS NC "1-jet" event

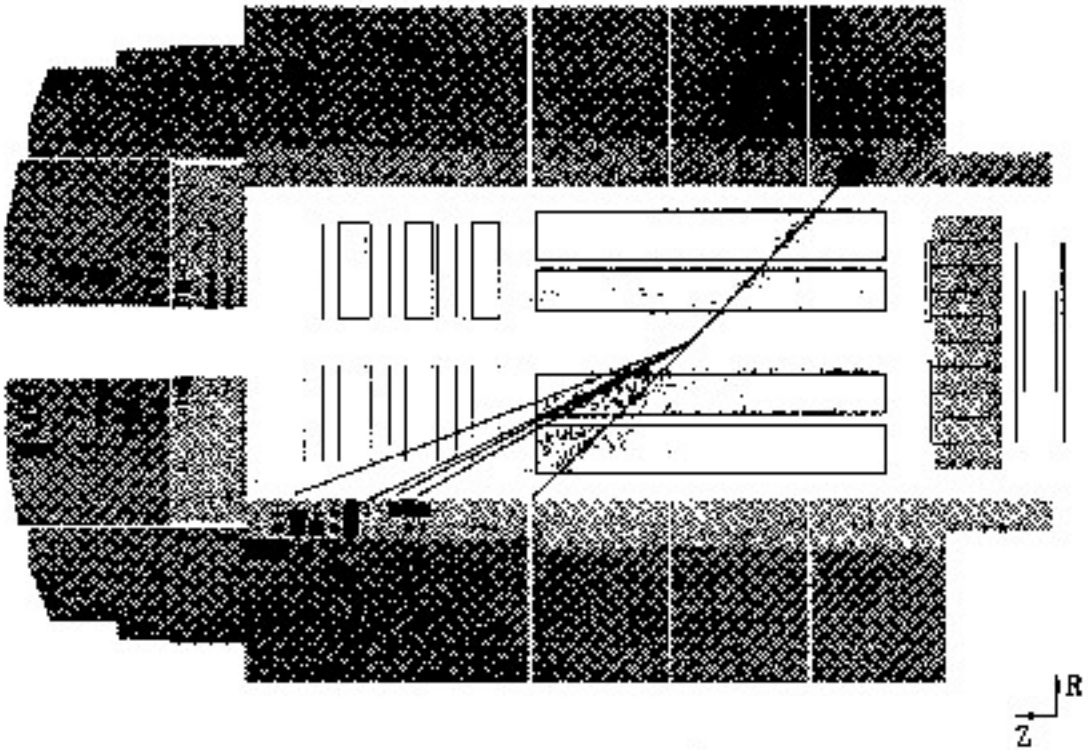

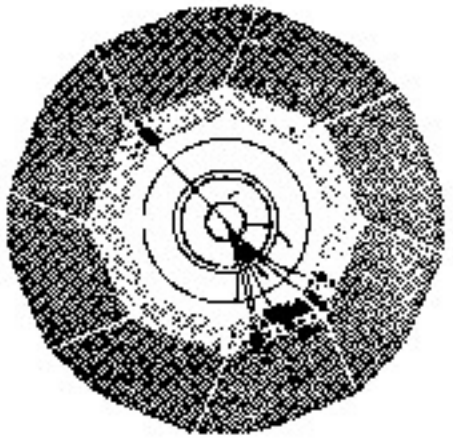

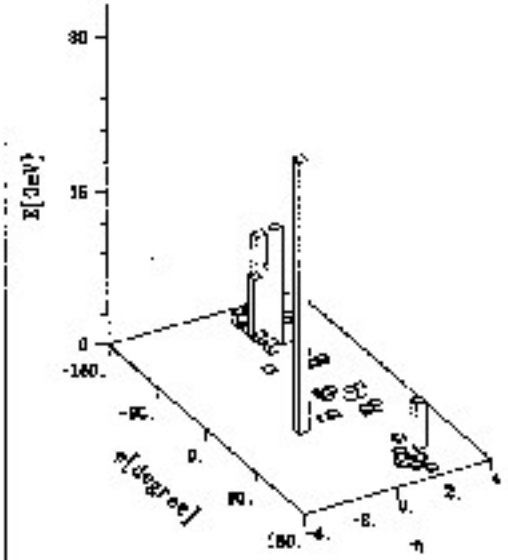

LIQUID KRYPTON: GEM[†]
ARGON: ATLAS

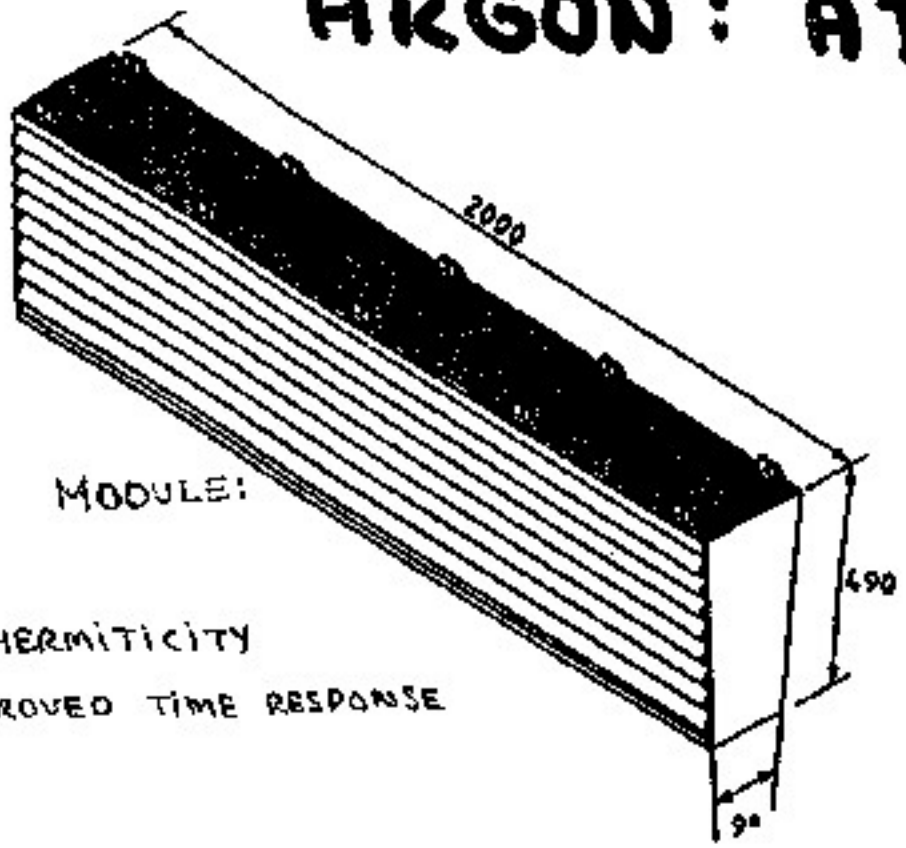

MODULE:

BETTER HERMITICITY

MUCH IMPROVED TIME RESPONSE

ACCORDEON STRUCTURE:

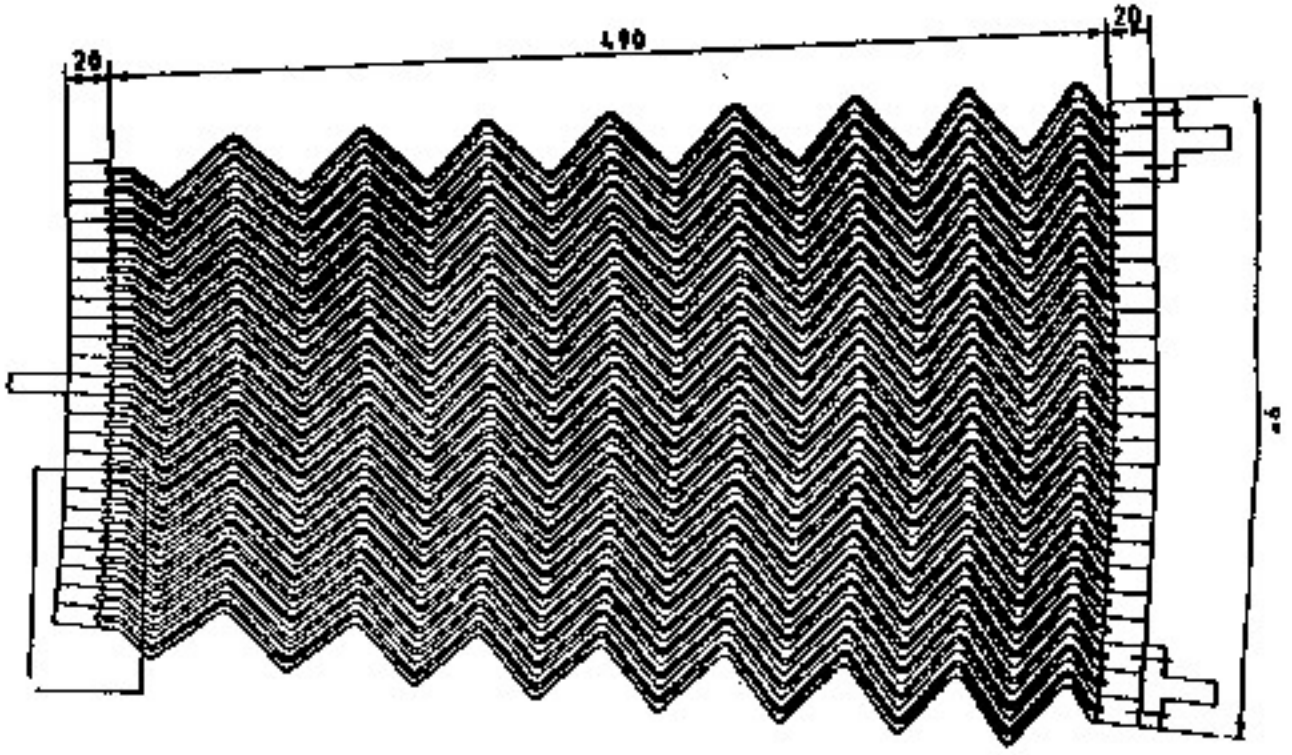

LIQUID ARGON: SLD

PROJECTIVE

OPTICAL FIBER READOUT

Pb plates

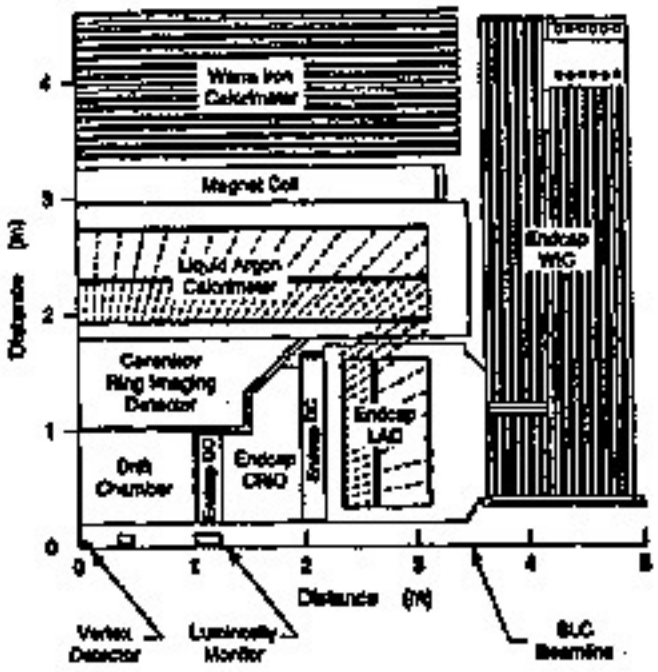

LIQUID FIBER: SSC†/LHC

RADIATION HARD !

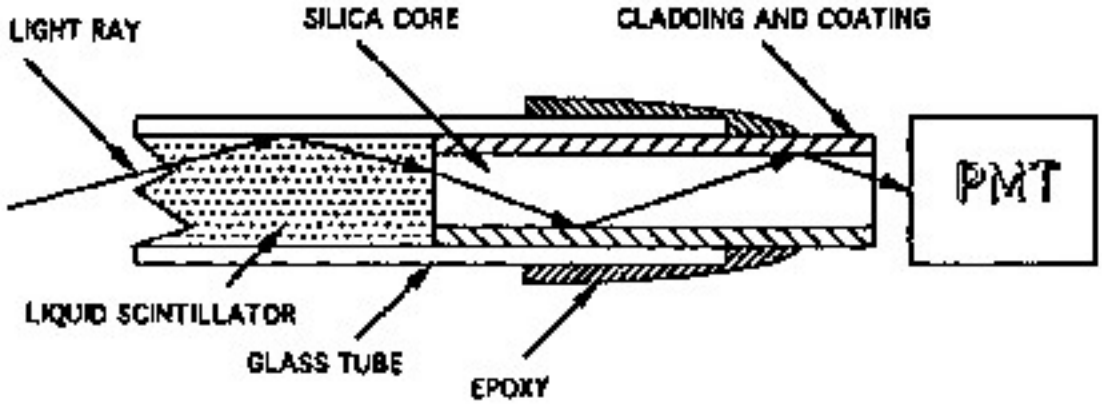

SCINTILLATING FIBER: RD1

MODULE STRUCTURE
AS SEEN BY
INCOMING PARTICLES:

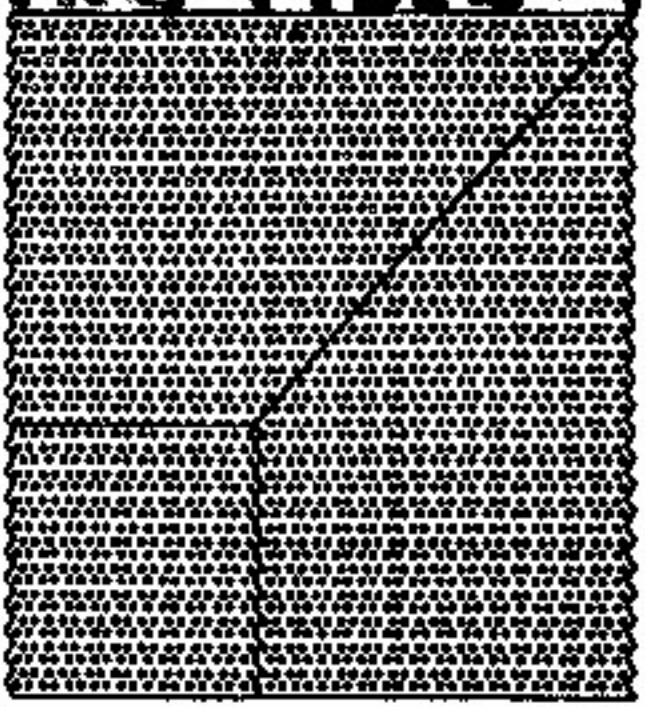

Pb FILLING

SIDE VIEW - READOUT:

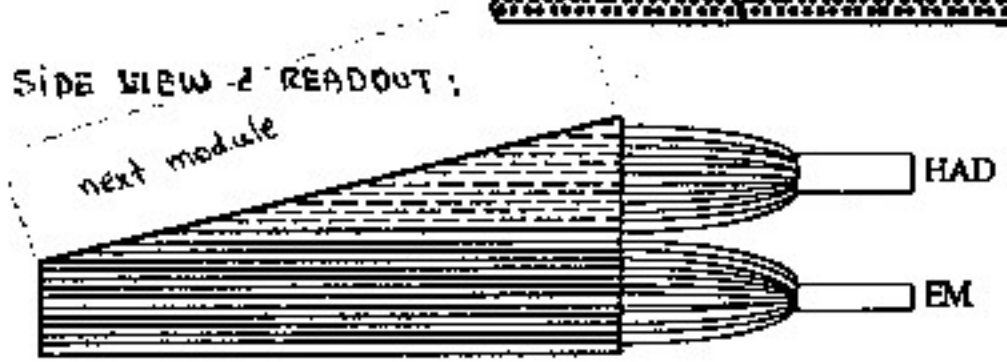

RESOLUTION:

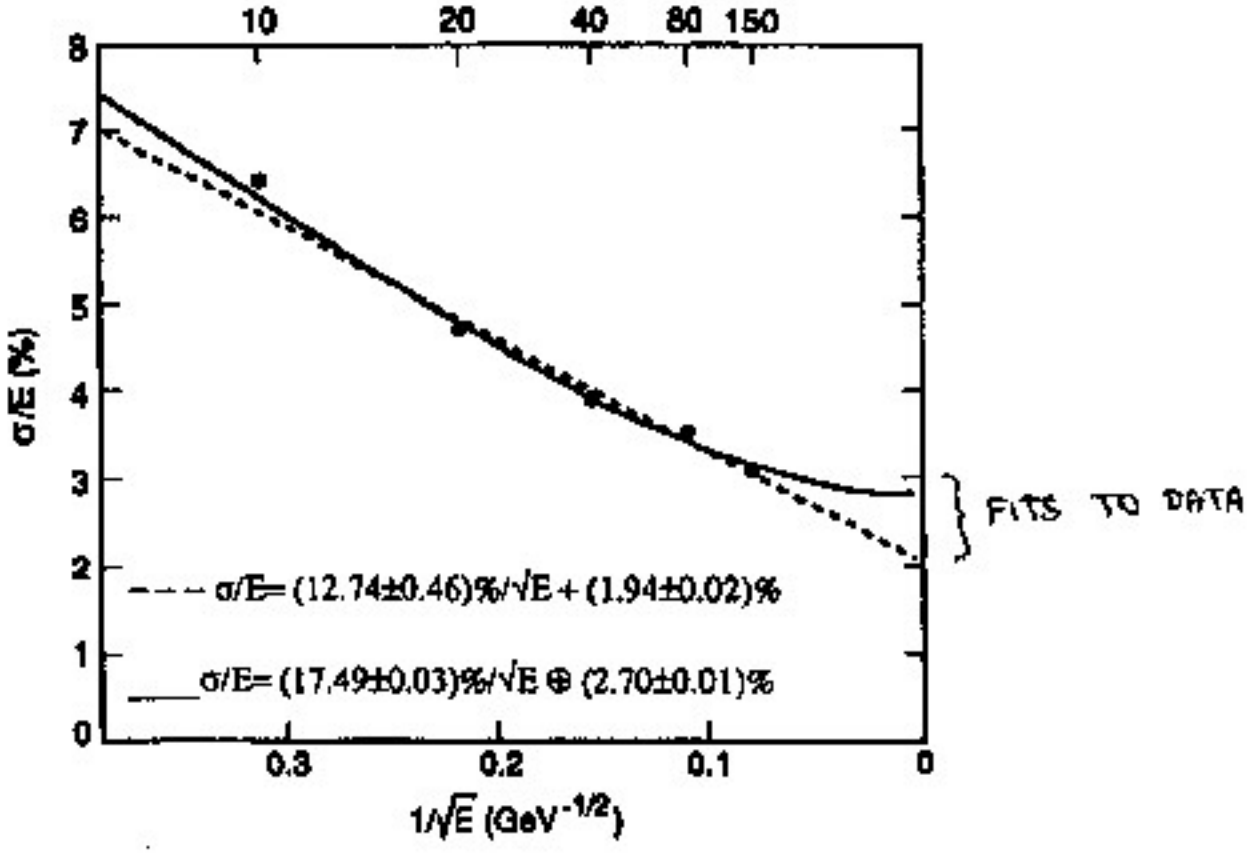

SAMPLING CAL.: SDC†

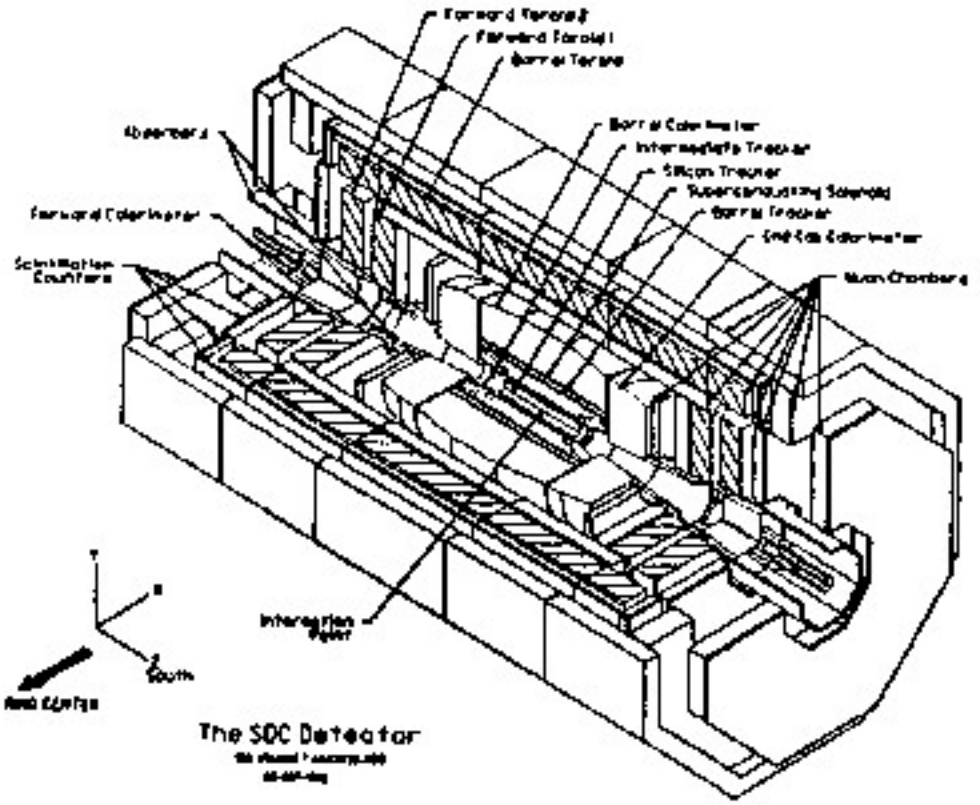

WLS - FIBER READOUT

PROJECTIVE

E.M.: Pb plates

HAD.: Steel plates

Tile/Fiber Central Calorimeter
(Quadrant Cross Section)

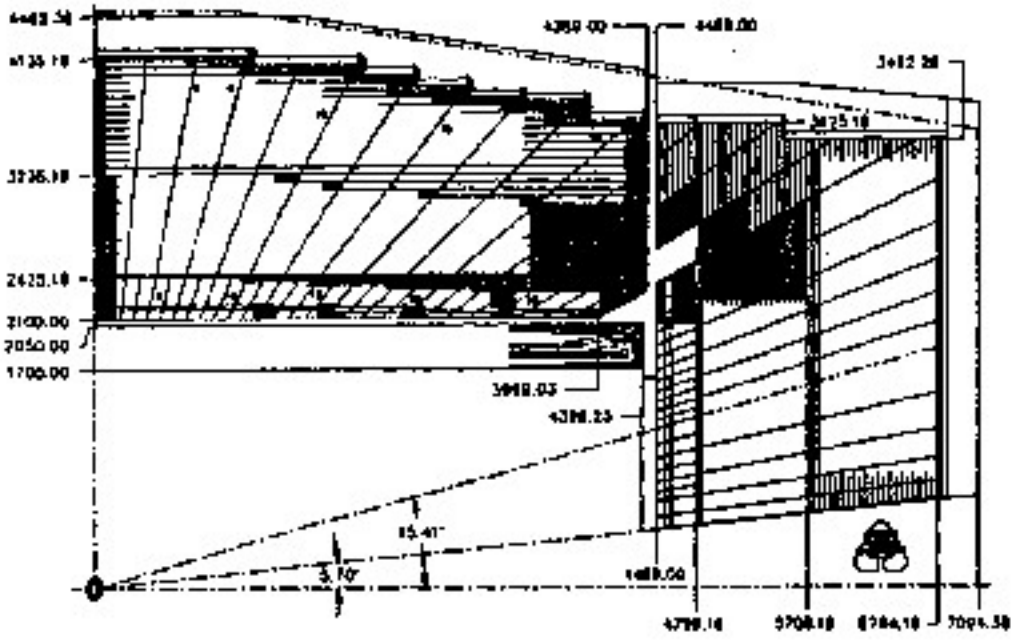

SCINTILLATING TILES: CDF

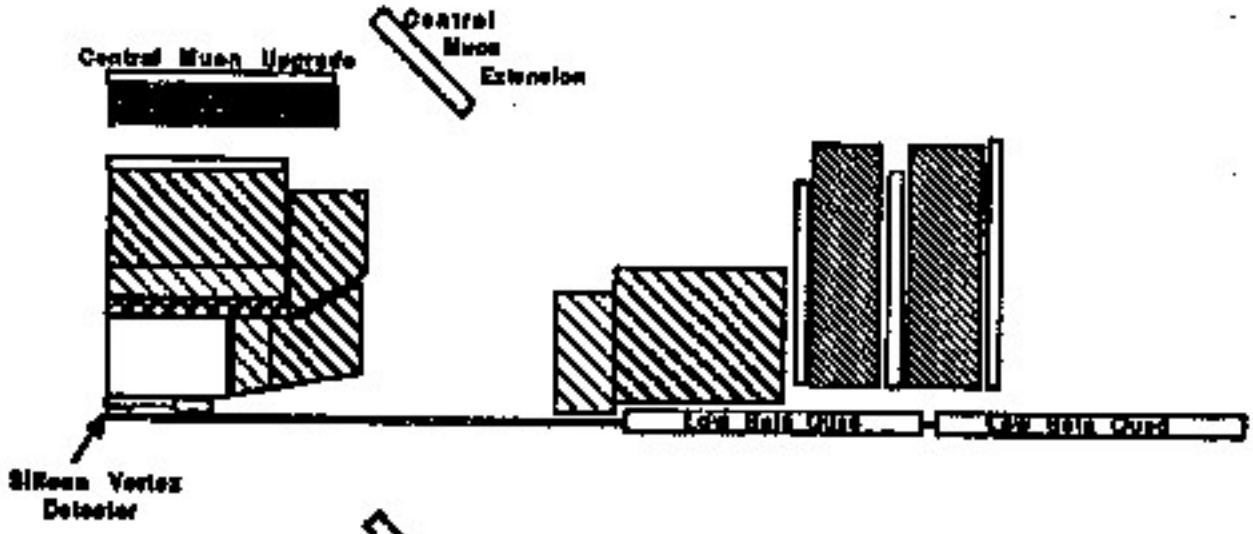

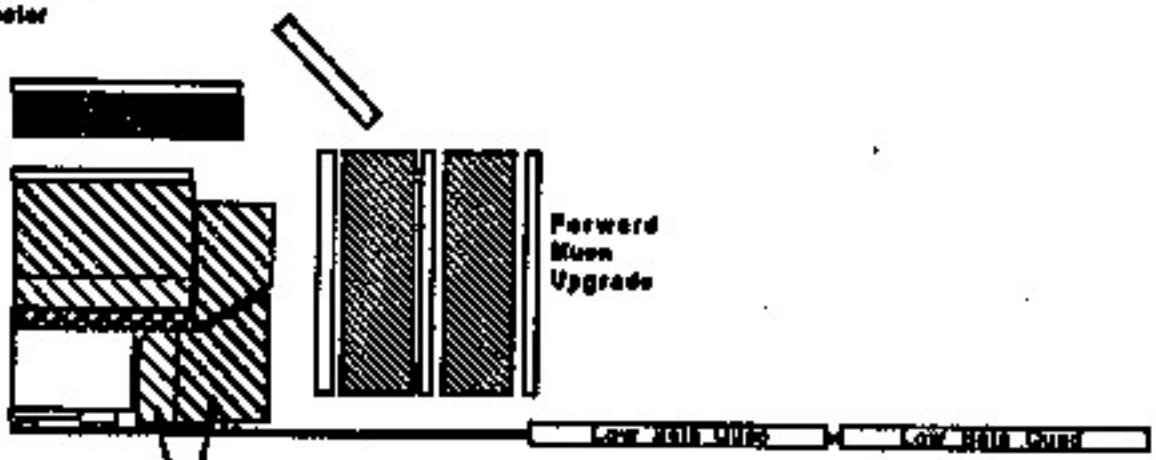

Plug Upgrade

E.M.: Pb plates | HAD.: Steel plates

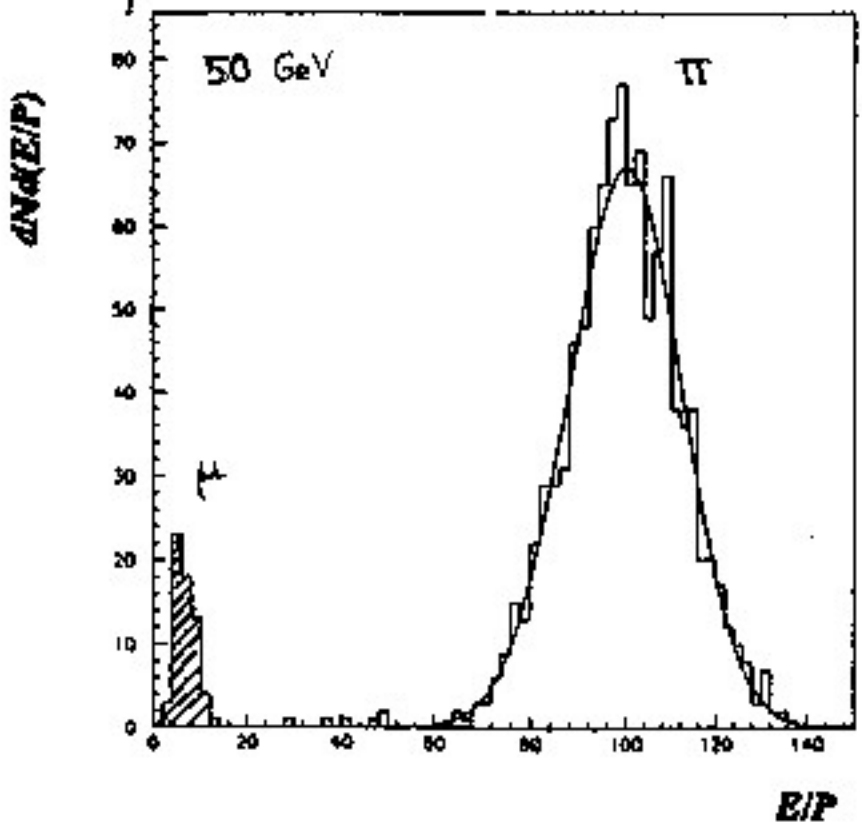

CDF : RESOLUTIONS

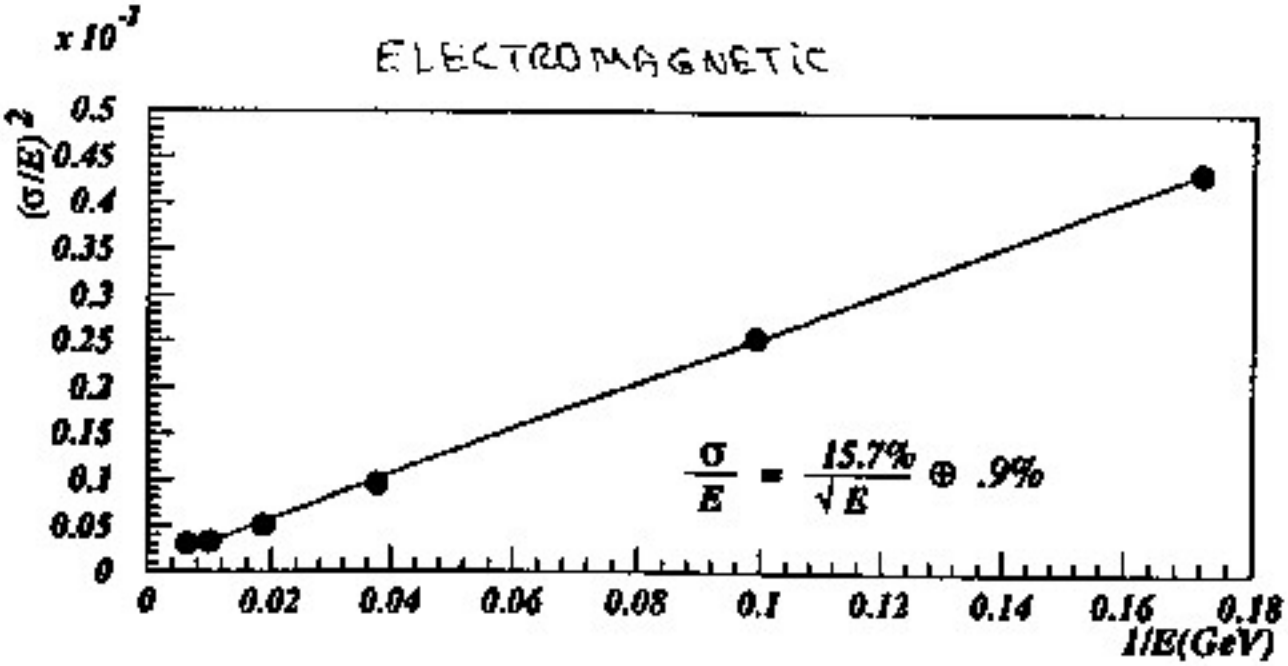

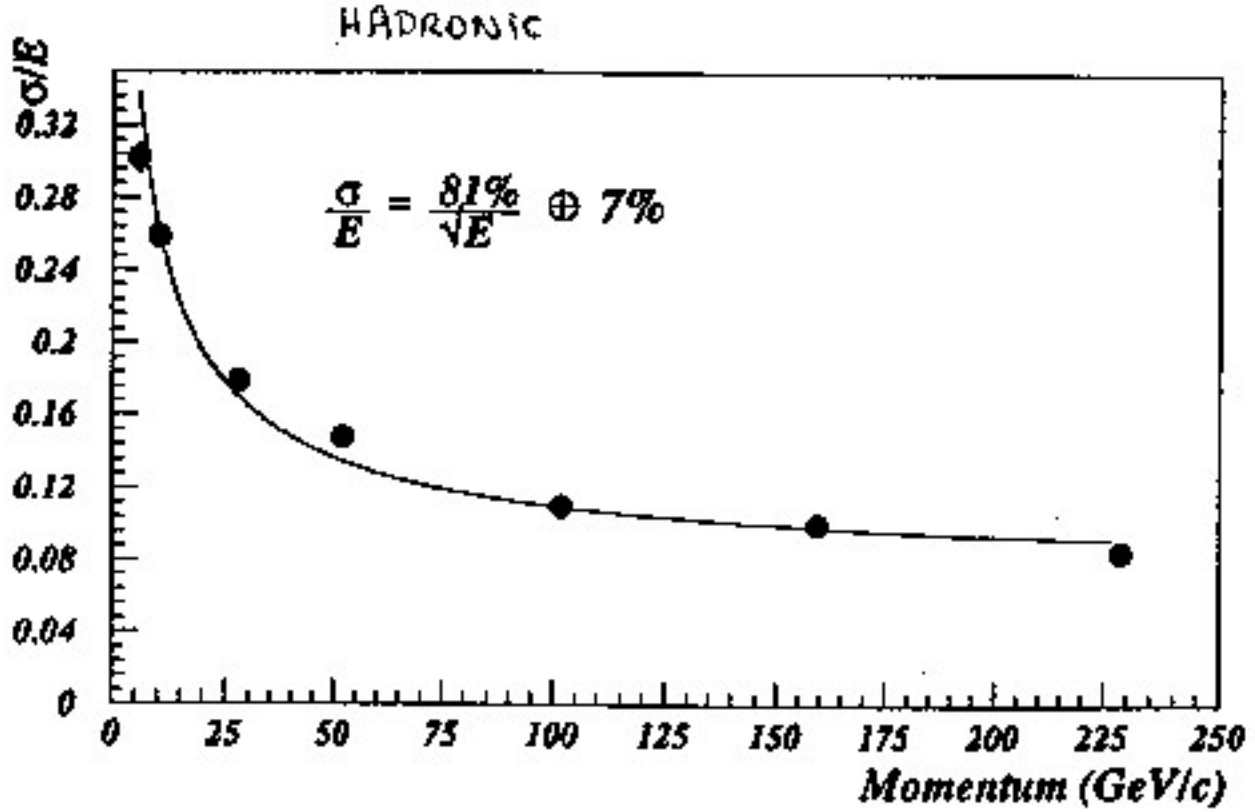

RECENT CALORIMETERS

	ABSORBER / READOUT E.M.	HAD.	e/h	RESOLUTION E.M.	HAD.
SCINTILLATION					
ZEUS	U/Scint		1.00	$\frac{15\%}{\sqrt{E}}$	$\frac{35\%}{\sqrt{E}}$
CDF	Pb/Scint	Steel/Scint	1.28	$\frac{14\%}{\sqrt{E}} \oplus 1\%$	$\frac{80\%}{\sqrt{E}} \oplus 7\%$
SDC	Pb/Scint	Fe/Scint	1.02	$\sim\frac{15\%}{\sqrt{E}} \oplus 1\%$	$\frac{35\%}{\sqrt{E}} \oplus ?$
GEM		Cu/Scint (fibre)	1.10		$\frac{91\%}{\sqrt{E}} \oplus 1\%$
RD1	Pb/Scint (fibre)		?	$\frac{17\%}{\sqrt{E}} \oplus 3\%$	$\frac{50\%}{\sqrt{E}} \oplus 7\%$
( )	Pb-epoxy/Scint (fibre)			$\frac{5\%}{\sqrt{E}} \oplus 3\%$	
(LHC)	Pb/liquid scint.		?	$\frac{10\%}{\sqrt{E}} \oplus ?$	$\frac{51\%}{\sqrt{E}} \oplus ?$
LIQUID IONISATION					
H1	Pb/LAr	Steel/LAr	?	$\frac{12\%}{\sqrt{E}} \oplus 1\%$	$\frac{50\%}{\sqrt{E}} \oplus 3\%$
DØ	U/LAr		1.06	$\frac{16\%}{\sqrt{E}} \oplus 1\%$	$\sim\frac{45\%}{\sqrt{E}} \oplus 4\%$
GEM	Pb/LKr	Steel/LKr	0.9-1.3	$\frac{7\%}{\sqrt{E}}$	$\frac{60\%}{\sqrt{E}} \oplus 2\%$
SLD	Pb/L.Ar.		?	$\frac{12\%}{\sqrt{E}} \oplus 2\%$	$\sim\frac{60\%}{\sqrt{E}} \oplus ?$
ATLAS	Pb/L.Ar.		?	$\frac{10\%}{\sqrt{E}} \oplus 1\%$	$\frac{50\%}{\sqrt{E}} \oplus 3\%$
CRYSTALS					
GEM	BaF_2			$\frac{2\%}{\sqrt{E}} \pm 0.5\%$	
L3	BGO			$\frac{2\%}{\sqrt{E}} \pm 0.5\%$	
CTBV	CsI			$\frac{0.5\%}{\sqrt{E}} \oplus 0.3\% \oplus \frac{1.9\%}{E}$	
OTHERS					
( )	Pb/Solid Ar		~1.0	$\frac{23\%}{\sqrt{E}}$	$\frac{100\%}{\sqrt{E}}$
( )	W/Si			$\sim\frac{15\%}{\sqrt{E}}$	
( )	Steel/Ar (high pressure gas)		?	$\frac{45\%}{\sqrt{E}}$	$\frac{60\%}{\sqrt{E}}$

PHYSICS AT HERA

DEEP INELASTIC SCATTERING (D.I.S.)

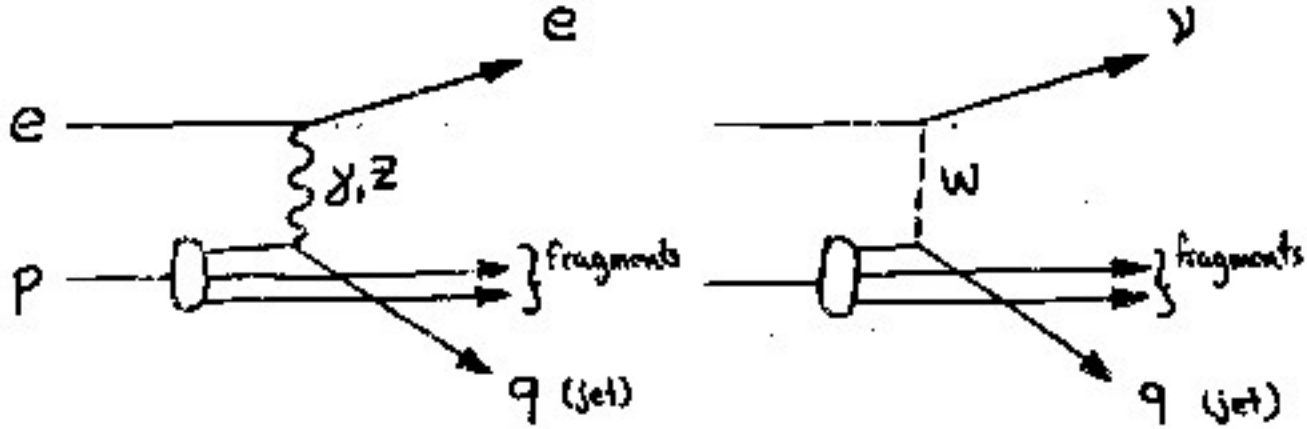

Neutral Current event Charged Current event

KINEMATICS : $X \doteq$ FRACTION OF P-MOMENTUM IN STRUCK QUARK
$Q^2 \doteq$ EXCHANGED MOMENTUM (SQUARED)

X & Q^2 ARE COMPLETELY DEPENDENT ON CALORIMETER-MEASURED ENERGIES. THEY DETERMINE HOW GOOD WE WILL KNOW THE PROTON STRUCTURE FUNCTIONS.

PHOTO-PRODUCTION

QUARK-GLUON FUSION

etc...

DIS: RATES

ACCEPTANCE

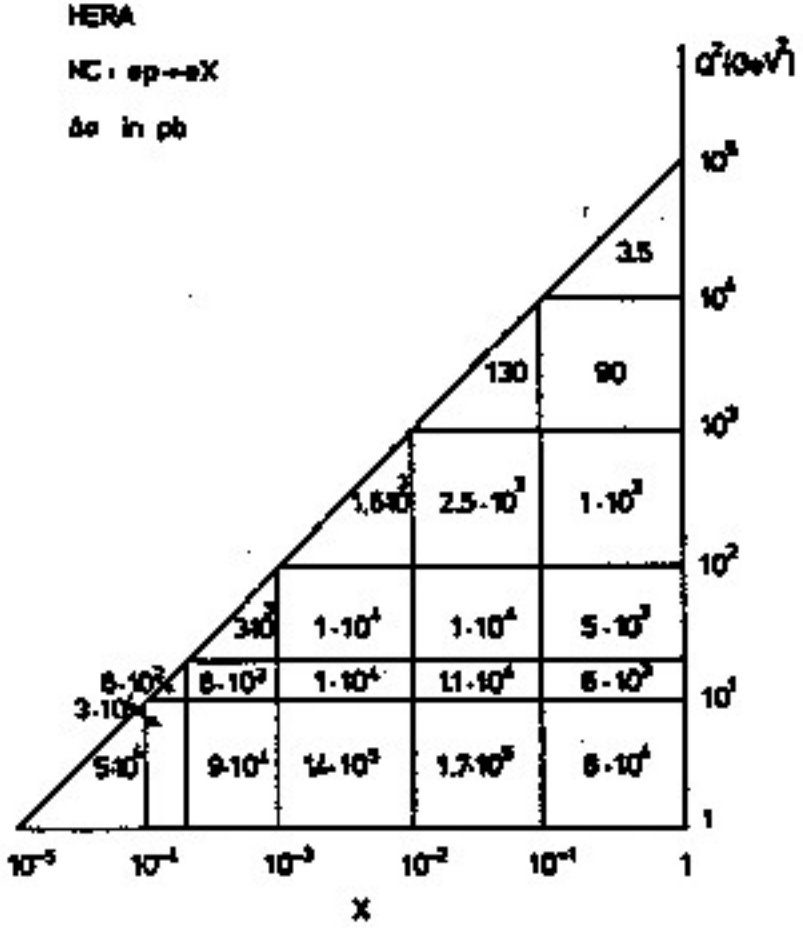

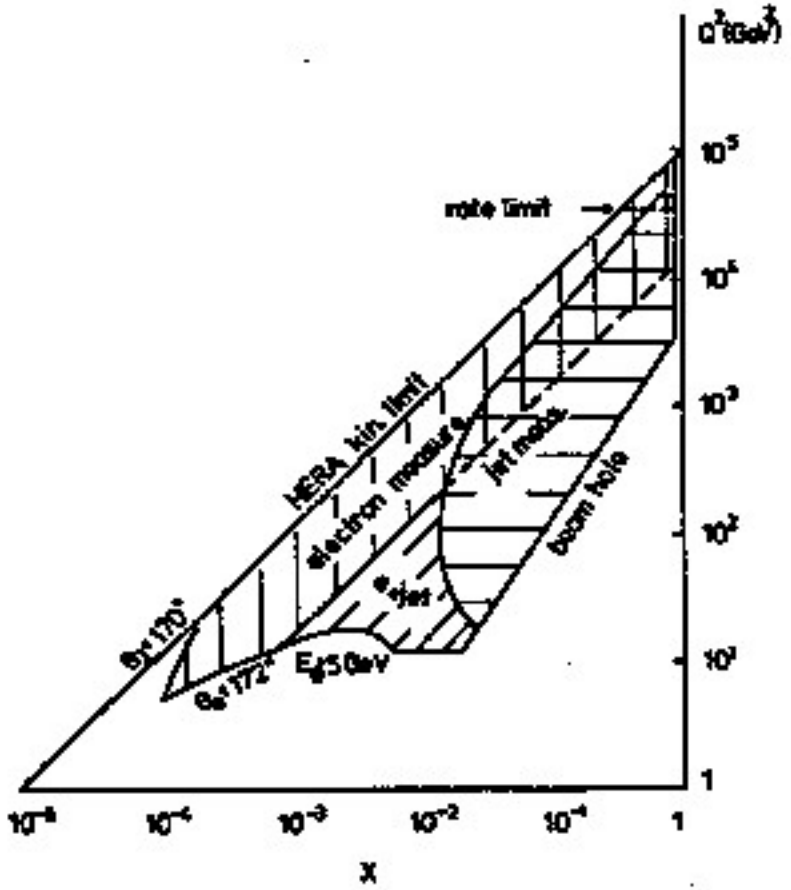

DIS : 1992 DATA

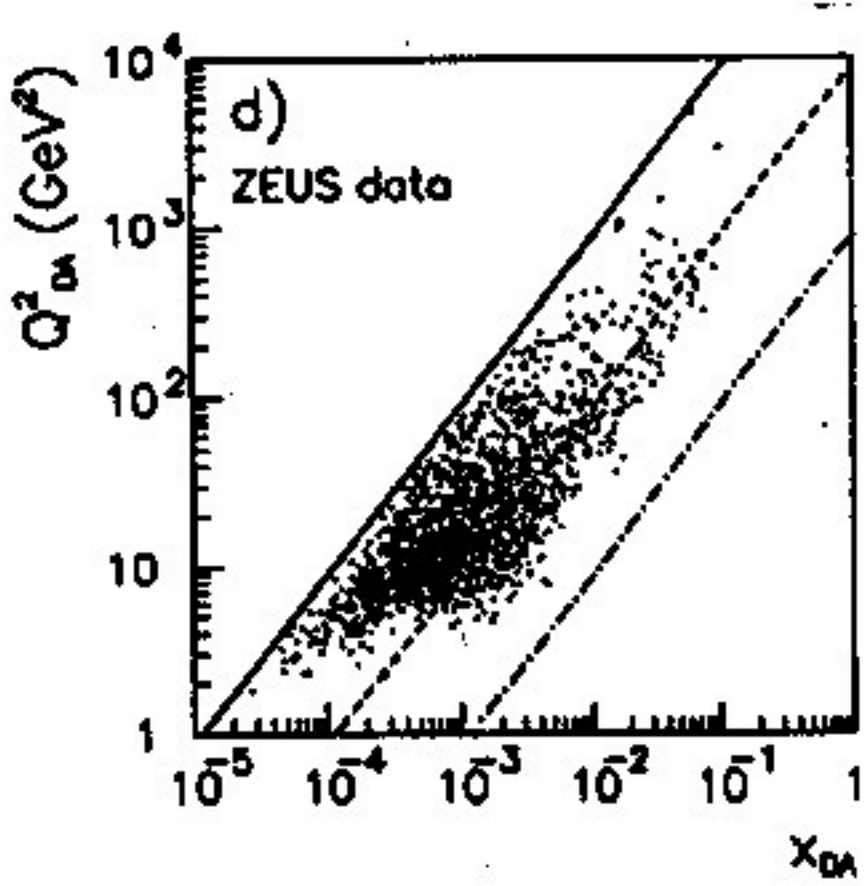

PRE-ZEUS ERA OF U/Scint. CAL's

AFS AT CERN ISR

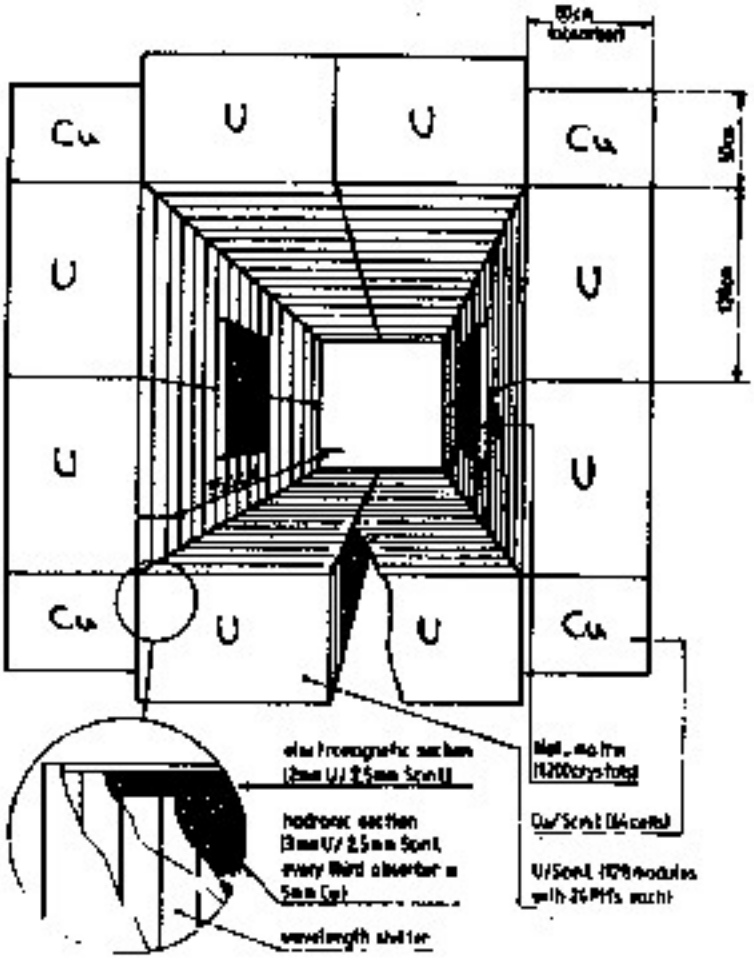

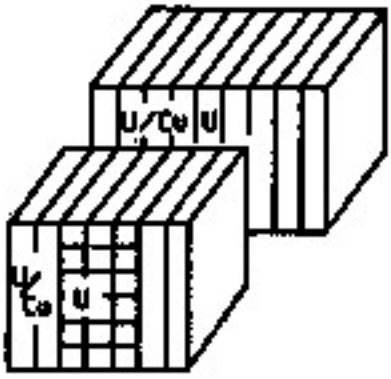

HELICS (NA34)
AT CERN SPS

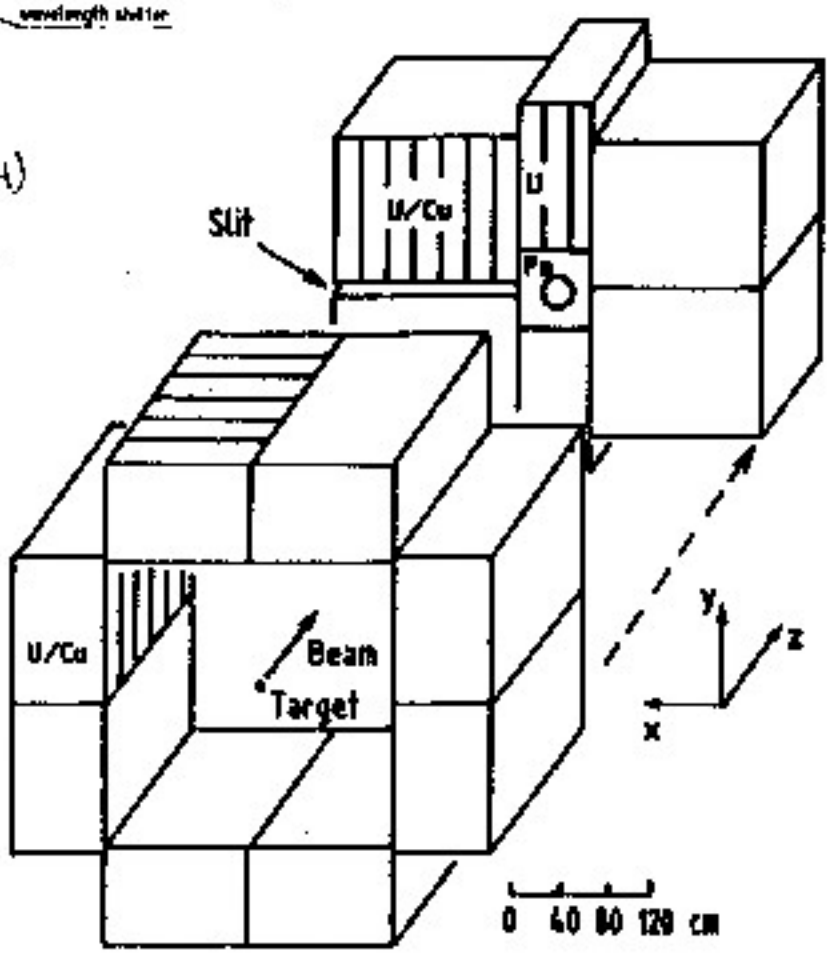

HELIOS : RESOLUTION

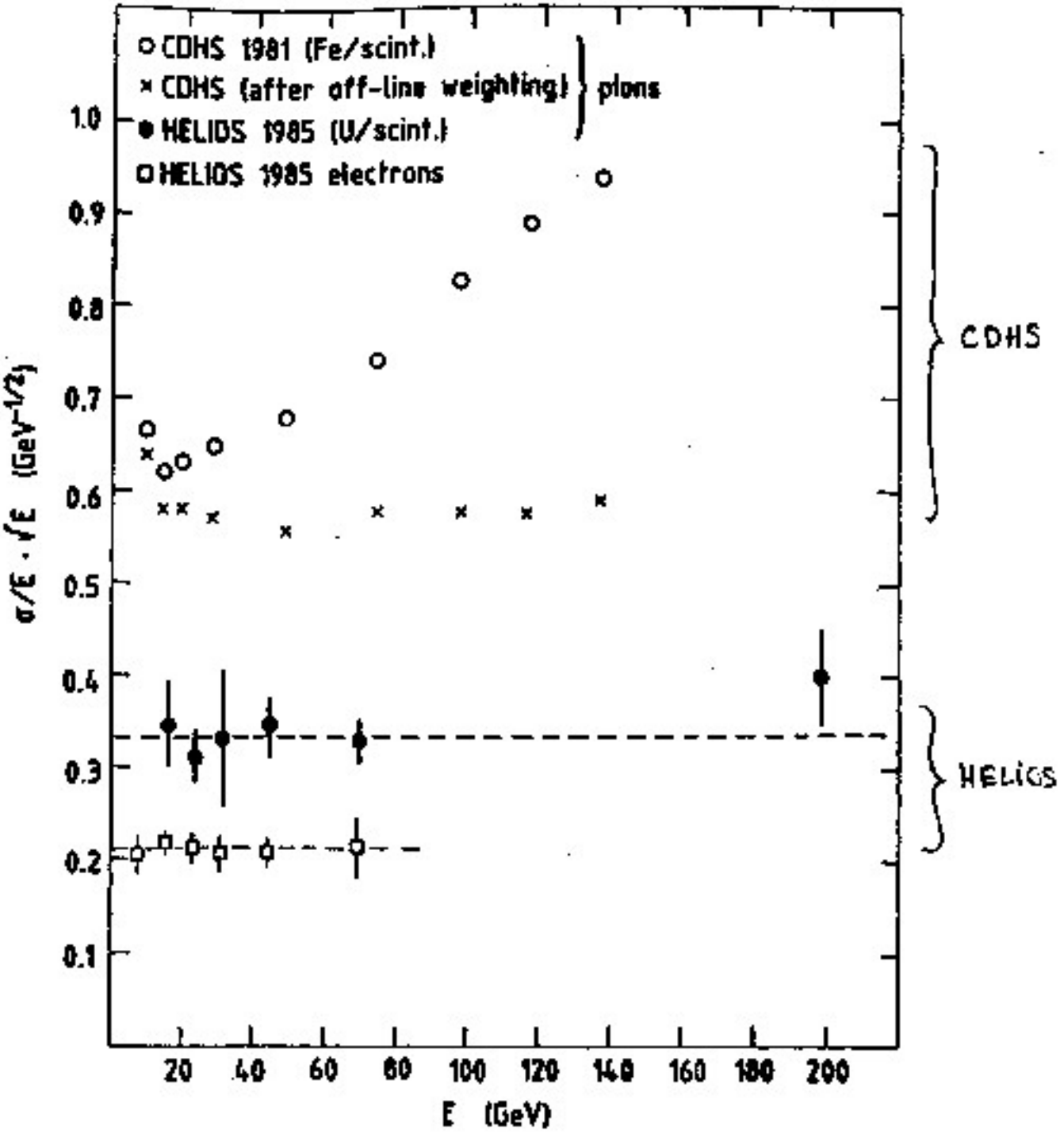

HELIOS & HEAVY IONS

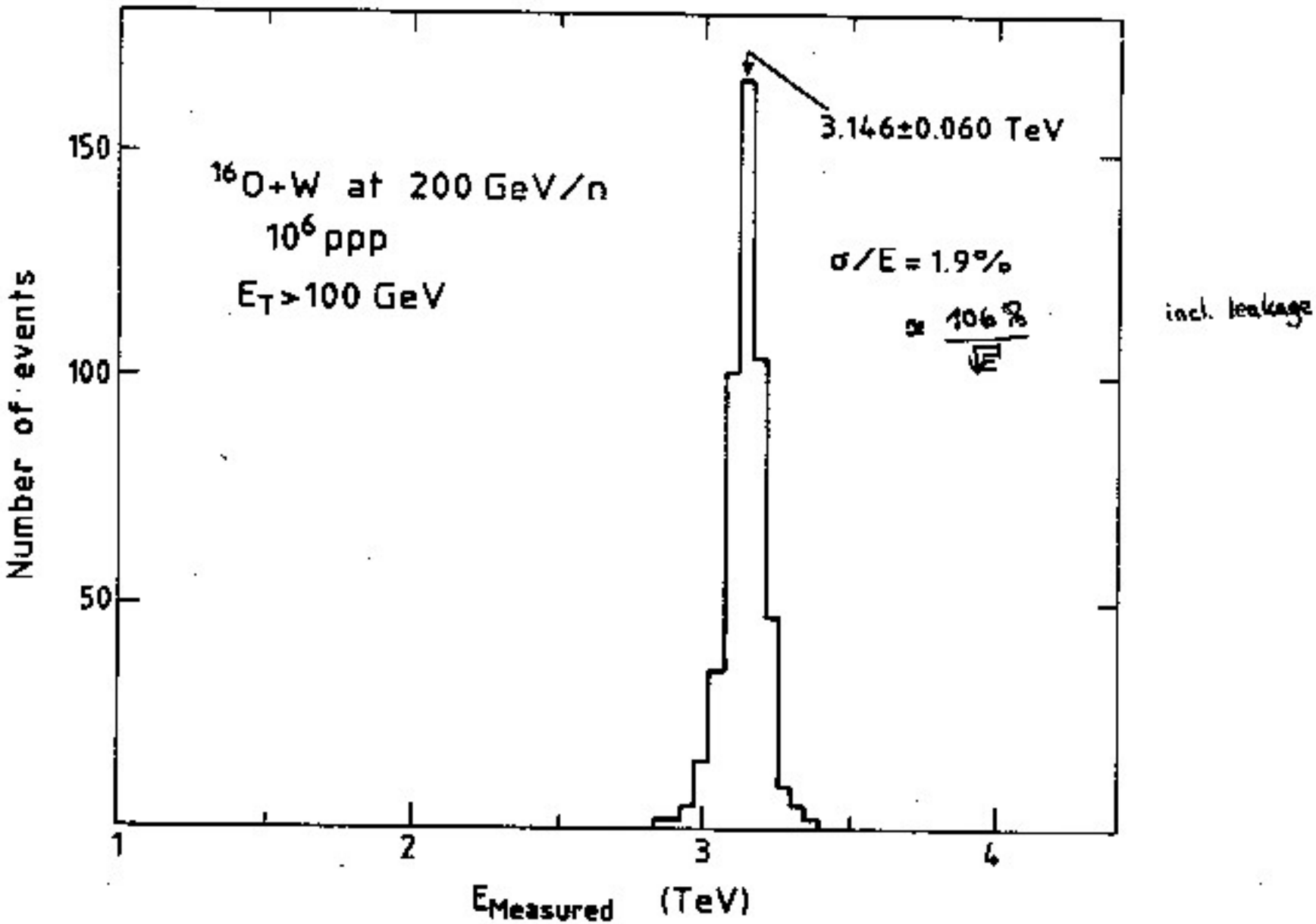

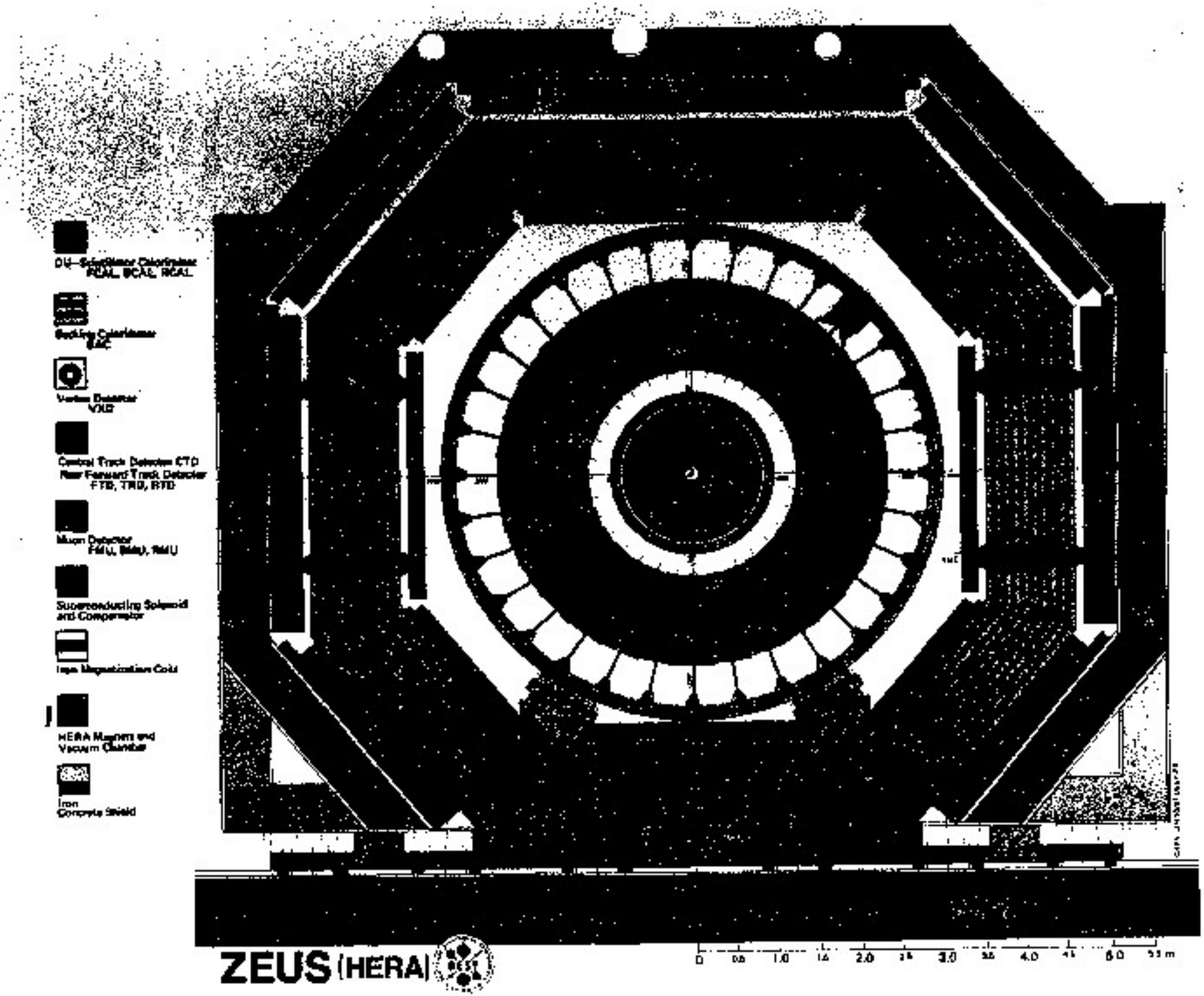
ZEUS (HERA)

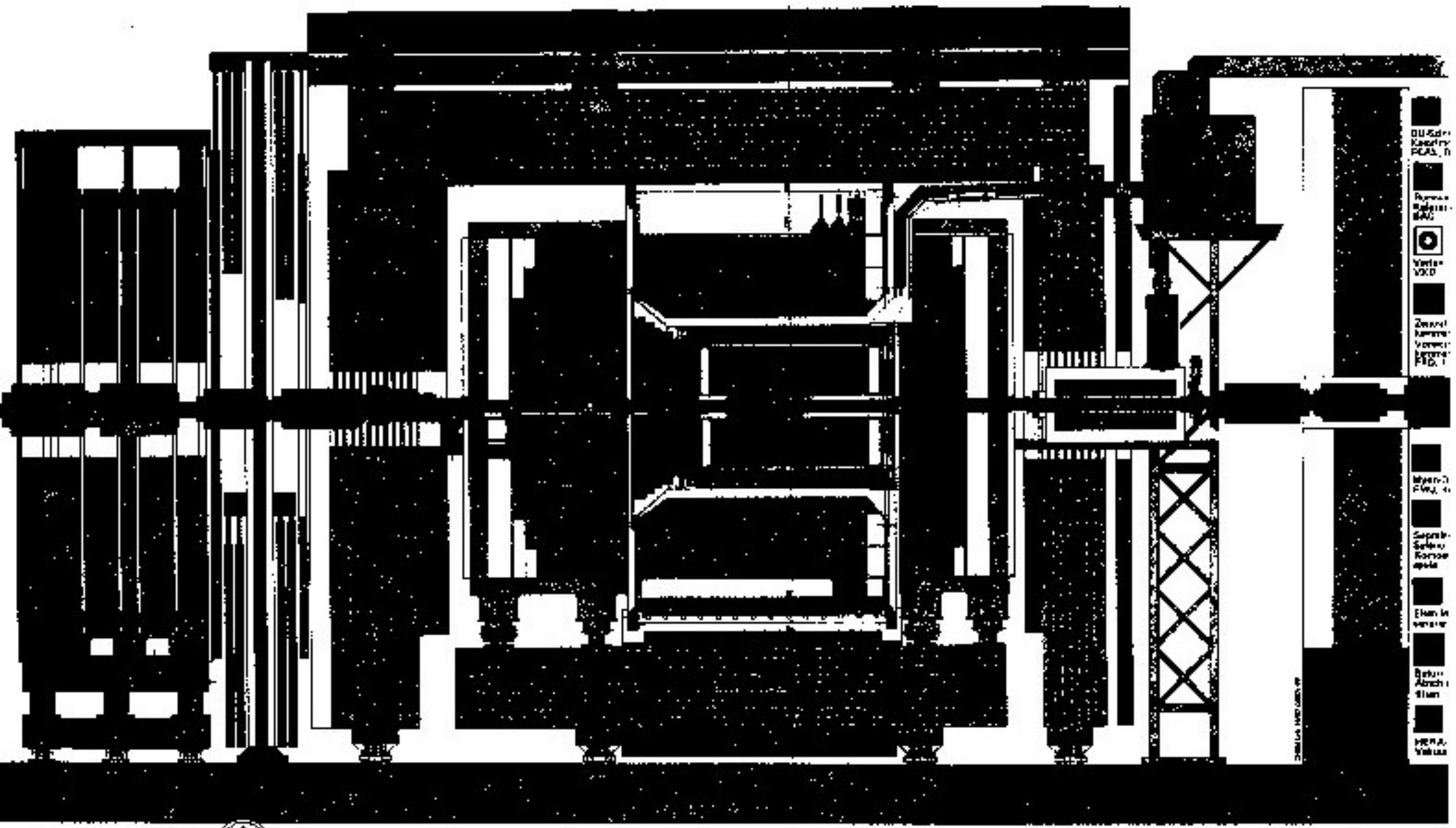

ZEUS (HERA)

ZEUS CALORIMETERS

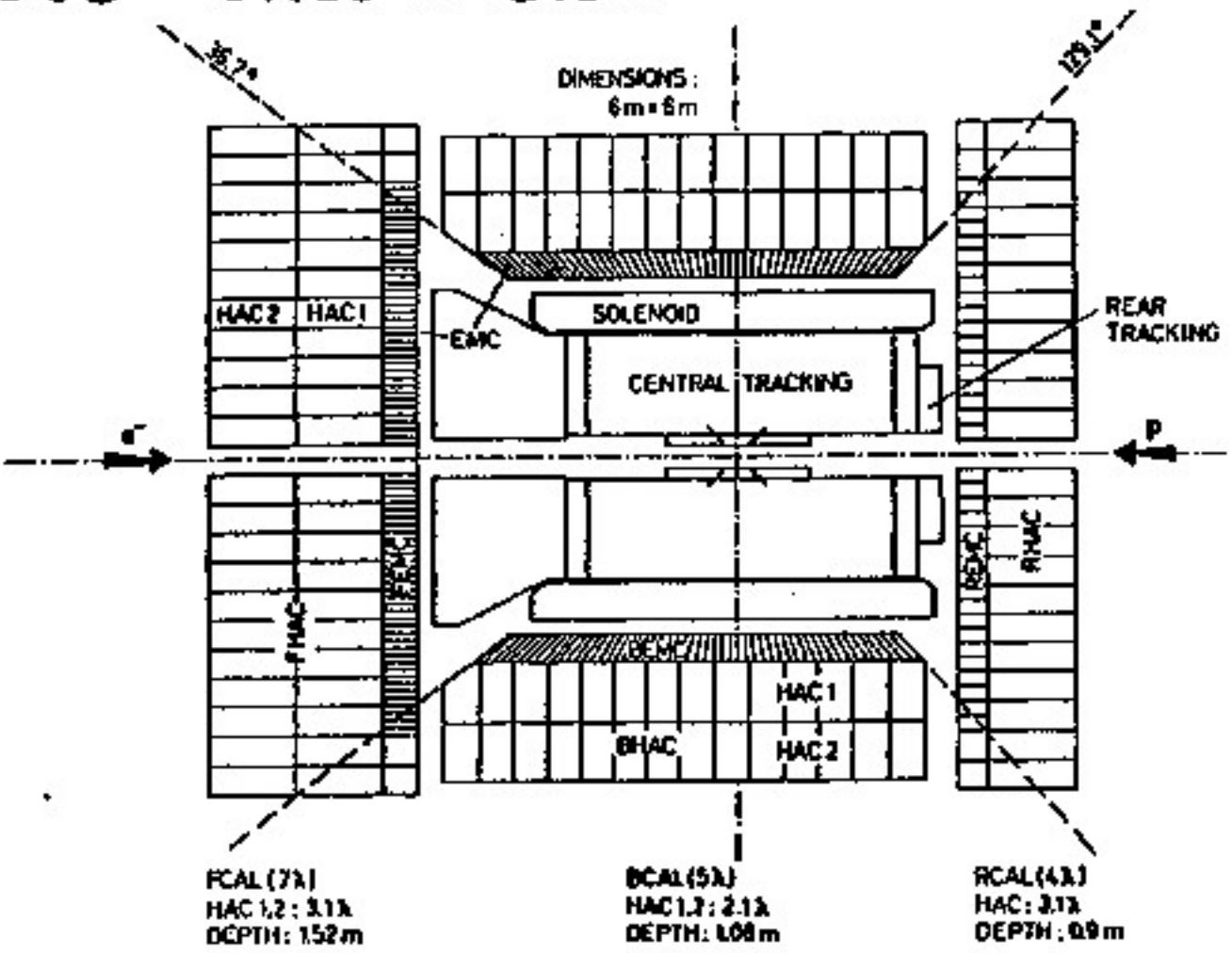

BARREL CALORIMETER MODULE

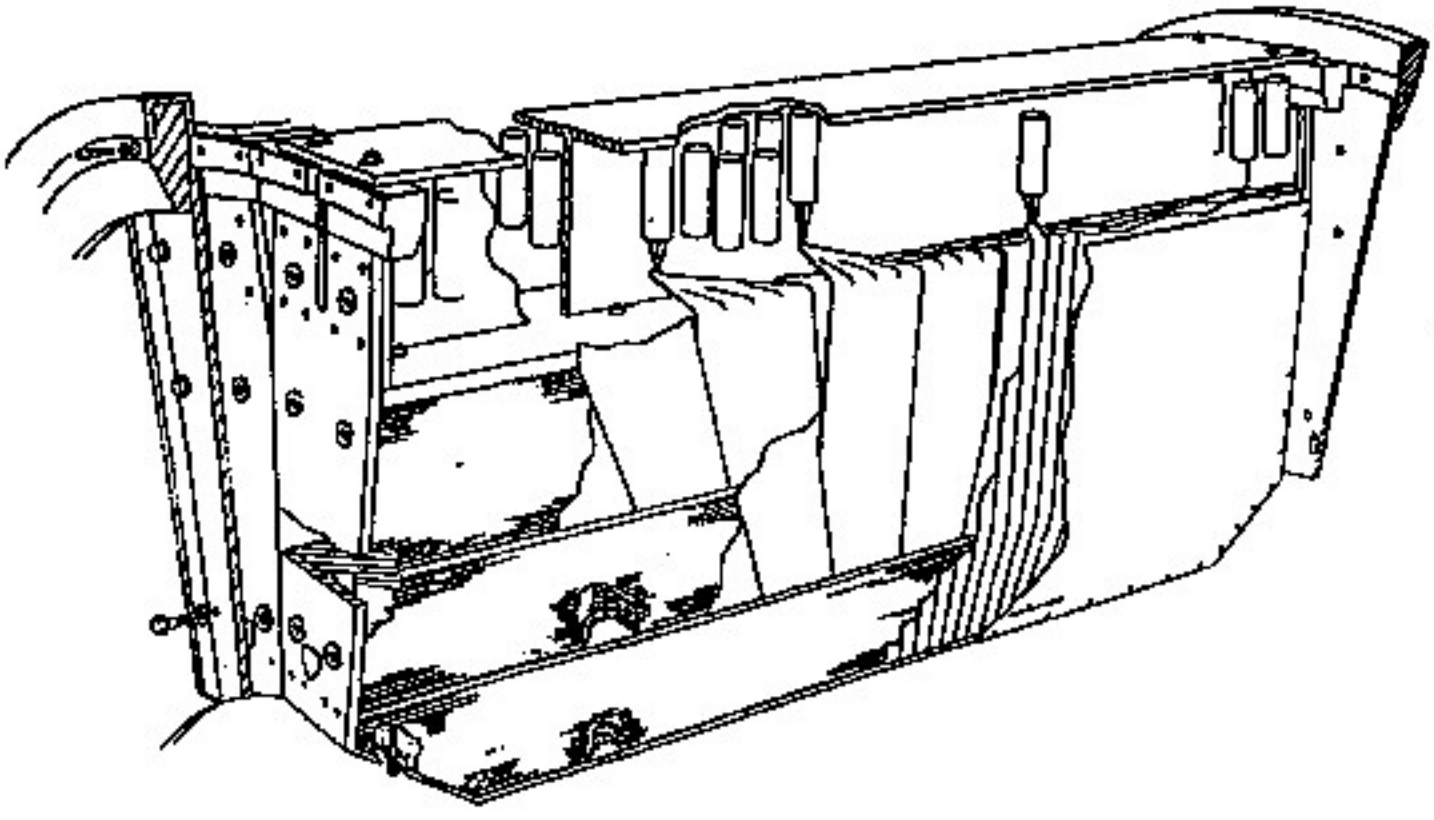

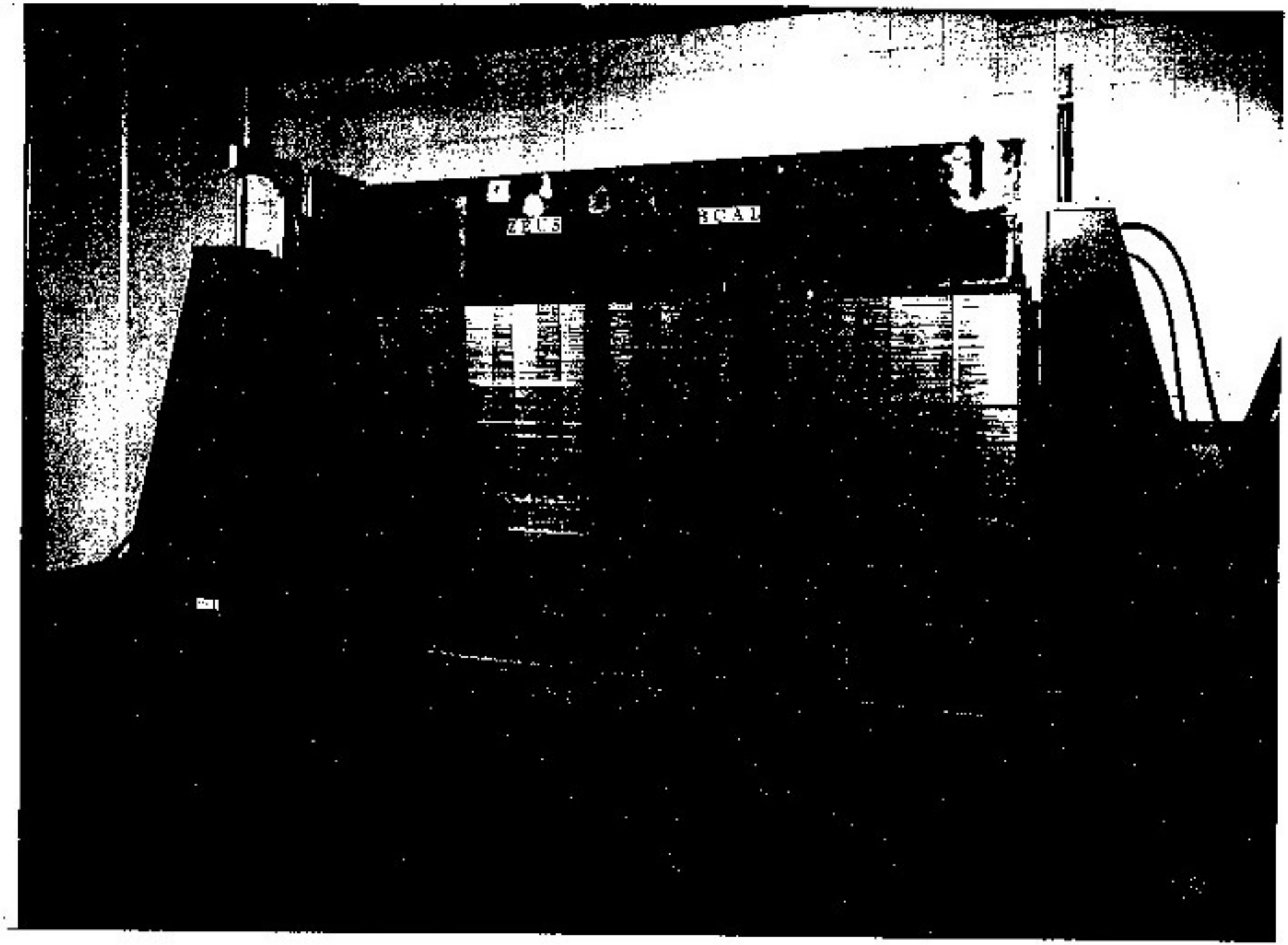
ZEISS
SCAL

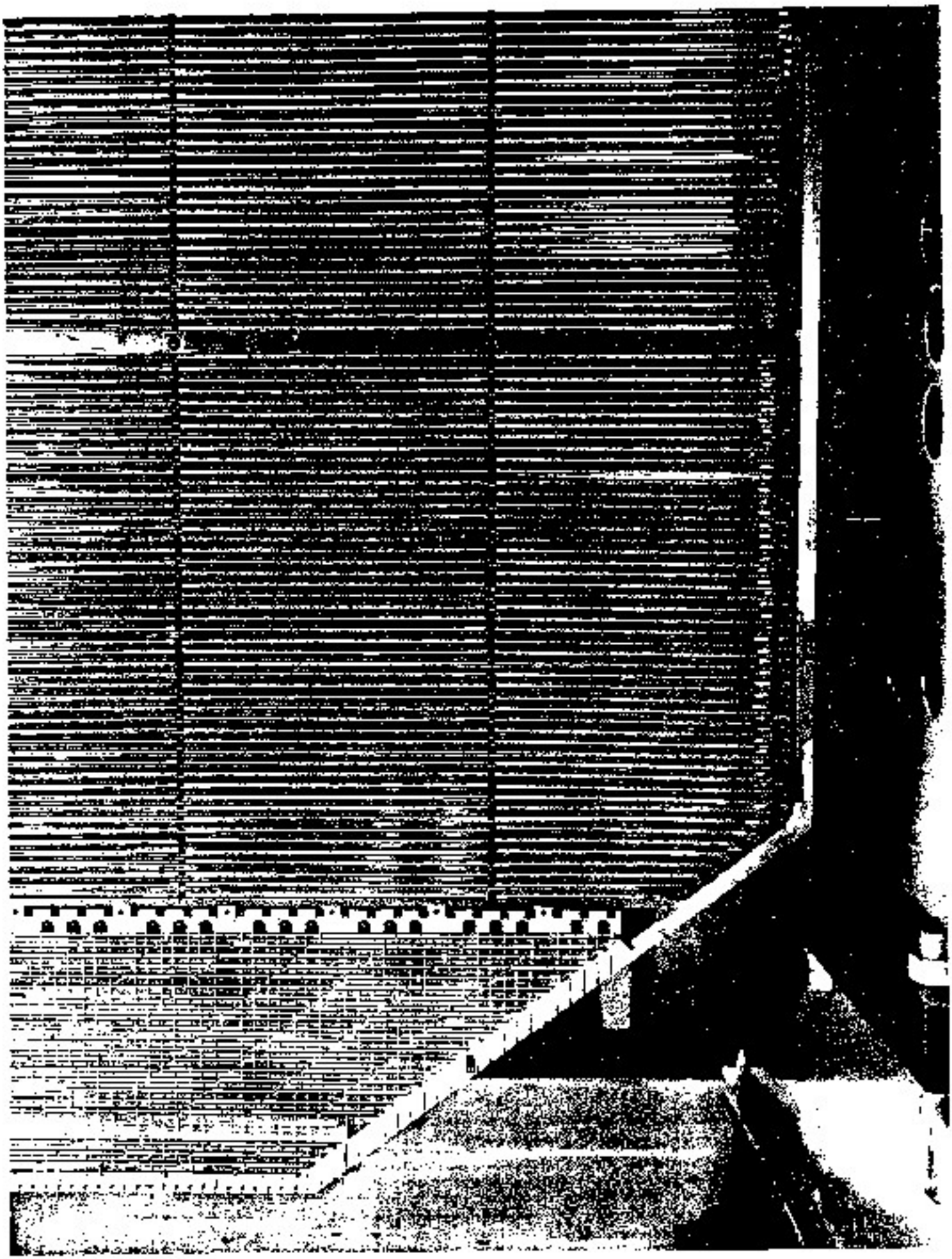

FORWARD CALORIMETER MODULE

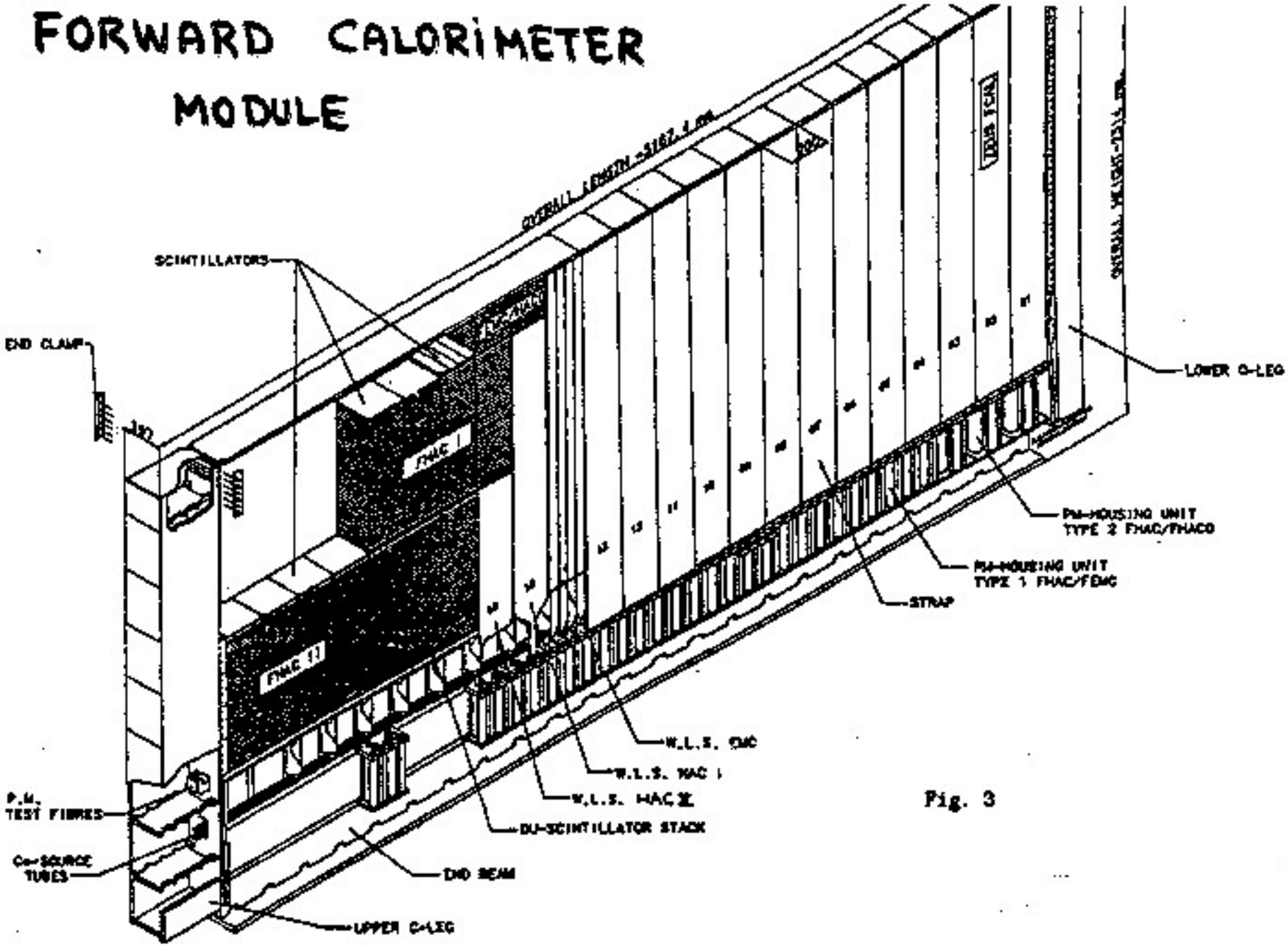

Fig. 3

ZEI

CALORIMETER TOWER STRUCTURE

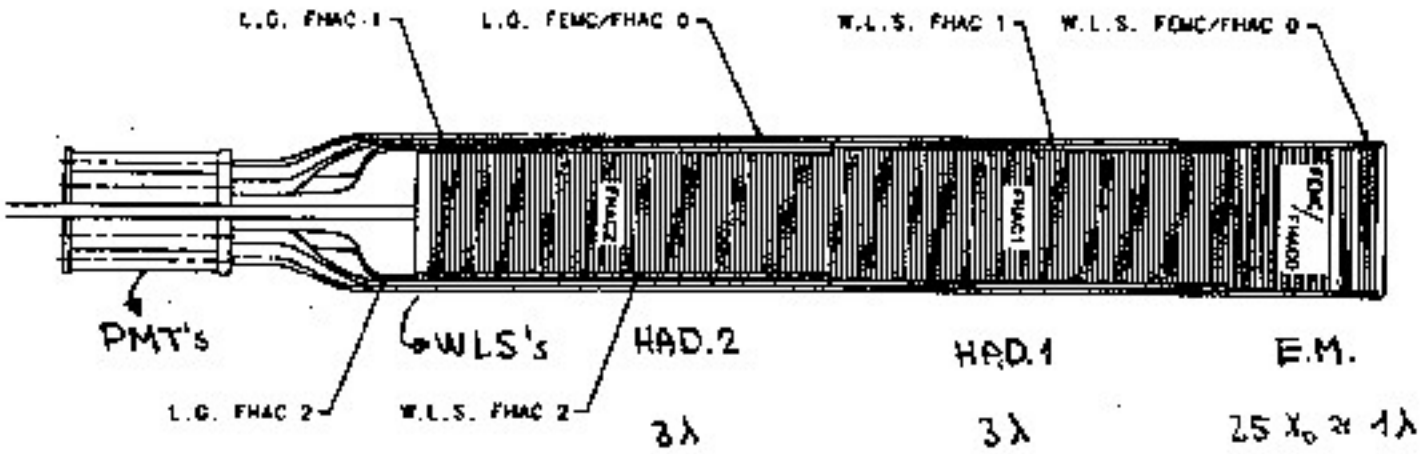

CLADDING OF DEPLETED URANIUM PLATES

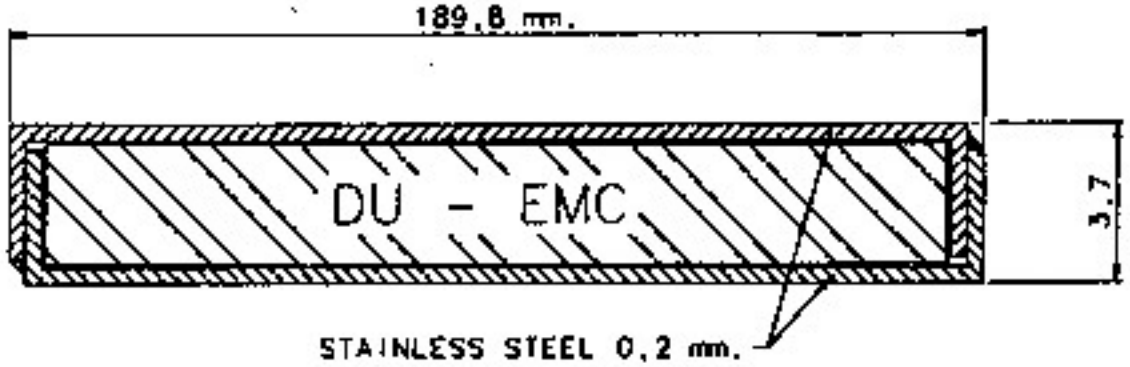

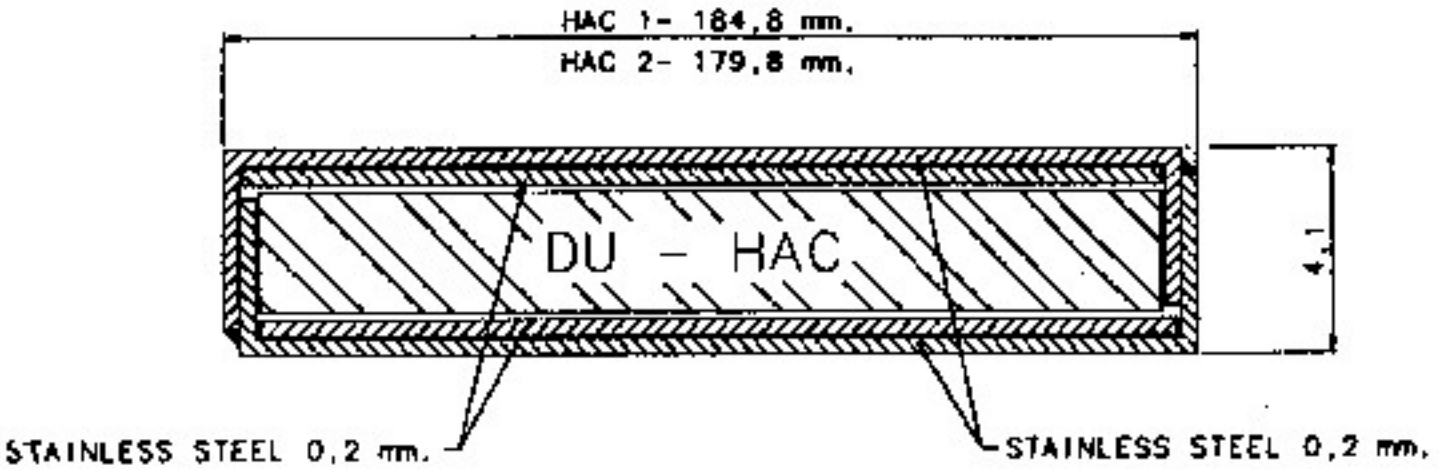

LATERAL SEGMENTATIONS

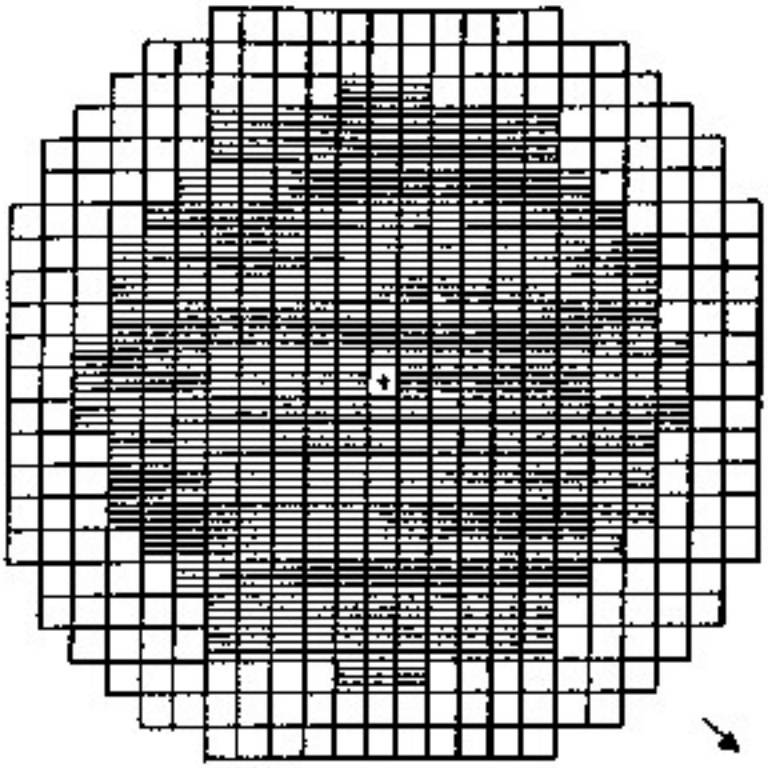

FINER EMC SEGMENTATIONS

FCAL front view

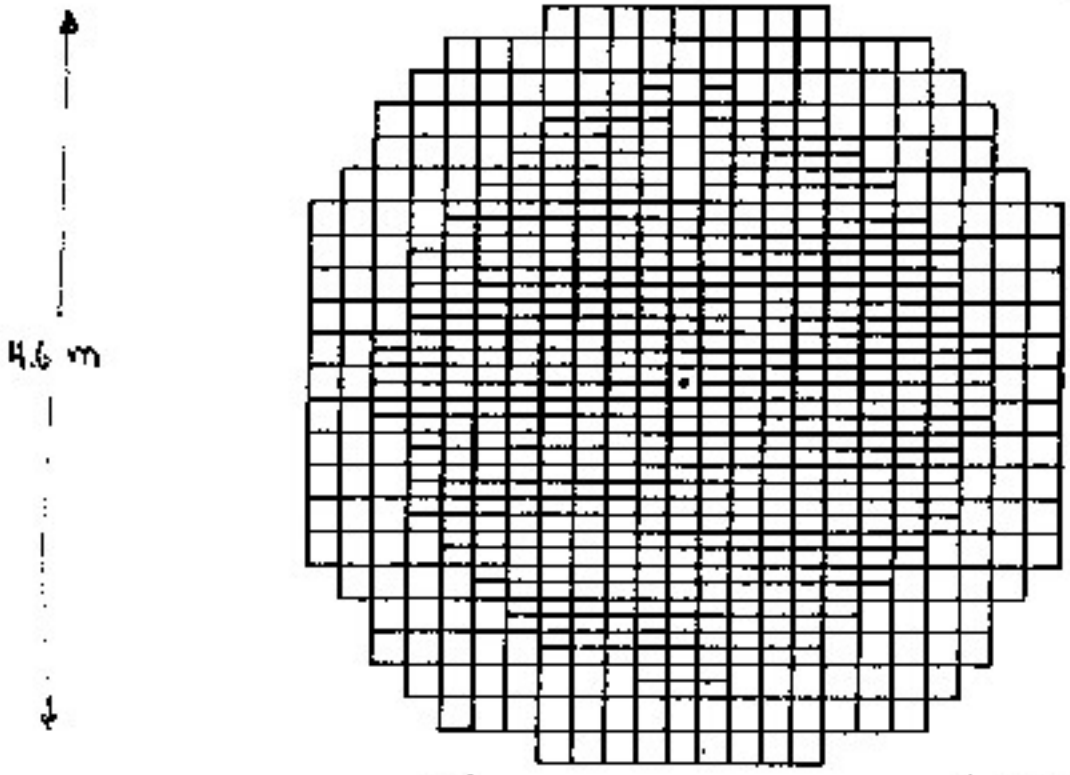

24 MODULES APIECE

RCAL front view

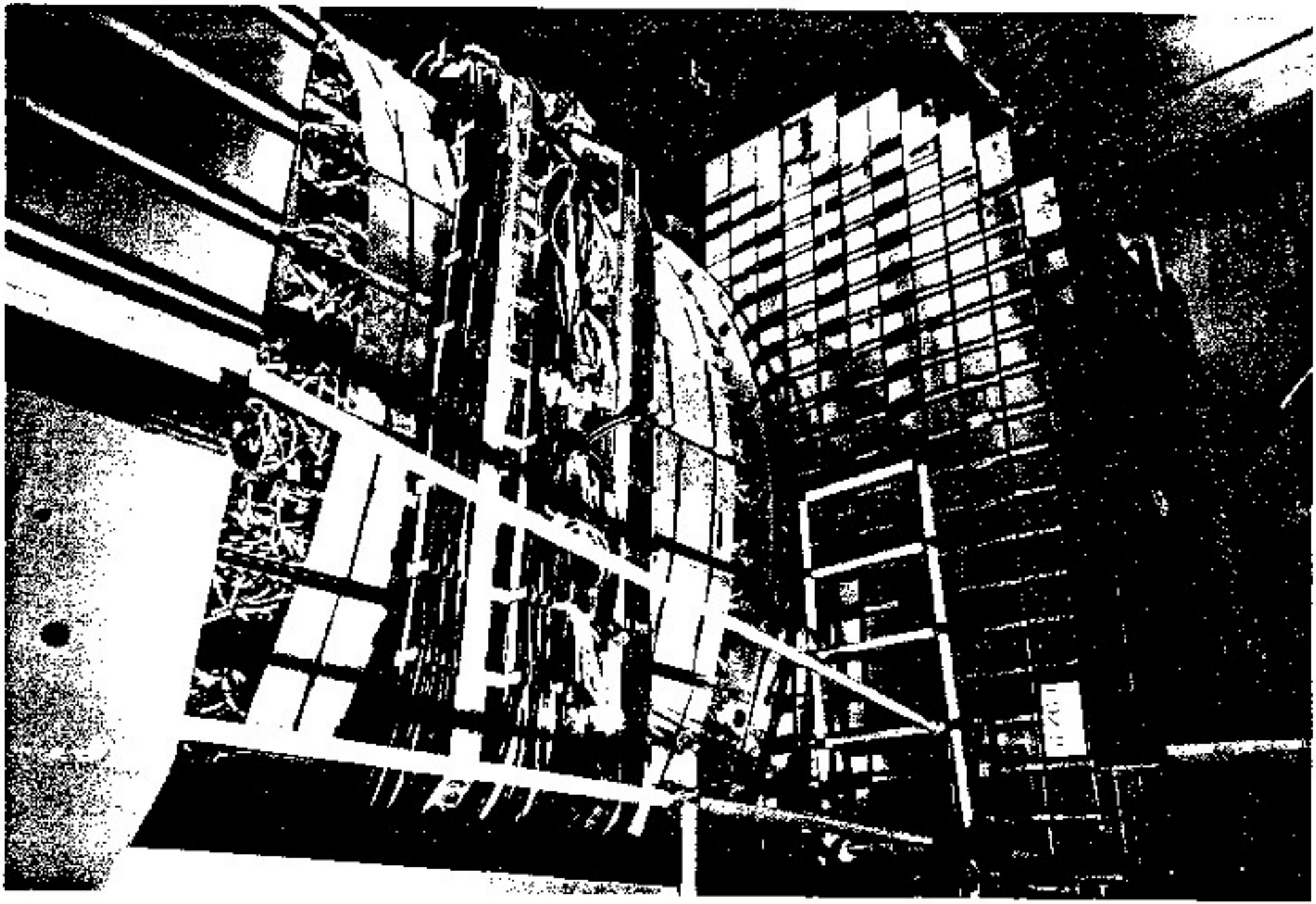

SCINTILLATORS

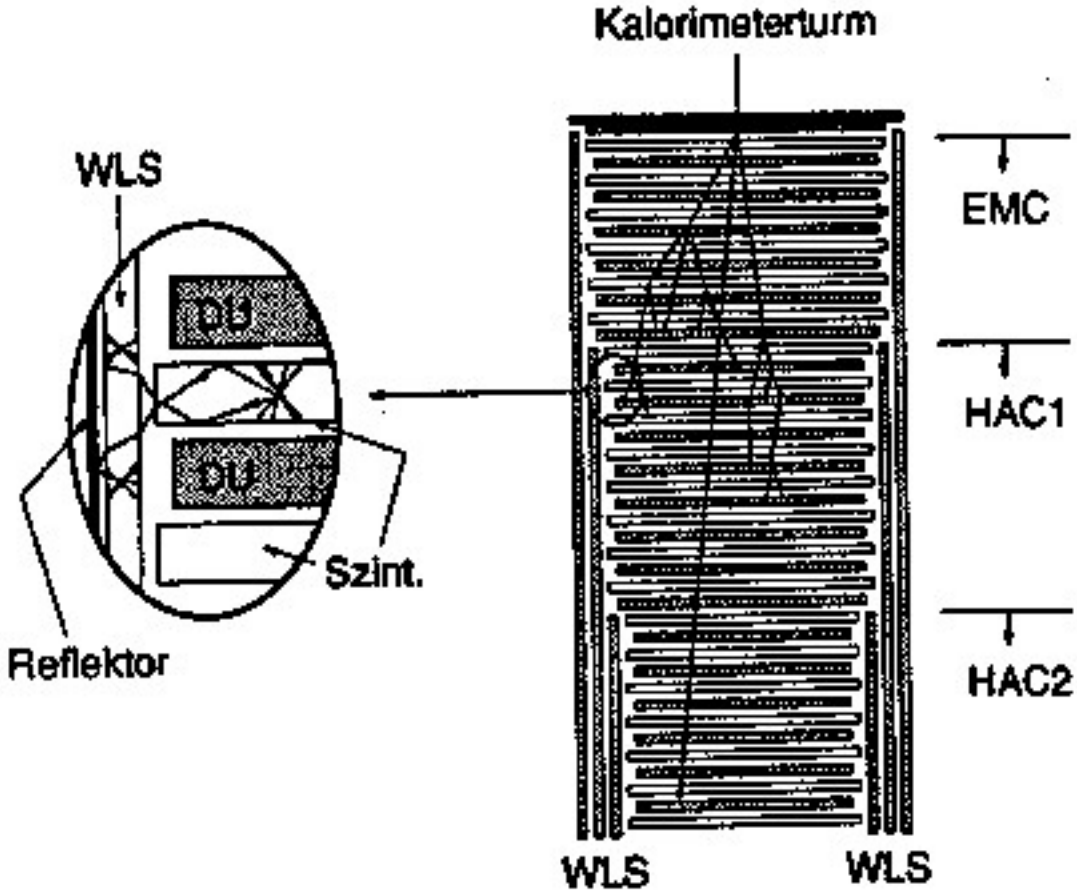

WAVELENGTH SHIFTERS

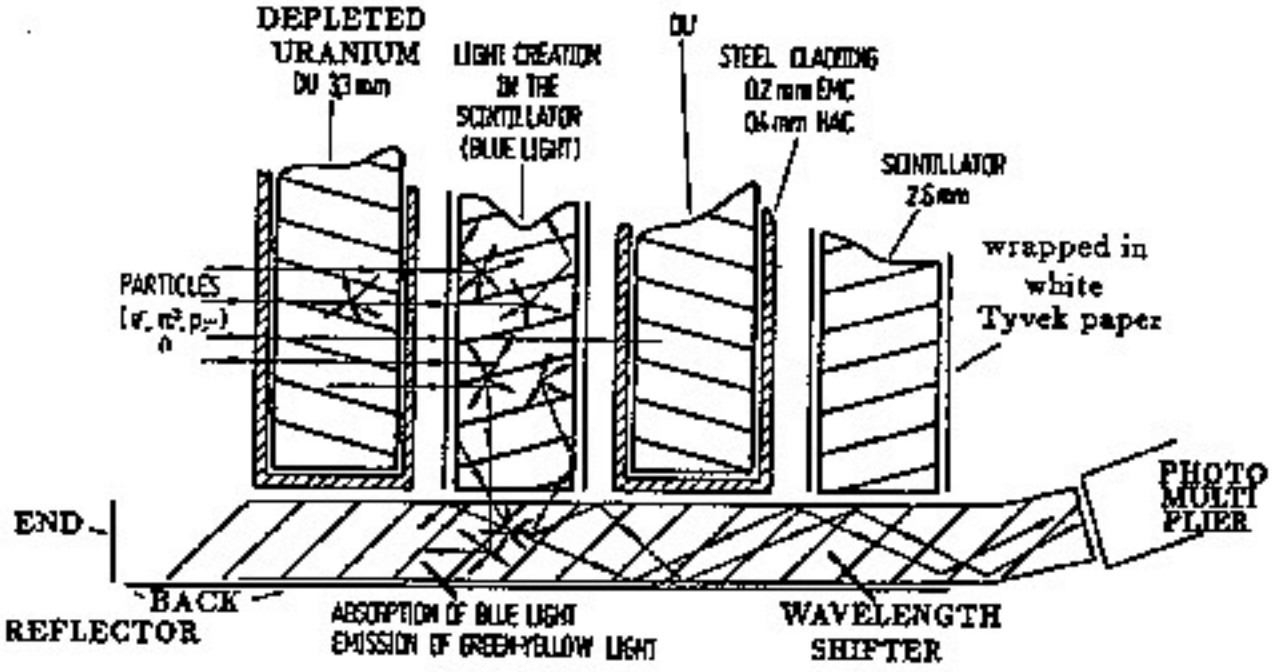

SCINTILLATOR (UNIFORMITY CORRECTION PATTERN)

FOR EMC TILE

BEFORE:

	0.989	0.981	0.984	0.984	0.978	0.981	0.994	0.979
1.035	1.012	1.000		0.996	0.991	0.993	0.988	0.994
1.113	1.075	1.025	1.010	0.993	1.000	1.013	1.004	1.006
1.111	1.100	1.050	1.015	1.009	1.013	1.009	1.005	0.997
1.133	1.096	1.067	1.027	1.016	1.010	1.004	0.993	1.000
1.142	1.106	1.070	1.036	1.029	1.009	1.006	1.001	1.000
1.136	1.101	1.076	1.037	1.026	1.019	1.007	1.008	0.999
1.126	1.109	1.071	1.045	1.030	1.018	1.006	0.995	0.993
1.100	1.088	1.064	1.036	1.025	1.013	0.990	0.990	0.972
1.109	1.084	1.061	1.050	1.019	1.017	0.991	0.984	0.974

45 35 25 15 5

10 30 50 70 90 (mm)

AFTER:

	0.960	0.972	0.972	0.985	0.996	0.988	0.996	0.985
0.968	0.973	0.986	0.968	0.985	0.990	0.997	0.998	0.996
0.988	0.995	0.975	0.965	0.978	1.004	0.999	1.002	0.995
0.982	1.006	0.994	0.977	0.989	1.005	1.002	1.001	1.004
0.980	1.000	0.996	0.990	0.987	1.001	1.009	1.001	1.004
0.974	1.005	0.996	0.991	0.995	1.013	1.012	1.010	1.000
0.972	0.995	0.993	0.987	0.996	1.000	1.006	1.002	0.998
0.960	0.989	0.983	0.976	0.991	0.998	0.990	0.984	0.989
0.937	0.966	0.971	0.970	0.976	0.988	0.979	0.986	0.975

45 35 25 15 5

15 35 55 75 95 (mm)

--- nonuniformity < 2.5 %
—— nonuniformity < 5.0 %

WAVELENGTH SHIFTER

TEST SETUP:

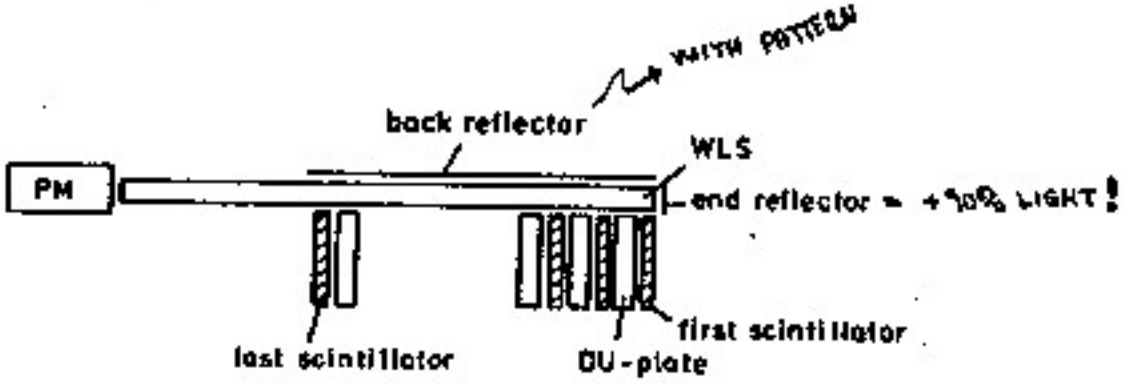

WLS - CASSETTE:

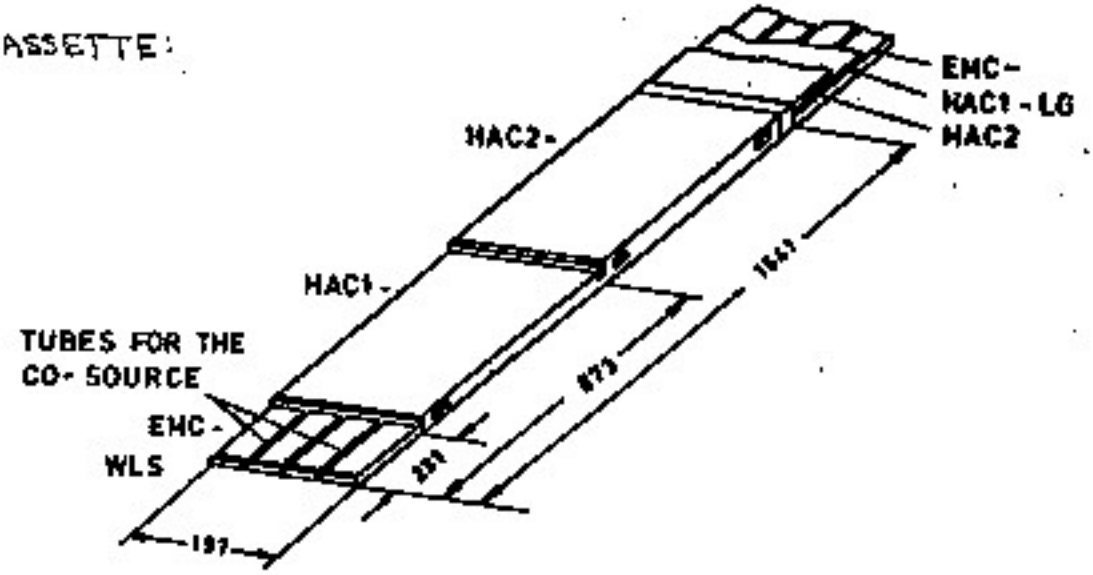

CORRECTIVE PATTERN :

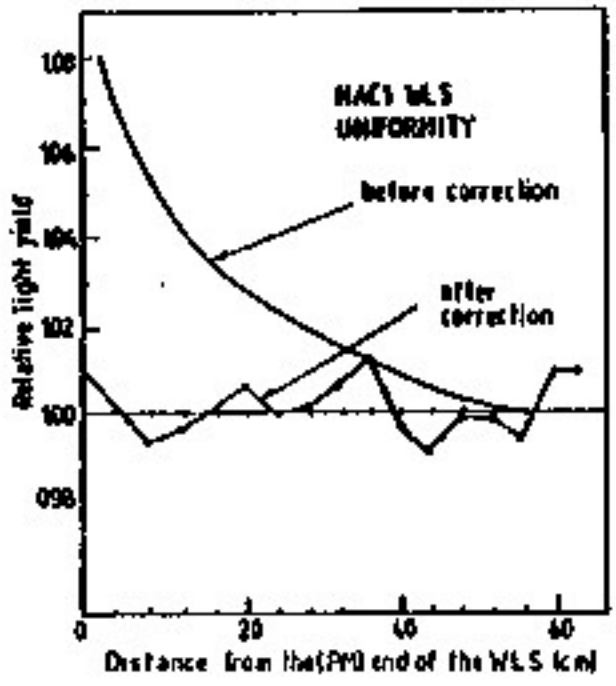

OPTICAL CHAIN PROCESSES

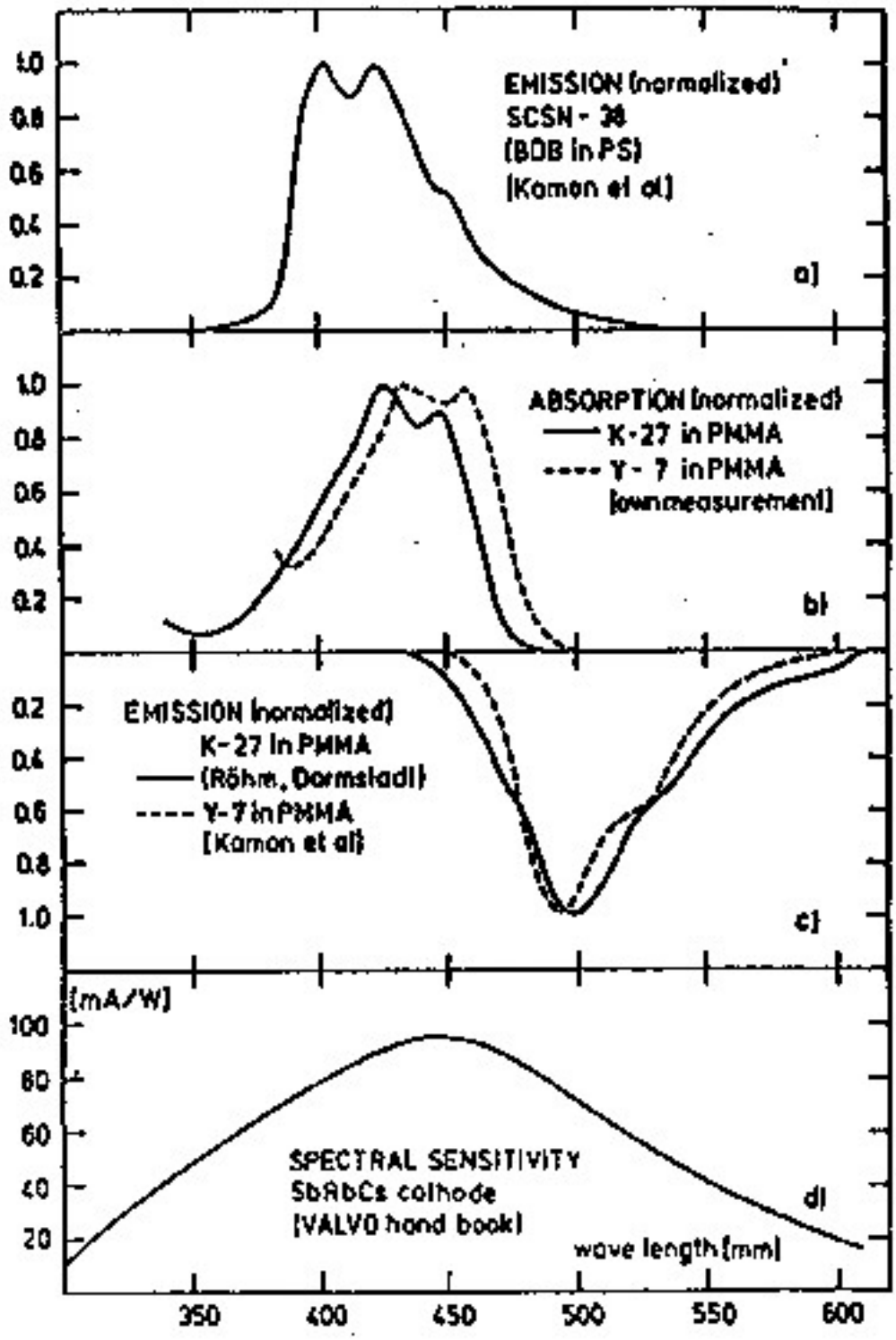

ZEUS CALORIMETER PROTOTYPE

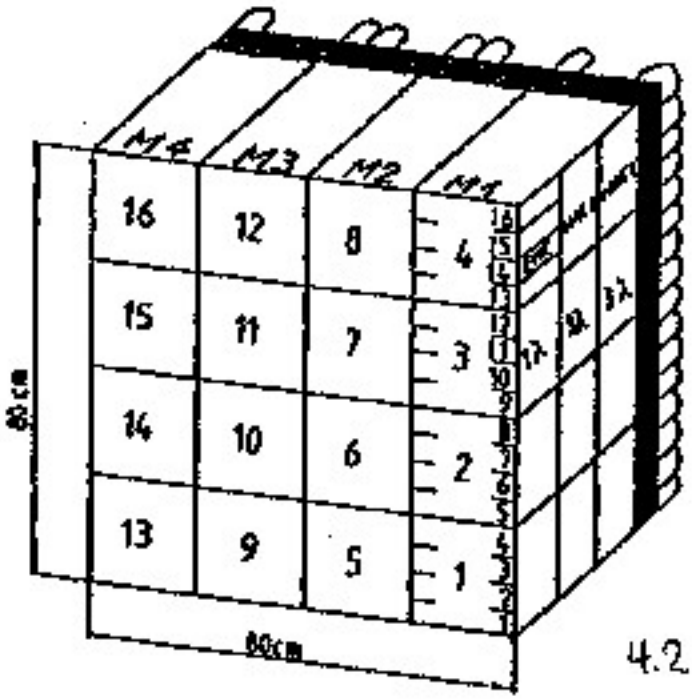

4.2 λ DEEP

SETUP:

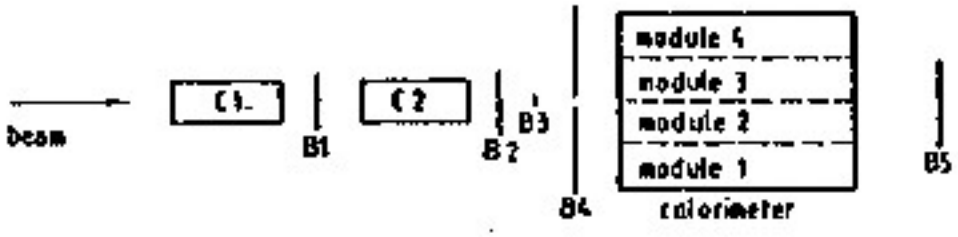

Beam = B1. B2. B3. $\overline{B4}$
e trigger = Beam. C2
h trigger = Beam. $\overline{C2}$
μ trigger = Beam. B5

ENERGY SCANS — ABSOLUTE ENERGY CALIBRATION

CERN - PS

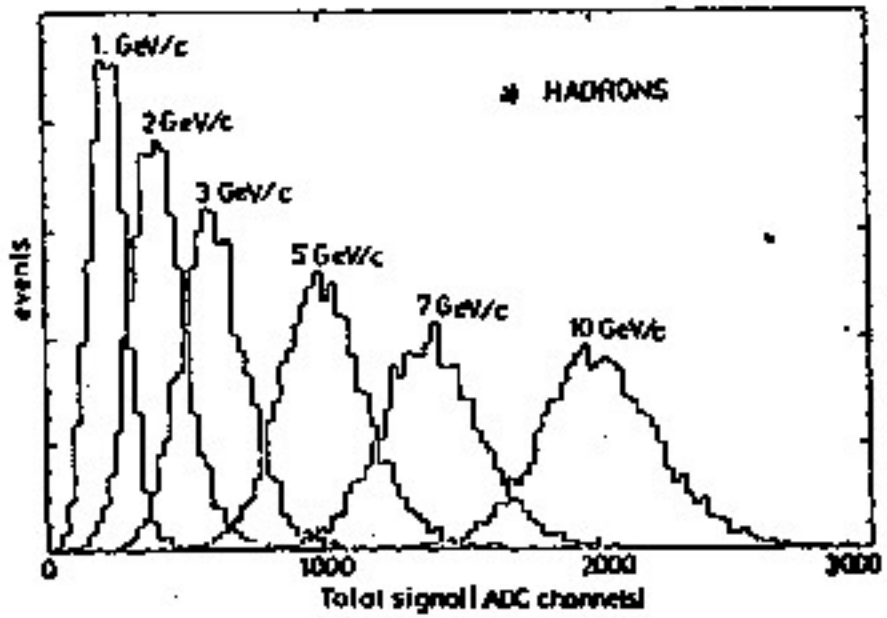

CERN - SPS

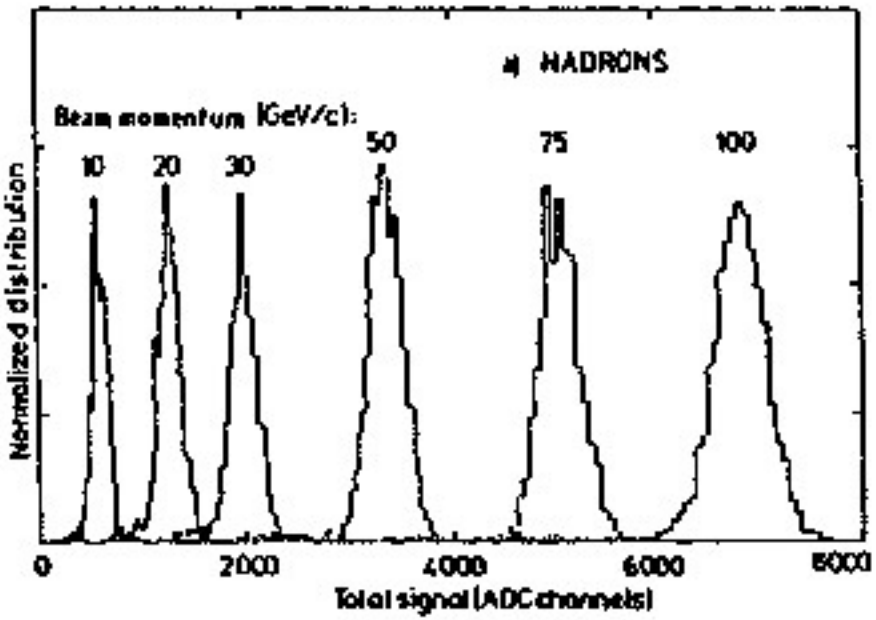

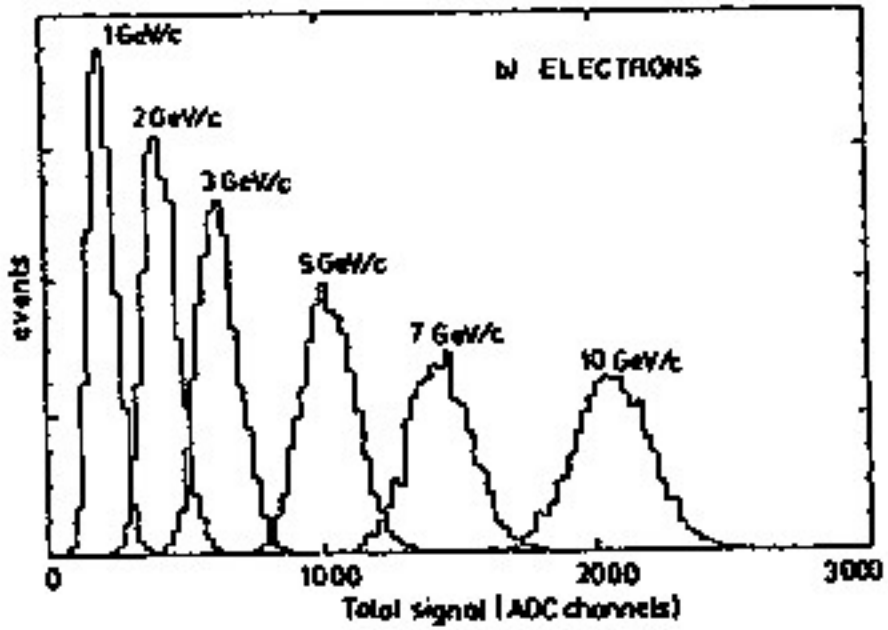

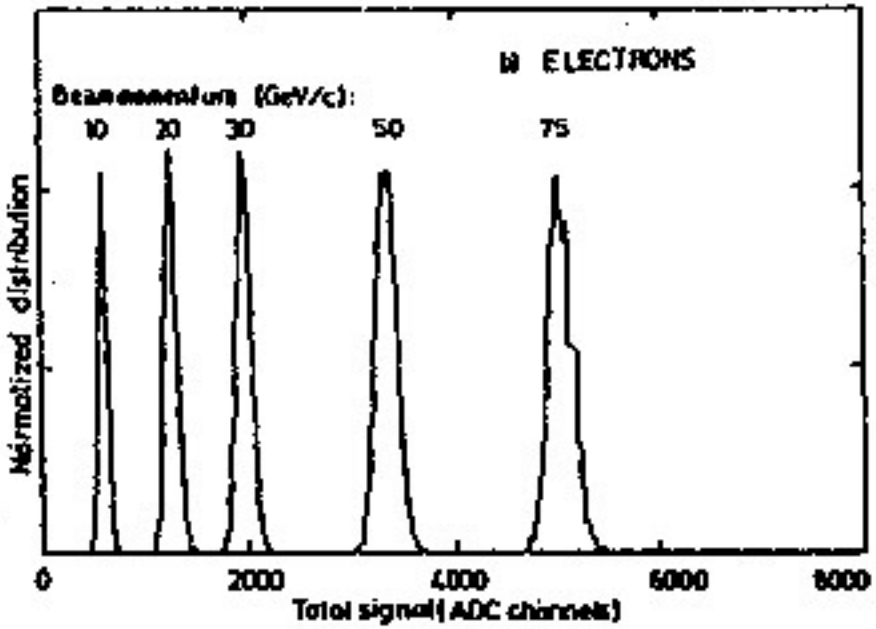

ENERGY DISTRIBUTIONS

LONGITUDINAL:

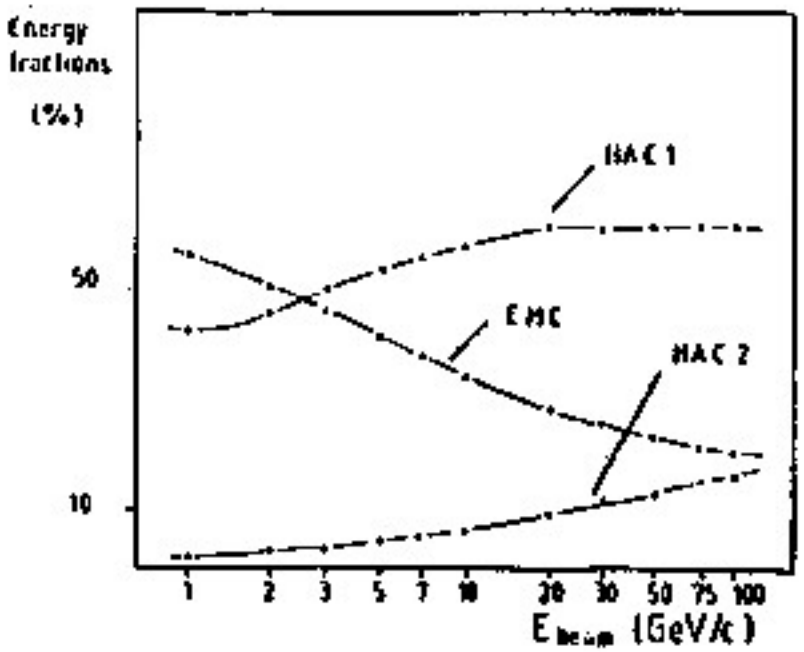

LATERAL:

Lateral spread of 30 GeV/c hadron showers

0.01	002	0.07	004	007	002	001
002	009	0.25	0,30	0,25	0.09	002
0.07	025	1,3	3,7	1,3	0,25	007
004	0,30	3,7	75,5	37	0,30	0.04
0.07	0,25	1,3	3,7	1,3	0,25	007
002	0,09	0,25	0,30	0,25	0,09	002
001	002	007	004	007	002	001

Total sum = 100

LONGITUDINAL INTERCALIBRATION

α = INTERCALIBRATION PARAMETER

ENERGY RESOLUTION:

→ DIFFERENT MINIMA!

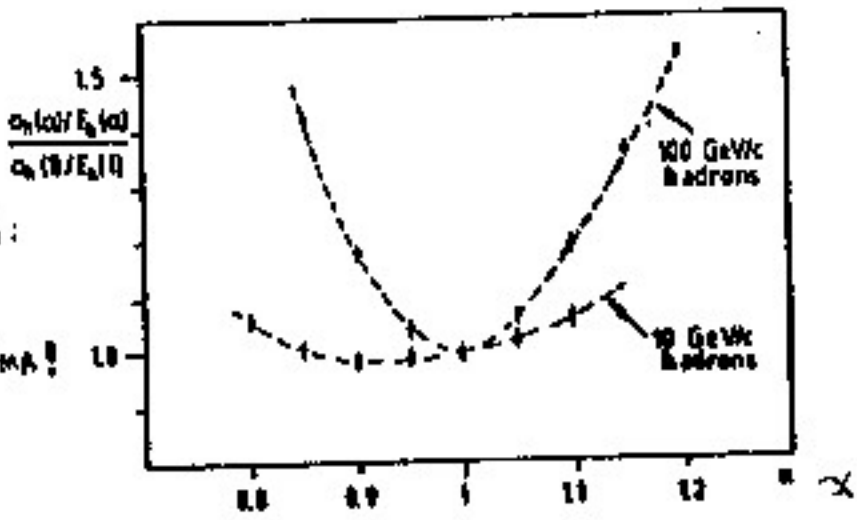

α WHILE MINIMIZING

THE HADRONIC RESOLUTION

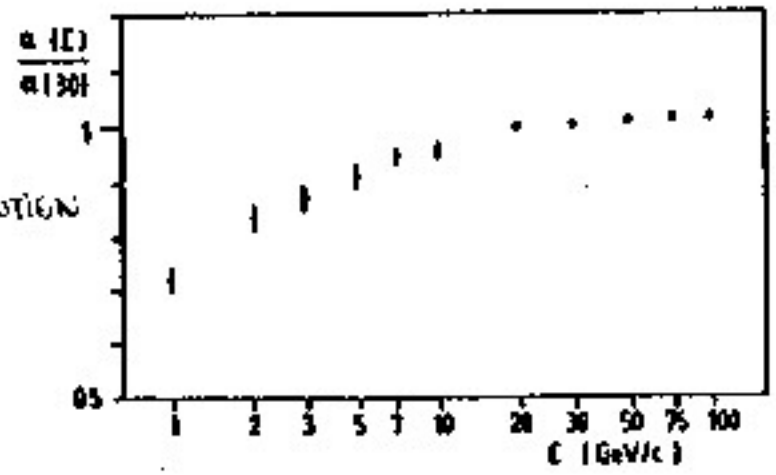

e/h RATIO

→ NO UNIQUE SOLUTION!

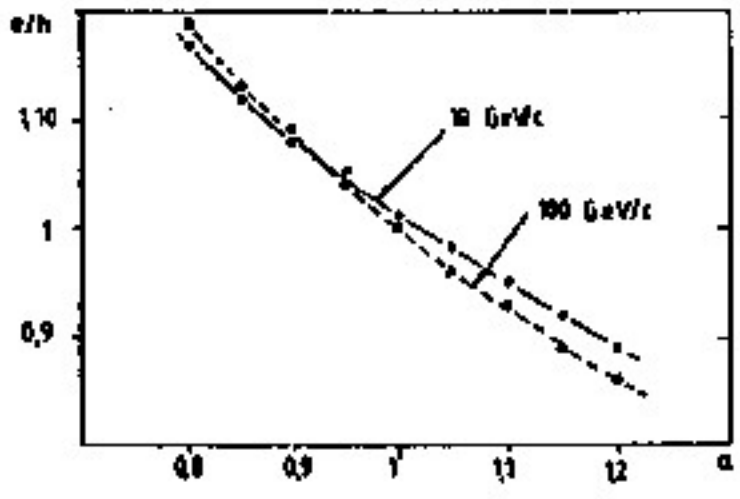

LINEARITY .

OR HOW WELL IS THE ENERGY PROPORTIONAL TO THE SIGNAL ?

DEVIATIONS FROM LINEARITY

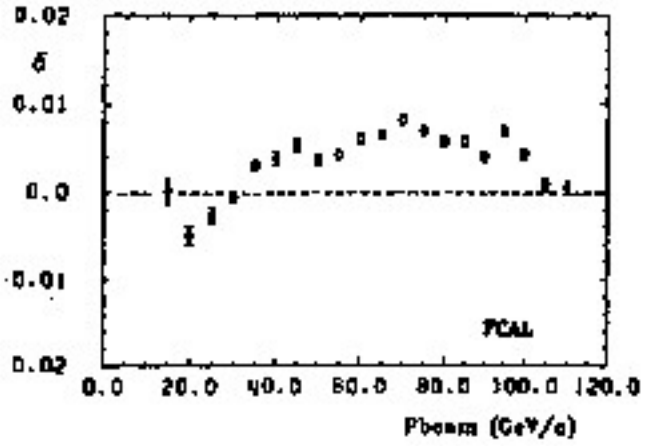

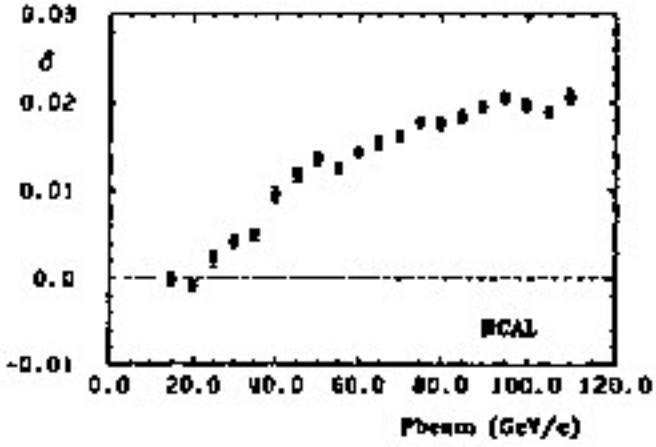

RESOLUTION

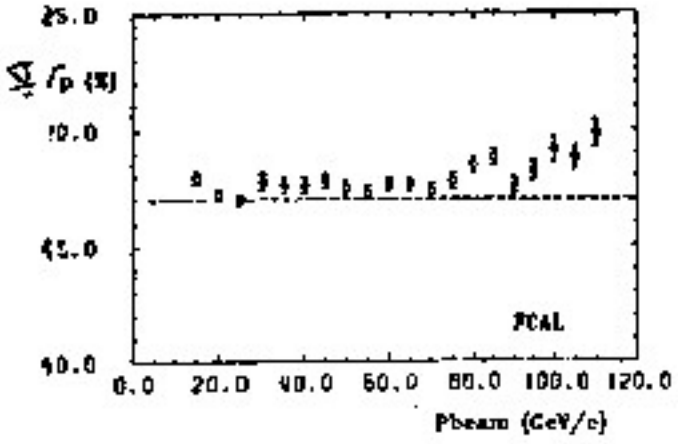

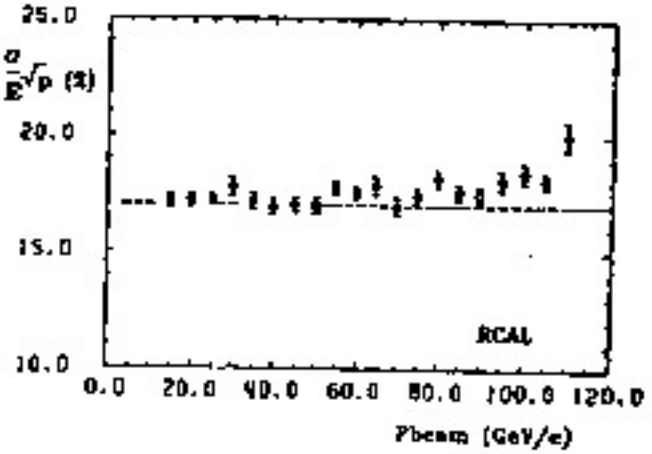

PERFORMANCES

e/h RATIO

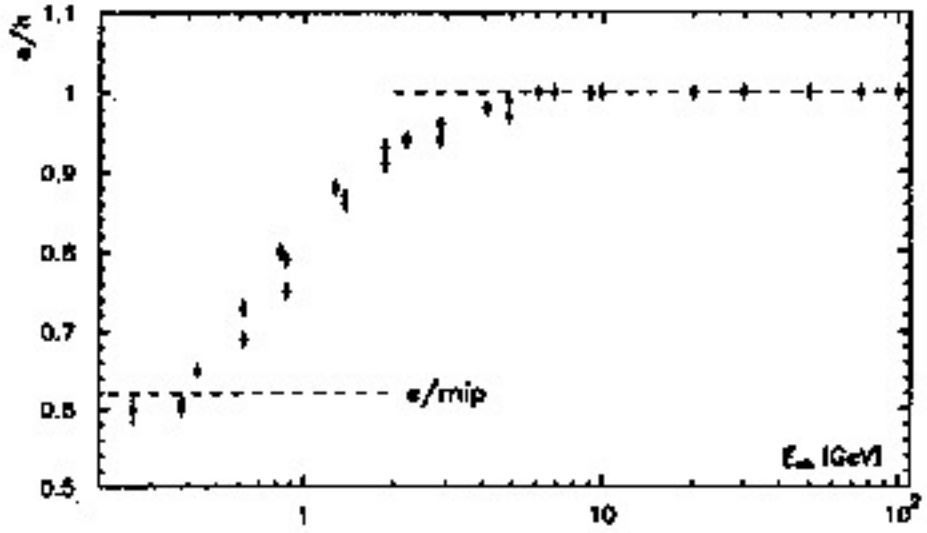

{ 3.3 mm U ≈ 1 X_0
{ 2.6 mm Scintillator

ENERGY RESOLUTIONS

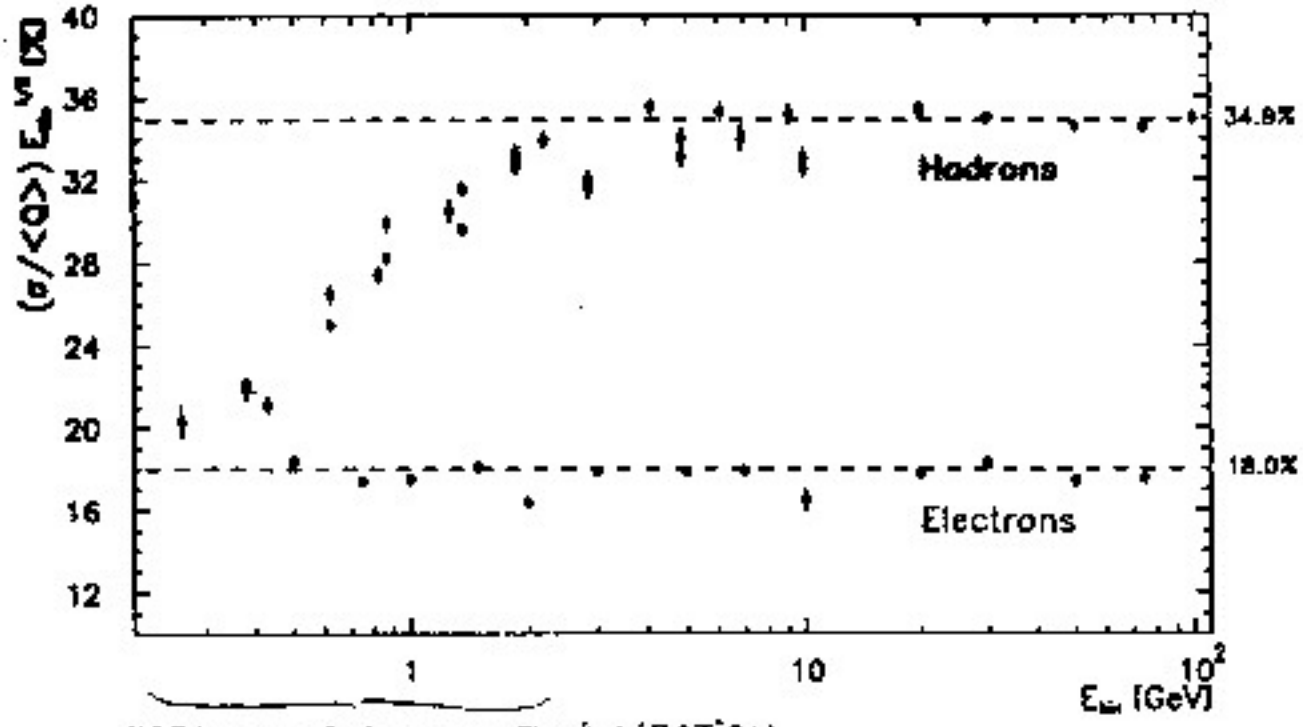

HADRONS: MORE LOSSES BY IONIZATION

PERFORMANCES

e/h RATIO (LOWER ENERGY RANGES)

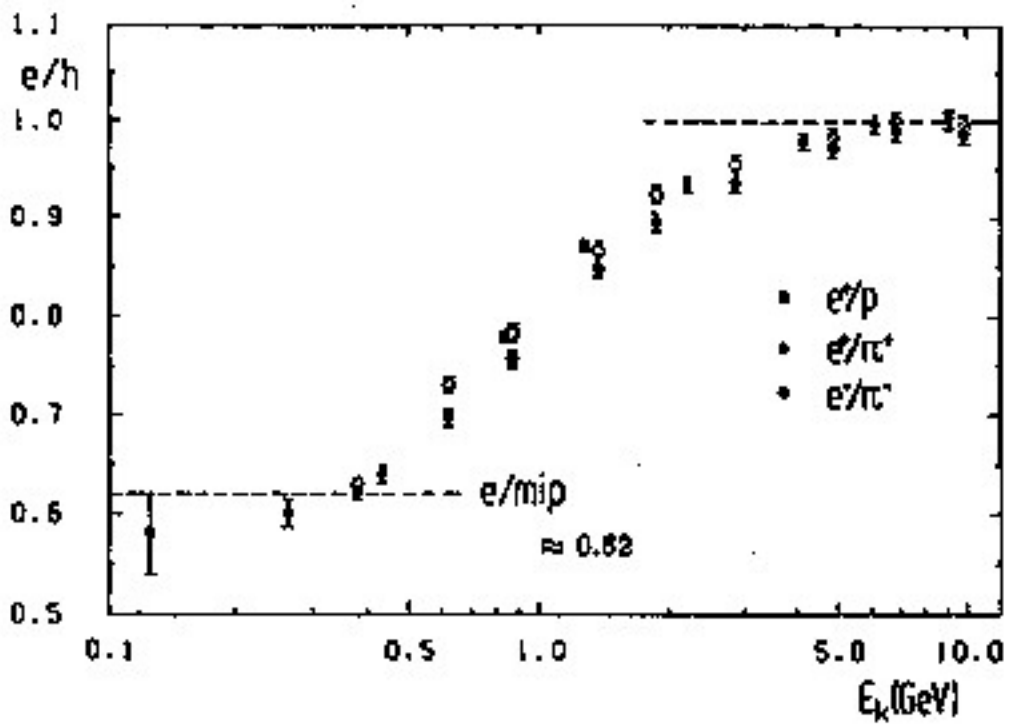

ENERGY RESOLUTIONS

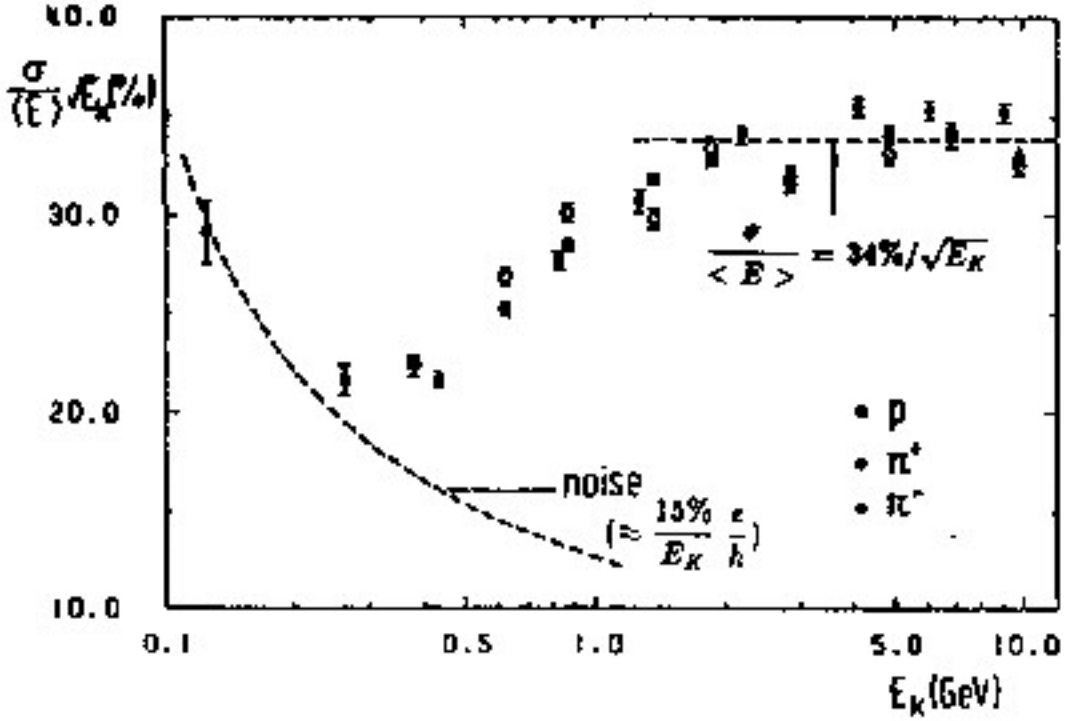

RESPONSE NON-UNIFORMITY BETWEEN MODULES (HELIOS' WORST CASE)

TOTAL SIGNAL

SINGLE SIGNALS

RESOLUTION

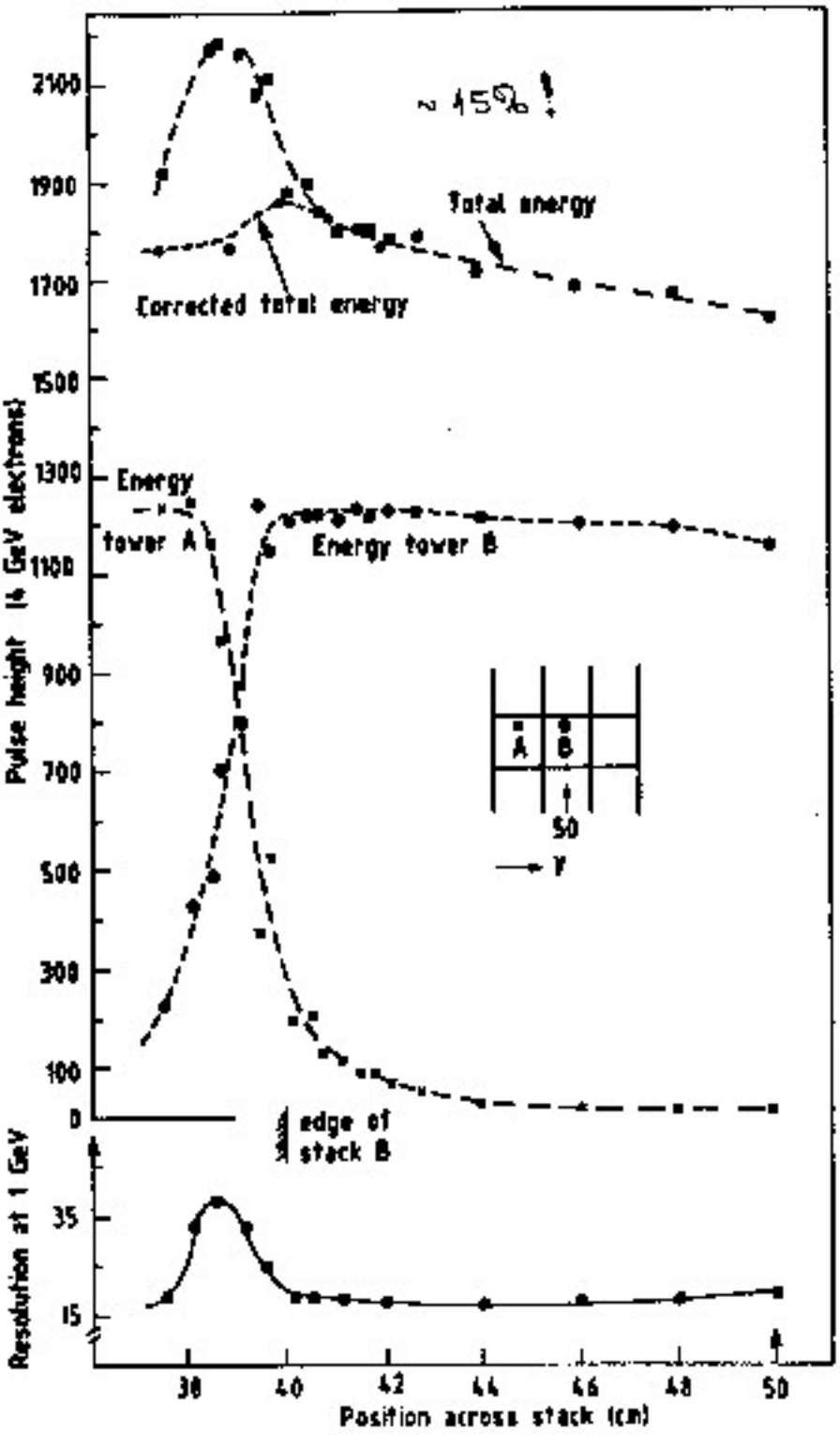

UNIFORMITY TEST SCANS

VS POSITION AND ANGLE

ADD BETWEEN MODULES :

no Pb ↓ | 2 mm Pb ↓ | 3 mm Pb ↓

INCIDENCE ANGLE ↓

Electrons (30 GeV/c)

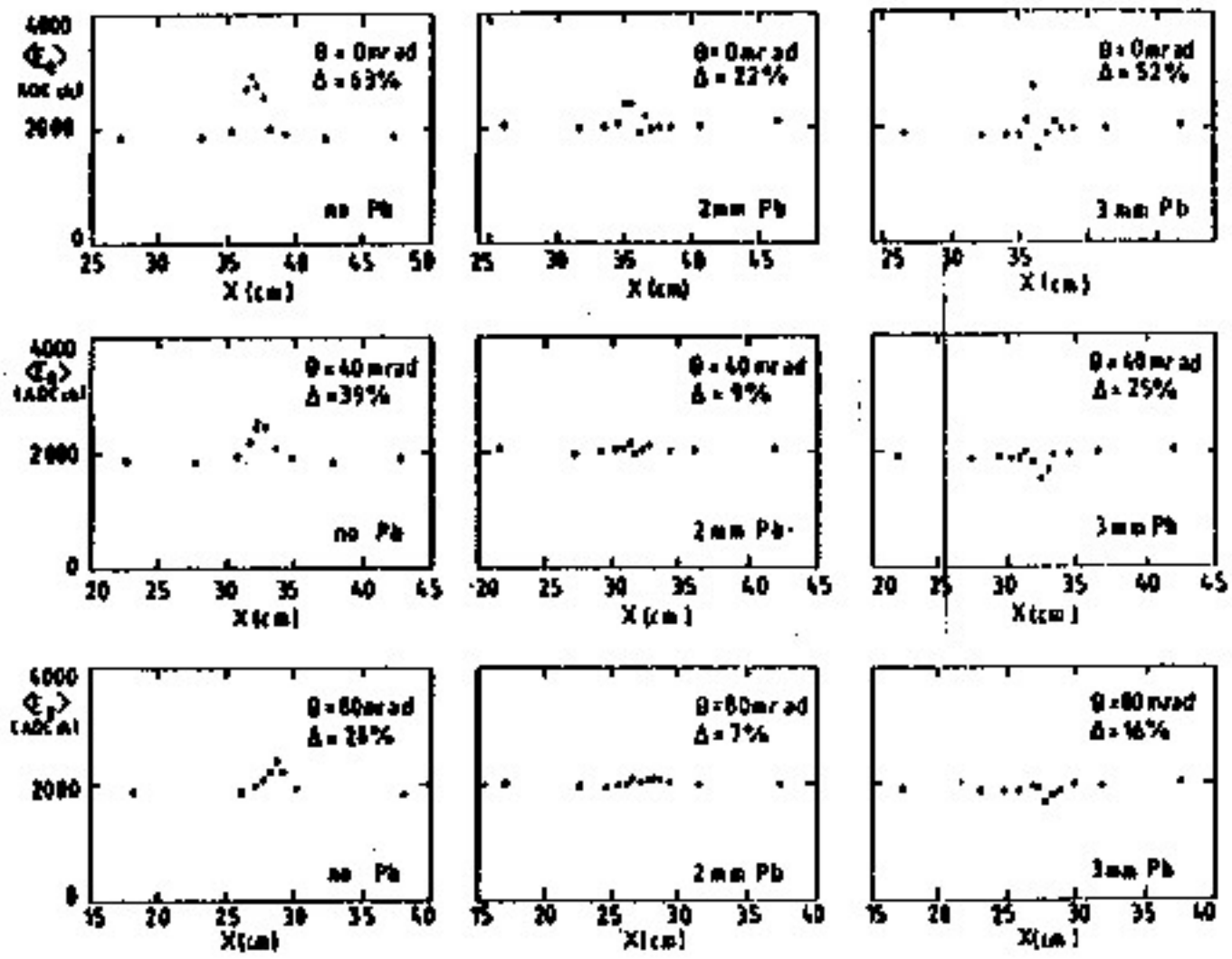

CALIBRATION SCHEMES

URANIUM NOISE SIGNALS (UNO):

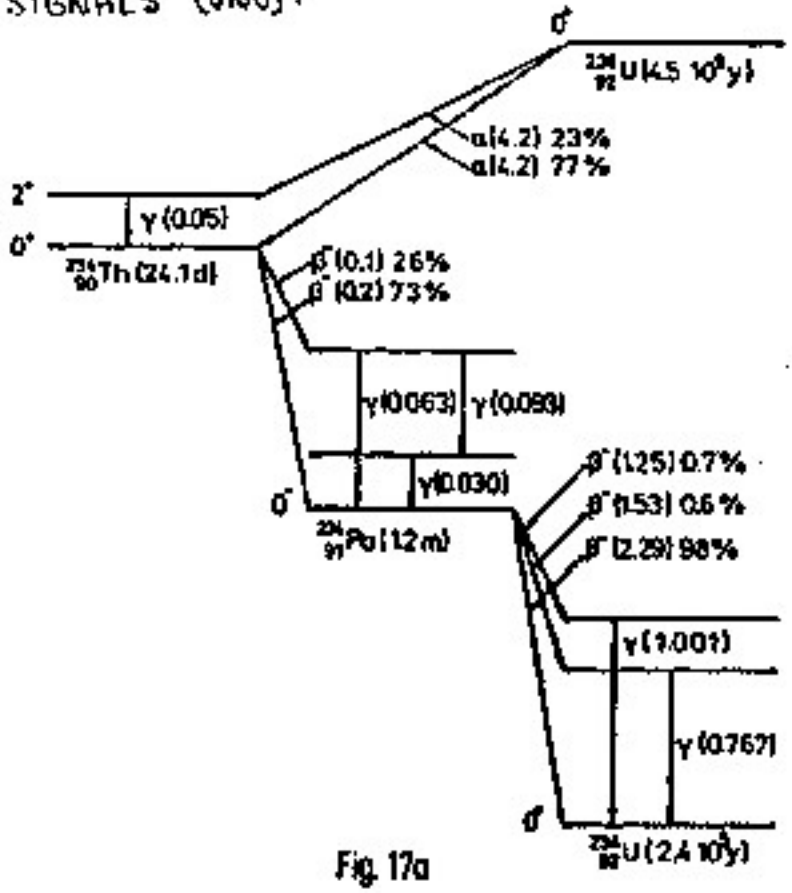

Fig. 17a

4 BEAM-INDEPENDENT CALIBRATION METHODS

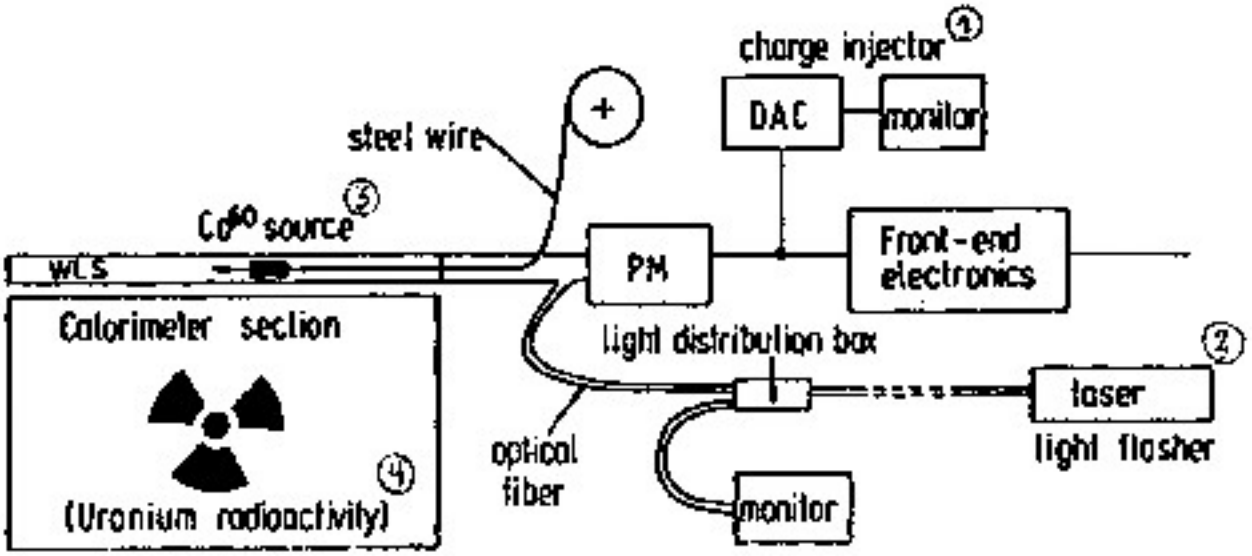

STABILITY CHECKS vs TIME

DEFINITIONS

δ = SHORT-TERM VARIATION

Δ = LONG- " "

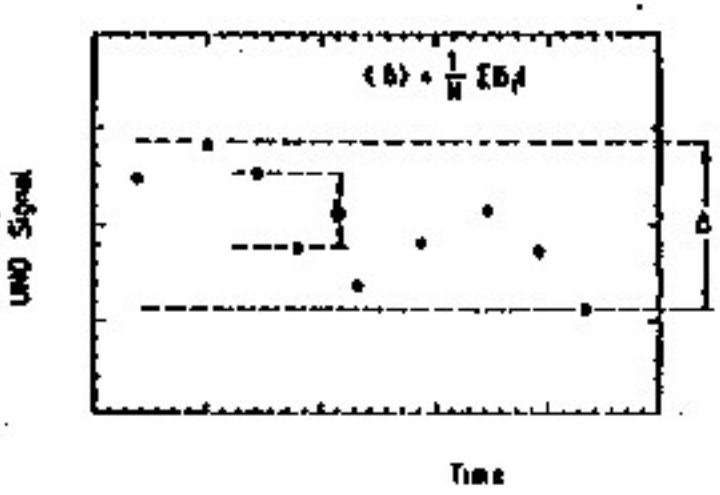

UNO SIGNAL

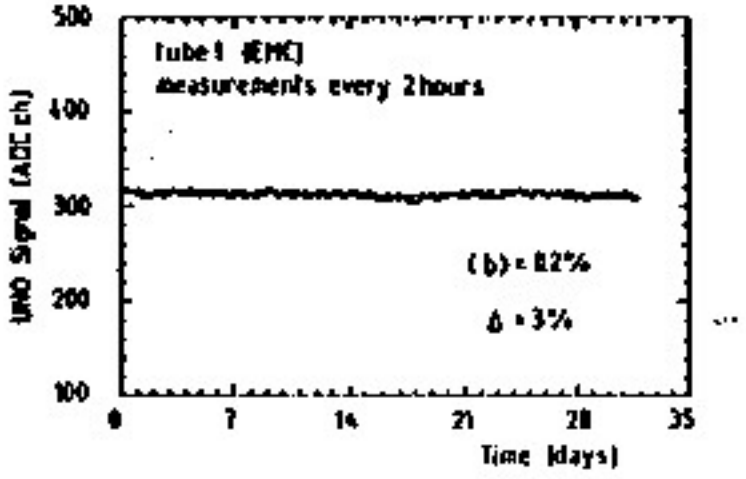

COBALT SOURCE SCANS

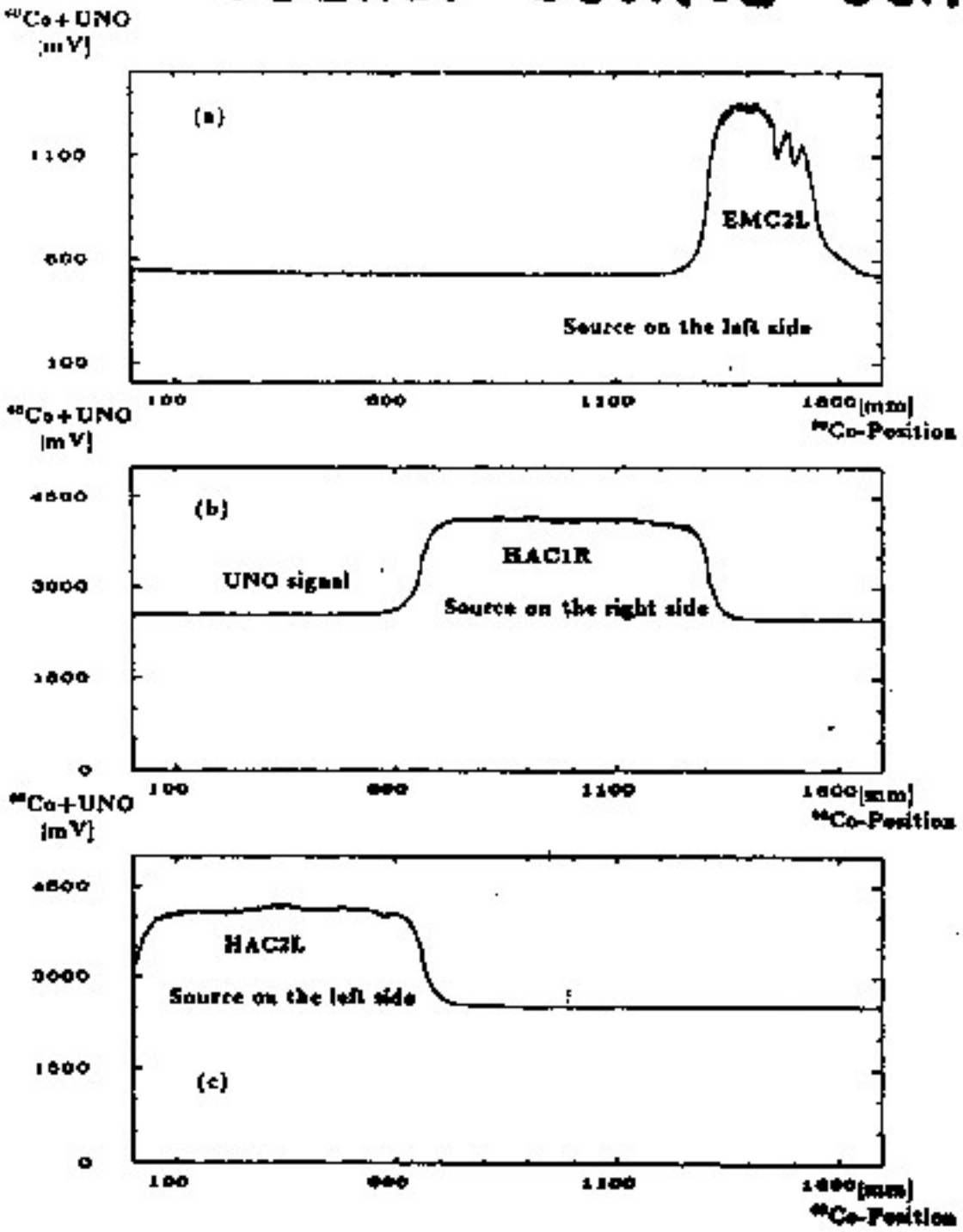

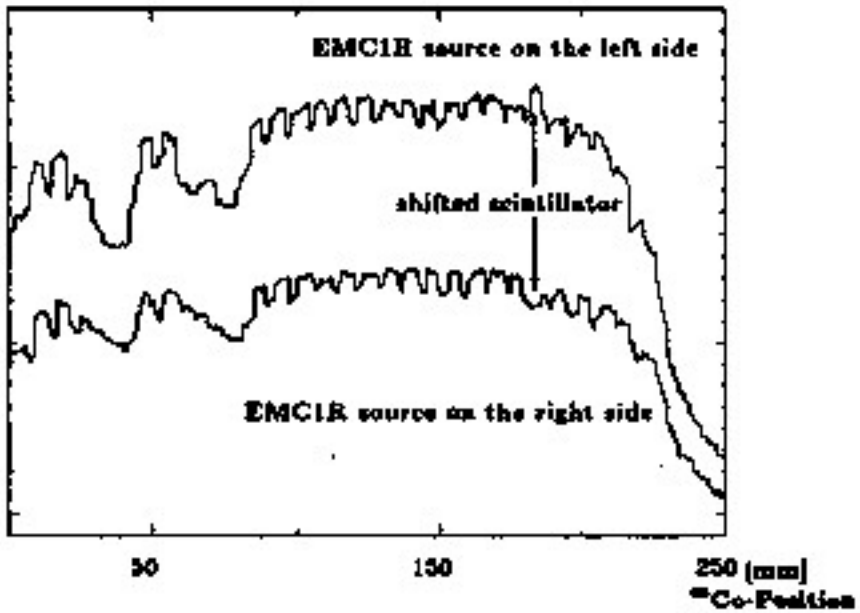

SCAN ALONG THE WLS's,
AT THE END OF THE SCINTILLATORS

... A GOOD DIAGNOSTIC TOOL
E.G. FOR MECHANICAL PROBLEMS

COSMIC MUON SIGNALS

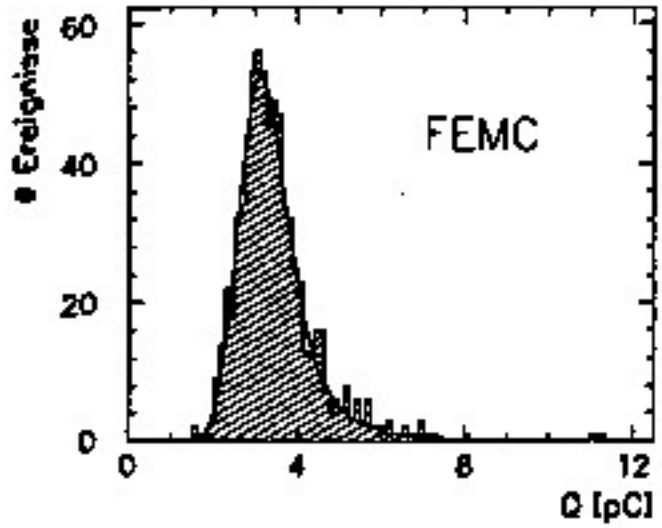

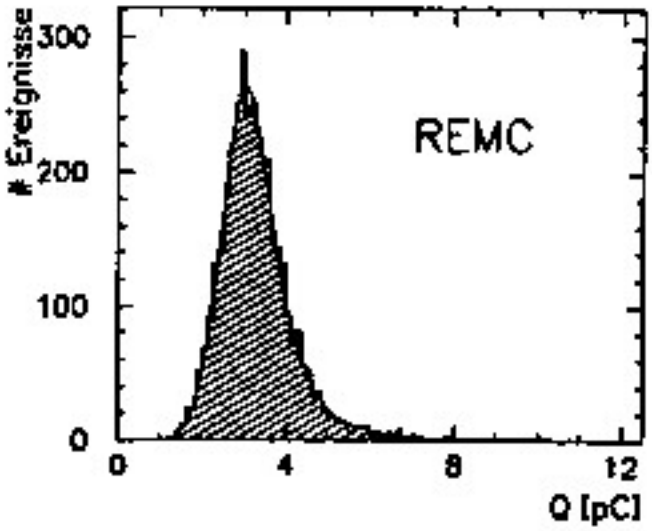

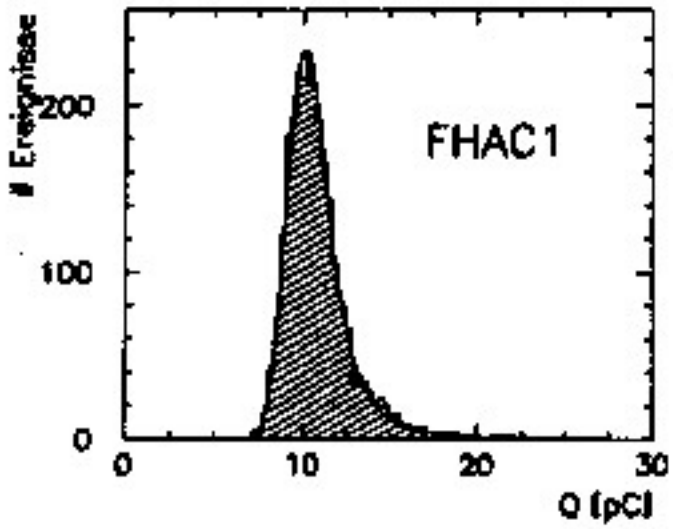

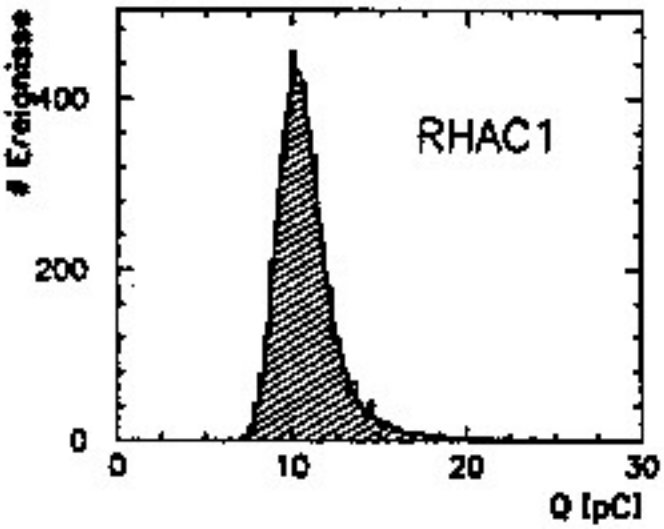

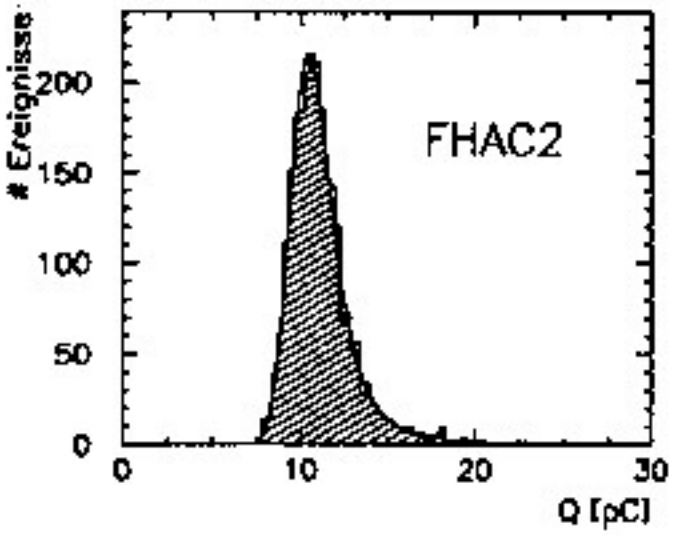

... BEFORE INSTALLING THE MODULES IN THE DETECTOR

HALO MUON SIGNALS

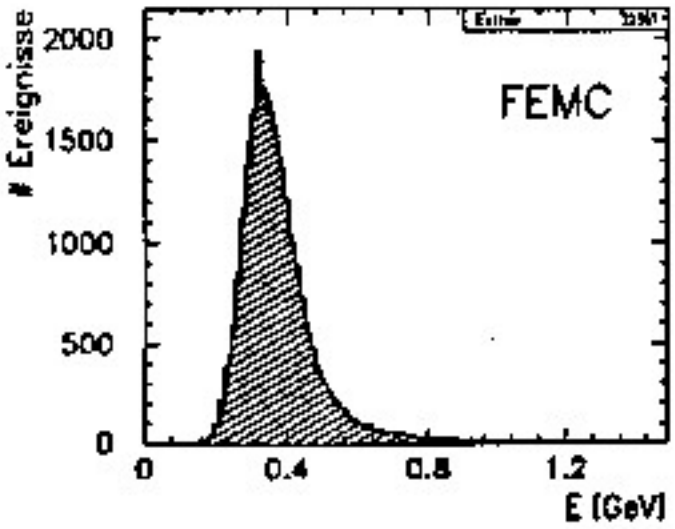

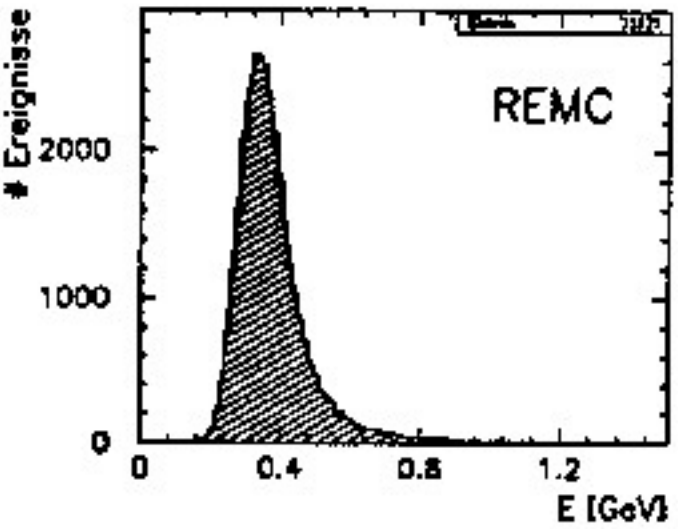

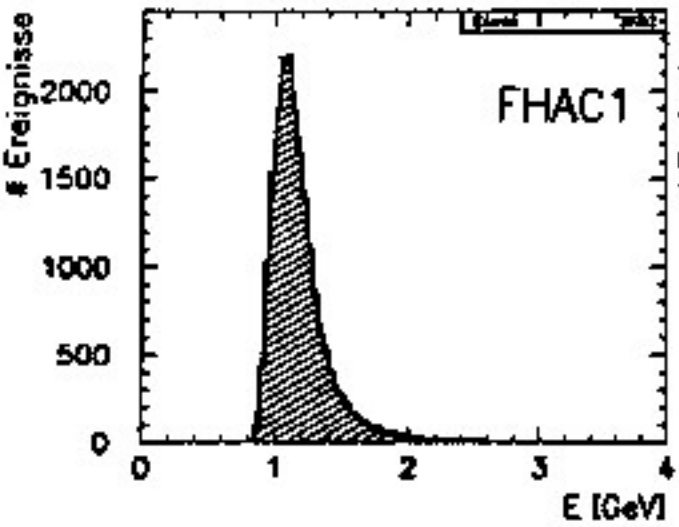

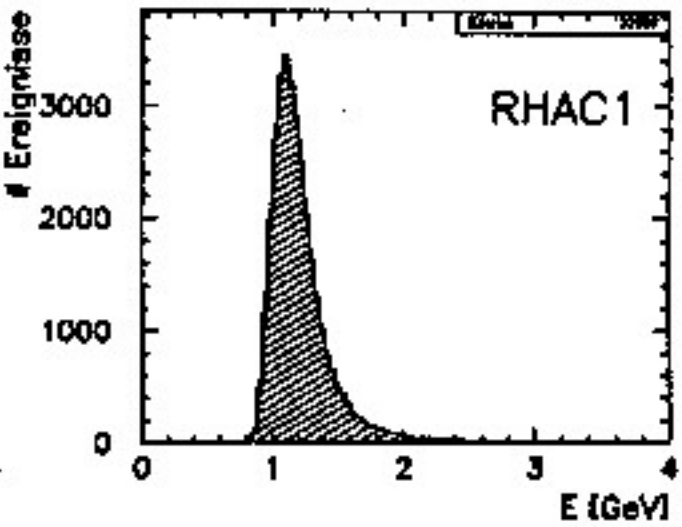

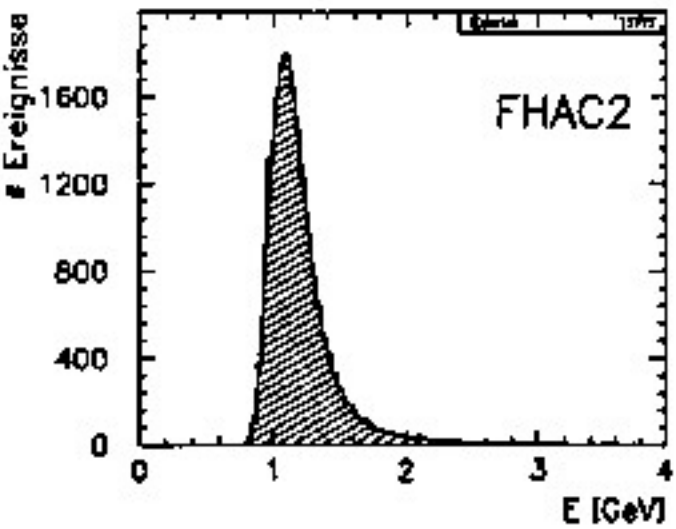

... AFTER INSTALLATION OF THE MODULES IN THE DETECTOR

CALORIMETER TEST SET UP

TO INVESTIGATE THE MAGNETIC FIELD DEPENDENCE OF THE CALIBRATION

SINCE THE SCINTILLATOR LIGHT OUTPUT IS $\vec{B}$- DEPENDENT

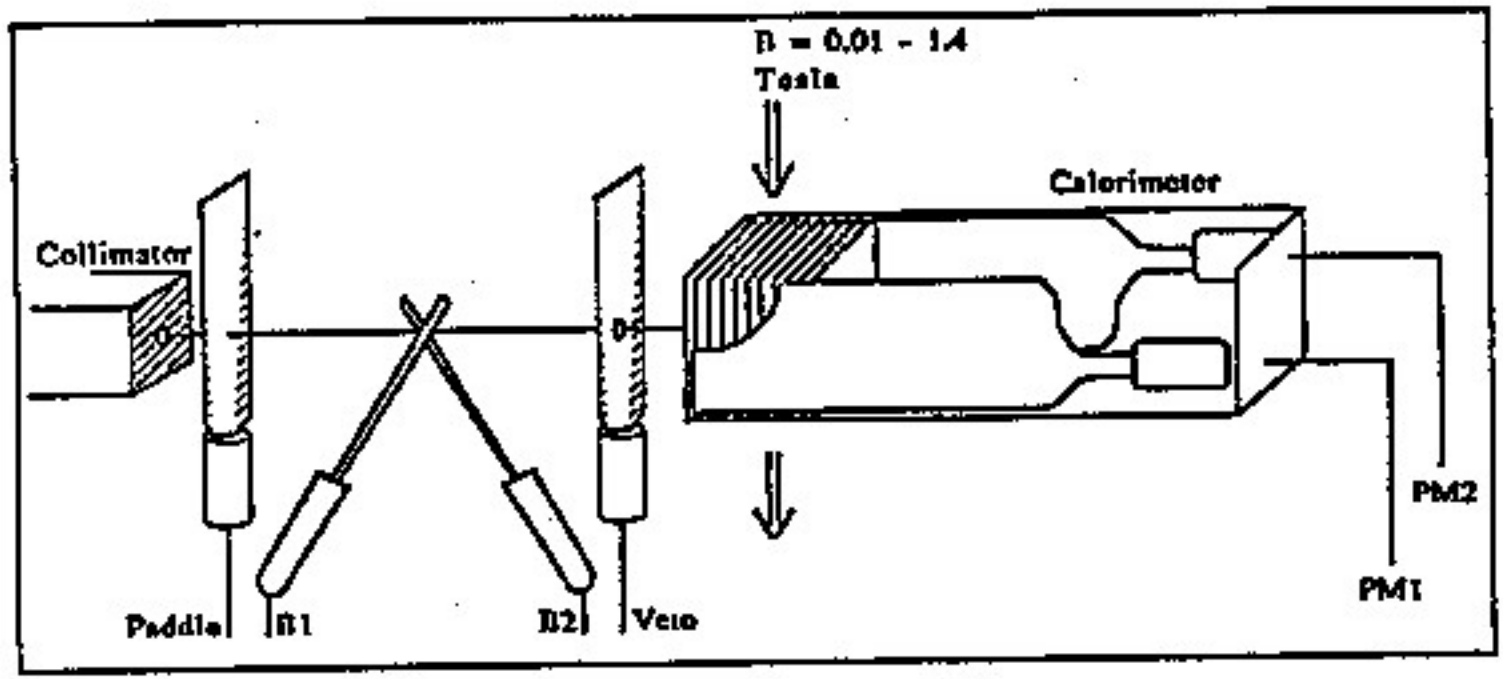

LIGHT OUTPUT VARIATION vs $B_\perp$

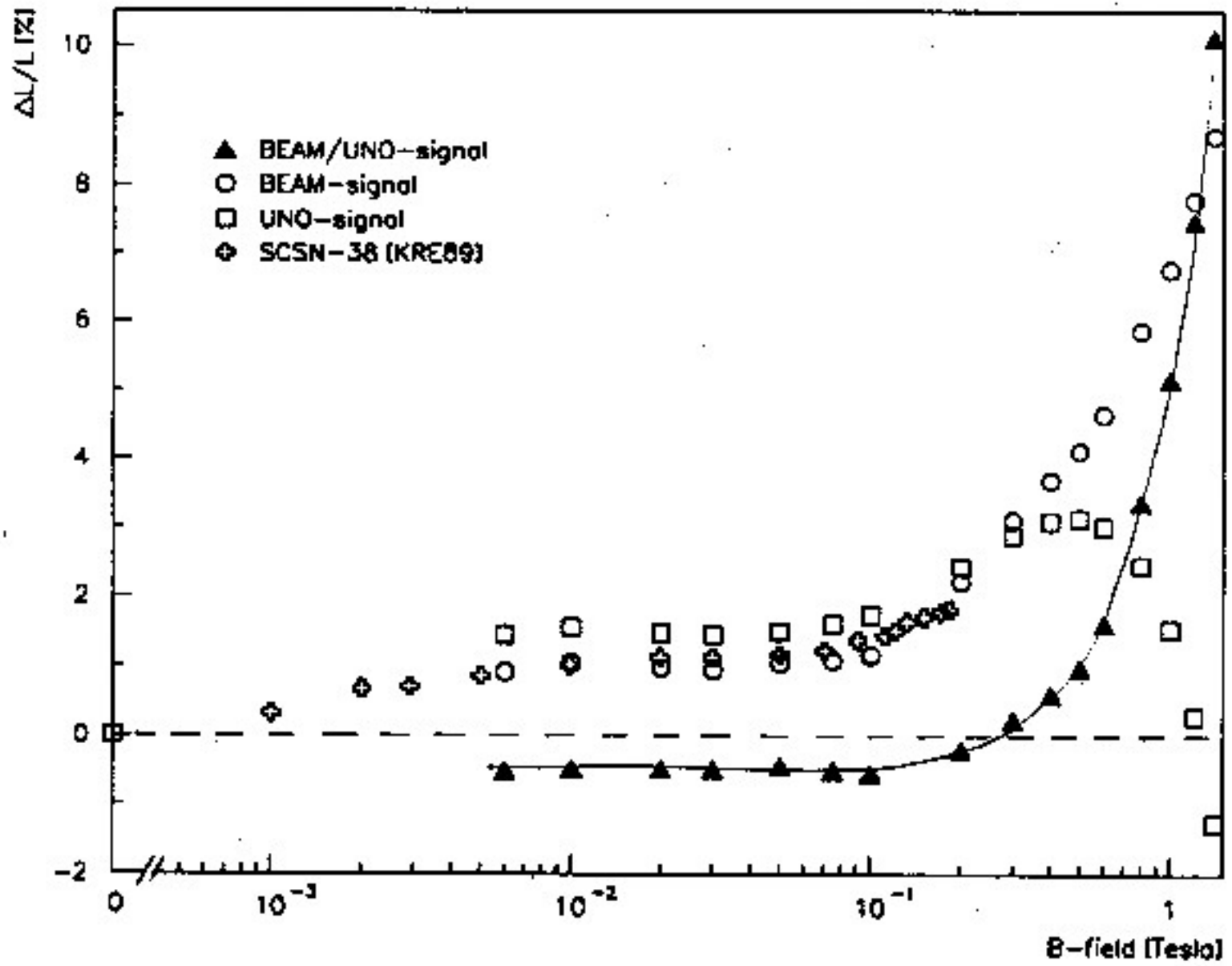

CALORIMETER SIGNAL : TIME SAMPLING

THE PULSE HEIGHT IS SAMPLED AT EACH 96 ns (BEAM CROSSING TIME) AND STORED IN A PIPELINE FOR LATER RETRIEVAL IF THE EVENT IS ACCEPTED BY THE TRIGGER.

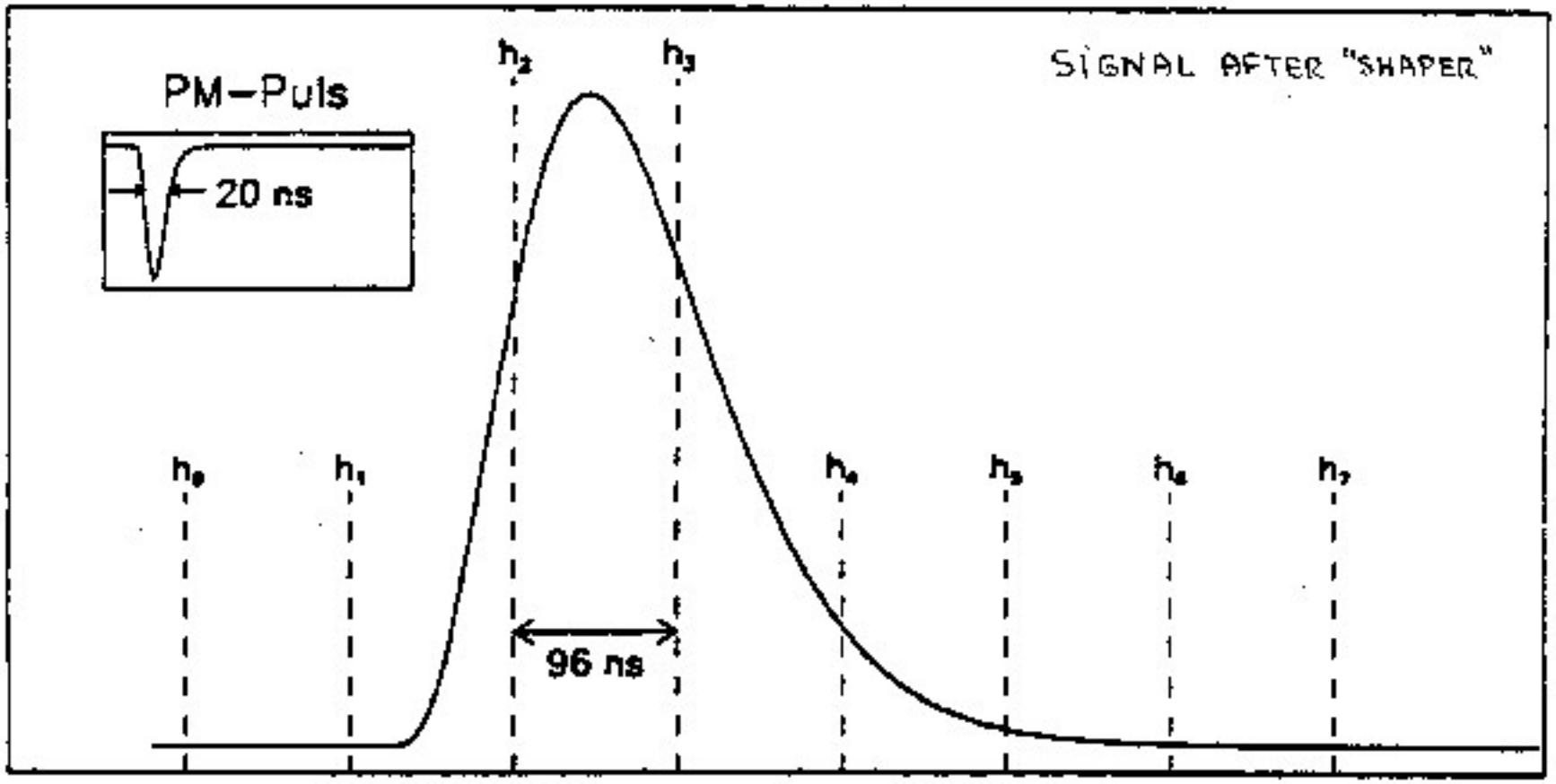

NC

$y = 0.07$

$Q^2 = 2500\ \mathrm{GeV}^2$

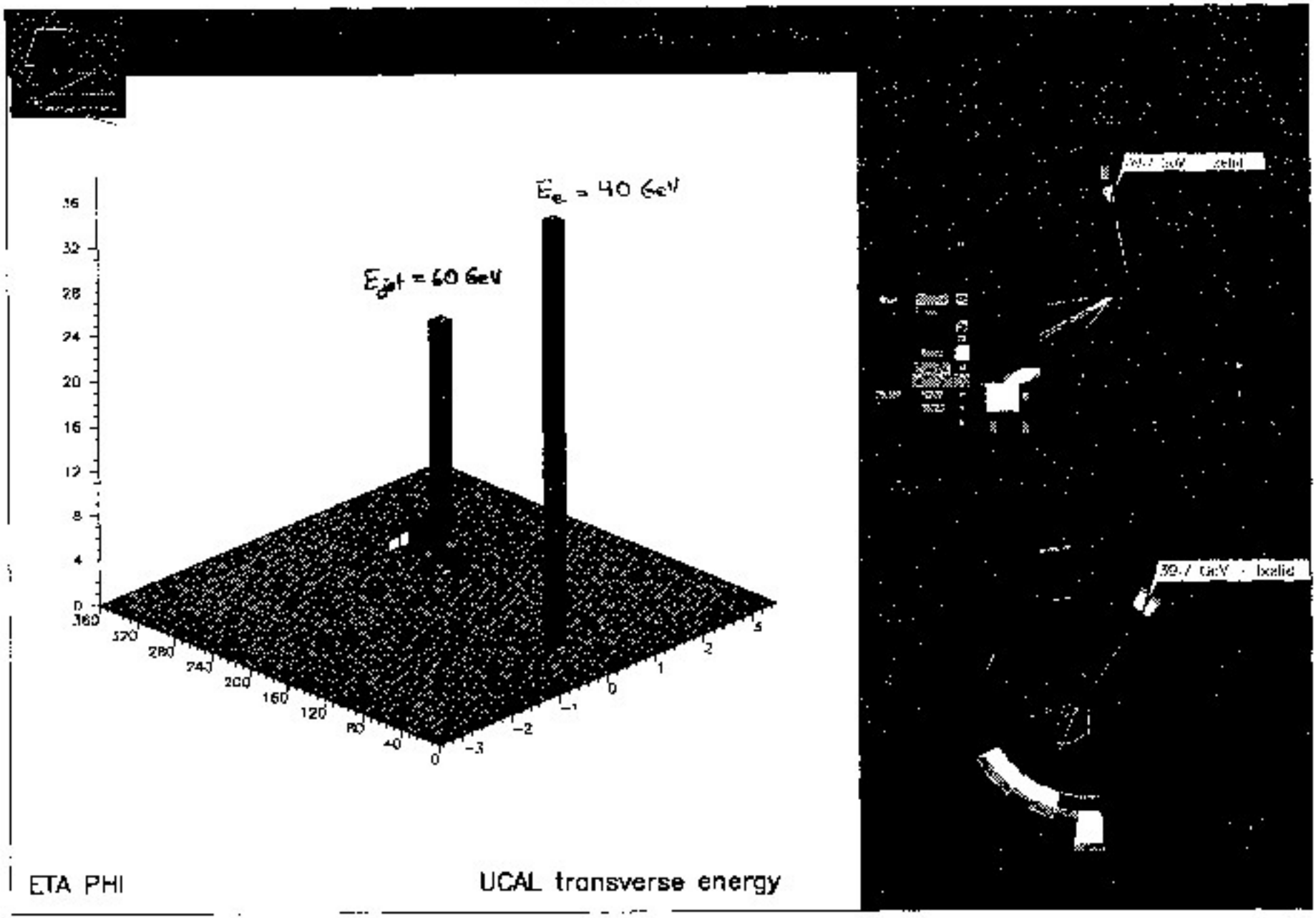

SHIFTED VERTEX EVENT

10157 66140

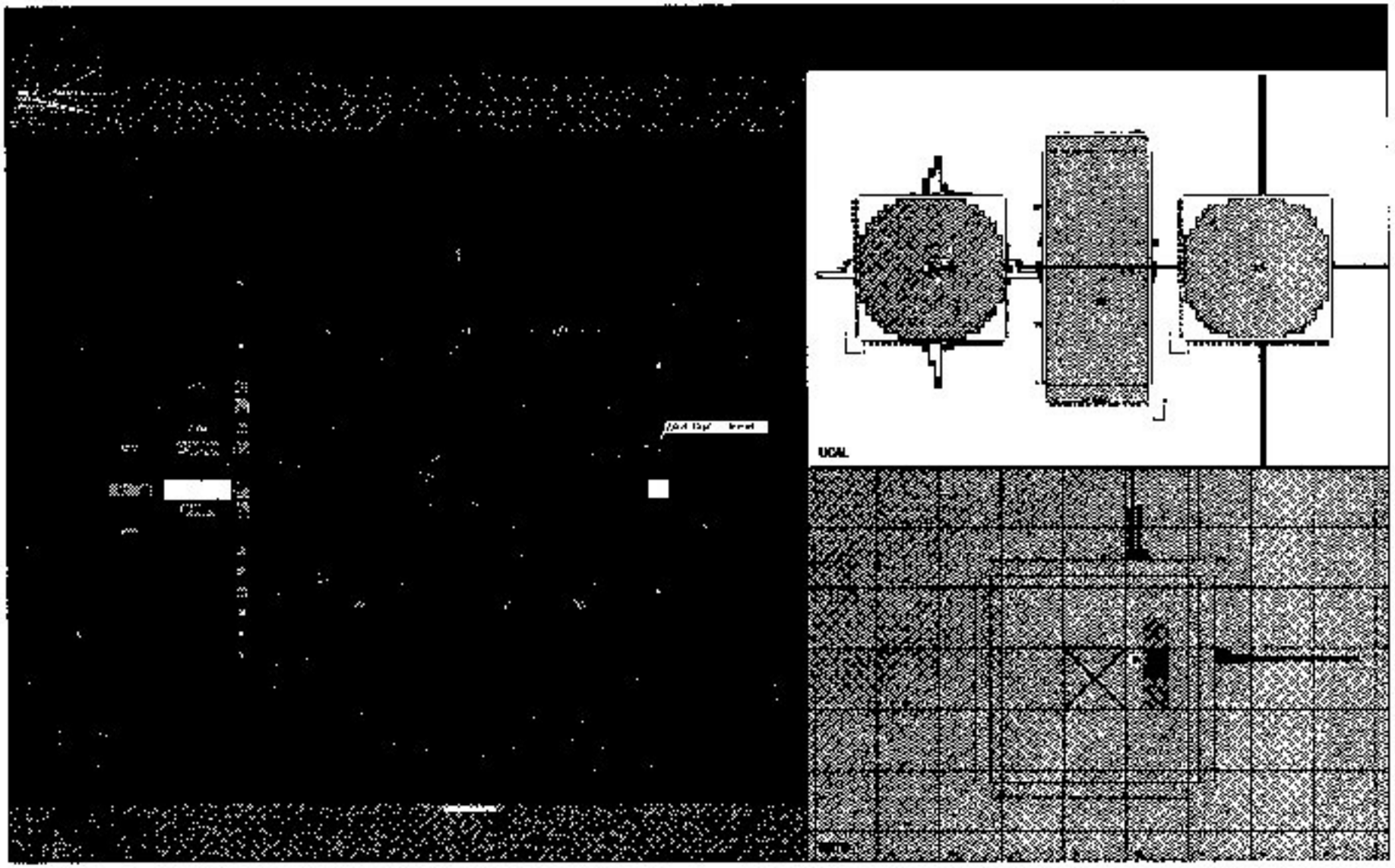

"SRTD" DATA

CALORIMER TIME INFORMATION

IT IS USE ON-LINE IN THE TRIGGER TO SELECT EVENTS

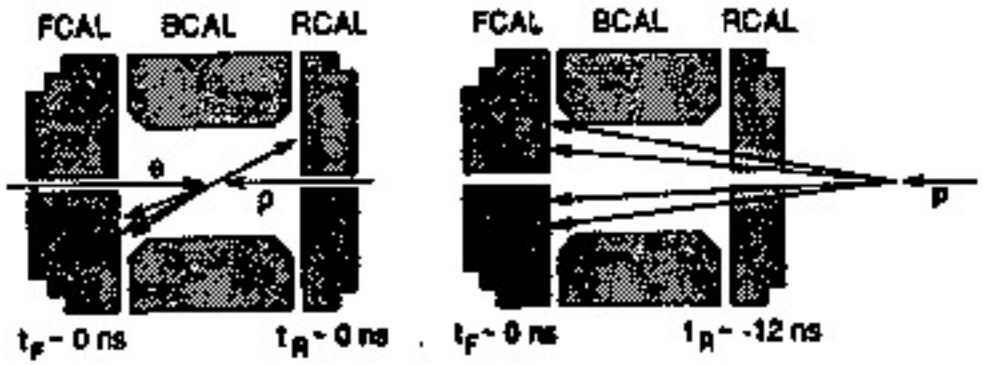

e-p EVENT

BACKGROUND EVENT

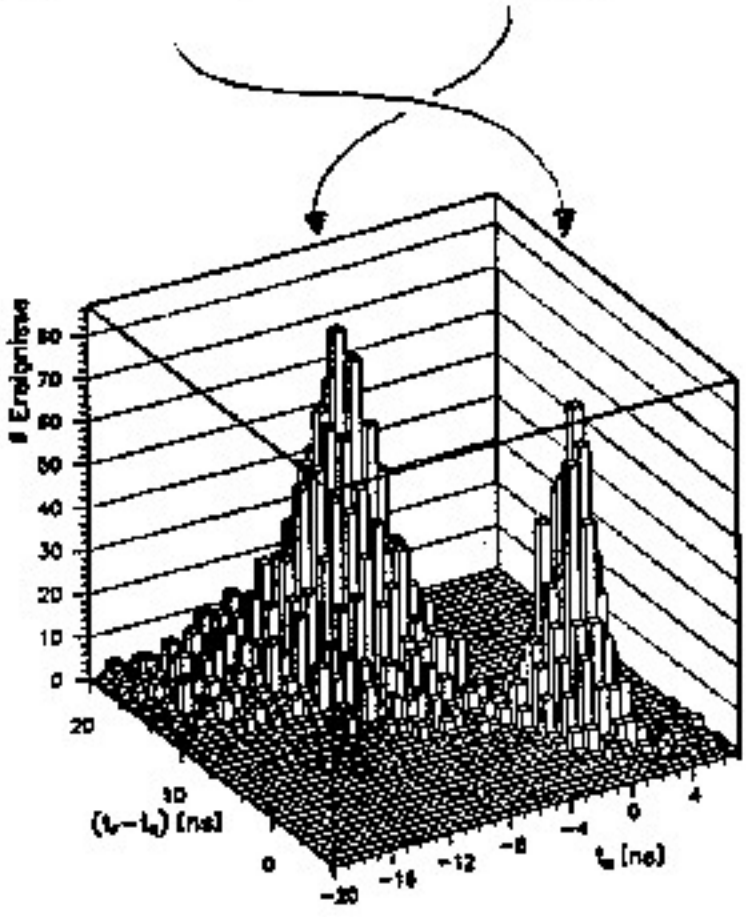

FUTURE DETECTORS

e.g. linear colliders with WW, ZZ, .. productions

PHYSICS REQUIREMENTS: few GeV mass resolution

→ good jet resolution
" angular "

HOW ?

HERMETICITY
- missing E
- forward / backward coverage

TRACK MOMENTUM
- high resolution
- large tracking volume

JET FLAVOR TAGGING
- vertexing
- efficiencies

ENERGY FLOW
- tracking
- calorimetry

⇒ OPTIMIZE DETECTOR DESIGN

ENERGY FLOW

GOAL: OPTIMIZE THE JET ENERGY RESOLUTION

1- CHARGED PARTICLES (hadrons, e, μ)

high momentum resolution tracker

2- PHOTONS

electromagnetic calorimeter

3- NEUTRAL HADRONS

hadronic calorimeter

each device optimized for response vs. granularity, etc...

$$E_{JET} = \sum_i E_i^1 + \sum_i E_i^2 + \sum_i E_i^3$$

CURRENT DETECTORS

examples

CALORIMETRY ENERGY INFORMATION CAN BE IMPROVED BY :

- SHOWER MAX DETERTORS e.g. CDF
- TRACKING e.g. ALEPH
- PRESHOWERING e.g. ZEUS

CLEAR IMPROVEMENTS ARE OBSERVED, <u>BUT</u> THEY ARE LIMITED BY THE CURRENT DESIGN :

- CALORIMETER GRANULARITY MAY BE TOO COARSE
- TRACKING MAY NOT REACH FORWARD ENOUGH
- ...

PROJECTS

TRACKING

MINIMUM MATERIAL
ALSO FORWARD COVERAGE
HIGH ANGULAR RESOLUTION
GOOD MOMENTUM RESOLUTION
} TPC ?

E-CAL

DENSE → SMALL R_M
≈ TRANSVERSE SEGMENTATION

X_0/λ_I SMALL → GOOD LONGITUDINAL SEPARATION HAD vs EM

W absorber + Si Pad 1×1 cm^2 ?

H-CAL

INTEGRATED APPROACH NEEDED

PROBLEM : TOO MANY CELLS NEEDED ? (BECAUSE OF OVERLAPS)

SOLUTION : TINY CELLS WITH 1 BIT INFO ??

STILL, ALGORITHMS ARE NEEDED TO DISENTANGLE OVERLAPS AS BEST AS POSSIBLE : LOTS OF SIMULATIONS

THE ALGORITHM(S) MAY BECOME MORE IMPORTANT THAN THE CALORIMETER ITSELF.